BOEING

Unclassified
Security Classification

DOCUMENT CONTROL DATA - R & D

(Security classification of title, body of abstract and indexing annotation must be entered when the overall report is classified)

1. ORIGINATING ACTIVITY *(Corporate author)*
Vertol Division
The Boeing Company
P. O. Box 16858, Philadelphia, PA 19142

2a. REPORT SECURITY CLASSIFICATION
Unclassified

2b. GROUP
N/A

3. REPORT TITLE
Four Prop Tilt Wing with Leading Edge BLC: Results of Semi-Span Wind Tunnel Test

4. DESCRIPTIVE NOTES *(Type of report and inclusive dates)*
Contractor Test Report (2-16 April 1970)

5. AUTHOR(S) *(First name, middle initial, last name)*
Kolesar, Charles
Kassianides, G, and Andrews, J.

6. REPORT DATE	7a. TOTAL NO. OF PAGES	7b. NO. OF REFS
May 1970	195	None

8a. CONTRACT OR GRANT NO.	9a. ORIGINATOR'S REPORT NUMBER(S)
F33615-70-C-1000	Boeing Vertol Document D170-10036-1
b. PROJECT NO. 698BT	
c. Task Area Number: 02	9b. OTHER REPORT NO(S) *(Any other numbers that may be assigned this report)*
d. Work Unit Number: 005	AFFDL TR 71-91, Reference 1

10. DISTRIBUTION STATEMENT
Approved for public release; distribution unlimited.

11. SUPPLEMENTARY NOTES	12. SPONSORING MILITARY ACTIVITY
	Air Force Flight Dynamics Laboratory Wright-Patterson AFB, Ohio 45433

13. ABSTRACT

This report presents the results of wind tunnel test BVWT 055 performed in the Boeing Vertol V/STOL wind tunnel on a powered four prop tilt wing semi-span model. The purpose of the test was to establish the effect of leading edge boundary layer control (BLC) coupled with cyclic pitch on the descent capability of the aircraft.

Configuration changes including "both-down-between-nacelles" and "both-down-inboard" propeller rotations, double slotted flaps and single slotted flaps, full span leading edge slats on and off, and all but the inboard wing fence removed were investigated during this test.

DD FORM 1 NOV 65 1473

Unclassified
Security Classification

14. KEY WORDS	LINK A		LINK B		LINK C	
	ROLE	WT	ROLE	WT	ROLE	WT
Cyclic Pitch Propellers						
Double Slotted Flaps						
Leading Edge Boundary Layer Control (BLC)						
Slats						
Tilt Wing Aircraft						

REV LTR

THE BOEING COMPANY

VERTOL DIVISION · PHILADELPHIA, PENNSYLVANIA

CODE IDENT. NO. 77272

NUMBER D170-10036-1

TITLE FOUR PROP TILT-WING WITH LEADING EDGE BLC: RESULTS OF SEMI-SPAN WIND TUNNEL TEST

ORIGINAL RELEASE DATE MAY 1970. FOR THE RELEASE DATE OF SUBSEQUENT REVISIONS, SEE THE REVISION SHEET. FOR LIMITATIONS IMPOSED ON THE DISTRIBUTION AND USE OF INFORMATION CONTAINED IN THIS DOCUMENT, SEE THE LIMITATIONS SHEET.

MODEL _____ CONTRACT F33615-70-C-1000

ISSUE NO. _____ ISSUED TO: _____

George Kassianides.

PREPARED BY J Andrews, C Kolesar DATE 5/25/70
G. Kassianides, J. Andrews, C. Kolesar

APPROVED BY Charles E Kolesar DATE 5/25/70
C. Kolesar

APPROVED BY D Bevan DATE MAY 26/70
D. Bevan, Chief, V/STOL Aerodynamics

APPROVED BY K B Gillmore DATE 5/27/70
K. B. Gillmore, Mgr., V/STOL Technology

APPROVED BY P C Prager DATE 5/26/70
P. C. Prager, Program Manager

LIMITATIONS

This document is controlled by V/STOL Aerodynamics-Org 7481

All revisions to this document shall be approved by the above noted organization prior to release.

ACTIVE SHEET RECORD

SHEET NUMBER	REV LTR	ADDED SHEETS				SHEET NUMBER	REV LTR	ADDED SHEETS			
		SHEET NUMBER	REV LTR	SHEET NUMBER	REV LTR			SHEET NUMBER	REV LTR	SHEET NUMBER	REV LTR
i						35					
ii						36					
iii						37					
iv						38					
v						39					
vi						40					
1						41					
2						42					
3						43					
4						44					
5						45					
6						46					
7						47					
8						48					
9						49					
10						50					
11						51					
12						52					
13						53					
14						54					
15						55					
16						56					
17						57					
18						58					
19						59					
20						60					
21						61					
22						62					
23						63					
24						64					
25						65					
26						66					
27						67					
28						68					
29						69					
30						70					
31						71					
32						72					
33						73					
34						74					

FORM 46288 (7/67)

ACTIVE SHEET RECORD

SHEET NUMBER	REV LTR	ADDED SHEETS				SHEET NUMBER	REV LTR	ADDED SHEETS			
		SHEET NUMBER	REV LTR	SHEET NUMBER	REV LTR			SHEET NUMBER	REV LTR	SHEET NUMBER	REV LTR
75						115					
76						116					
77						117					
78						118					
79						119					
80						120					
81						121					
82						122					
83						123					
84						124					
85						125					
86						126					
87						127					
88						128					
89						129					
90						130					
91						131					
92						132					
93						133					
94						134					
95						135					
96						136					
97						137					
98						138					
99						139					
100						140					
101						141					
102						142					
103						143					
104						144					
105						145					
106						146					
107						147					
108						148					
109						149					
110						150					
111						151					
112						152					
113						153					
114						154					

FORM 46288 (7/67)

ACTIVE SHEET RECORD

SHEET NUMBER	REV LTR	ADDED SHEETS				SHEET NUMBER	REV LTR	ADDED SHEETS			
		SHEET NUMBER	REV LTR	SHEET NUMBER	REV LTR			SHEET NUMBER	REV LTR	SHEET NUMBER	REV LTR
155											
156											
157											
158											
159											
160											
161											
162											
163											
164											
165											
166											
167											
168											
169											
170											
171											
172											
173											
174											
175											
176											
177											
178											
179											
180											
181											
182											
183											
184											
185											
186											
187											
188											
189											

FORM 46283 (7/67)

REVISIONS			
LTR	DESCRIPTION	DATE	APPROVAL

ABSTRACT

This report presents the results of wind tunnel test BVWT 055 performed in the Boeing Vertol V/STOL wind tunnel on a powered four prop tilt wing semi-span model. The purpose of the test was to establish the effect of leading edge boundary layer control (BLC) coupled with cyclic pitch on the descent capability of the aircraft.

Configuration changes including "both-down-between-nacelles" and "both-down-inboard" propeller rotations, double slotted flaps and single slotted flaps, full span leading edge slats on and off, and all but the inboard wing fence removed were investigated during this test.

KEY WORDS

Cyclic Pitch Propellers

Double Slotted Flaps

Leading Edge Boundary Layer Control (BLC)

Slats

Tilt Wing Aircraft

NOMENCLATURE

The following nomenclature was used for Model VRO40Q-3 in test BVWT 055. Additional nomenclature is included in the Data Reduction section of this report.

Symbol		
A_p	Propeller disc area	ft^2
α_F	Fuselage angle of attack relative to freestream	degrees
$\alpha_{W_{EFF}}$	Effective wing angle of attack	degrees
B_1	Half-fuselage used with semispan model	
b	Wing span	ft.
c	Wing chord	ft.
γ	Cyclic angle	degrees
D	Propeller diameter	ft.
δ_F	Flap angle	degrees
F_1	Wing fence configuration	
f_1	Basic single-slotted flap	
f_2	Basic double slotted flap	
$\theta_{.75}$	Propeller blade pitch angle at .75R	degrees
i_w	Wing incidence relative to waterline	degrees
L	Lift	lbs.
M	Pitching moment (about wing hinge), positive nose up	ft. lbs.
N_1	Nacelle configuration	
P_1	Collective hubs	
P_2	Cyclic hubs	

Symbol		
Q_3	Slats used with Wing 3	
q	Freestream dynamic pressure	lbs/ft^2
R	Blade radius	ft.
S	Wing area	$ft.^2$
T	Thrust	lbs.
V_T	Freestream velocity	ft/sec
W_{3t}	Wing 3, tip panel on	
w	Propeller induced velocity	ft/sec
X	Longitudinal force, positive forward	lbs.
Y	Side force, positive to the right	lbs.

Superscripts	(Superscripts are in sequence left wing tip to fuselage centerline)	
f^{60}	Flap at 60°	
$p^{1,1}$	Both propellers turning down inboard	
$p^{1,2}$	Left wing O/B propeller turning down inboard, I/B propeller turning outboard	
Q^{10}	Slat setting, see Notes	
Q^*	Slat setting, see Notes	

NOTES: 1) According to the notation used, slat $Q_3^{10,10,10,*}$ indicated that all slat segments inboard of the wing tip were set at Q^{10} position with the exception of the slat segment inboard of the inboard nacelle which was set at Q^* position.

FORM 46284 (2/66)

TABLE OF CONTENTS

TABLE OF CONTENTS

1.0 INTRODUCTION

Wind tunnel test BVWT 055 was carried out on a semi-span powered model of the Model 170 four propeller tilt-wing, in the 20ft.x 20ft. test section of the Boeing-Vertol V/STOL wind tunnel. The test was performed during the period of April 2nd to April 16th, 1970 inclusive.

The objective of this test program was to investigate leading edge boundary layer control (BLC) as a means of improving the descent performance of a four propeller tilt wing incorporating cyclic pitch propellers for pitch control. In the initial phase of the program, several values of blowing coefficient, C_{μ_s}, were evaluated with BLC employed over the full wing span and over selected sections of the span. This testing with collective hubs was utilized to establish the blowing configurations to be used for the cyclic pitch phase of the program.

The portion of the wing extending over the fuselage was of special concern since this section of the wing is "not bathed" in the propeller slipstream and consequently stalls early. Leading edge BLC was evaluated as a method of maintaining flow attachment on the wing center section to a higher angle of attack.

From previous test results it was known that positive (nose down) cyclic has a detrimental effect on the rate of descent performance. The effect on rate of descent of BLC coupled with cyclic was the primary investigatory item of the test.

"Both-down-between-nacelles" propeller rotation was found to be the optimum rotation in past testing. The effect of changing the inboard propeller rotation to "down inboard" when blowing was employed was also investigated with and without cyclic.

The majority of runs were made with 60° of large chord double slotted flaps that incorporate a movable fore flap which "nests" when the flap is retracted. Less complex single slotted flaps were also tested at 30° and 45° of deflection with full span blowing and positive cyclic.

Slats have been found to be beneficial for maintaining flow attachment to higher wing angles and thereby improving the descent performance of the tilt wing aircraft. With leading edge BLC, a clean wing leading edge can probably be used if the loss in descent performance is minimal. Consequently, the effect of removing the slats was evaluated.

Wing fences (two at the side of the fuselage and two mid-span for a total of four per semispan) have been used to contain the stall over the wing center section and at the fuselage side plus any mid-span stall that occurs in the low dynamic pressure region between propeller tips. All but the inboard fence were removed for a series of runs to investigate the effect of their removal.

2.0 MODEL DESCRIPTION AND INSTALLATION

The general arrangement and geometry of semispan Model VRO40Q-3 and wind tunnel installation details are presented in this section. Figure 1 is a photograph of this model as installed in the Boeing-Vertol V/STOL wind tunnel for this test.

2.1 WING GEOMETRY (See Figure 2)

The model utilized the No.3 wing of basic Model VRO40Q. This rectangular wing has the following geometry:

Span (2xSemispan to round tip)	9.450 ft
Chord	1.2065 ft
Area	11.401 ft^2
Aspect Ratio	7.84
Wing Pivot Position	
X-Axis	40%c aft of wing L.E.
Z-Axis	11%c below w.c.p.
Basic Wing Section	NACA 63_3418
Wing Chord/Prop. Diameter	0.563
Slats	15% basic wing chord
Flaps	
Single slotted	40.00% basic wing chord 25% chord Fowler action
Double slotted	35.52% basic wing chord (when retracted) 22.2% chord Fowler action

Slats

The wing incorporated full span leading edge slats of the design depicted in Figure 3. These were attached to the basic wing leading edge with preset brackets, and were arranged in four spanwise segments. The inboard slat segment covered the leading edge from the $\mathcal{L}$ of the aircraft to the inboard nacelle side; the between-nacelles slat was in two equal pieces and the outboard segment extended from the outboard nacelle side to the wing tip. It was thus possible to set the slats differentially according to

the direction of rotation of the propeller blades in front of each slat segment.

The slat angle, gap and location for the two different propeller rotations had been optimized in previous tests and these were used during this test.

BLC Slot (See Figure 4)

The BLC slot, located at the 0.5% chord station, was of the design shown in this figure. Slot gap could be varied by using different thicknesses of shim spacer in the lower movable surface of the wing leading edge.

Three spanwise slot segments were provided. The first segment extended from the aircraft centerline to the inboard nacelle side, the second extended between the nacelles and the third extended outboard of the outboard nacelle to the wing tip. Slot segments were given letter designations as shown in Figure 2.

The pressure ratio applied to each of these slots could be adjusted individually by separate pressure valves.

Flaps

Both double slotted and single slotted flaps were used during this test. The majority of runs were made with double slotted flaps of the configuration depicted in Figure 5. These had been designed for a wing of the same span as the wing used in this test but with a basic wing chord of 1.0715 ft. instead of 1.2065ft. The flap chord (retracted position) of 40% for the small chord wing reduced to 35.5% for the larger chord wing. The fore flap "nests" against the main flap in the retracted position. This movable fore flap feature results in an extended flap chord of 49% for the small chord wing or 43.5% of the larger chord wing.

The single slotted flaps shown in Figure 6 were specifically designed for the wing used in this test. They had a flap chord of 40% and 25% chord Fowler action.

All runs with double slotted flaps were made with a flap deflection of 60°. Single slotted flap deflection was limited to 45° due to flow separation on the flap as established from previous testing.

The gaps and locations used for both the double slotted flaps (at 60°) and single slotted flaps (at 30° and 45°) with reference to the wing, were determined from previous test data.

Figure 1.

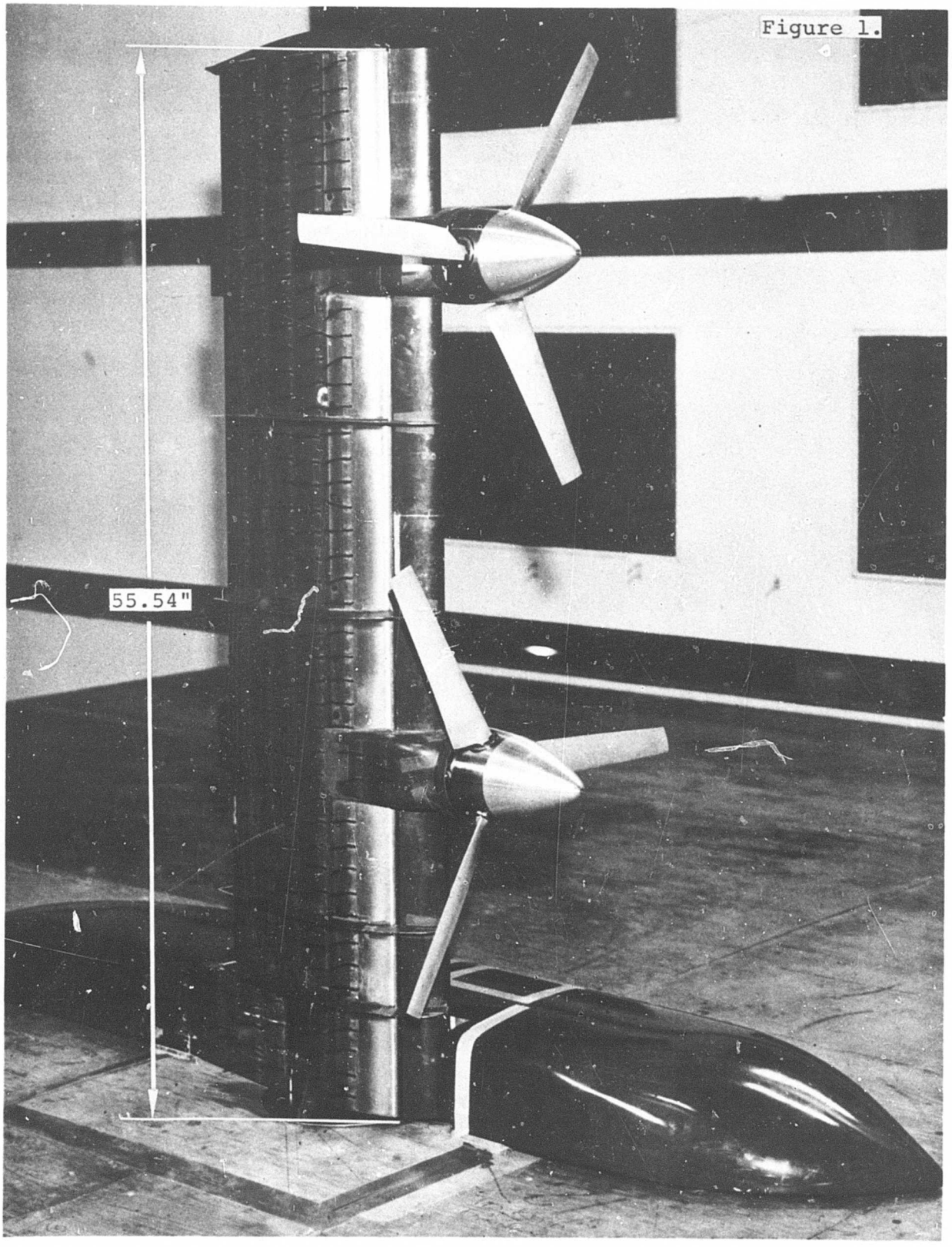

Semi-span Model VRO40Q-3 Installation
in Boeing-Vertol V/STOL Wind Tunnel

MODEL VRO40Q-3: BLC TEST

NOTES:

1. Wing Area = 11.401 ft^2
2. Prop Area = 3.607 ft^2
3. Aspect Ratio = 7.84
4. c/D = 0.563
5. F Defines Wing Fence
6. (A) to (G) Define Blown Regions

Not to scale

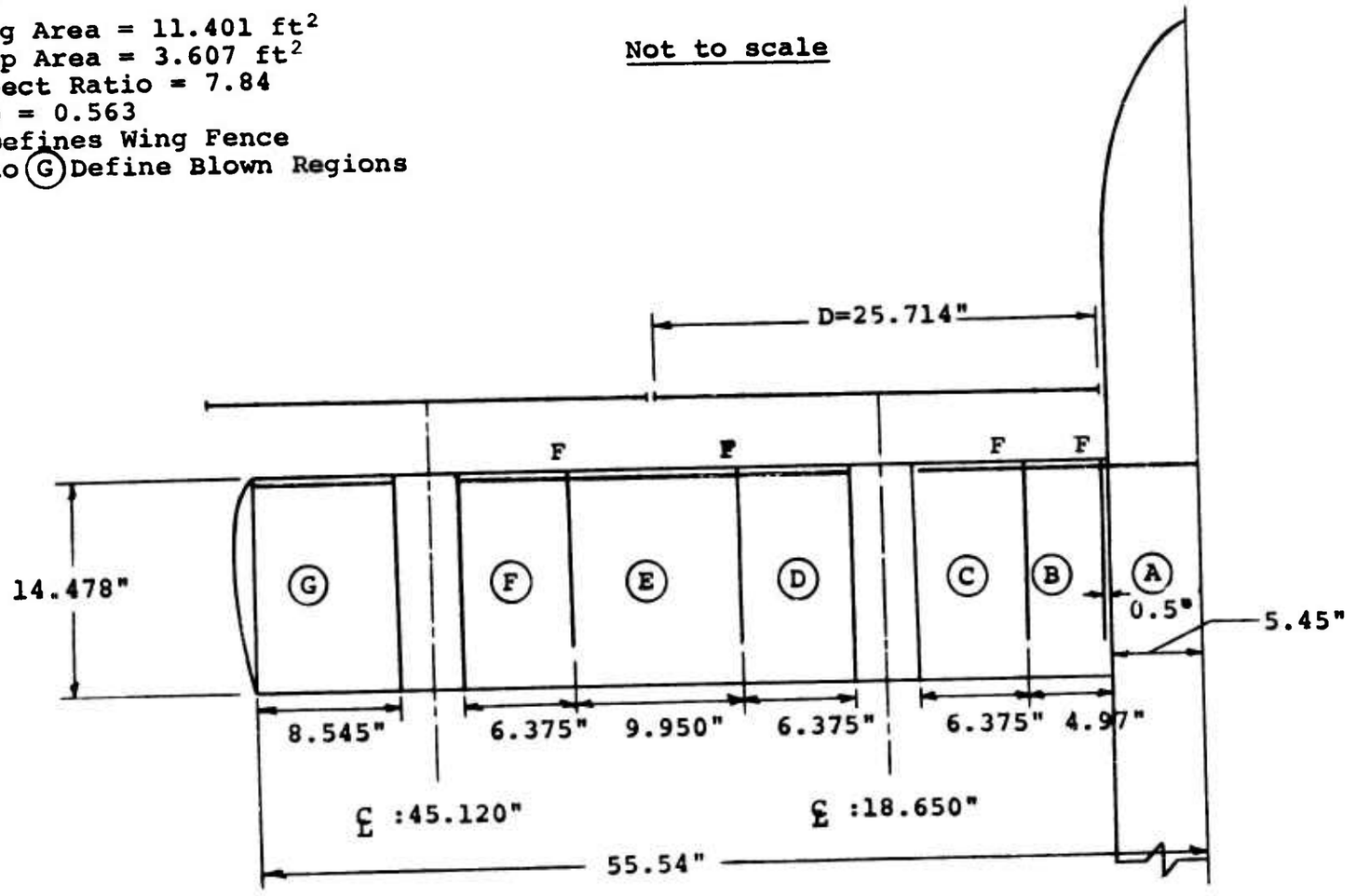

BASIC WING GEOMETRY AND SLOT LOCATIONS

Figure 2

MODEL VRO40Q-3: BLC TEST

Figure 3

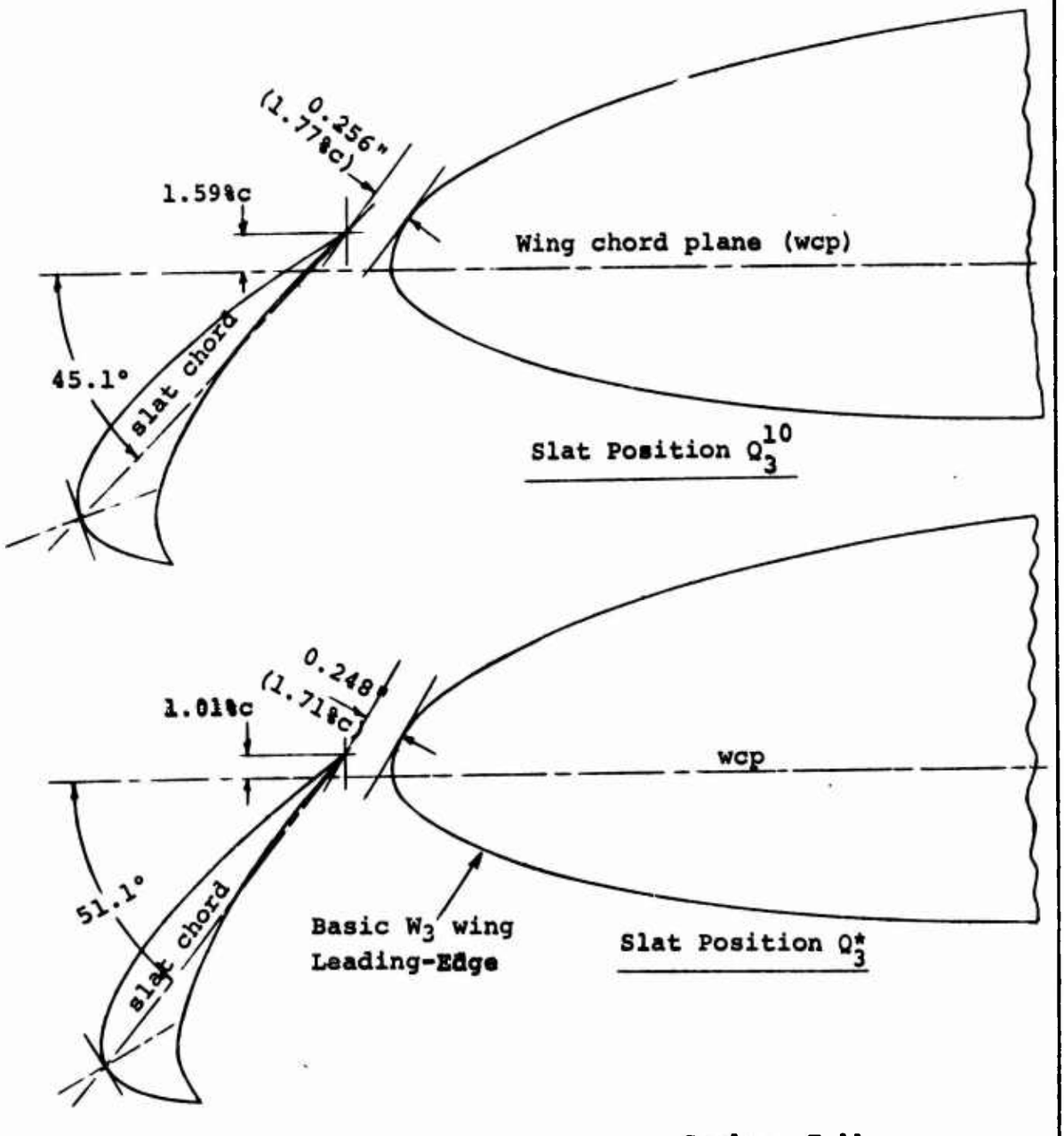

Scale: Full
c: Basic Wing Chord

DETAILS OF Q_3 SLAT ARRANGEMENT

FORM 11180 (6/67)

Figure 4

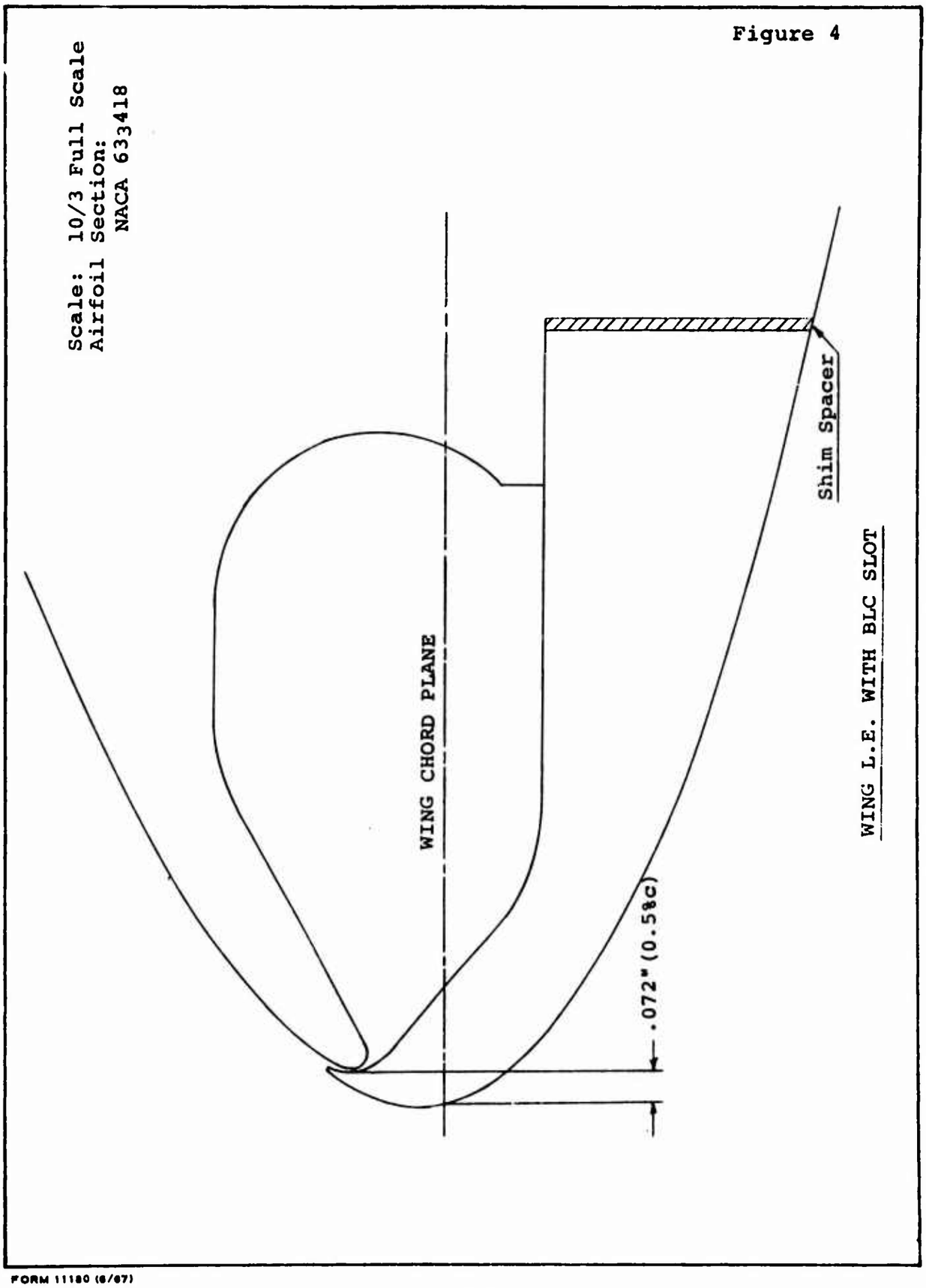

FORM 11180 (6/67)

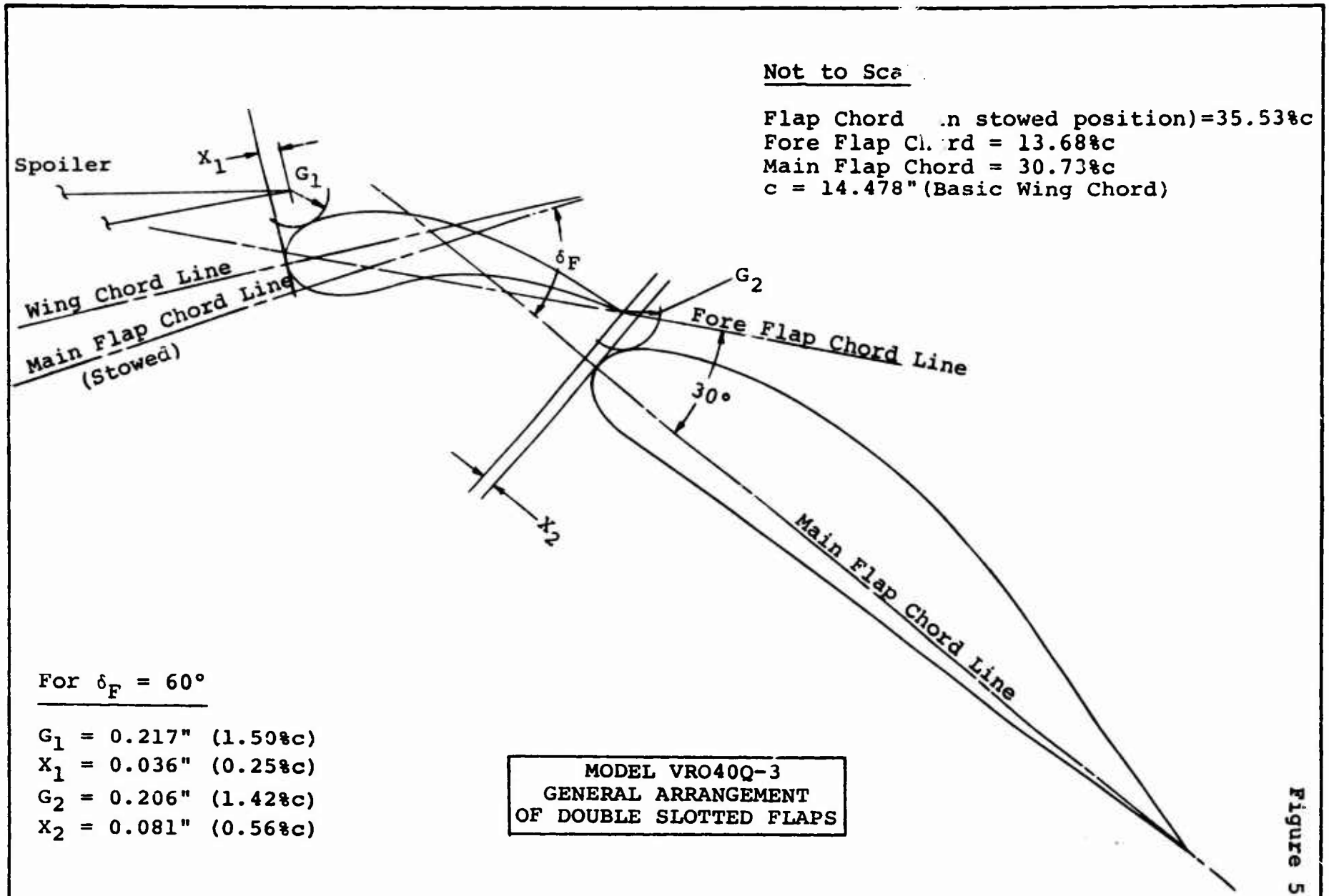

For δ_F = 60°

G_1 = 0.217" (1.50%c)
X_1 = 0.036" (0.25%c)
G_2 = 0.206" (1.42%c)
X_2 = 0.081" (0.56%c)

MODEL VRO40Q-3
GENERAL ARRANGEMENT
OF DOUBLE SLOTTED FLAPS

Figure 5

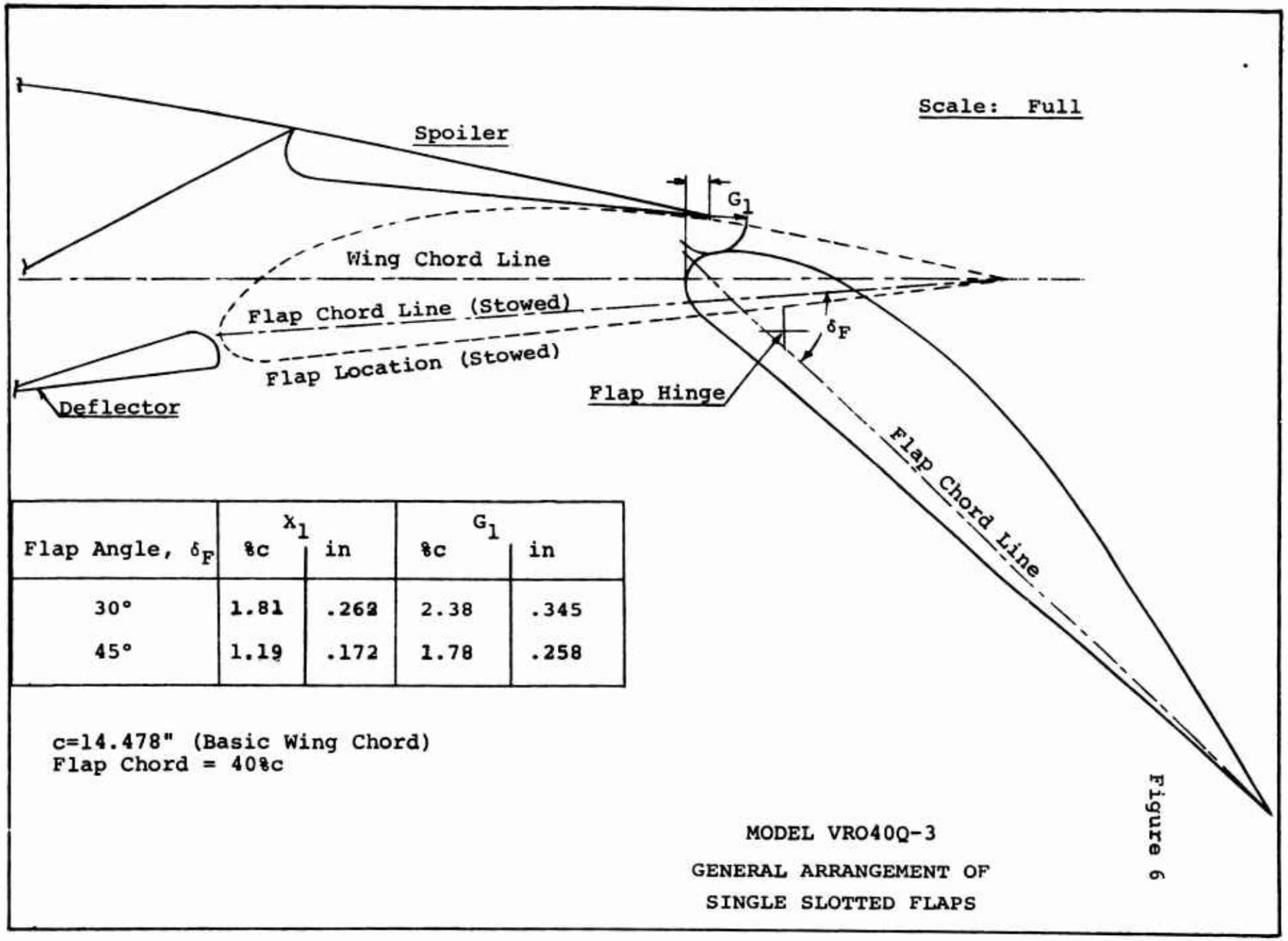

Flap Angle, δ_F	X_1 %c	X_1 in	G_1 %c	G_1 in
30°	1.81	.262	2.38	.345
45°	1.19	.172	1.78	.258

c=14.478" (Basic Wing Chord)
Flap Chord = 40%c

MODEL VRO40Q-3
GENERAL ARRANGEMENT OF
SINGLE SLOTTED FLAPS

Figure 6

2.2 PROPELLERS, HUBS

Two three-bladed propellers were used on this model. These were located .35c ahead of the basic wing leading edge with the thrust line .155c below the wing chord plane. Geometric characteristics of the collective hub propellers are given below:

Diameter	- 2.143 ft
Disc Area	- 3.61 ft^2
Root Chord (at 2.571 in.radius)	- 2.071 in.
Tip Chord	- 1.385 in.
Root Section	- NACA 63_{2015}
Tip Section	- NACA 63_{2012}
Activity Factor	- 91 per blade

The blades had a constant taper in both chord and thickness with an unswept 27% chord line. Overall blade twist was 24.5° as shown in the Figure 7 blade twist distribution plot.

Collective hubs were used during the non-cyclic portion of the test. These were replaced by cyclic hubs when cyclic was required. Propeller collective and cyclic angles were manually adjusted.

The cyclic hubs employed a swashplate mounted on a cyclic stack fixed to the front of the electric nacelle motor housing. The outer annulus of the swashplate was driven by scissors mounted on the rear face of the hub. Cyclic pitch was applied to the blades through a set of pitch links.

Both sets of 3-way hubs utilized the same propeller blades; however, in the case of the cyclic hubs, the propeller tips were trimmed to match the larger diameter incorporated into the hub to allow sufficient space for the cyclic mechanism.

2.3 FUSELAGE GEOMETRY

The half-fuselage used is shown in Figure 8 and 9. This body had a shape generally representative of a four propeller tilt-wing aircraft fuselage. Since only the wing was mounted to the balance, no physical contact or interference between the wing and the fuselage was allowed.

A wing-fuselage fairing attached to the fuselage (See Figure 8) was remotely driven to provide a small clearance between the wing and the fairing. The fairing was incorporated to eliminate the

"hole" aft of the wing which would have resulted due to the wing tilt and wing/body juncture requirements.

2.4 MODEL INSTALLATION

The model was installed in the tunnel as shown in Figure 9 and 10. A platform or ground board 144.90 inches above the tunnel floor served as a plane of symmetry. The four component balance mounted to the wing root, and all the electrical, water and air leads were neatly arranged in a streamlined fairing below the platform. A cylindrical tube extension was used to attach the four component balance and thereby the wing to the tunnel yaw table. All yaw table driving gears plus motor were below the tunnel floor (Figure 10).

As an additional point, the tubing used to transmit blowing air to the wing was "looped around" the wing root balance in a manner which virtually eliminated any balance interactions. This was verified during the balance calibration.

2.5 TEST FACILITY

As mentioned previously, the test was conducted in the 20ft x 20ft test section of the Boeing-Vertol V/STOL wind tunnel. See Figure 11 for a detailed schematic of the tunnel.

Two test section configurations are currently available, namely: closed throat, and slotted throat. Walls, floor and ceiling used for the closed throat configuration are also used for the slotted throat configuration by simply removing covers from slots which are built into the walls. The slotted throat was used during BVWT 055 to minimize wall effects.

Figure 7

HALF MODEL VRC400-3

PROPELLER BLADE TWIST DISTRIBUTION

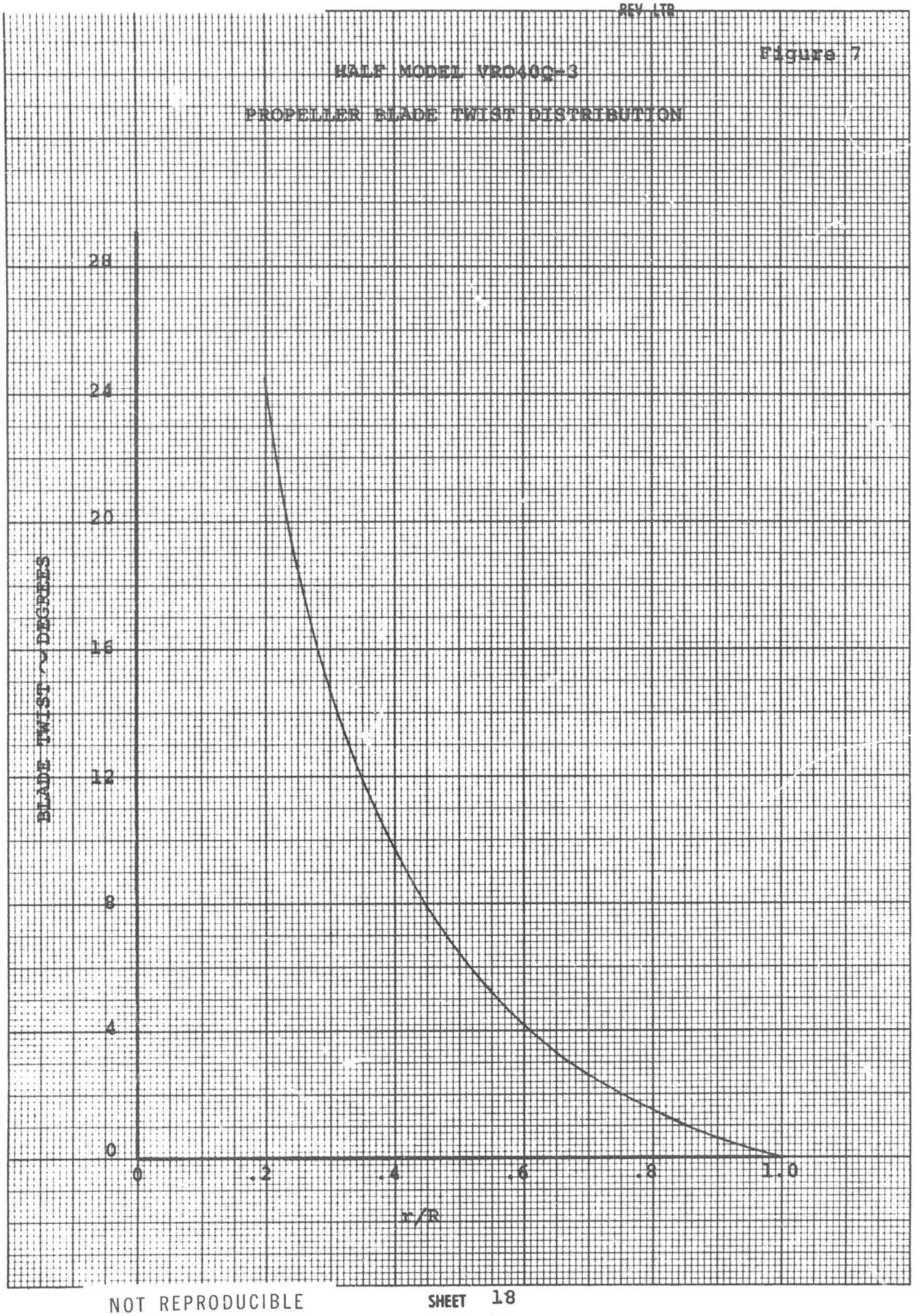

A

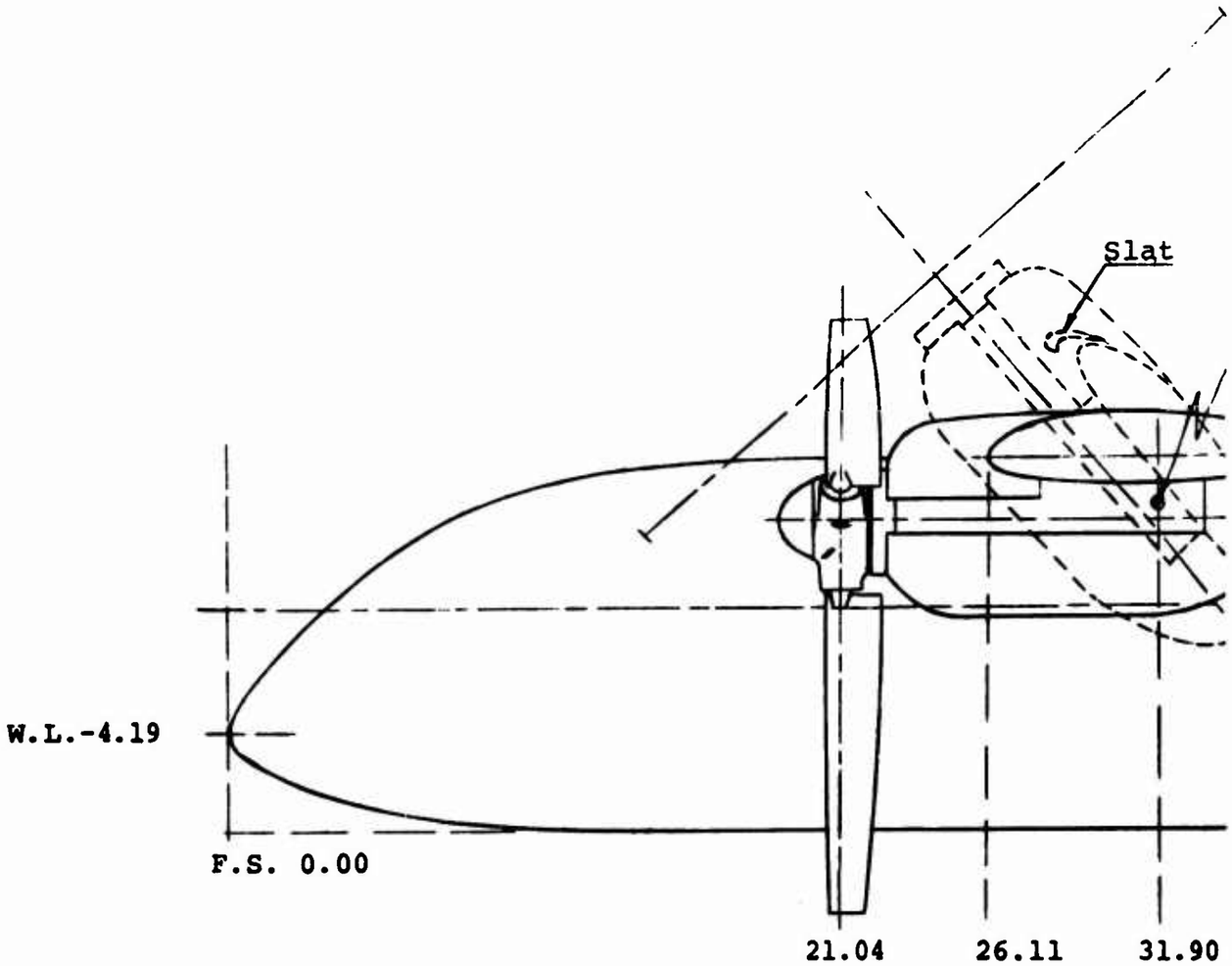

END VIEW OF VRO40Q-3

HALF MODEL

FORM 13910 (6/66)

Figure 6

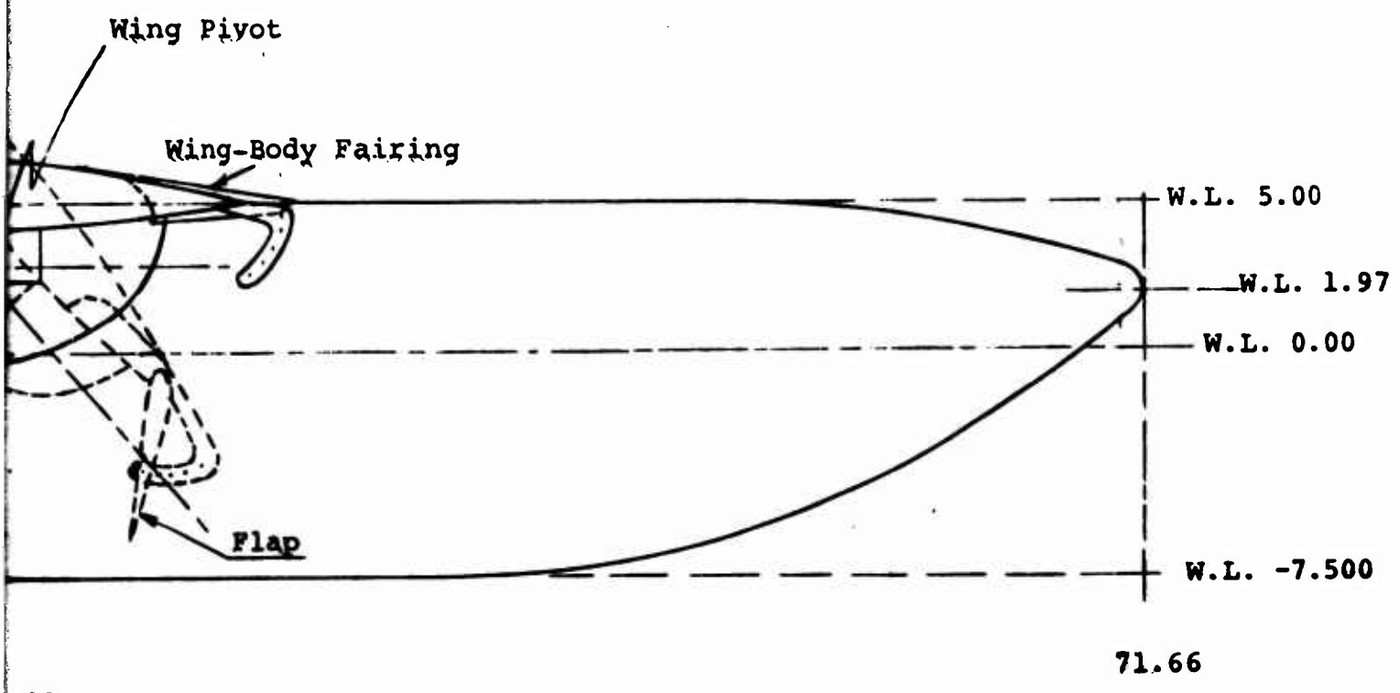

.90

Q-3

A

GENERAL ARRANGEMENT
OF VRO40Q-3 HALF MODEL
AND INSTALLATION DETAILS

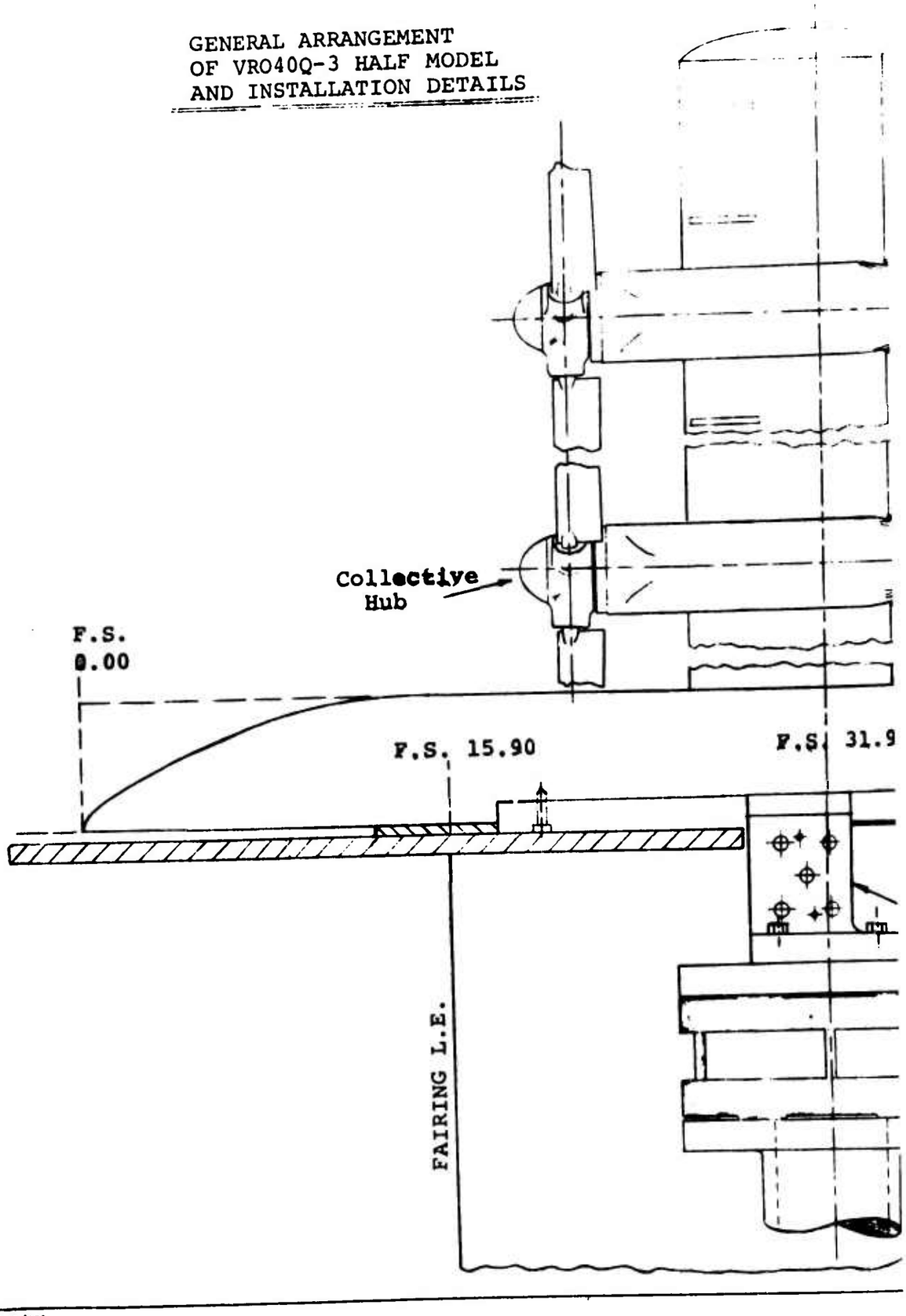

FORM 13910 (8/66)

Figure 9

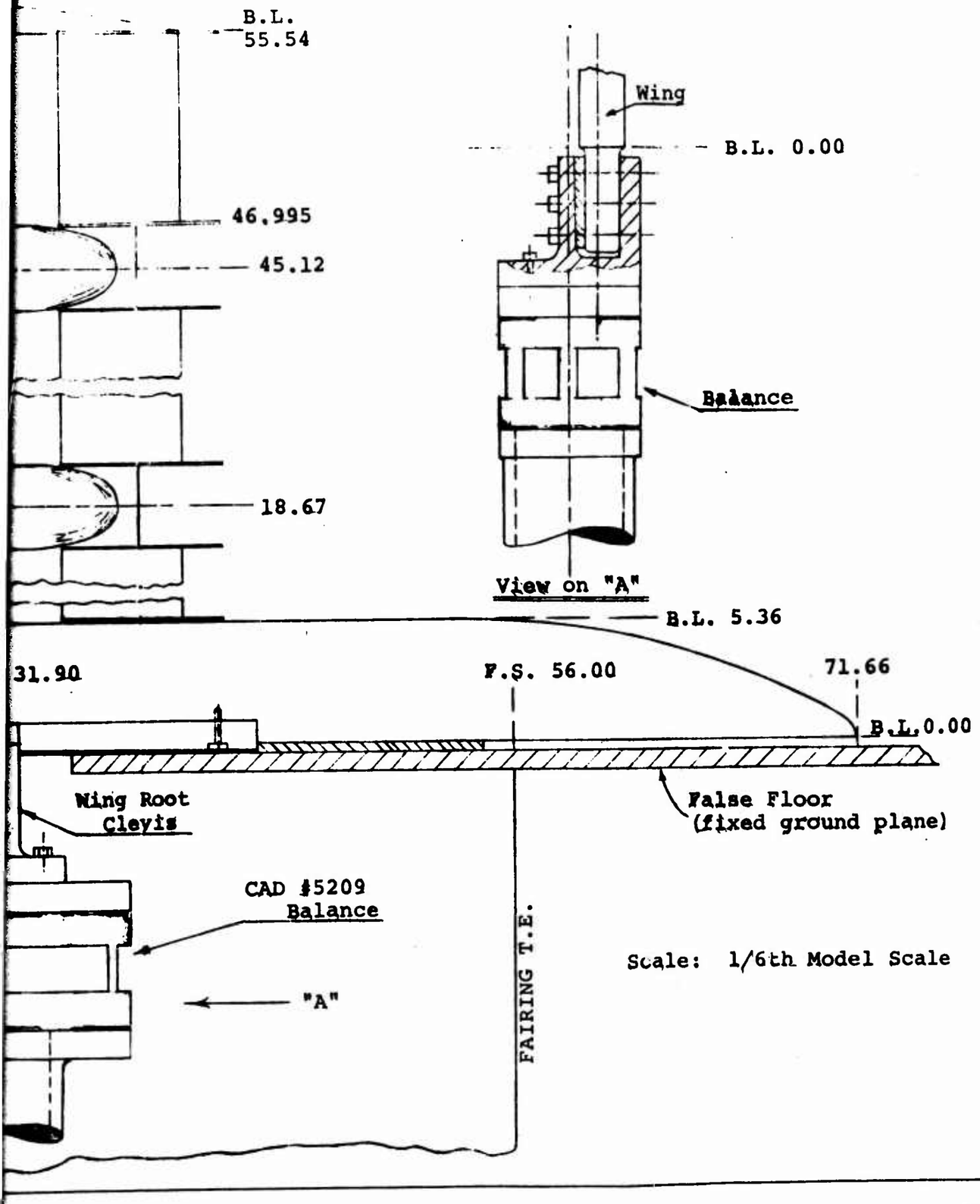
B.L.
55.54
Wing
B.L. 0.00
46.995
45.12
Balance
18.67
View on "A"
B.L. 5.36
31.90
F.S. 56.00
71.66
B.L.0.00
Wing Root
Clevis
False Floor
(fixed ground plane)
CAD #5209
Balance
"A"
FAIRING T.E.
Scale: 1/6th Model Scale

A

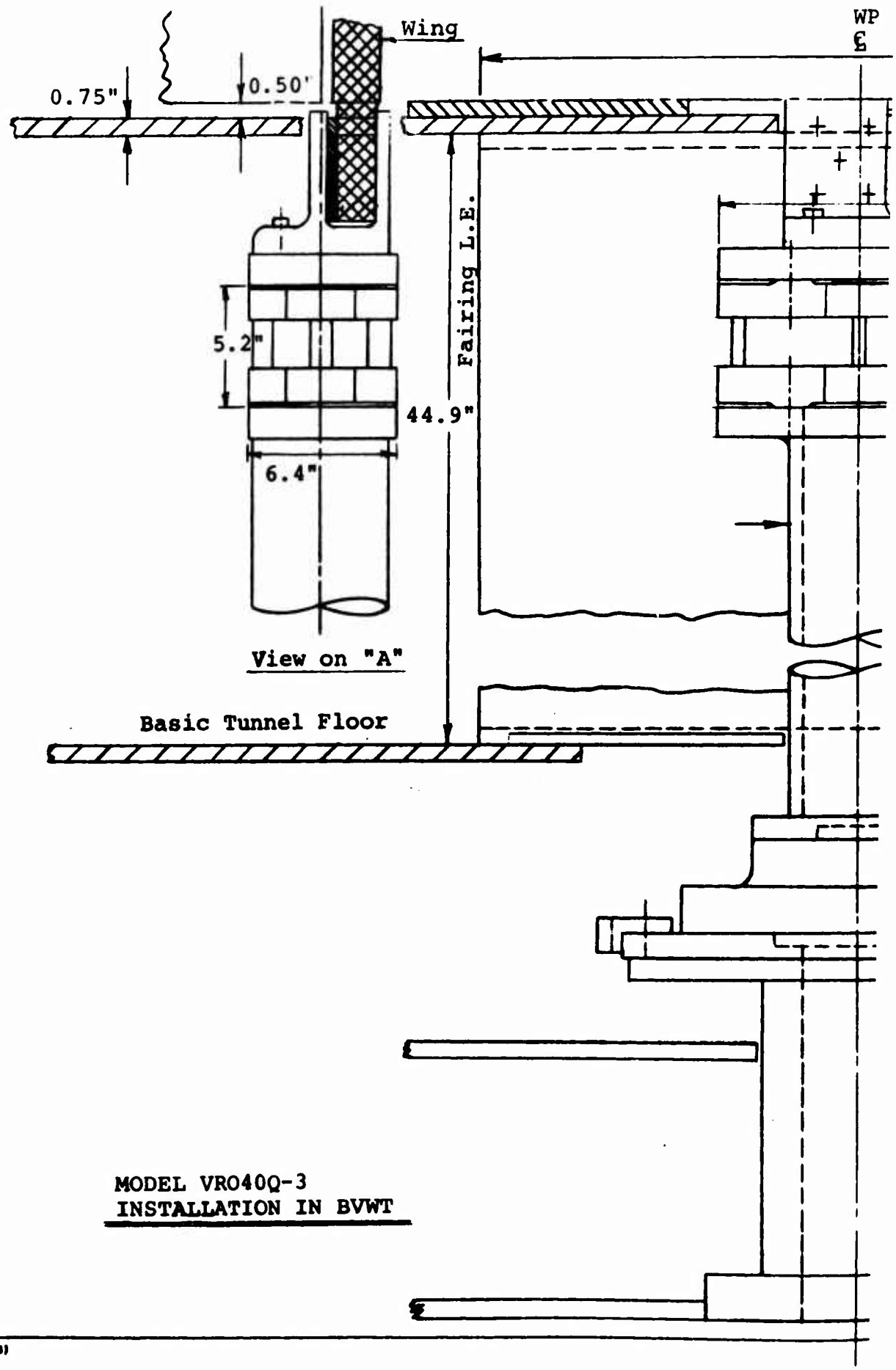

MODEL VR040Q-3
INSTALLATION IN BVWT

Figure 10

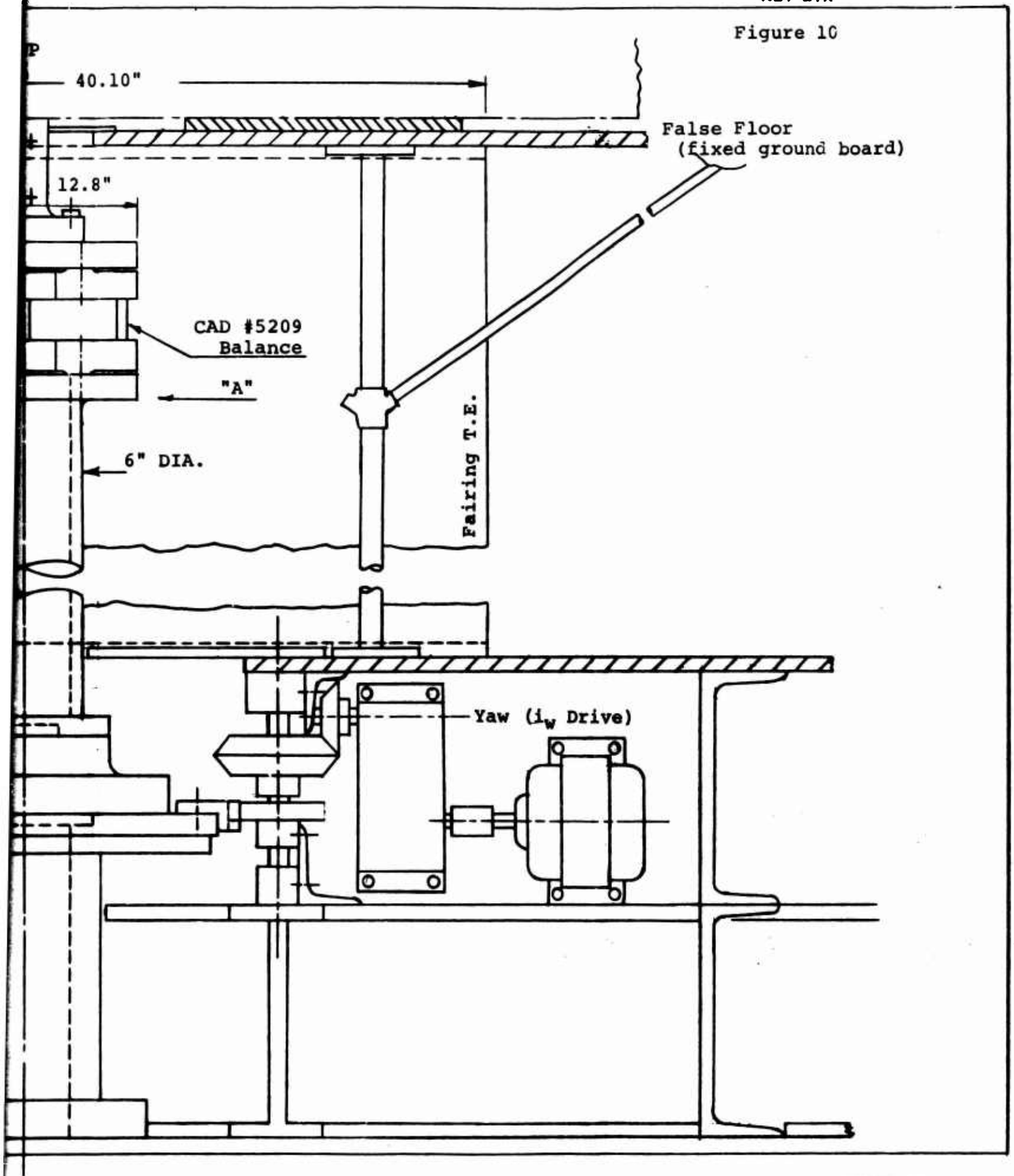
40.10"
False Floor
(fixed ground board)
12.8"
CAD #5209
Balance
"A"
6" DIA.
Fairing T.E.
Yaw (i_w Drive)

Figure 11

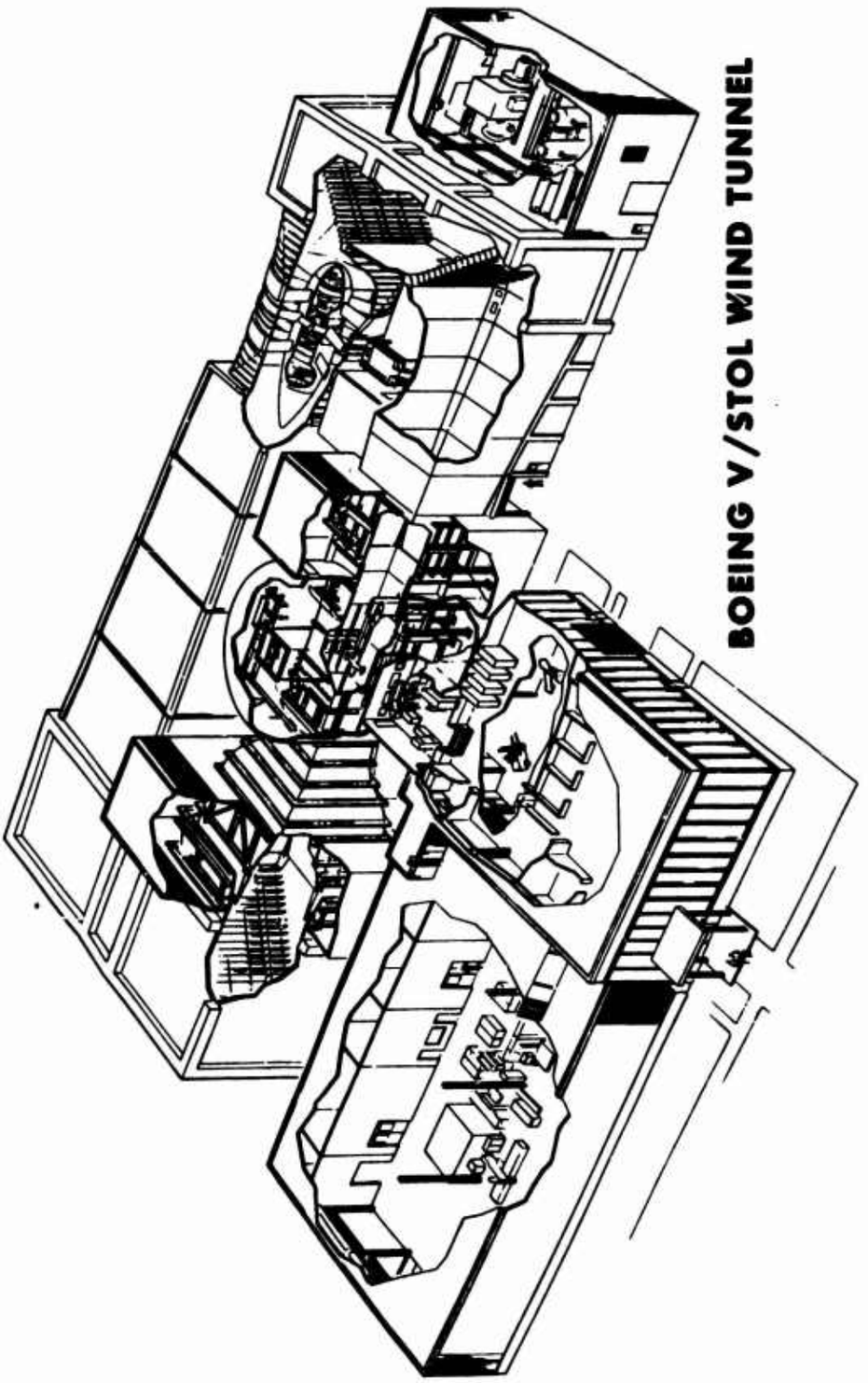

3.0 INSTRUMENTATION AND EQUIPMENT

3.1 MODEL INSTRUMENTATION

Model instrumentation consisted of the following:-

a) Four component strain gauge balance

This was located at the wing root as shown in Figures 9 and 10 and was mounted with its axis parallel to the wing chord. The balance itself, turned with the wing. Components measured by this balance were: normal force, axial force, pitching moment and rolling moment.

b) Thrust/torque flexures in each nacelle

In addition to measuring steady thrust and torque values, the normal force from each nacelle was displayed on an oscilloscope so that dynamic loads in the flexures could be monitored.

c) Tachometer on each nacelle motor

The propeller RPM was measured by a tachometer, installed at the rear of the motor, that worked on the pulse generator principle (ten pulses per cycle).

d) Wing tilt angle potentiometer

The wing tilt angle (same as yaw table angle) was calibrated and measured using a potentiometer.

e) Thermocouple in main air duct

The duct air temperature was required for the purpose of calculating slot jet velocity and blowing coefficient.

f) Mass flow nozzle in main duct

Another quantity needed for the purpose of blowing coefficient calculations was the mass flow rate of blowing air. This was measured via an ASME nozzle located in the main air duct.

g) Pressure tap in each of three wing air ducts

The main air duct was subdivided into three wing air ducts supplying air to the three BLC slots shown in Figure 2. Static pressure in each of these ducts was sensed by a static pressure tap.

h) A supply control valve in each of the three wing air ducts

The pressure in each of the three wing air ducts was controlled by a valve which could be closed to completely shut-off the air flow to a given wing section.

3.2 DATA ACQUISTION SYSTEM

The flow diagram of the wind tunnel data system used in this test is shown in Figure 12. This data system can accept up to 120 channels from a model and the tunnel itself. These signals are routed as illustrated to an IBM 1800 computer for processing and data reduction. The computed results are tabulated by a line printer and selected quantities are plotted by the X-Y plotters. Final data is stored on magnetic tape.

A digital display of any nine channels is also available during testing for monitoring purposes. Dynamic data of six quantities can be continuously displayed on oscilloscopes. This provides assistance in preventing balance or structural limits from being exceeded.

A choice of sampling rates of 2, 4, 10, 20, 40, 100 and 200 samples per channel/sec. is available. The sampling process is accomplished with channel switching devices called multiplexers (MPX).

3.3 TEST EQUIPMENT

Auxiliary Air Supply

Auxiliary air for the BLC test was supplied by a 20 pound per second, 1000 pounds per square inch compressor system.

Auxiliary Power Supply

The power to drive the two electric propeller motors was supplied by a 375 KVA, variable frequency power system. This power supply was controlled from the main tunnel control console.

Figure 12

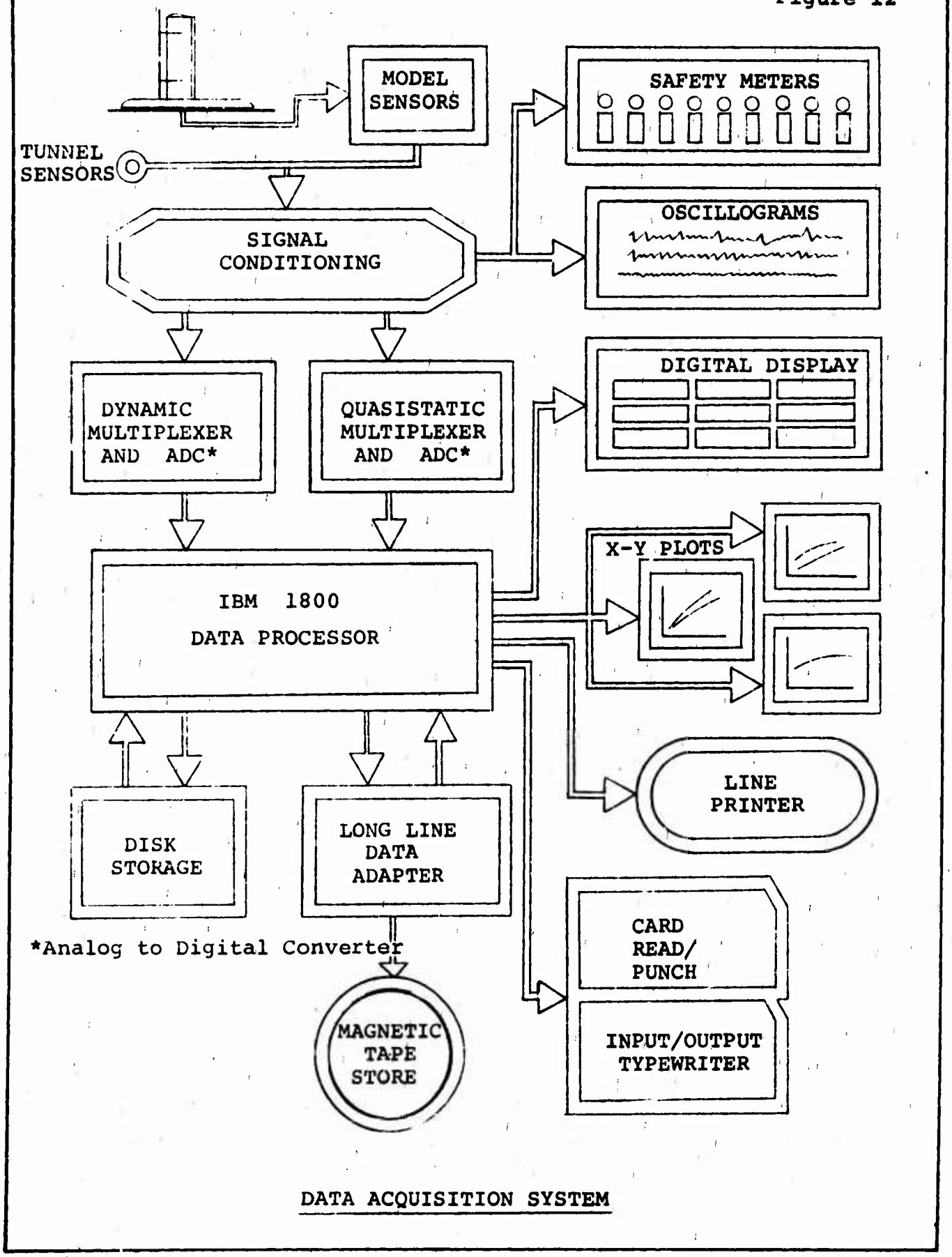

DATA ACQUISITION SYSTEM

FORM 11180 (8/67)

4.0 DATA REDUCTION

At each test point the following quantities were computed and printed out. All values noted were printed out on-line.

Freestream dynamic pressure, q	lbs/ft^2
Power (for each propeller), P	ft.lbs/sec.
RPM (of each propeller)	
Thrust (for each propeller plus total), T	lbs.
Torque (for each propeller), Q	ft.lbs.
Tunnel velocity, V	ft/sec.
Wing tilt angle, i_w	deg.
Chord force	lb.
Normal force	lb.
Pitching moment (about wing hinge), M	ft.lbs.
Rolling moment	ft.lbs.

The last four quantities, from the wing root balance, were resolved into the wing axis system in order to compute

Lift, L	lbs.
Longitudinal force (positive forward), X	lbs.

Force and moment coefficients in the slipstream notation were calculated as follows

Lift coefficient, $C_{L_s} = \frac{L}{q_s S}$

Longitudinal force coefficient, $C_{X_s} = \frac{X}{q_s S}$

Pitching moment coefficient, $C_{M_s} = \frac{M}{q_s S}$

Slipstream dynamic pressure (of each propeller, also average), $q_s = q + \frac{T}{A_p}$

Thrust coefficient (of each propeller, also average), $C_{T_s} = \frac{T}{q_s A_p}$

Lift and longitudinal force were also transcribed into coefficients of $\frac{L}{qb^2}$ and $\frac{D}{qb^2}$ (positive aft for drag).

The following propeller coefficients were computed.

Thrust coefficient (for each propeller, also average), $C_T = \frac{T}{\rho n^2 D^4}$

Power coefficient (for each propeller, also average),

$$C_P = \frac{P}{\rho n^3 D^5}$$

where ρ = density S.L./STD slug/ft^3
n = propeller speed rps

Advance ratio, $J = \frac{V}{nD}$

Each of the following blowing parameters were determined for the three wing air ducts separately.

Duct pressure, P_D lb/in^2

Duct pressure ratio, $\frac{P_D}{P_O}$

where P_O = test section static pressure

Jet velocity, V_J ft/sec

$$V_J = 109.6\sqrt{t_D+459.7}\cdot\sqrt{1-(P_O/P_D)^{2/7}}$$

where t_D= main air duct temperature, deg. F

An ASME nozzle was used to calculate

Mass flow rate, $\dot{\omega}$ lb/sec.
and thereby the

Blowing coefficient, $C_{\mu_s} = \frac{\dot{\omega} V_J}{32.2 q_s S_E}$

where S_E = slot span, ℓ, times wing chord, c ft^2

Full scale aircraft parameters of rate of descent in ft/min and velocity in knots were also computed for each test point.

$$R/D = 60\left(\frac{D}{qb^2}\right)\cdot\sqrt{\frac{2W}{\rho b^2}}\cdot\sqrt{\frac{1}{\left[\left(\frac{L}{qb^2}\right)^2+\left(\frac{D}{qb^2}\right)^2\right]^{3/2}}}$$

$$V = .592\sqrt{\left(\frac{2W}{\rho b^2}\right)\cdot\left(\frac{qb^2}{L}\right)}$$ S.L./STD conditions this report

Propeller induced velocity, w, in ft/sec was calculated at each test point from the following equation.

$$w^4 + w^3\ 2V\cos i_w + w^2\ V^2 = \left(\frac{T}{2\rho A_p}\right)^2$$

The above parameter was used to determine the effective wing angle of attack, $\alpha_{W_{EFF}}$. at buffet onset. This angle is defined as the angle between the wing chord and the resultant velocity at the

wing. The resultant velocity was obtained by adding vectorially, the tunnel velocity and the induced velocity at the leading edge of the wing. Full contraction of the propeller wake was assumed at the wing leading edge.

The three wind tunnel X-Y plotters were used to produce on-line plots of the

Force polars in terms of $\frac{L}{qb^2}$ vs $\frac{D}{qb^2}$

Lift curves in terms of $\frac{L}{qb^2}$ vs i_w

Pitching moment curves in terms of C_{m_s} vs i_w

Aircraft rate of descent was calculated from buffet onset angles presented as curves of

Wing tilt angle at buffet onset vs C_{T_s}

Effective wing angle of attack at buffet onset vs C_{T_s}

The method used to determine "buffet onset" is described on Page 45.

5.0 TEST PROCEDURE AND TEST CONDITIONS

5.1 TEST PROCEDURE

The wing root balance and nacelle strain gauge balances were calibrated statically by applying known forces and moments. Resultant calibration data was incorporated into the computer program.

With no wind in the tunnel, the blowing slots were calibrated as follows: starting with slot span A→B (Refer to Figure 2) and with all slots on the remainder of the wing sealed off, increasingly larger pressure ratios were applied in the duct leading to the slot. For each value of pressure ratio, the momentum force per unit slot span, $\frac{\dot{w}V_j}{g}$, was calculated. Thus a relation between applied pressure ratio and blowing coefficient, C_{μ_s}, was established for a mean value of slipstream dynamic pressure, q_s. The same procedure was followed for all the slot spans to be blown, including full span blowing. Figure 13 presents the results of the calibration.

Available power from the electric motors driving the propellers limited the slipstream q to approximately 12 psf at buffet onset when the collective hub propellers were used. This limitation necessitated utilizing a minimum slot gap (a .005" slot gap was the smallest gap that could be accurately set) so that reasonable C_{μ_s} values of the numerical order of 0.10 could be achieved with a choked slot nozzle. A choked nozzle condition was desired for maintaining a good spanwise distribution of flow from the nozzle.

Thrust balancing preceded every change of propeller hub or propeller rotation. This was achieved by adjusting the collective blade angle of each propeller manually until the thrusts were within 1.5 lb. maximum from each other at representative wing tilt angles and at all the tunnel dynamic pressures for which data was to be acquired.

All test runs or i_w sweeps were performed with a constant propeller RPM (5500 RPM with collective hubs and 4500 RPM with cyclic hubs), constant blade pitch (approximately 12° at 0.75 blade radius) and constant tunnel q. Previous testing on the same propeller/hub/motor nacelle packages plus known characteristics of the electric motor and propeller/hubs established the combination of propeller RPM and collective pitch that would achieve a maximum slipstream q.

Every configuration tested (flap setting, propeller rotation, blowing configuration, cyclic angle, etc.) was evaluated over a series of four runs which comprised four specific tunnel q's. Values of tunnel q were chosen so as to achieve an appropriate

spread of C_{T_S}, i.e. .35 to .84 at buffet onset. The maximum value of C_{T_S} was predicated by considerations of electric propeller motor power limitations and the lowest tunnel q that could accurately be achieved.

Each run with leading edge BLC was conducted with a constant duct pressure ratio. When more than one blown segment was being evaluated the wing air duct valves were ground adjusted to equalize the duct pressure ratios. A target C_{μ_S} value was achieved prior to a series of runs by varying the duct pressure with the air supply control installed in the control console. This was accomplished with the tunnel and propeller running and the wing set near buffet onset. Slipstream q at buffet onset for each tunnel q of a run series is essentially constant for the procedure used in conducting the test, i.e. constant RPM and collective pitch. Consequently, the C_{μ_S} at buffet onset was also essentially constant over the run series. The three duct pressure ratios and the blowing coefficient were presented on the overhead digital display board for monitoring and control purposes.

From results obtained from a test conducted on an isolated propeller identical to the type used during the BLC test, it was found that when cyclic was employed, there was about 15° of phase lag before the peak value of moment was attained, i.e., instead of maximum moment being applied at 0° and 180°, it was applied at 15° and 195°. This was due to non-rigidities in the propeller/hub system. During this test, cyclic pitch was introduced with 15° of phase lead.

A Polaroid photograph of the tufted side of the wing was taken at each data point along with tuft comments by an observer. In addition to the normal tufts attached to a wing, vertical "tuft stalks" were installed on the wing center section fairing (aft of the tilting portion of the wing), flap surface, and at the wing trailing edge.

5.2 TEST CONDITIONS

Figures 14 through 16 and Figures 17 through 19 depict typical ranges of propeller thrust, slipstream thrust coefficient, and slipstream q attained on collective hub and cyclic hub runs, respectively. As stated previously, test runs with cyclic hubs were performed at 4500 RPM compared to 5500 RPM with collective hubs. The net result was a lower total propeller thrust and thus lower tunnel q's for attaining the spread in C_{T_S} achieved during a run series with collective hubs.

The tabulation on the following page summarizes the data runs performed during the subject test (BVWT 055) in terms of key configuration parameters.

BVWT 055
RUN SUMMARY

RUNS	PROP ROTATION	FLAP	δ_F	BLOWN REGION	C_{μ_s}	HUBS	CYCLIC ANGLE	REMARKS
8-11	$P^{1,2}$	Double	60°	None	—	Coll.	—	
14-17		Slotted		A→B	.10			
19-22				A→C	.10			
23-26				A→C	.07			
27-31				A→C	.04			
32-35				A→C&B	.11			
36-39				A→C&G	.07			
40-43				A→C&G	.05			
44-47				A→G	.21			
48-51				A→G	.12			
52-55				A→G	.06			
58-61				A→G	.14			
65-68	$P^{1,1}$			A→G	.09			
69-72	$P^{1,2}$			A→G	.09			
82-85				A→G	.11	Cyclic	0°	
87-90				A→G	.11		+4°	15° Lead on Cyclic
93-96				A→C&G	.11		+4°	
97-100				A→C&G	.12		+4°	45° Lead on Cyclic
102-105				A→C&G	.11		0°	
106-109				A→C&G	.11		+6°	15° Lead on Cyclic for Rest of Cyclic Runs
110-113				A→G	.12		+6°	
114-117				A→G	.12		-4°	
119-122	$P^{1,1}$			A→G	.11		0°	
123-126				A→G	.11		+4°	
127-130				A→G	.12		+6°	
132-135	$P^{1,2}$			A→G	.11		+4°	LE. Slats off
136-139				A→G	.11		+4°	(3) Outboard
140-143		Single	45°	A→G	.11		+4°	Fences off
144-147		Slotted	30°	A→G	.11		+4°	
148-151			45°	A→G	.11		0°	
152-155				None	---		0°	
156				None	---		0°	Wing Root "Added Sealing" Removed

FORM 46284 (2/66)

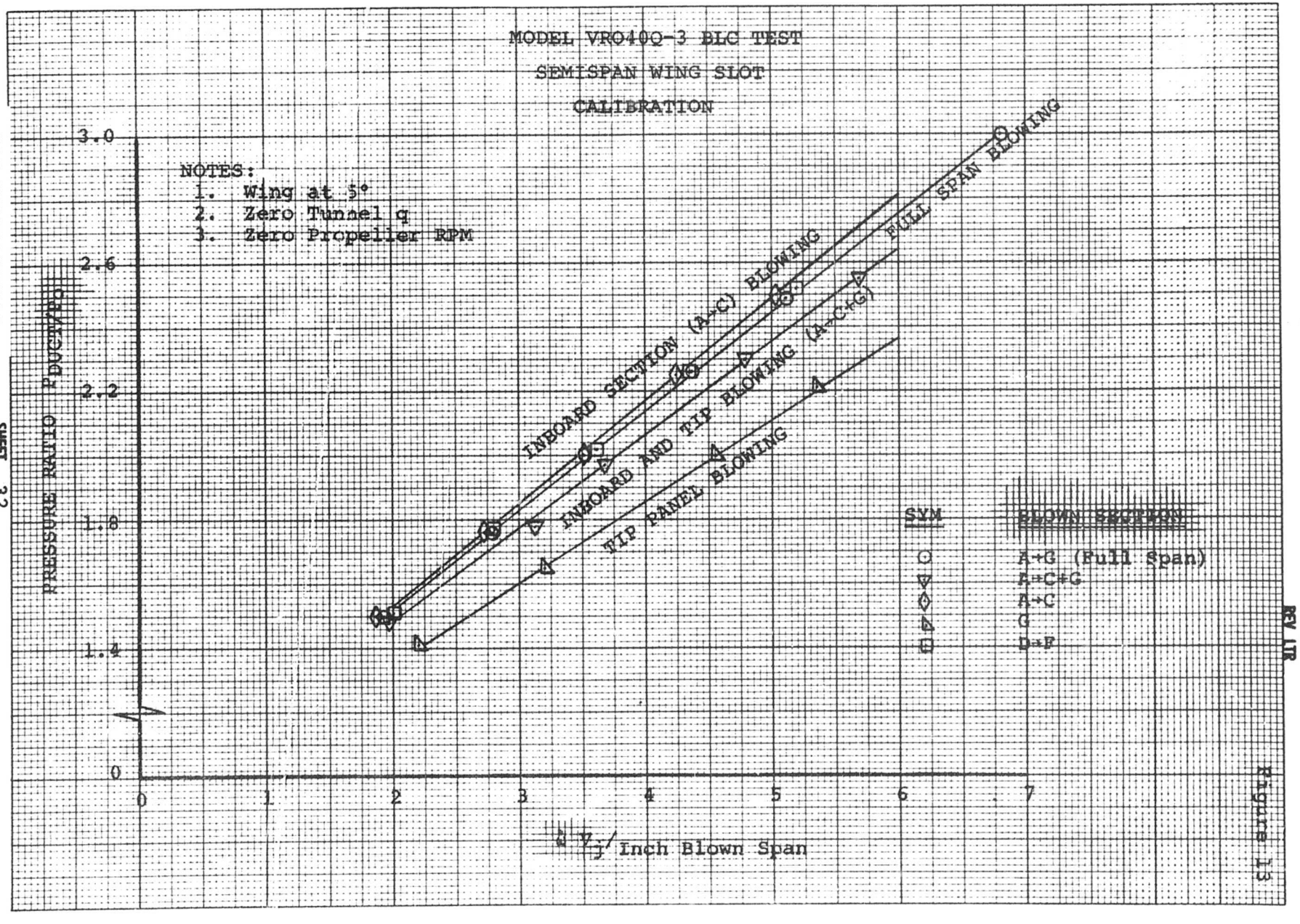

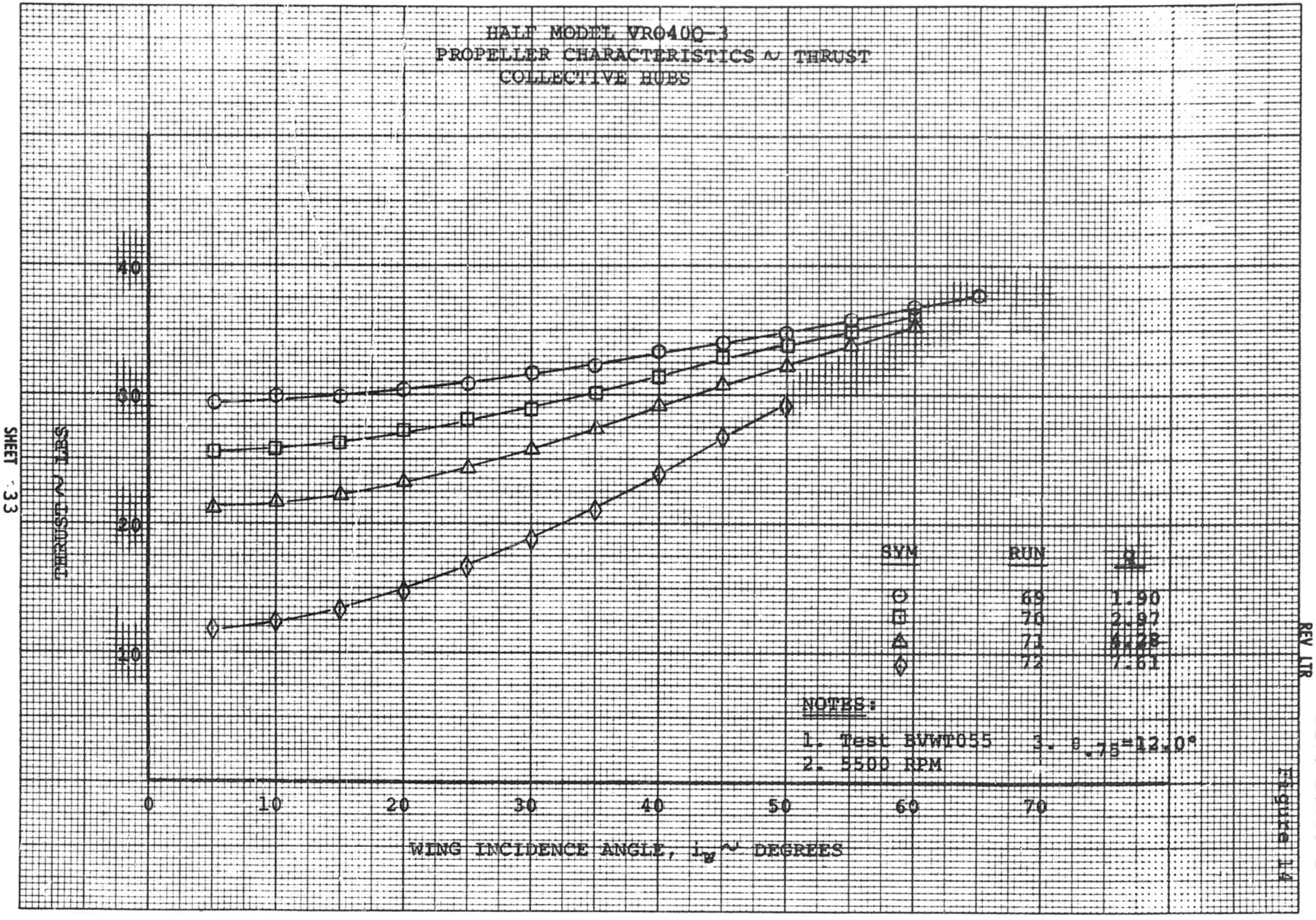

SHEET 33

NUMBER D170-10036-1
REV LTR

Figure 14

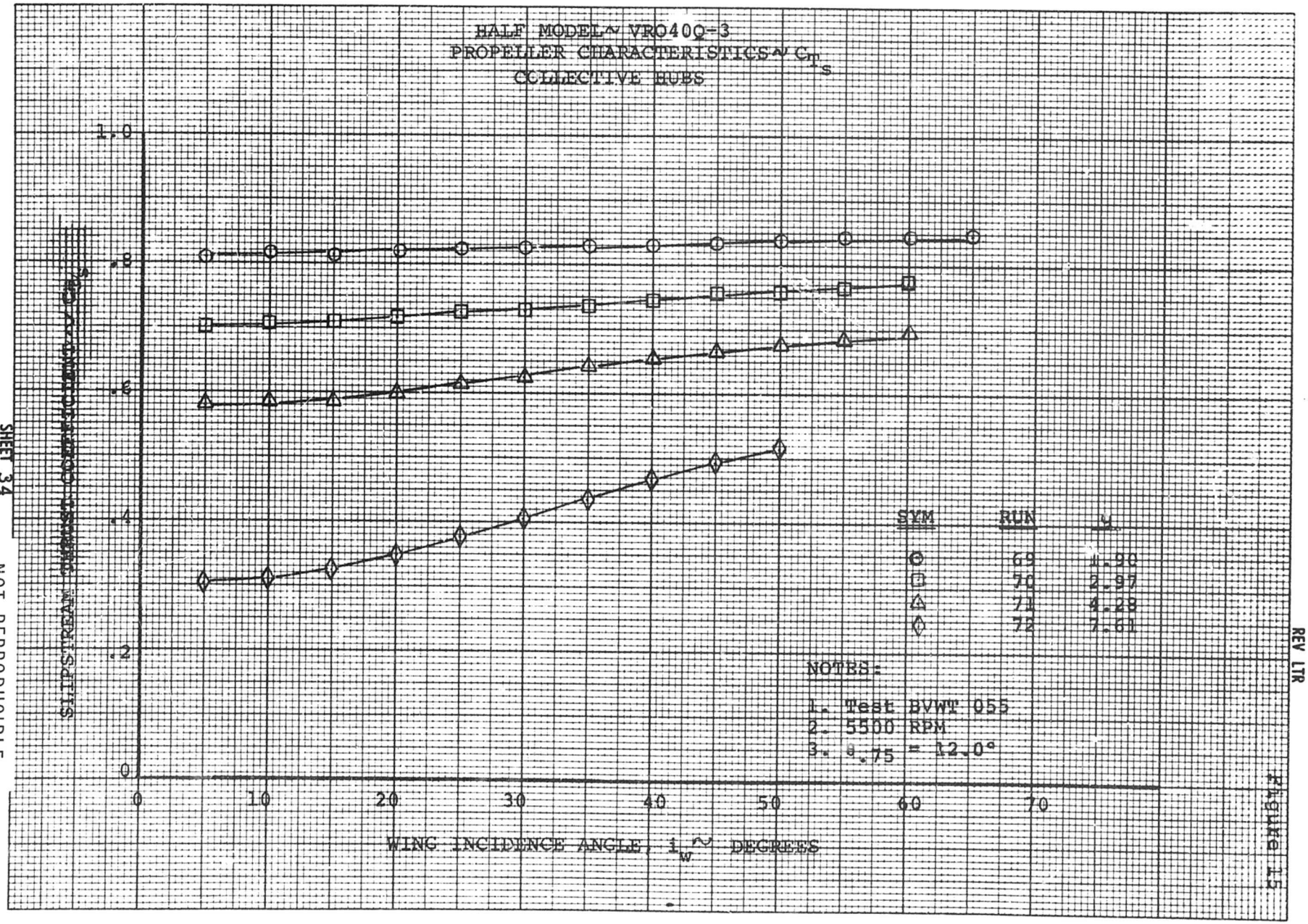

Figure 15

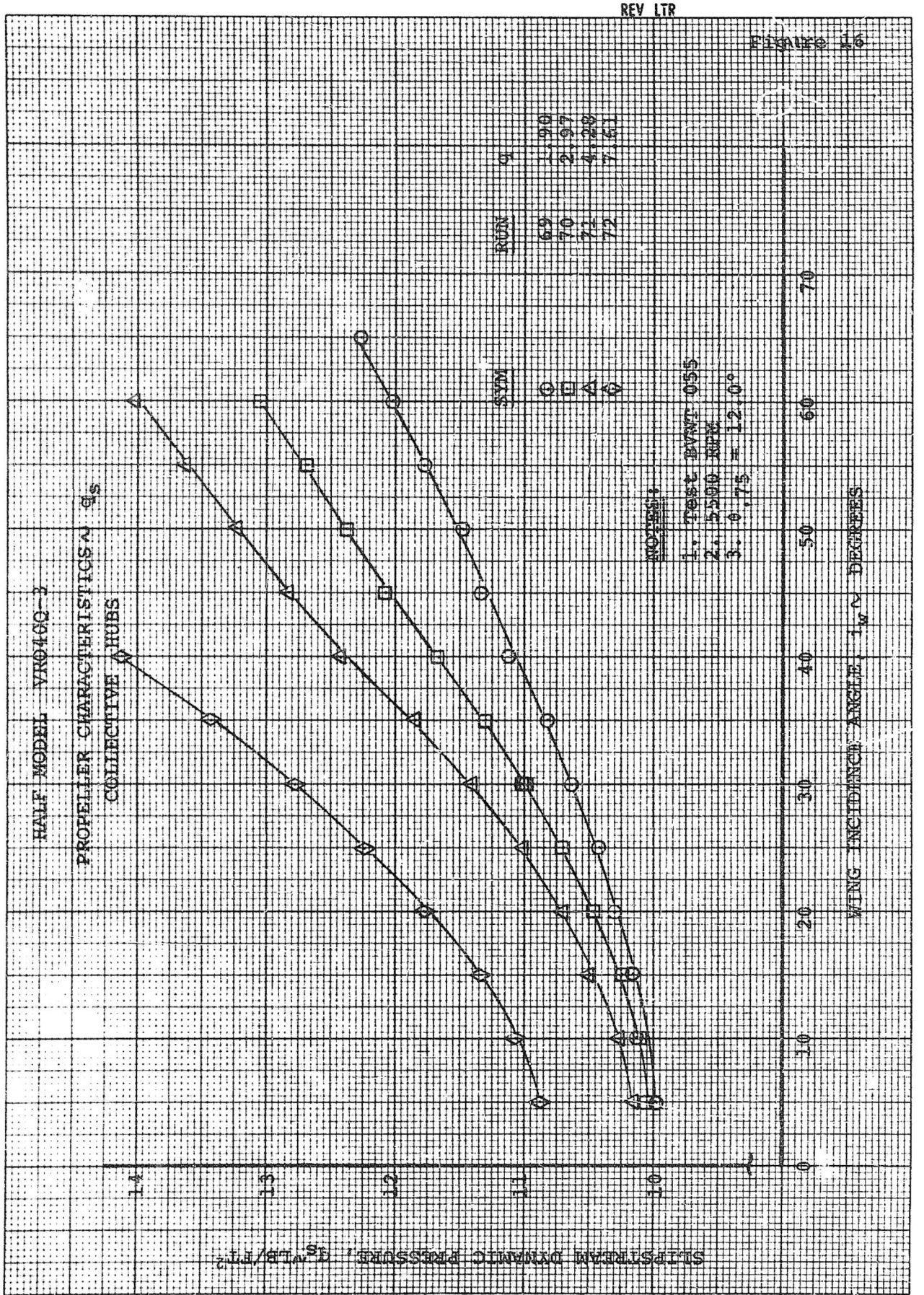

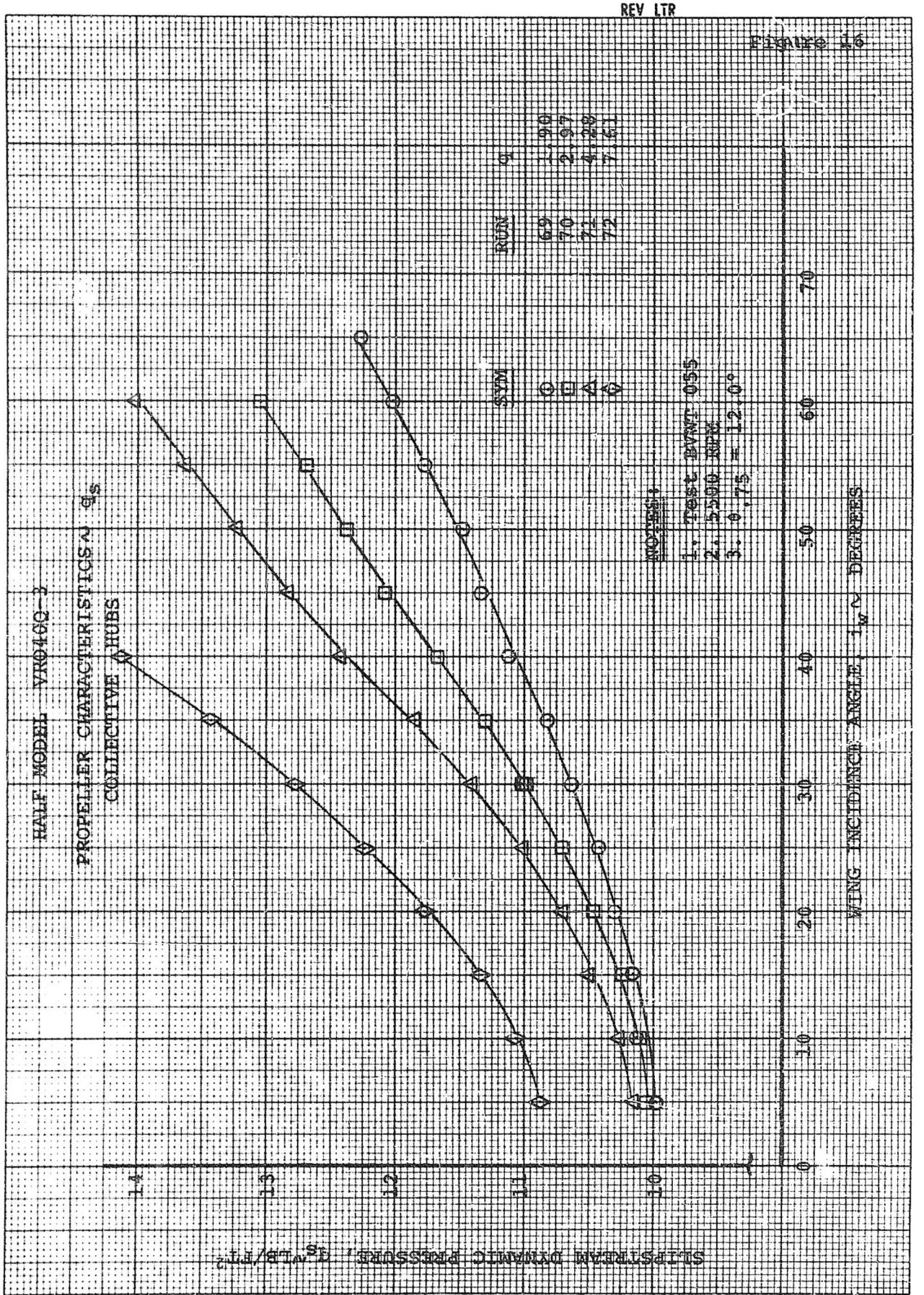

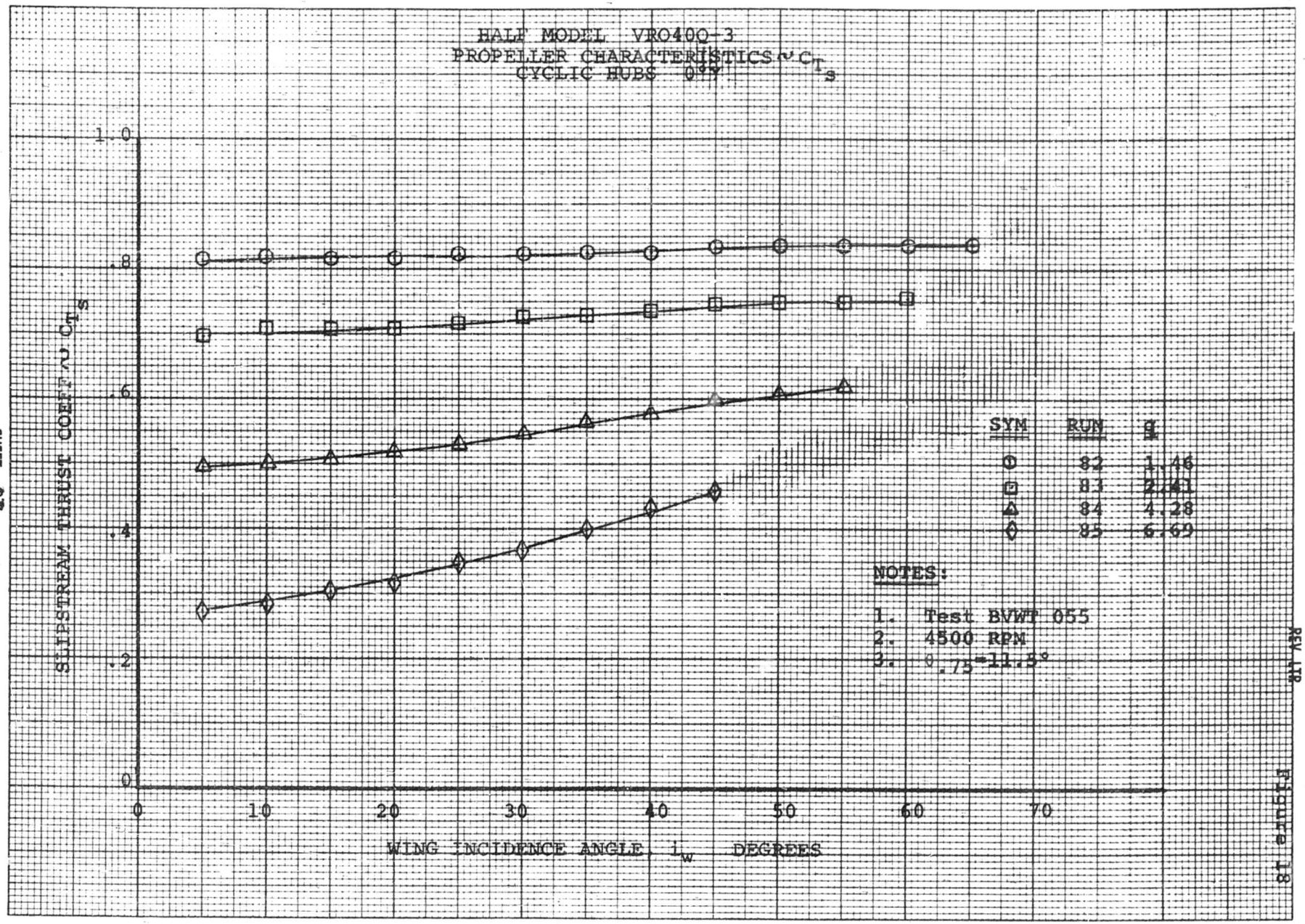

SHEET 37

NUMBER D170-10036-1
REV LTR
Figure 18

Figure 19

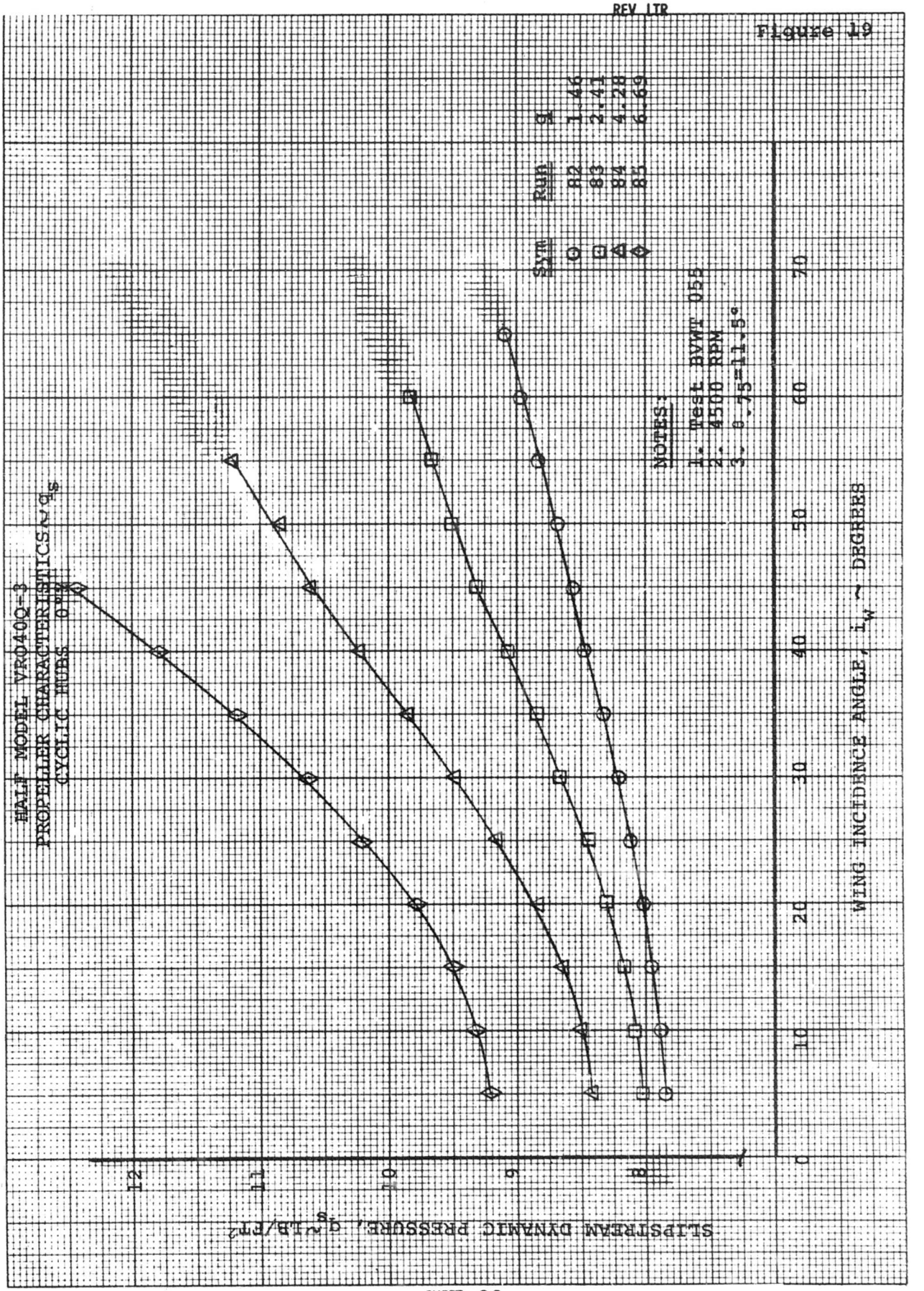

6.0 TEST RESULTS AND DISCUSSION

The primary objective of this test was to investigate the feasibility of improving the descent performance of a four prop tilt wing aircraft when cyclic pitch was employed, through leading edge BLC. Values of blowing coefficient ranging from .04 to .21 were used and selected sections of the span as well as the entire wing span including the wing center section over the fuselage were blown.

The majority of the test was conducted with a blowing coefficient, C_{μ_s}, of approximately .11. This rather large blowing magnitude resulted from a combination of three items: utilization of the smallest slot gap that could be accurately set across the wing span (approximately .005"), the relatively low q_s (summation of tunnel q and propeller disk loading) available in the model tilt wing landing descent regime, and the desire to maintain a choked slot nozzle (P_D/P_O=1.89) for a good spanwise distribution of jet efflux. Since this test was a feasibility test and was not primarily directed towards the problem of minimizing blowing power requirements, the test objectives were not compromised.

The descent capability for each configuration was obtained by determining the wing incidence angle at which initial stall or separation occurred on the wing outboard of the inboard wing fences, i.e. outboard of the "B" region shown in Figure 2. Inboard areas where stall was tolerated comprise the center section over the fuselage, the area behind the gap between the propeller tip and fuselage, and the area behind the propeller tip -- in summary, sections over which the low freestream q or less than full slipstream q prevail and where roll disturbances are minimal. It is to be noted that at the higher forward flight speeds tested with $P^{1,2}$ prop rotation, the "B" region separates later than the portion of the wing proper that initially stalls.

In choosing the buffet onset angle, tuft photographs and observer comments were studied in conjunction with the corresponding force polars. Analysis of previous tilt wing tests indicated that buffet onset angle choice was aided when the force polars were presented in terms of $\frac{L}{qb^2}$ vs $\frac{D}{qb^2}$ rather than C_{L_s} vs C_{X_s}. A "marked break" occurred in the curves at buffet onset for the lower C_{T_s} values tested.

A special effort was made in analyzing the data for consistency in the choice of buffet onset angle.

6.1 COMPARISON BETWEEN BLOWN AND NON-BLOWN WING LEADING EDGE

Figures 20 through 23 present the comparison between the non-blown wing and the wing with full span L.E. blowing ($C_{\mu_S} \approx .1$) for two flap configurations -- double slotted flaps at 60° and single slotted flaps at 45°. Prop rotation $P^{1,2}$ was used. The rate of descent capability obtained with no blowing and 60° double slotted flaps (Figure 20) compares favorably with previous test data acquired on tilt wing models with similar slat/wing/flap geometry.

With double slotted flaps, the noted blowing configuration improves the descent capability by an average of 400 fpm. The corresponding increase in effective wing stall angle was approximately 4°. (See Figure 21).

A similar incremental improvement in effective wing stall angle occurred with the single slotted flaps (Figure 22) and provided the increase in descent capability shown in Figure 23.

As can be noted in Figure 22, the stall angle for no blowing, does not increase at the expected rate with increasing C_{T_S}, above $C_{T_S}=0.6$. The single slotted flap runs were performed with all but the most inboard fence removed (i.e. only the fence next to the fuselage side remained). At the higher values of C_{T_S}, the B region (See Figure 2) is no longer contained and spreads to the adjacent C region, thus, reducing the stall angle.

NUMBER
REV LTR

Figure 20

EFFECT OF L.E. BLOWING ON DESCENT RATE
DOUBLE SLOTTED FLAPS @ 60°

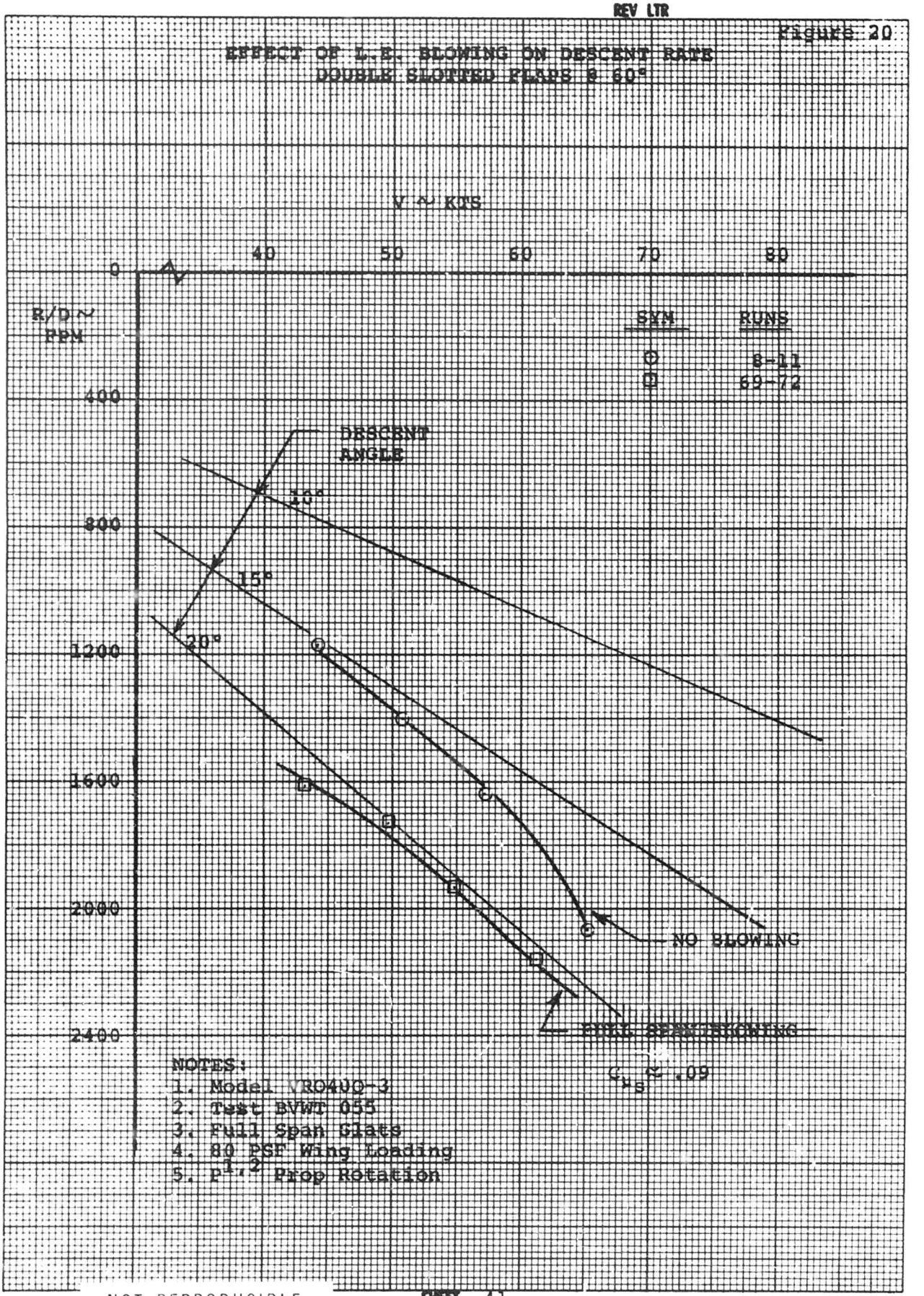

NOTES:
1. Model VR0400-3
2. Test BVWT 055
3. Full Span Slats
4. 80 PSF Wing Loading
5. $P^{1.2}$ Prop Rotation

EUGENE DIETZGEN CO.
MADE IN U. S. A.

NO. 340R-20 DIETZGEN GRAPH PAPER
20 X 20 PER INCH

Figure 21

EFFECT OF L.E. BLOWING ON BUFFET ONSET
DOUBLE SLOTTED FLAPS @ 60°

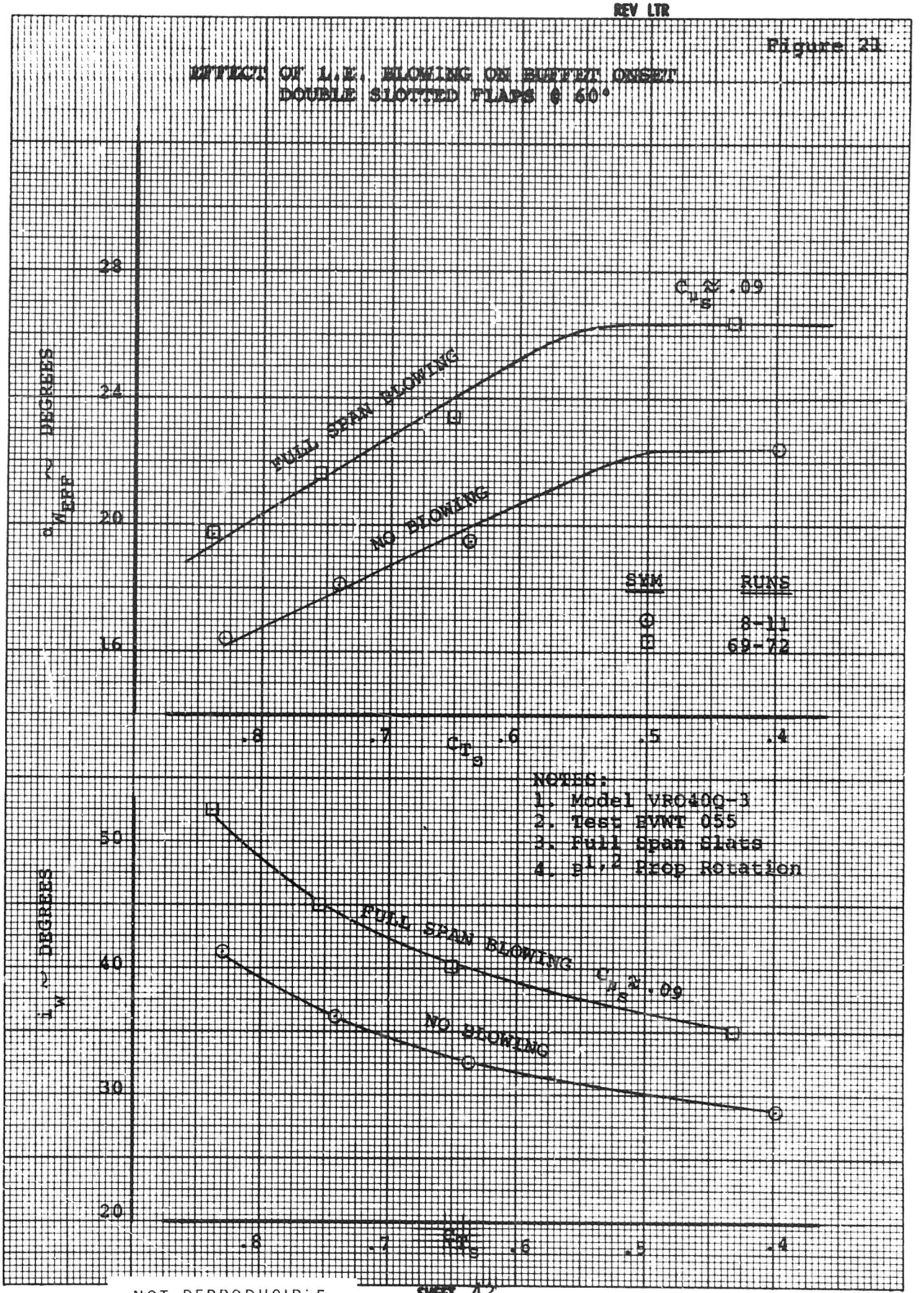

Figure 22

EFFECT OF L.E. BLOWING ON EFFET ONSET

SINGLE SLOTTED FLAPS @45°

NOTES:
1. Model VR0400-3
2. [illegible] $\bar{c}_{VWT}$ 0.55
3. Full Span Slats
4. (3) Outbd.Fences OFF
5. Cyclic Nubs, $\gamma=0°$

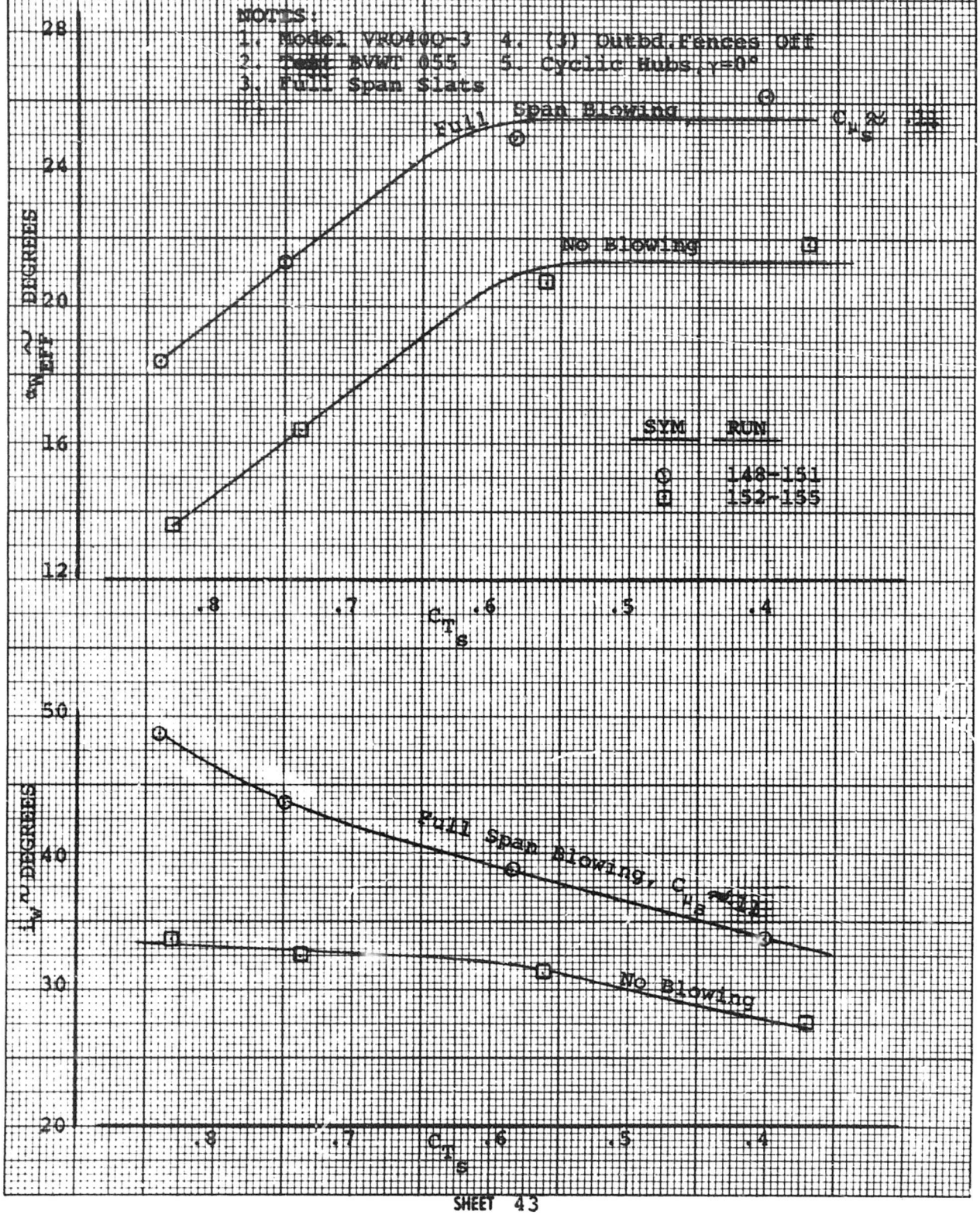

Figure 23

EFFECT OF L.E. BLOWING ON DESCENT RATE

SINGLE SLOTTED FLAPS @ 45°

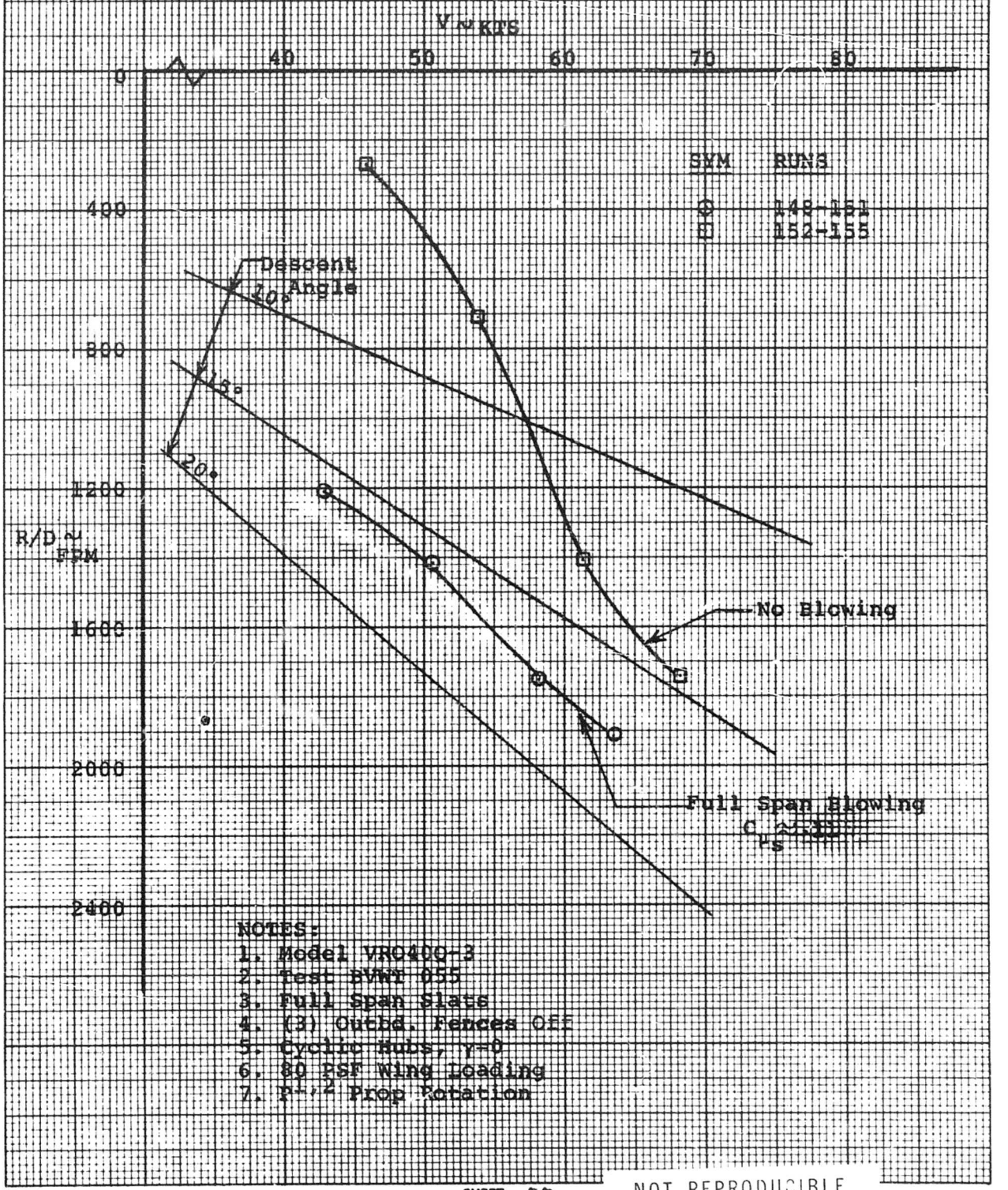

NOTES:
1. Model VRO400-3
2. Test 8VWT 655
3. Full Span Slats
4. (3) Outbd. Fences Off
5. Cyclic Hubs, γ=0
6. 80 PSF Wing Loading
7. $R^{+}/_{2}$ Prop Rotation

6.2 EFFECT OF BLC ON WING CENTER SECTION AND "B" REGION STALL

As stated previously, stall on the wing center section over the fuselage and in the "B" region of the wing (See Figure 2) was considered tolerable for the reasons stated and consequently, did not enter into the choice of buffet onset. On semispan model VR040Q-3, the leading edge slat extended across the wing center section in an attempt to delay stall in this region to the highest possible angle.

Data presented in Figure 24 (double slotted flaps at 60°) and Figure 25 (single slotted flaps at 45°) show that stall with the $P^{1,2}$ prop rotation, no L.E. blowing, occurred on the wing/body center section at 10°→15° of wing tilt angle and in the "B" region at a wing tilt angle which varied from 29° at .8 C_{T_s} to 38° at .4 C_{T_s} with the 60° double slotted flaps and from 24° at .8 C_{T_s} to 33° at .4 C_{T_s} with the 45° single slotted flaps (5° difference with flap configuration). Leading edge blowing (.11 C_{μ_s}) over the wing center section increased the stall angle by a constant delta of 18° over the range of C_{T_s} values tested. The resultant stall angle was thus increased from 10°→15° with no blowing to 28°→33° with blowing. Leading edge blowing over the "B" region increased the stall angle from 11° to 14° at .8 C_{T_s}. The increment decreased at lower C_{T_s} values.

Note that Figure 24 was with A→B region L.E. blowing (.10C_{μ_s}) and that Figure 25 was with full span blowing (.11C_{μ_s}). The incremental improvement in stall angle was essentially the same for both blowing configurations.

Of special concern when tufts are utilized to interpret the occurrence of stall is whether the tufts are recording only the flow activity on the surface of the wing and not the character of the flow a small distance above the surface. To resolve this factor, an inverted "V" shaped tuft stalk was mounted on the movable wing/body fairing aft of the tilting wing center section. Observations established that separated flow did not exist above the surface when the surface flow was attached, and that stall on and above the surface occurred essentially simultaneously.

Figure 24

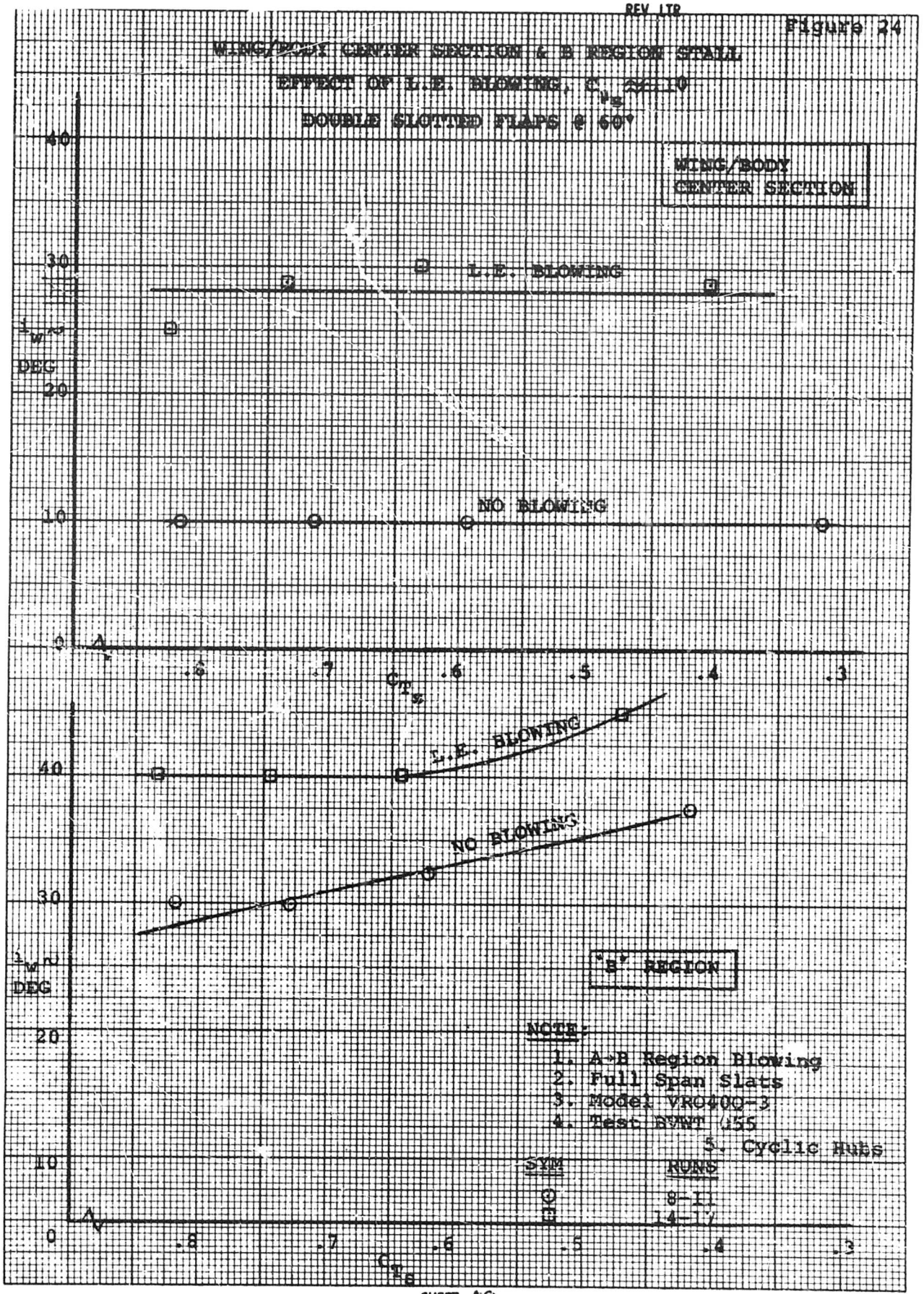

Figure 25

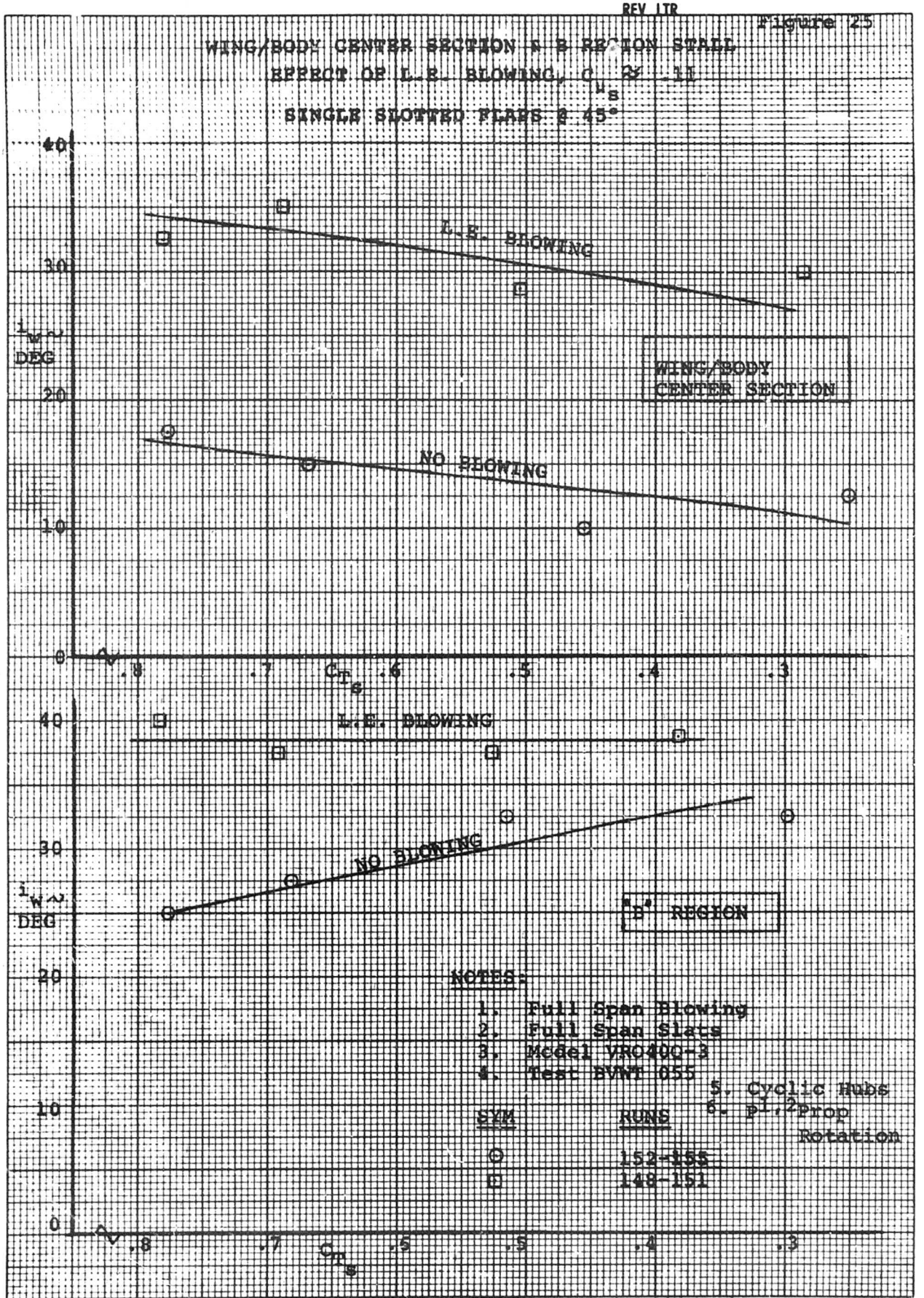

6.3 EFFECT OF CYCLIC WITH BLC, $P^{1,2}$ PROP ROTATION

The effect of cyclic pitch on descent capability was evaluated with both full span L.E. blowing and partial span L.E. blowing (panel inboard of inboard nacelle plus tip panel, A→C&G regions) for the $P^{1,2}$ prop rotation ("both-down-between-nacelles"). This comparison was made at a blowing coefficient, C_{μ_s}, of .12, the lowest value that could be attained with a choked blowing slot.

As has been the case in previous tests positive cyclic (nose down moment) has a detrimental effect on the descent performance. This is also the case with full span leading edge BLC, wherein positive cyclic reduces the descent capability in the order of 100 fpm per degree up to 6° of cyclic over the speed range tested. See Figure 26. However, a comparison of the +4°γ descent curve with the 0°γ no blowing curve, reveals that below 60 knots the loss in descent performance due to positive cyclic is equalized by the gain due to blowing.

Figure 27 presents the corresponding buffet onset angles for full span L.E. blowing. A positive cyclic angle of 4° reduced the effective wing stall angle from 1.5° to 2° over the C_{T_s} range evaluated. Increasing the cyclic angle to +6°, further reduced the effective stall angle by a maximum of 0.8°.

Negative cyclic does not result in a gain in effective wing stall angle (Figure 27), in spite of the gain in rate of descent performance (Figure 26). This indicates that negative cyclic provides an improvement in descent capability by improving the turning effectiveness (θ/δ). This also infers that a large part of the loss in descent performance with positive cyclic results from a decrease in turning effectiveness. Figure 28 validates this premise.

The choice of the second blowing configuration to be evaluated with cyclic and the $P^{1,2}$ prop rotation was predicated upon the spanwise location of initial stall. In the initial phase of this test, it was established that the most critical area for stall with $P^{1,2}$ rotation was inboard of the inboard nacelle, with the tip panel being the second most critical area. In addition, positive cyclic with $P^{1,2}$ rotation retained initial stall in the inboard region. As a consequence, partial span L.E. blowing which excluded blowing the area between nacelles was investigated as a second choice.

Figure 29 shows that with the partial span blowing configuration of inboard plus tip panels, the rate of descent capability is approximately 100 fpm less than with full span blowing for 0° of cyclic pitch. Except for the premature stall at 70 knots with 6° of positive cyclic (this occurred at the fence dividing the unblown wing section between the nacelles and the inboard blown area), positive cyclic reduced the rate of descent capability

approximately 90 fpm per degree of cyclic -- slightly less than the magnitude obtained with full span blowing.

The data presented in Figure 30 shows approximately the same decrease in effective wing stall angle for 4° of positive cyclic as obtained with full span blowing. Except for the premature stall point, a further increase in cyclic to +6° did not result in a further measurable reduction in stall angle.

Figure 26

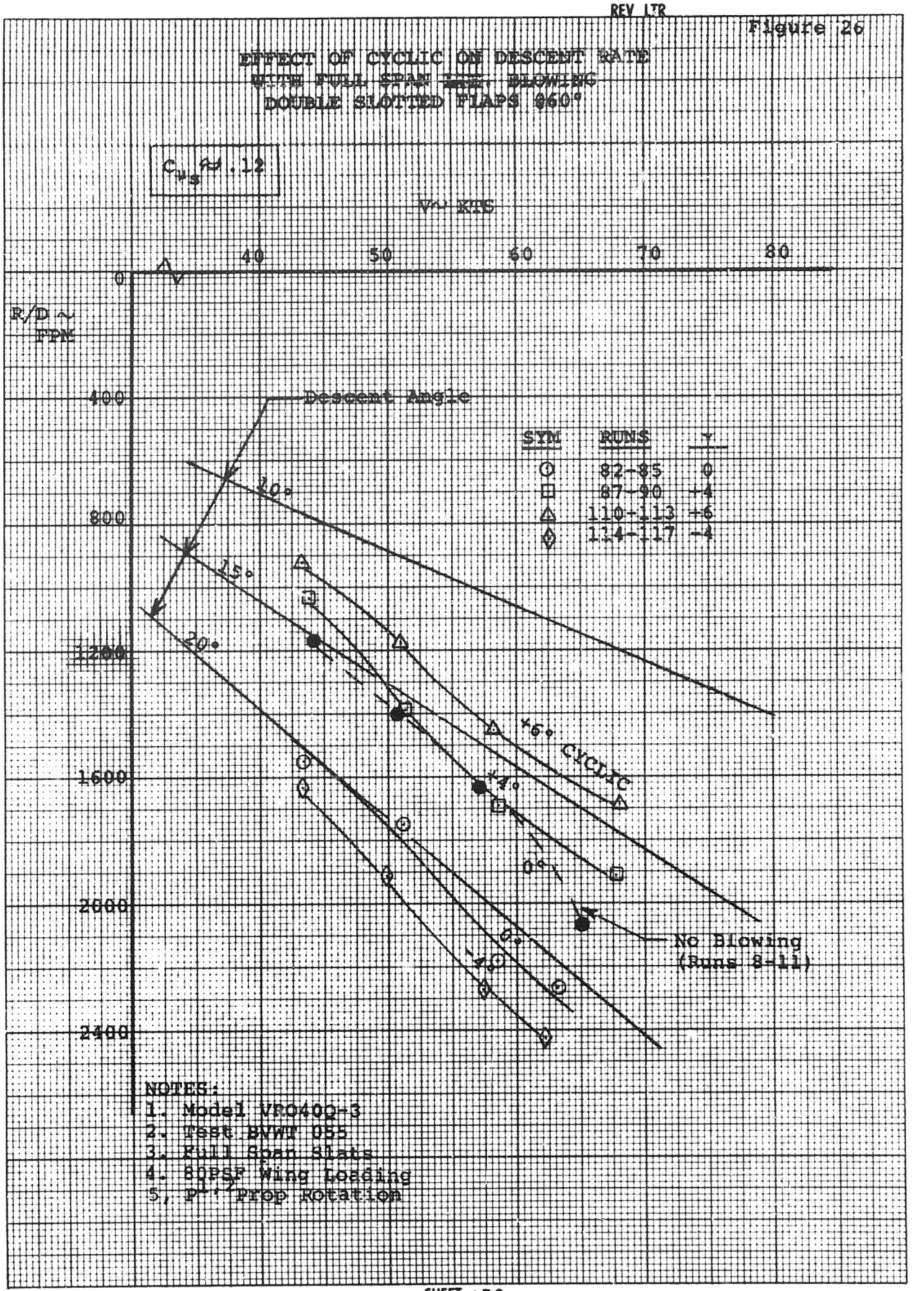

Figure 27

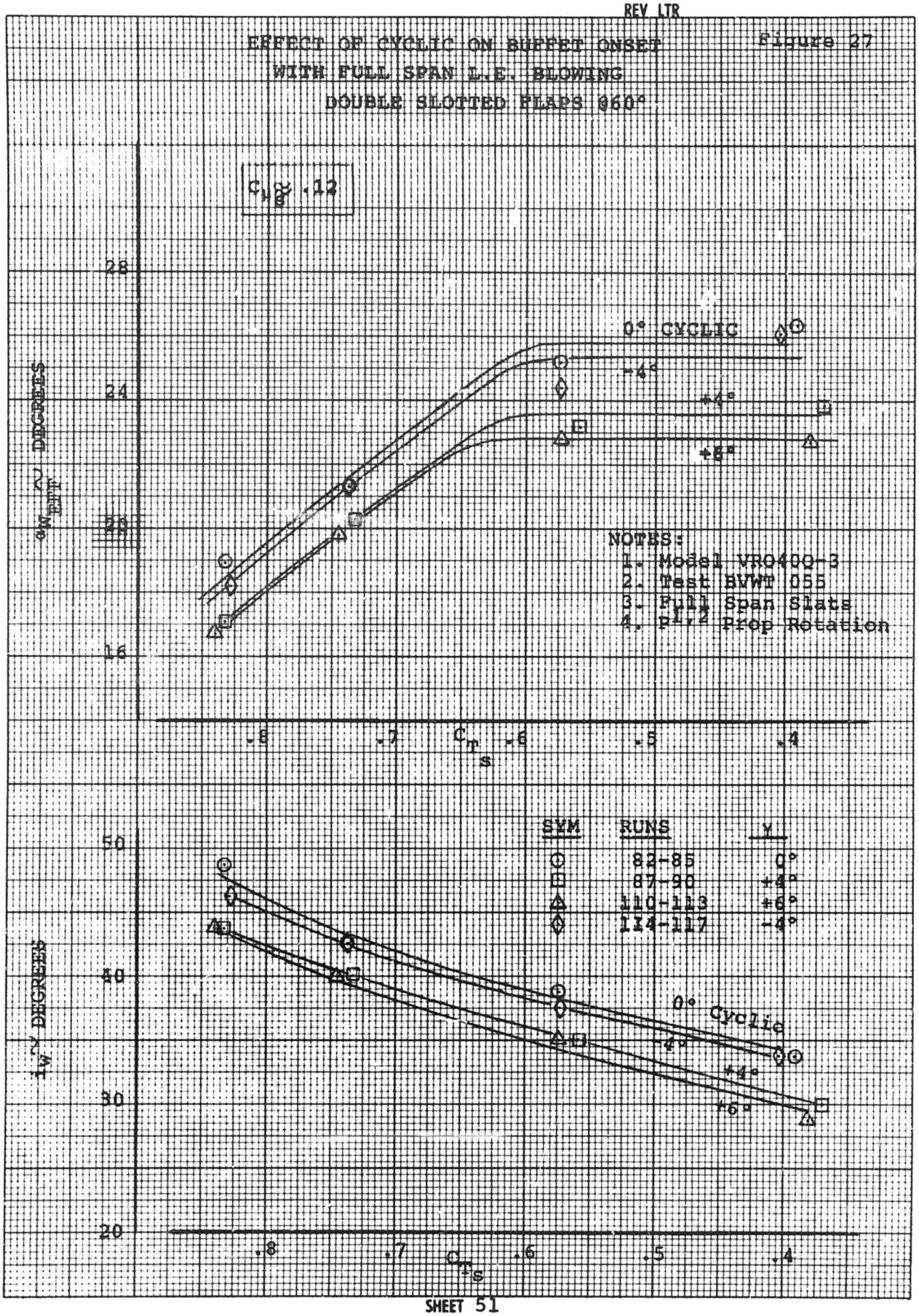

Figure 28

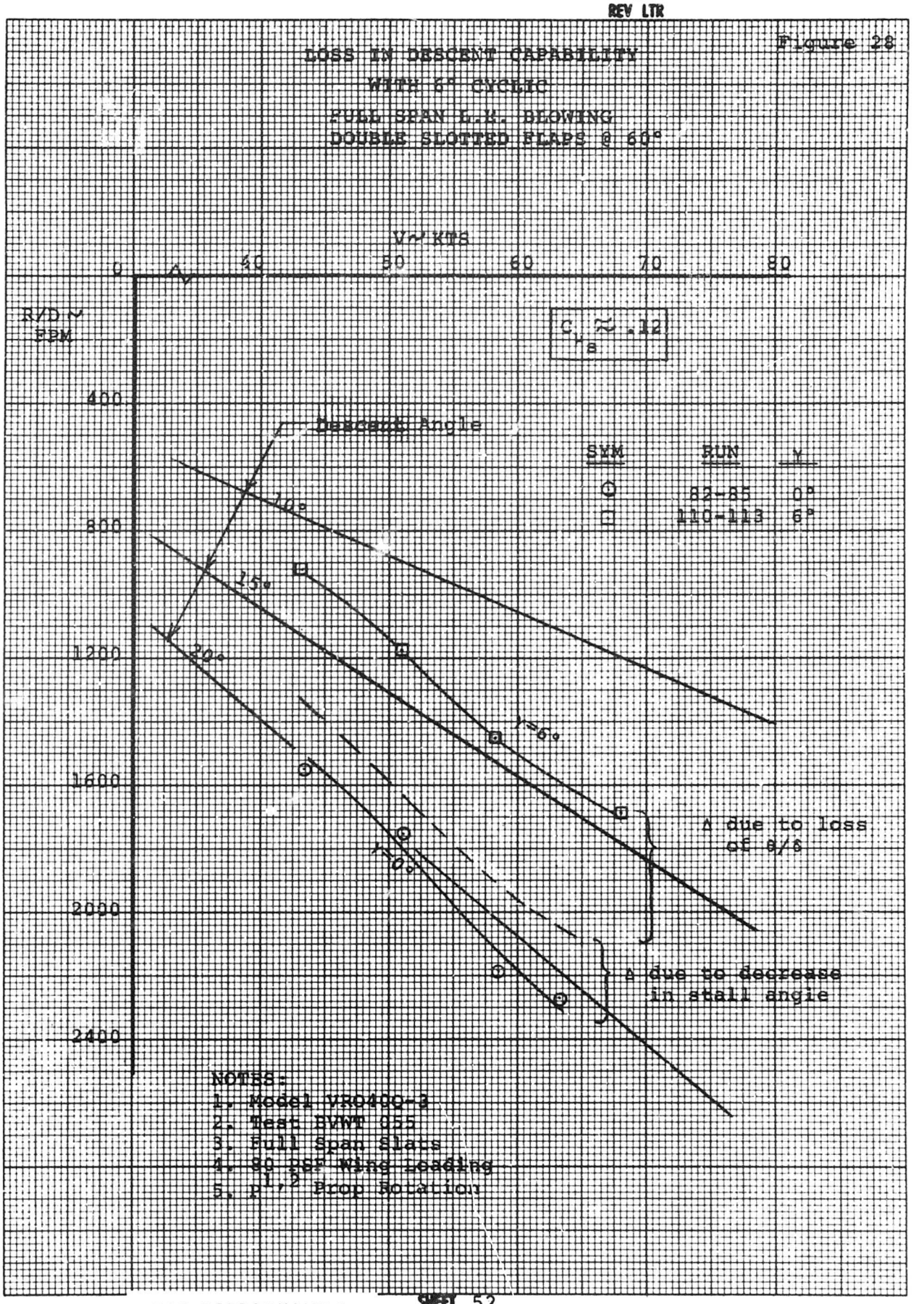

Figure 29

EFFECT OF CYCLIC ON DESCENT RATE
WITH PARTIAL SPAN L.E. BLOWING
DOUBLE SLOTTED FLAPS @ 60°

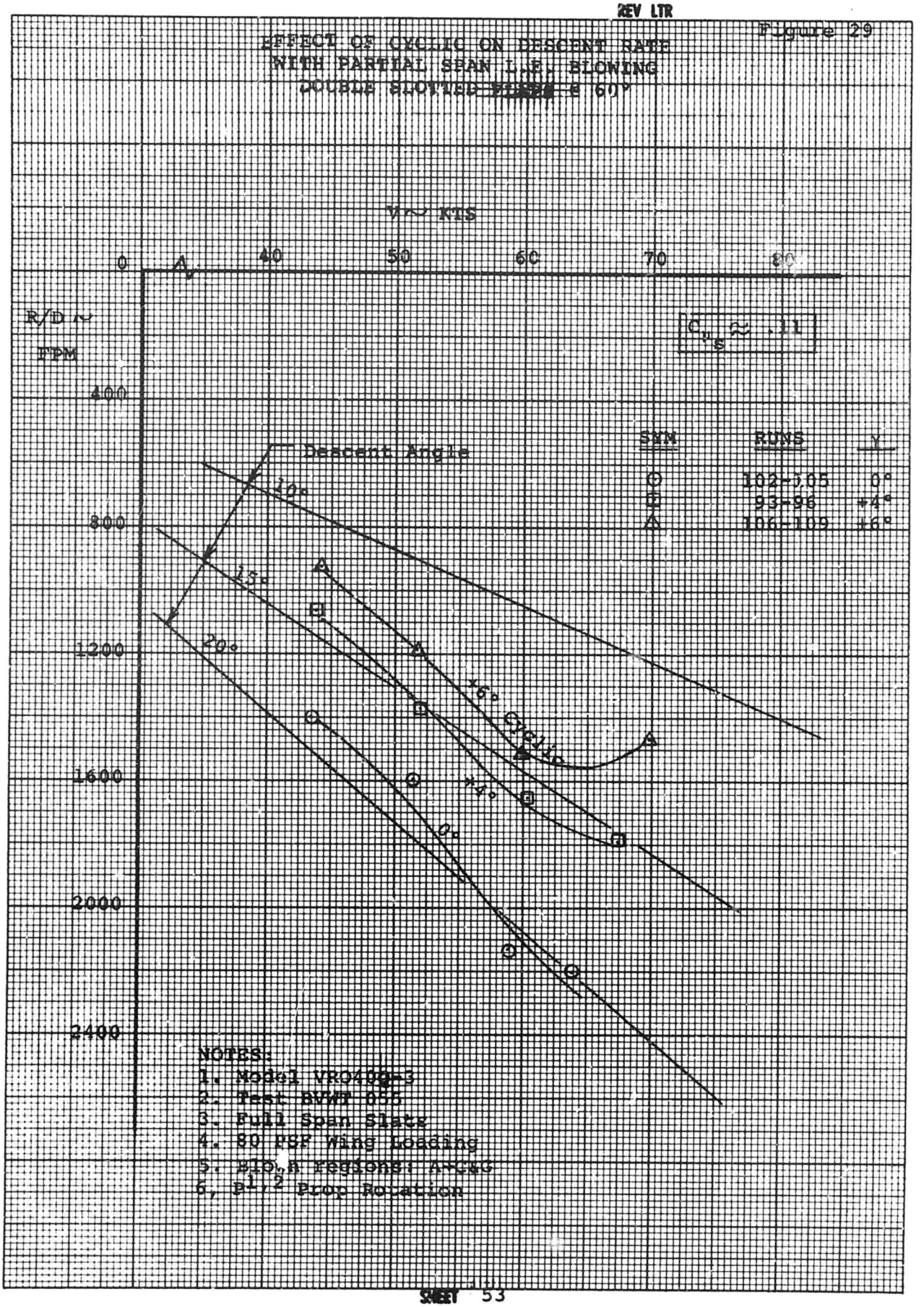

NUMBER
REV LTR

Figure 30

EFFECT OF CYCLIC ON BUFFET ONSET
WITH PARTIAL SPAN L.E. BLOWING
DOUBLE SLOTTED FLAPS @ 60°

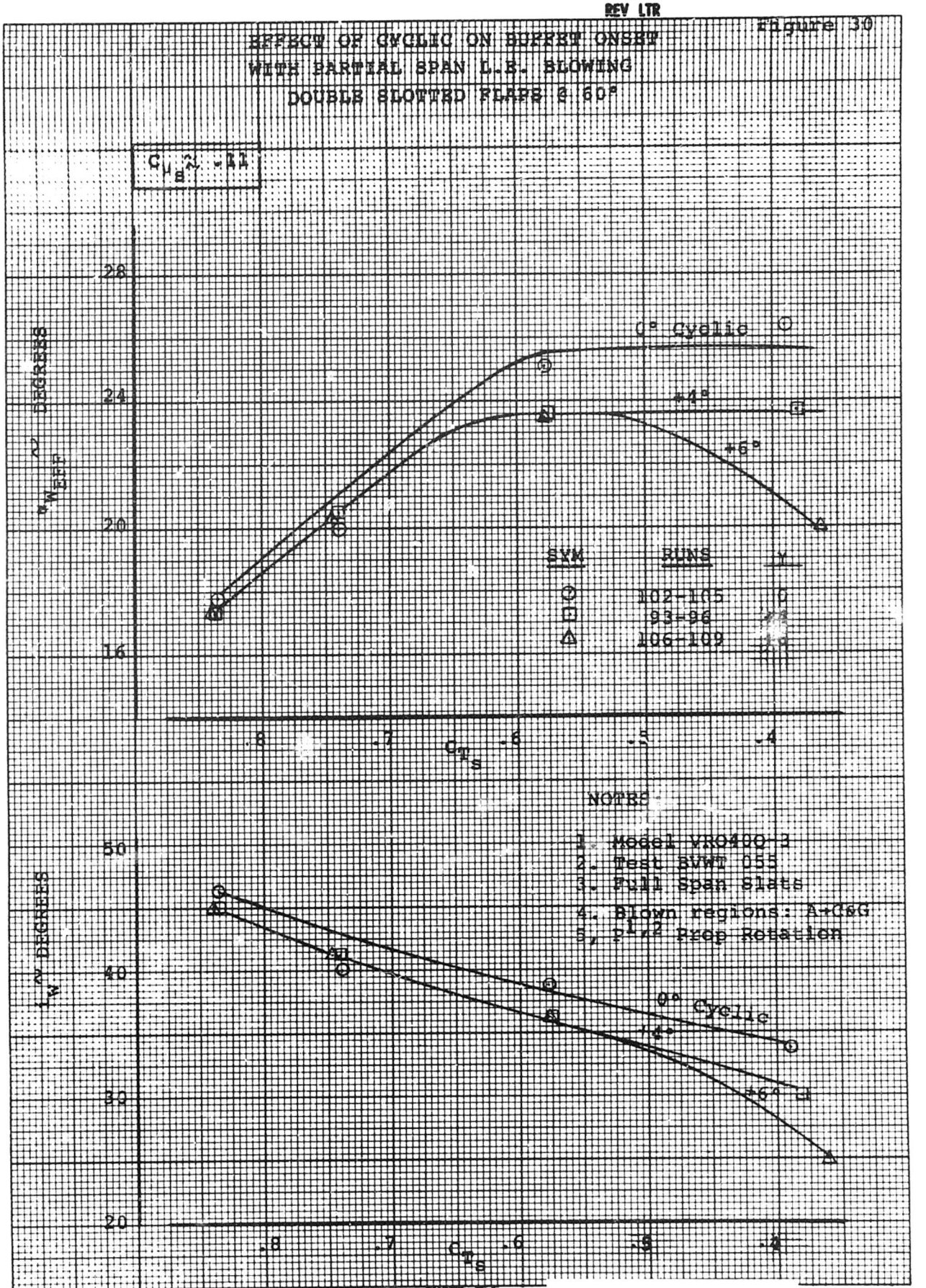

6.4 EFFECT OF CYCLIC WITH BLC $P^{1,1}$ PROP ROTATION

The most favorable blowing configuration (full span blowing) was chosen to evaluate the $P^{1,1}$ prop rotation (both props turning down inboard) with cyclic pitch. Figure 31 shows that with this rotation application of positive cyclic reduces the descent capability from 90 to 120 fpm per degree of cyclic over the speed range tested -- about the same average exhibited by the $P^{1,2}$ prop rotation. The decrease in effective wing stall angle (See Figure 32) due to positive cyclic was of the same magnitude as experienced with the $P^{1,2}$ prop rotation.

Figure 31

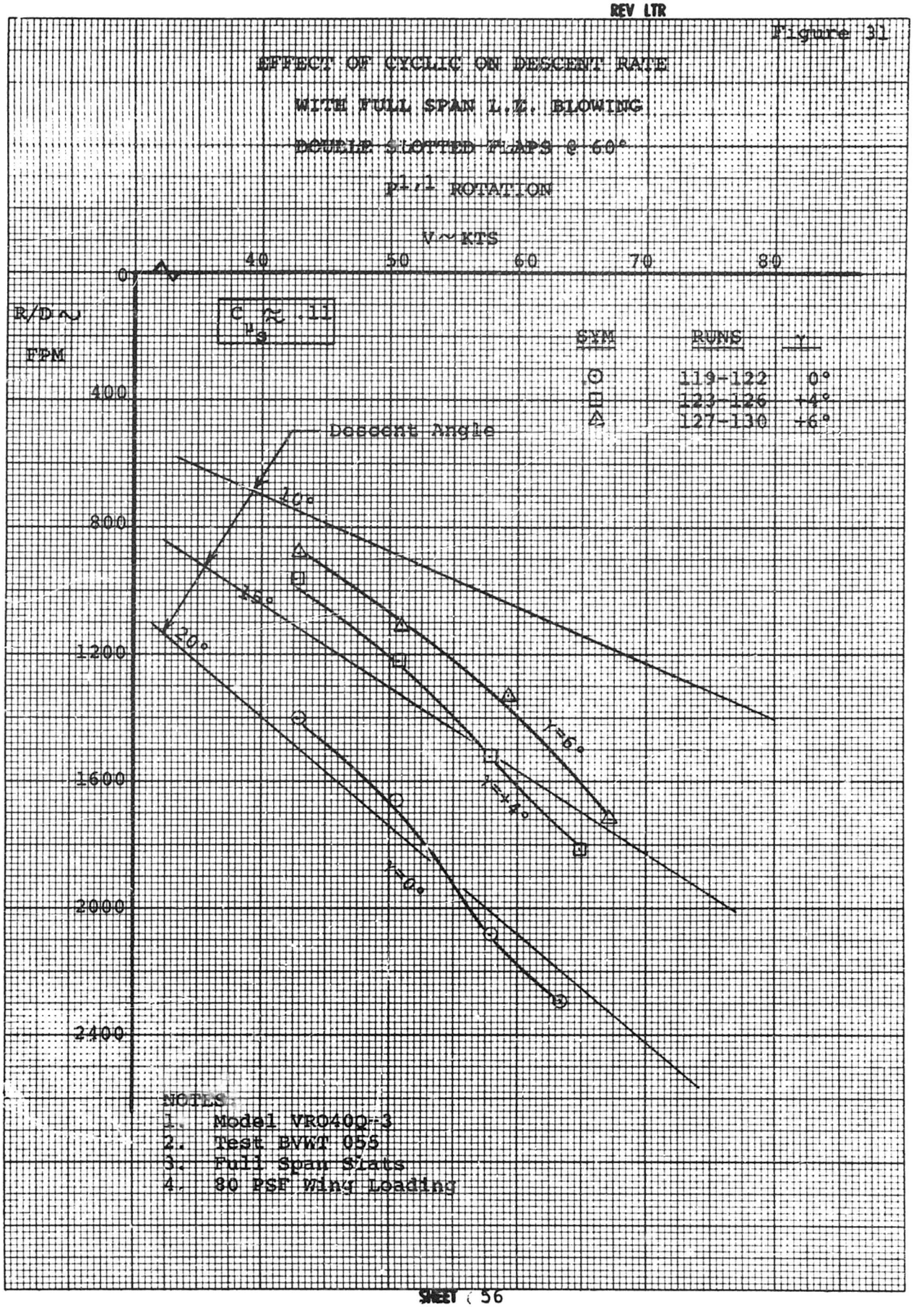

Figure 32

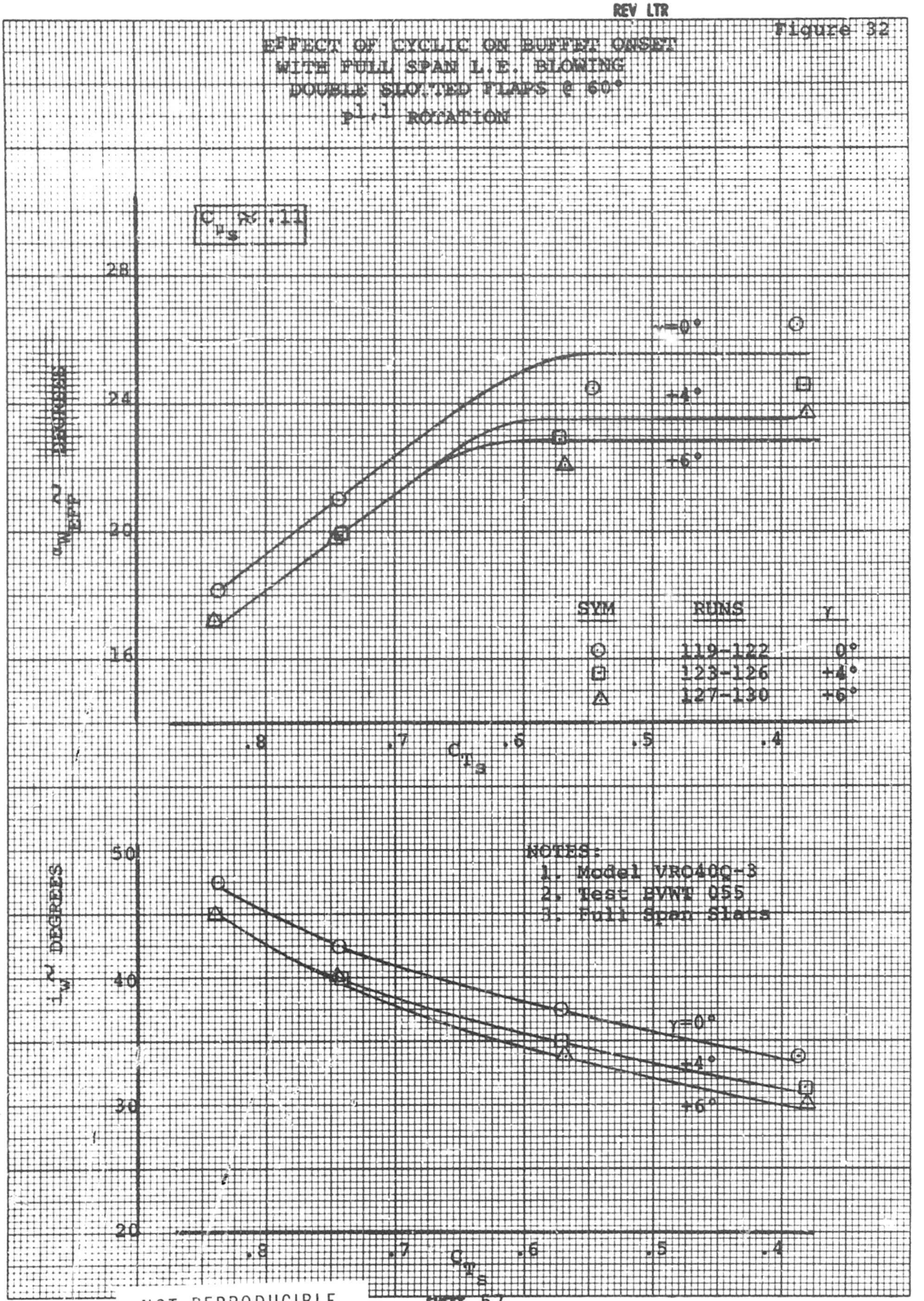

6.5 COMPARISON OF INBOARD PROP ROTATIONS

The effect of inboard prop rotation ($P^{1,2}$ vs $P^{1,1}$) on the landing descent performance was investigated with both collective and cyclic hubs during this leading edge BLC test. Figure 33 presents the rate of descent comparison with cyclic.

Unlike the results obtained in previous tests without leading edge blowing, wherein the $P^{1,1}$ rotation resulted in a large reduction in descent capability over that obtained with the $P^{1,2}$ rotation, leading edge blowing almost equalized the descent performance over the cyclic range evaluated (0° to °6° of cyclic).

Figures 34 and 35 depict the comparison with collective hubs. The buffet onset angles shown in Figure 34 are of a similar magnitude for both inboard prop rotations. The resultant descent capability with the $P^{1,1}$ prop rotation averaged 130 fpm less than with the $P^{1,2}$ rotation.

NUMBER
REV LTR

Figure 33

COMPARISON OF INBD PROP ROTATIONS
WITH FULL SPAN L.E. BLOWING & CYCLIC
DOUBLE SLOTTED FLAPS @ 60°

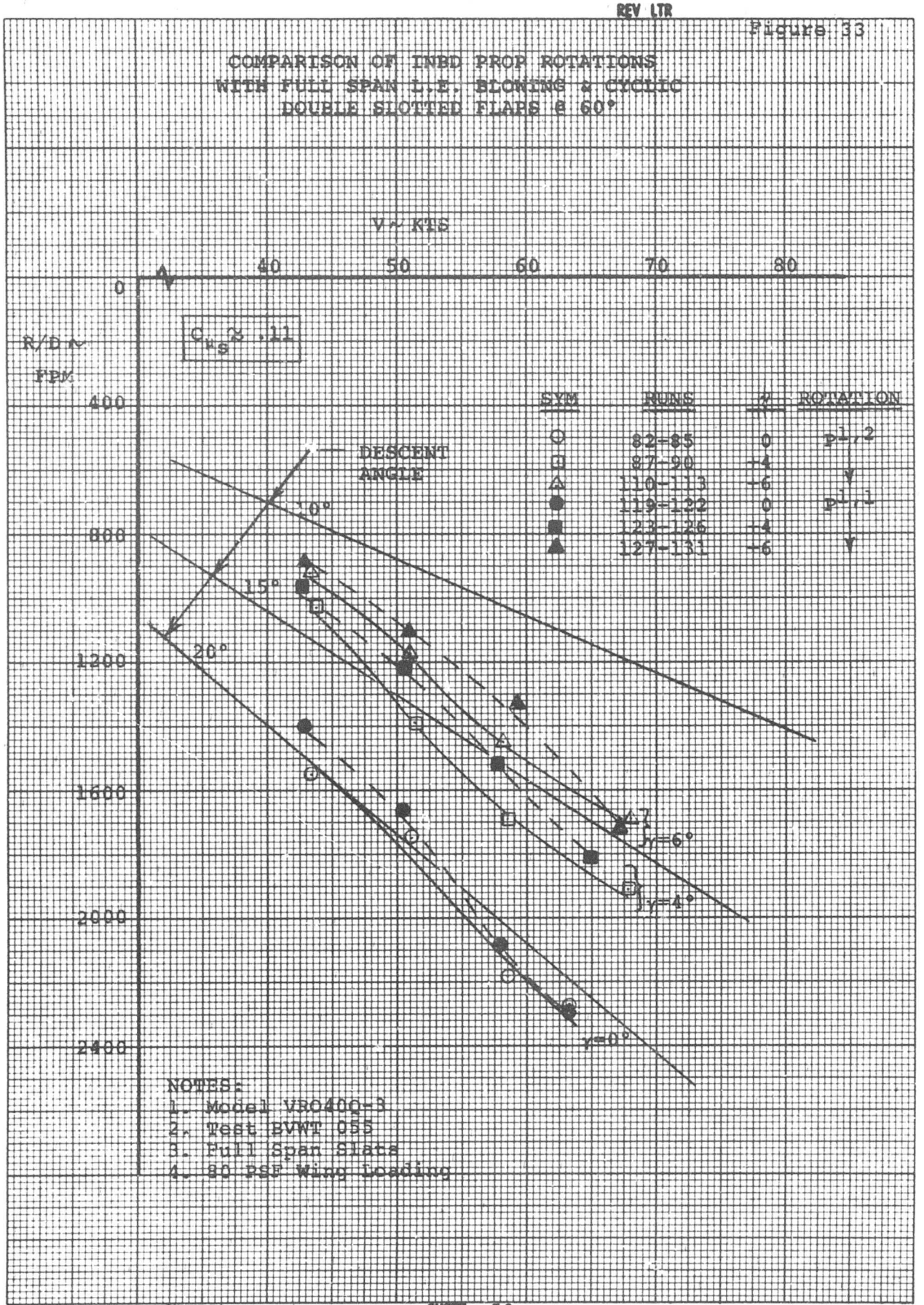

NUMBER
REV LTR

Figure 34

COMPARISON OF INBOARD PROP ROTATION
WITH FULL SPAN L.E. BLOWING
DOUBLE SLOTTED FLAPS @ 60°

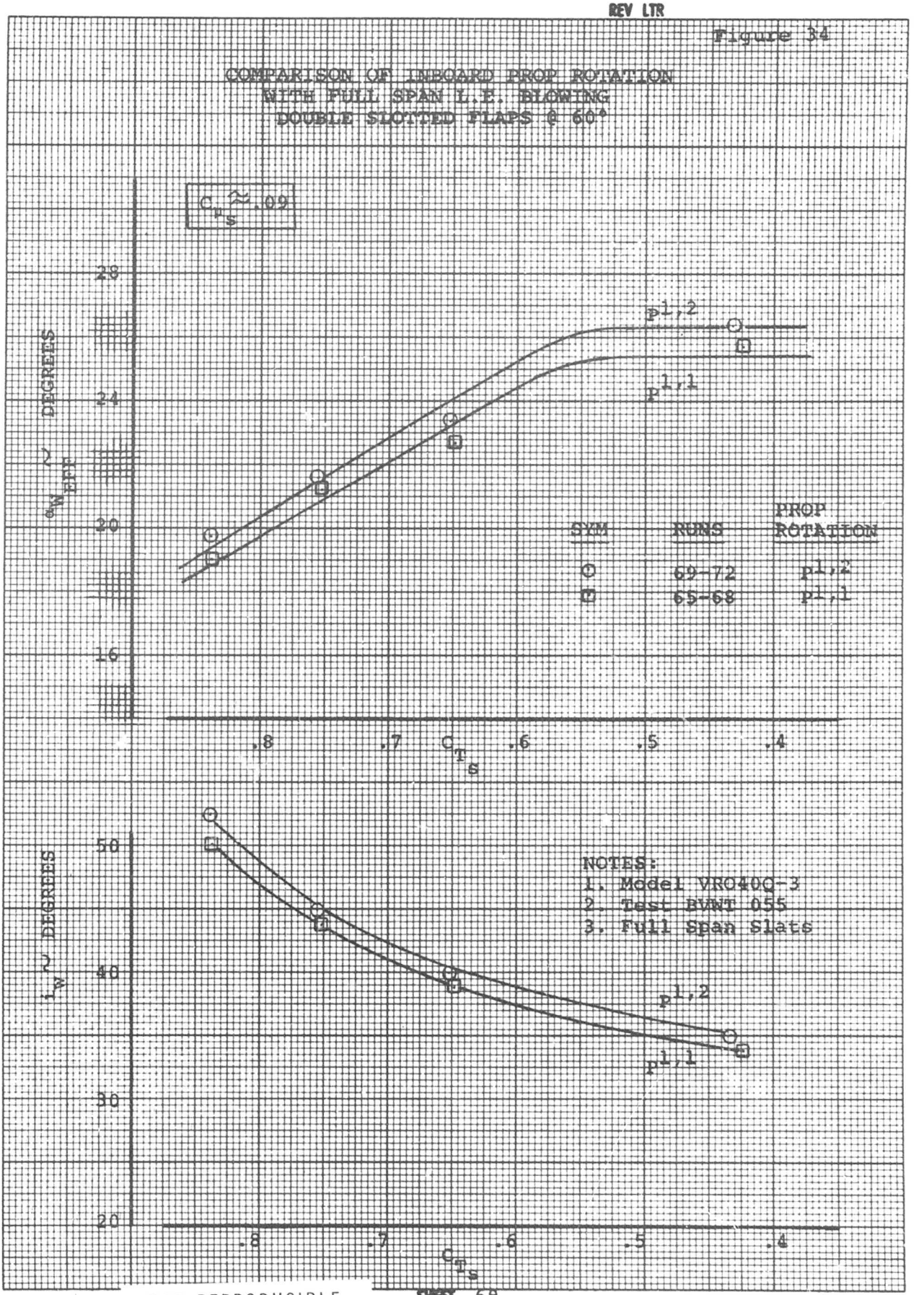

NOT REPRODUCIBLE

SHEET 60

Figure 35

COMPARISON OF INBOARD PROP ROTATION
WITH FULL SPAN L.E. BLOWING
DOUBLE SLOTTED FLAPS @ 60°

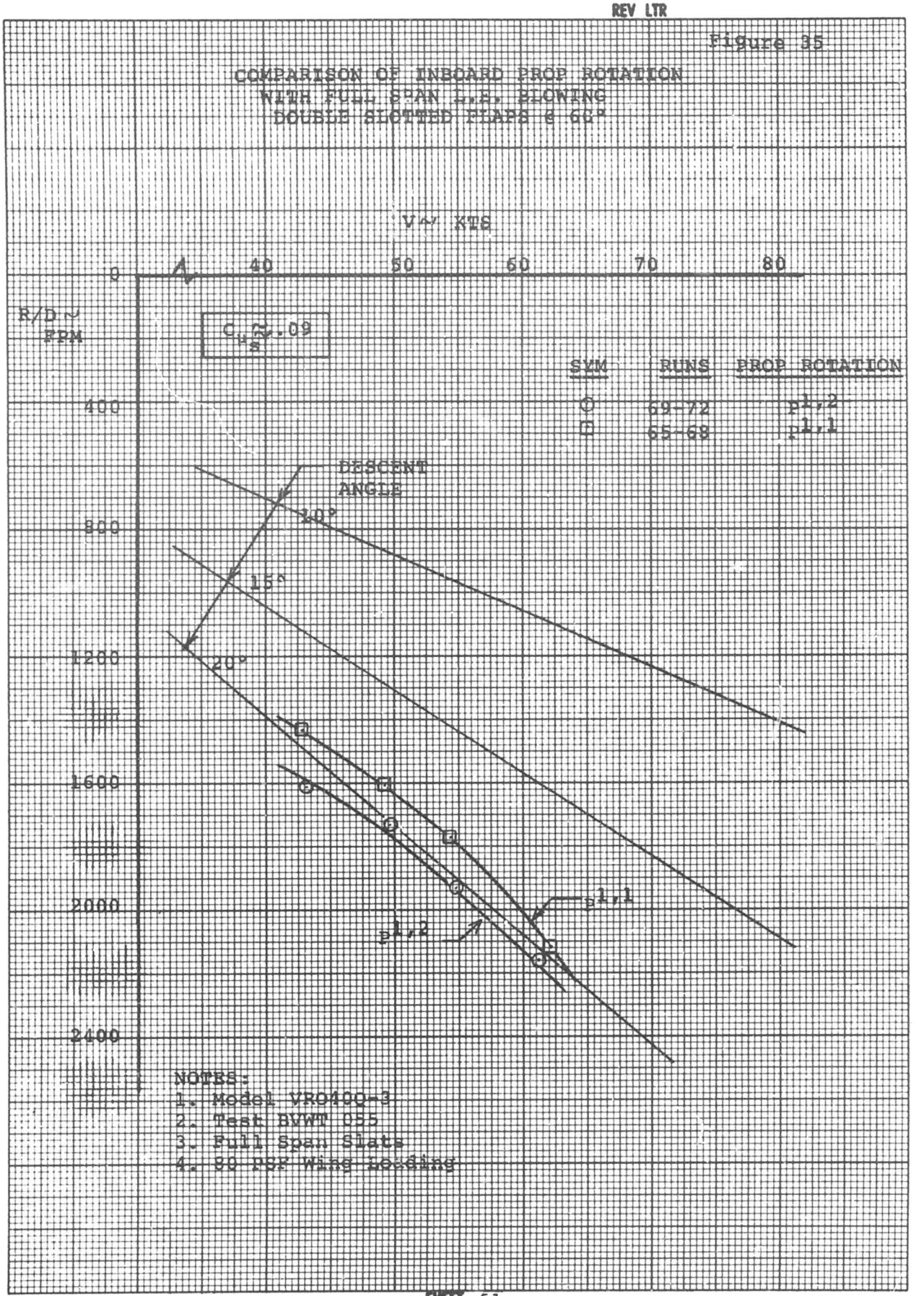

6.6 EFFECT OF CHANGING AZIMUTH LEAD OF CYCLIC ANGLE INPUT

Judging from results of a previous test on a isolated propeller/cyclic hub assembly identical to the one used in this test, an azimuth phase lag of about 15 degrees existed between initial application and full input of cyclic. This was attributed to blade/hub non-rigidities. An azimuth phase lead of 15 degrees was utilized on most cyclic runs to assure that full cyclic inputs occurred at 6 and 12 o'clock.

Previous tests reported by Canadair indicated an improvement in descent capability, where the application of nose down cyclic caused wing stalling, by the insertion of 22° of azimuth lead angle. To investigate the potential of phase lead for improving descent performance, a 45° phase lead (30° of net lead) on a +4° cyclic setting was incorporated during a series of runs with partial span leading edge blowing (A→C&G regions) and $P^{1,2}$ prop rotation. Figures 36 and 37 present the results. In the case evaluated, 45° of phase lead decreased the effective wing stall angle and the corresponding descent capability. Special note was taken of whether the 45° phase lead moved initial stall outboard into the unblown region between nacelles. There was some evidence of this at the two higher C_{T_S} values, but definitely not at the two lower C_{T_S} values.

EFFECT OF CHANGING PHASE LEAD ON CYCLIC ANGLE INPUT
WITH PARTIAL SPAN L.E. BLOWING, (A+C+G)
DOUBLE SLOTTED FLAPS @ 60°

Figure 36

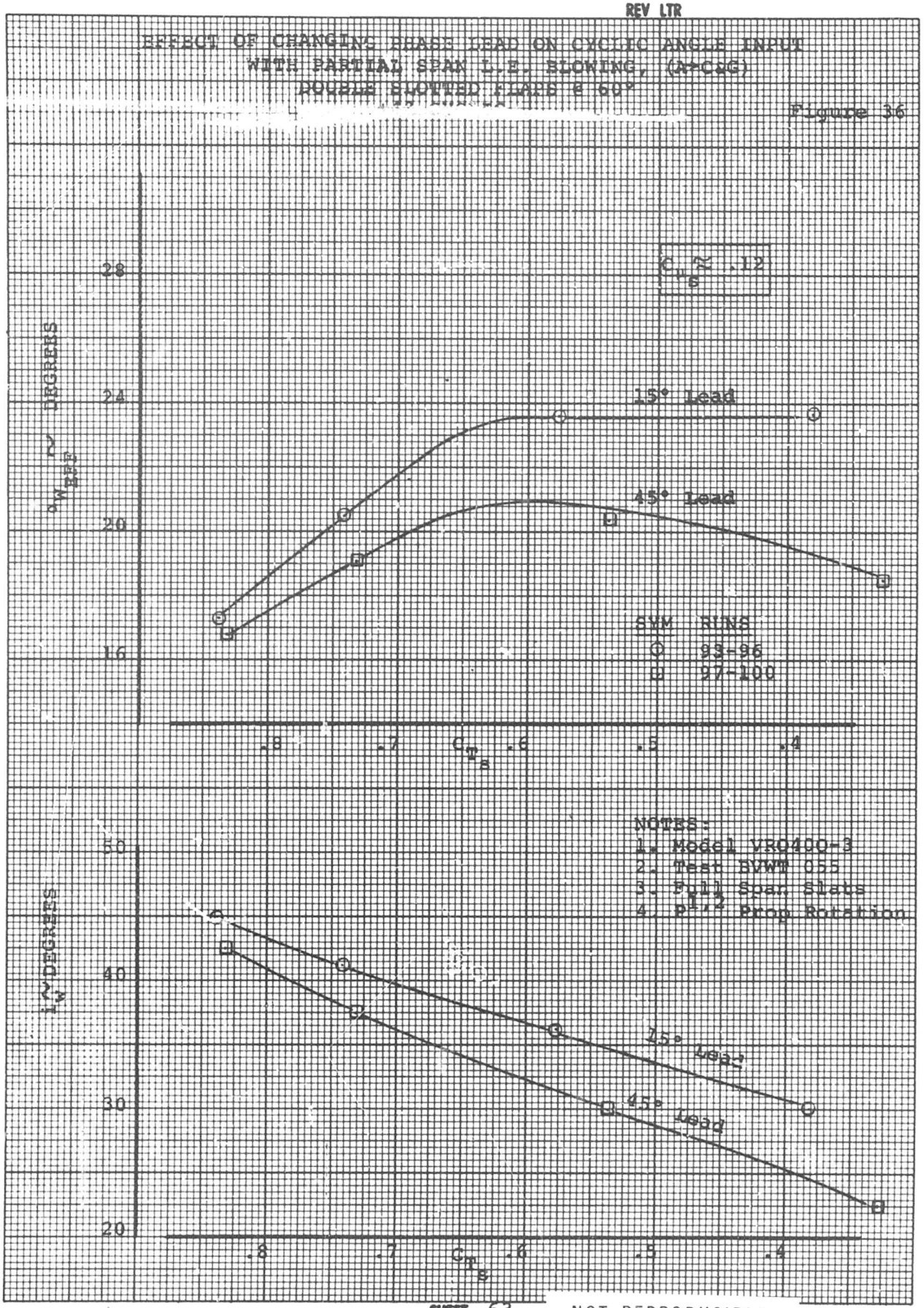

NUMBER
REV LTR

Figure 37

EFFECT OF CHANGING PHASE LEAD ON CYCLIC ANGLE INPUT
WITH PARTIAL SPAN L.E. BLOWING, (A_{1s}-C_{4G})
-4° CYCLIC

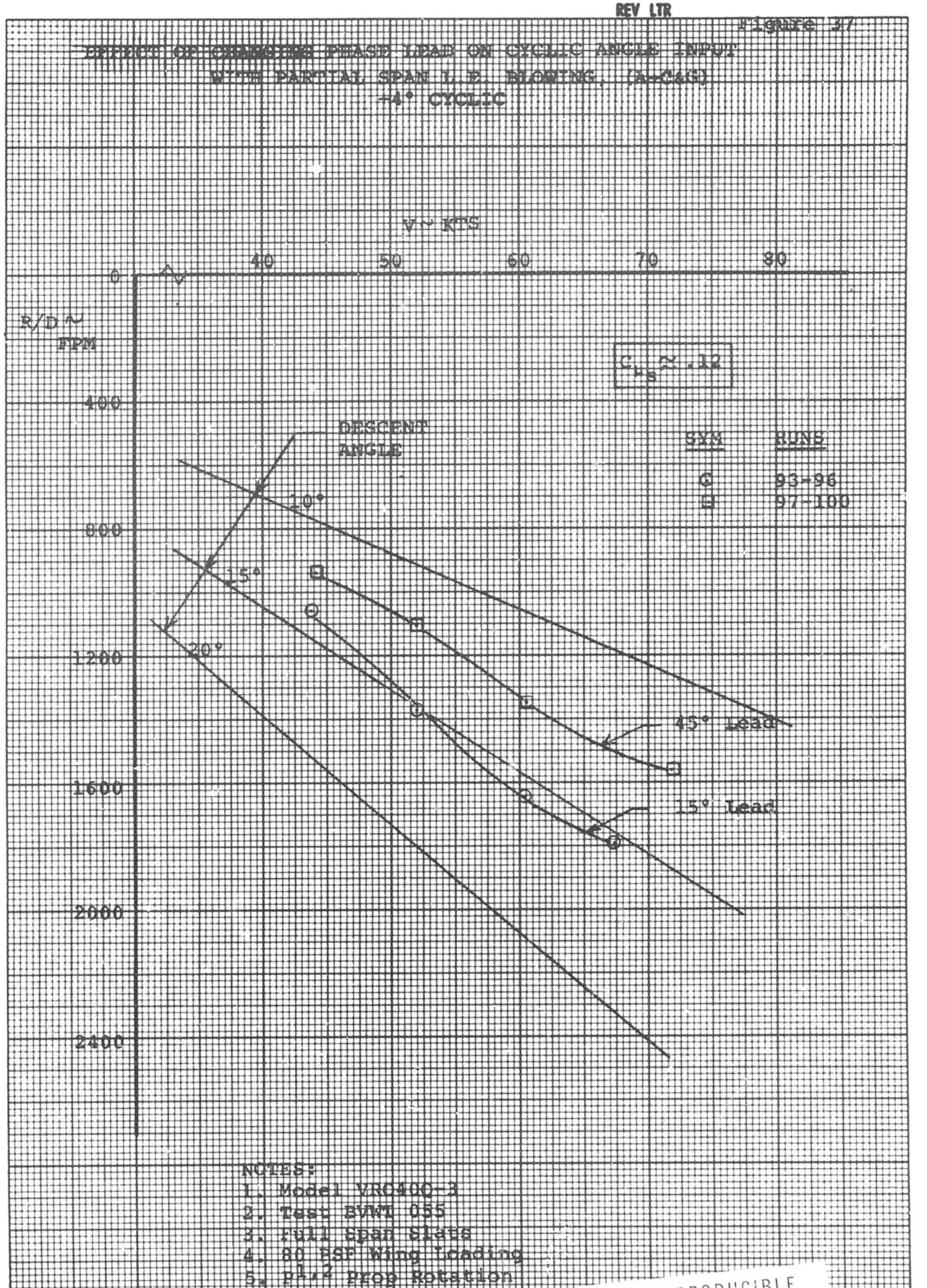

NOTES:
1. Model VR0400-3
2. Test BVWT 055
3. Full Span Slats
4. 80 PSF Wing Loading
5. $n_{A\times 2}$ Prop Rotation

6.7 SINGLE SLOTTED FLAPS WITH BLC AND CYCLIC

The investigation made with single slotted flaps (30° and 45° of deflection) was performed with full span blowing coupled with cyclic pitch angles of 0° and +4°. The average blowing coefficient (C_{μ_s}) was approximately .11 and the $P^{1,2}$ prop rotation was used.

Figure 38 shows a decrease in descent capability of 100 fpm per degree of positive cyclic with 45° of flap -- the same value that occurred with 60° of double slotted flaps. Reducing the flap deflection to 30° caused an additional reduction in descent performance. Corresponding buffet onset angles are presented in Figure 39. This figure again shows some decrease in effective wing stall angle with positive cyclic.

Figure 40 compares the descent capability measured with single slotted flaps at 45° and double slotted flaps at 60° for the same blowing configuration and +4° of cyclic. As can be noted, the 60° double slotted flap provides an incremental improvement of 300 fpm in descent rate over that measured with the 45° single slotted flaps. This result is in agreement with previous tilt wing test data acquired with similar flap configurations. Figure 41 presents the comparison of the corresponding buffet onset angles. It can be noted that both flap configurations exhibit the same effective wing stall angle, which is also in agreement with previous test data. The wing tilt angle at which buffet onset occurs with 60° of double slotted flaps is slightly less than with single slotted flaps set at 45°.

Figure 38

EFFECT OF CYCLIC ON DESCENT RATE
WITH FULL SPAN L.E. BLOWING
SINGLE SLOTTED FLAPS

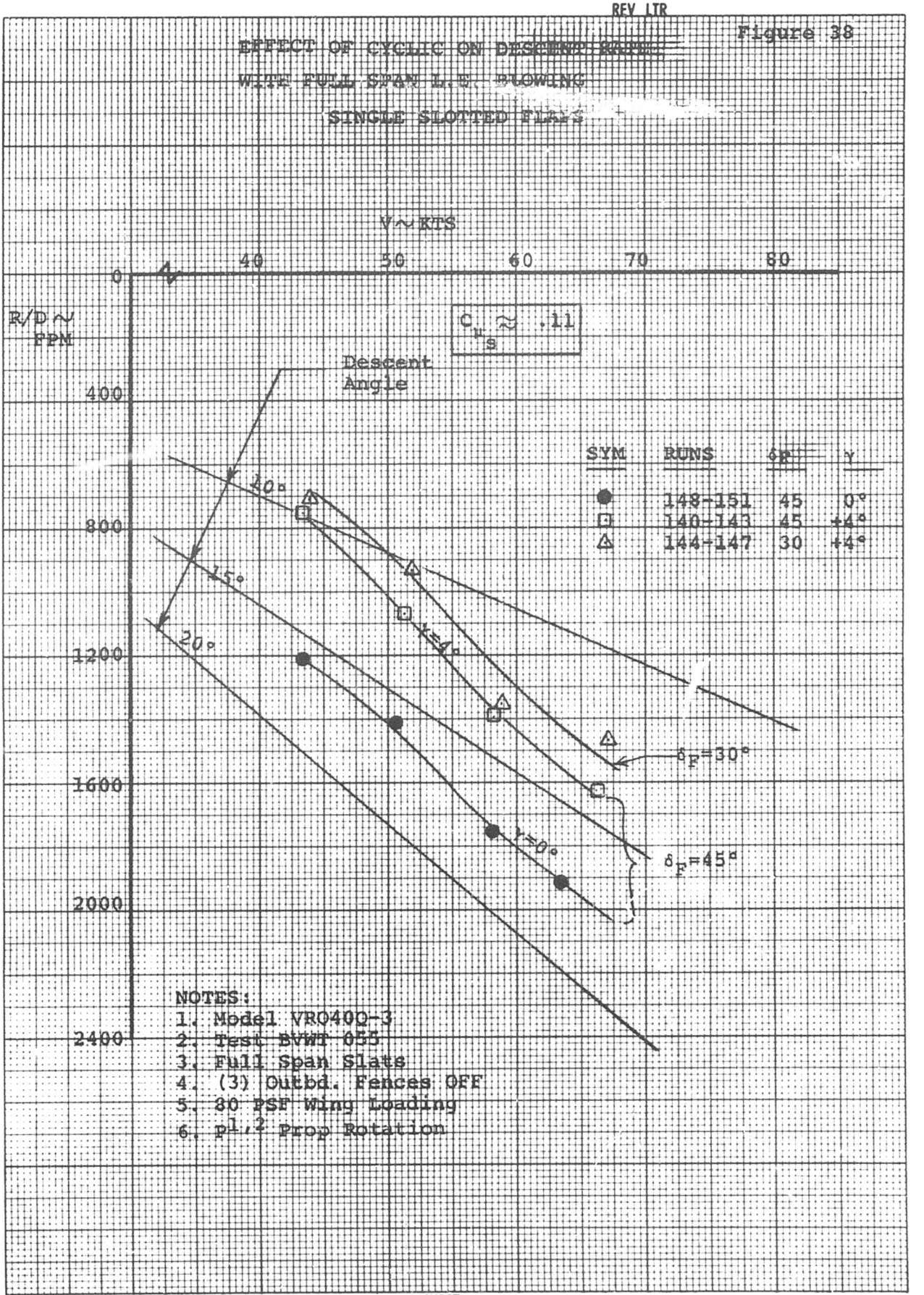

Figure 39

EFFECT OF CYCLIC ON BUFFET ONSET

WITH FULL SPAN L.E. BLOWING

SINGLE SLOTTED FLAPS

$C_{\mu_S} \approx .11$

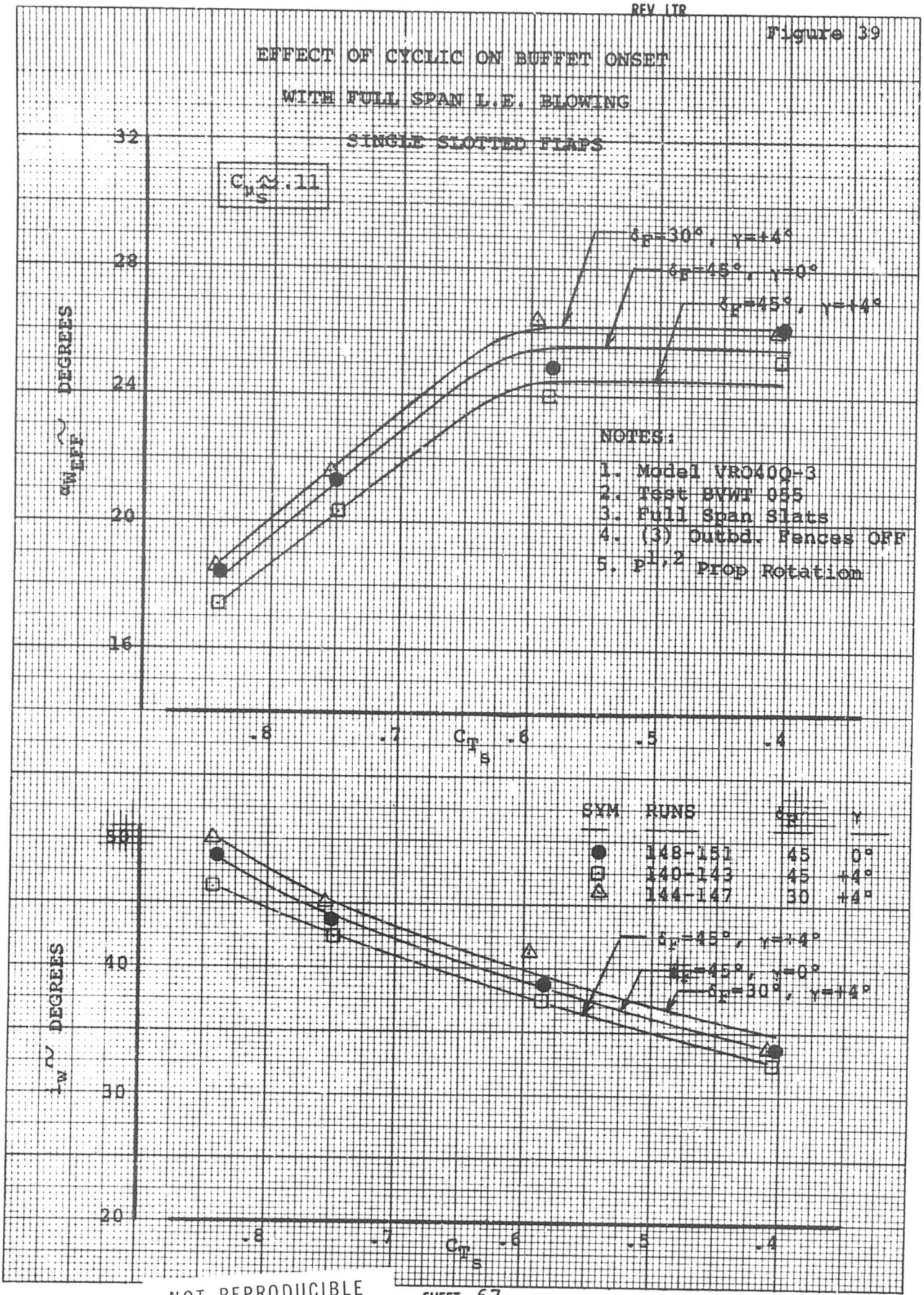

Figure 40

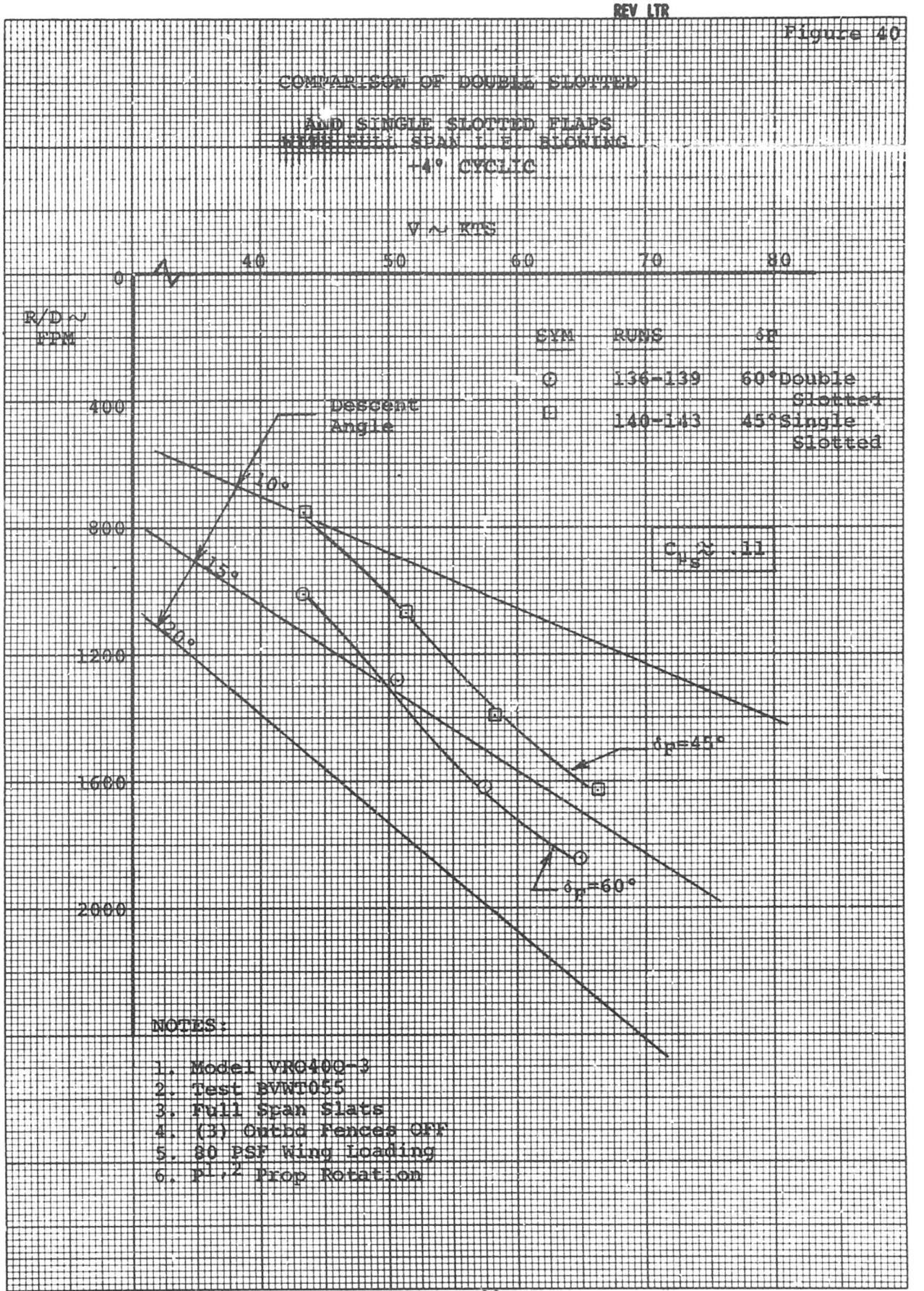

NOTES:

1. Model VRC400-3
2. Test BVWT055
3. Full Span Slats
4. (3) Outbd Fences OFF
5. 80 PSF Wing Loading
6. P1,2 Prop Rotation

Figure 41

COMPARISON OF DOUBLE SLOTTED AND SINGLE SLOTTED FLAPS WITH FULL SPAN L.E. BLOWING +4° CYCLIC

$C_{\mu_s} \approx .11$

NOTES:
1. Model VRO400-3
2. Test BVWT 055
3. Full Span Slats
4. (3) Outbd. Fences OFF
5. #1,2 Prop Rotation

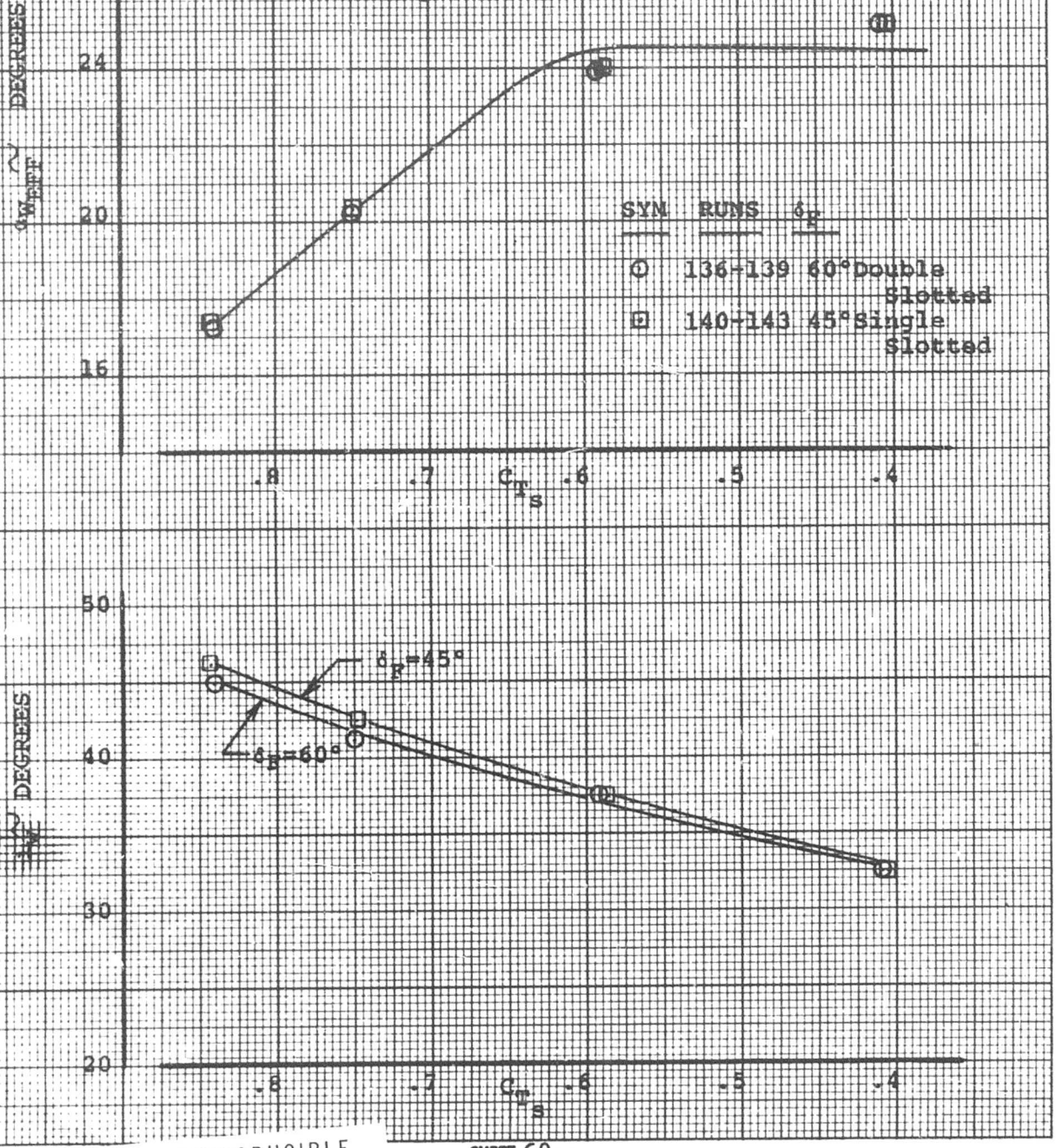

6.8 REMOVAL OF FULL SPAN SLATS WITH BLC

The effect on landing descent performance of removing the full span slats was investigated in a series of runs with full span blowing ($C_{\mu_s} \approx .11$), 4° of positive cyclic, double slotted flaps at 60°, and the $P^{1,2}$ prop rotation. Buffet onset angles and descent capability measured during these runs are compared with slats off base runs in Figures 42 and 43, respectively.

Figure 42 shows a small loss in effective wing stall angle due to slat removal at C_{T_s} values below .6, but an increasing incremental improvement at higher values. The net result was that the slats off configuration exhibited a higher rate of descent capability at lower speeds tested and a lower capability at the higher speeds. The small change in effective wing stall at the lower C_{T_s} values indicates that some loss in turning effectiveness occurred at the higher speeds when the slats were removed, (i.e. one degree in wing tilt stall angle represents about 45 fpm rate of descent).

Figure 42

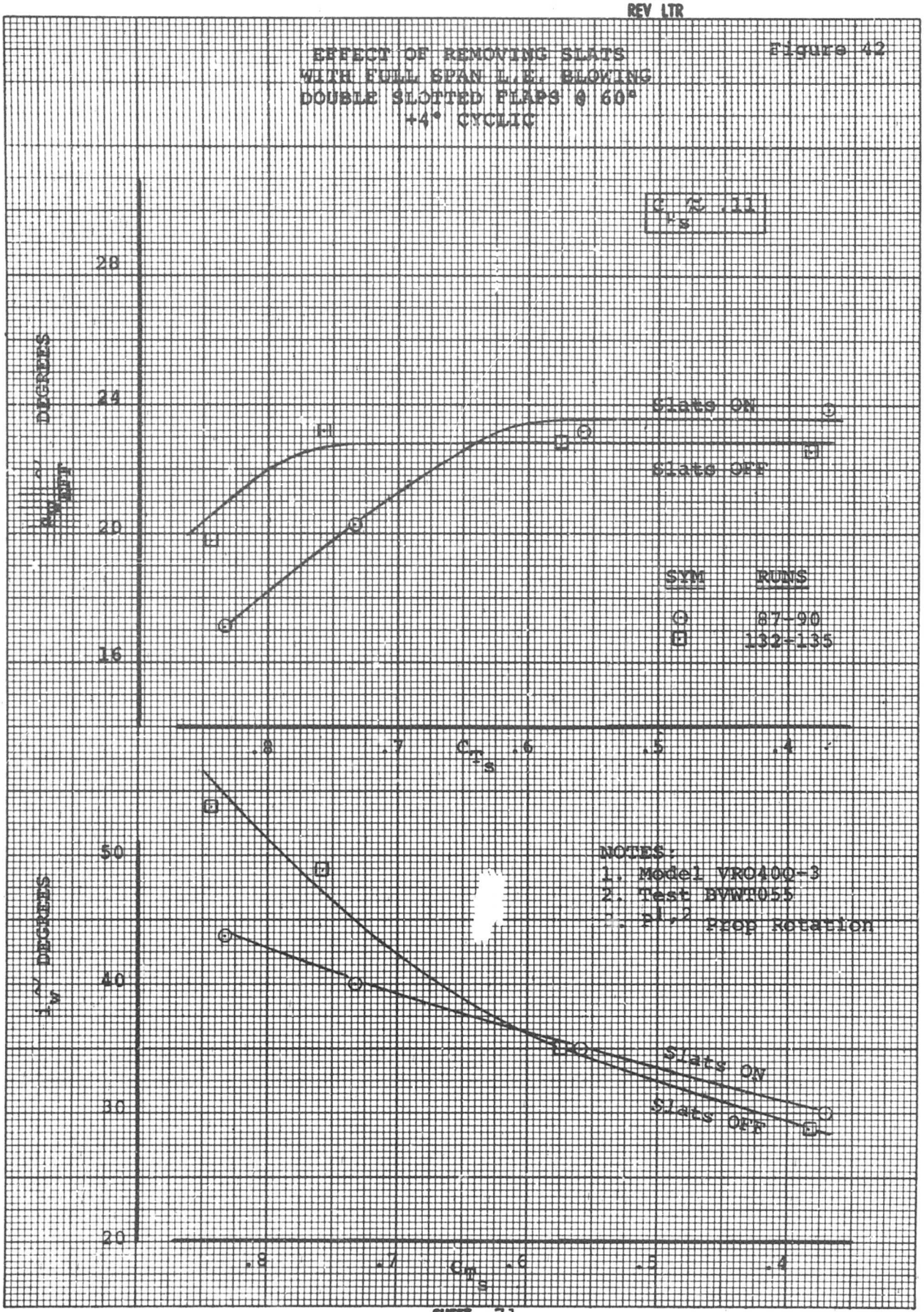

Figure 43

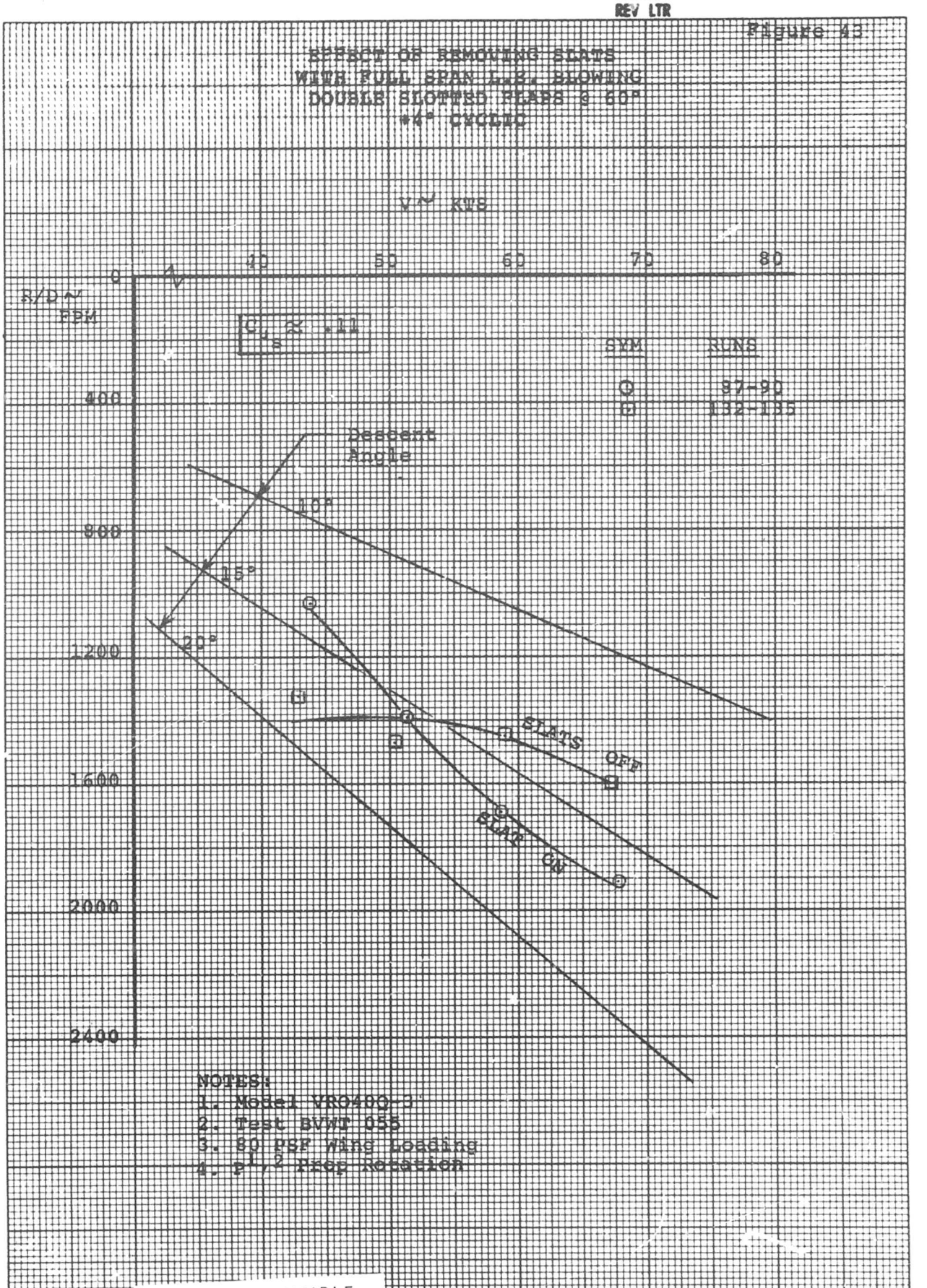

6.9 REMOVAL OF WING FENCES WITH BLC

The wing fence configuration (two midspan between nacelles and two inboard at the side of the body - see Figure 2) used on semispan model VR040Q-3 were developed on previous tests of the model to contain any stall occurring on the wing/body center section and in the B region, or the stall that initially occurred, depending upon the configuration/conditions tested, in the E region. The same wing fence geometry was retained for the current test. A series of runs were performed with the three most outboard fences removed to evaluate the effect on descent performance when full span blowing ($C_{\mu_s} \simeq .11$) and +4° of cyclic were employed. Figures 44 and 45 compare the "fences off" runs with a suitable series of "fences on" runs.

Removing the fences resulted in a small gain in wing stall angle, however, this is not reflected in an increase in descent capability.

Figure 44

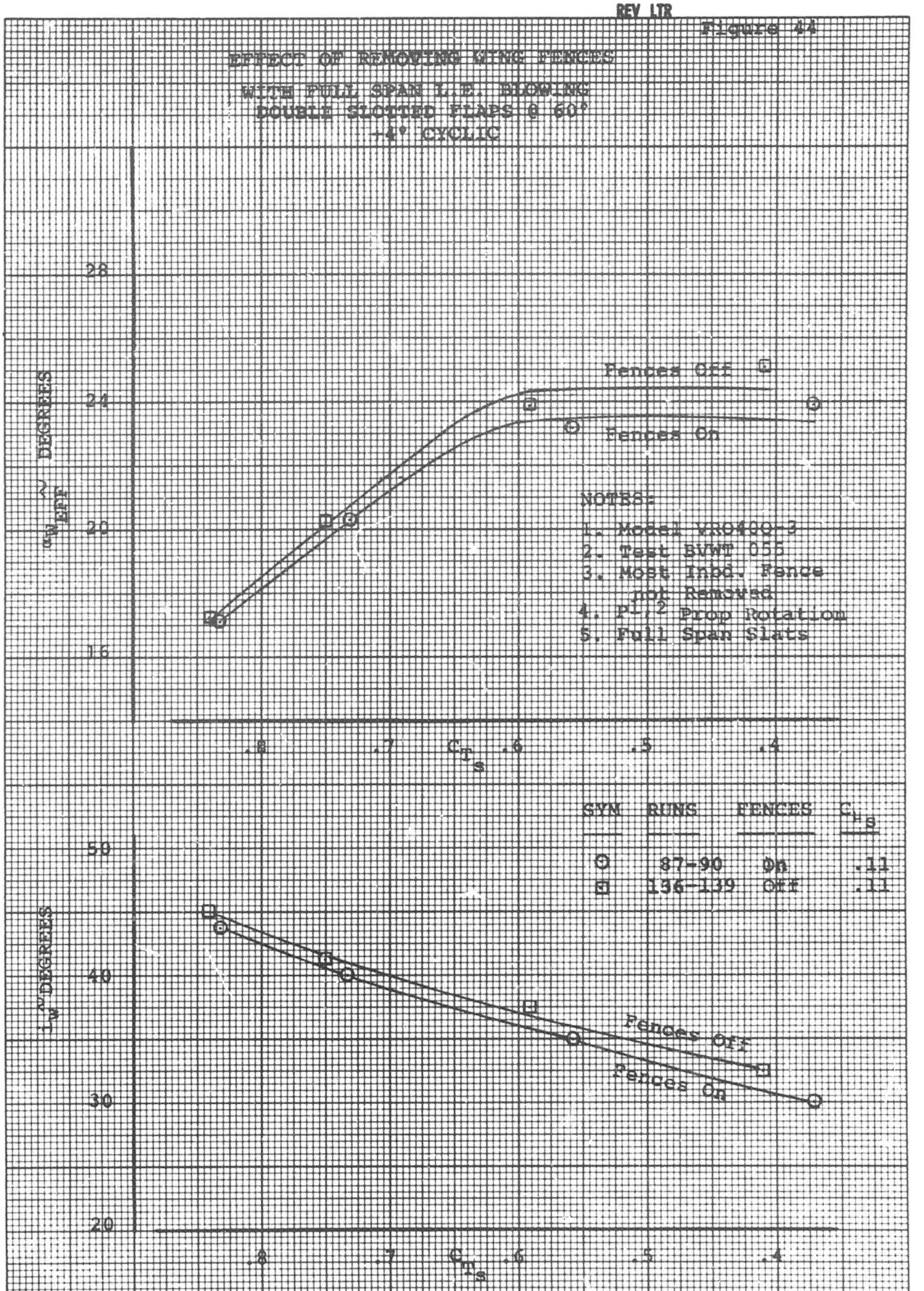

Figure 45

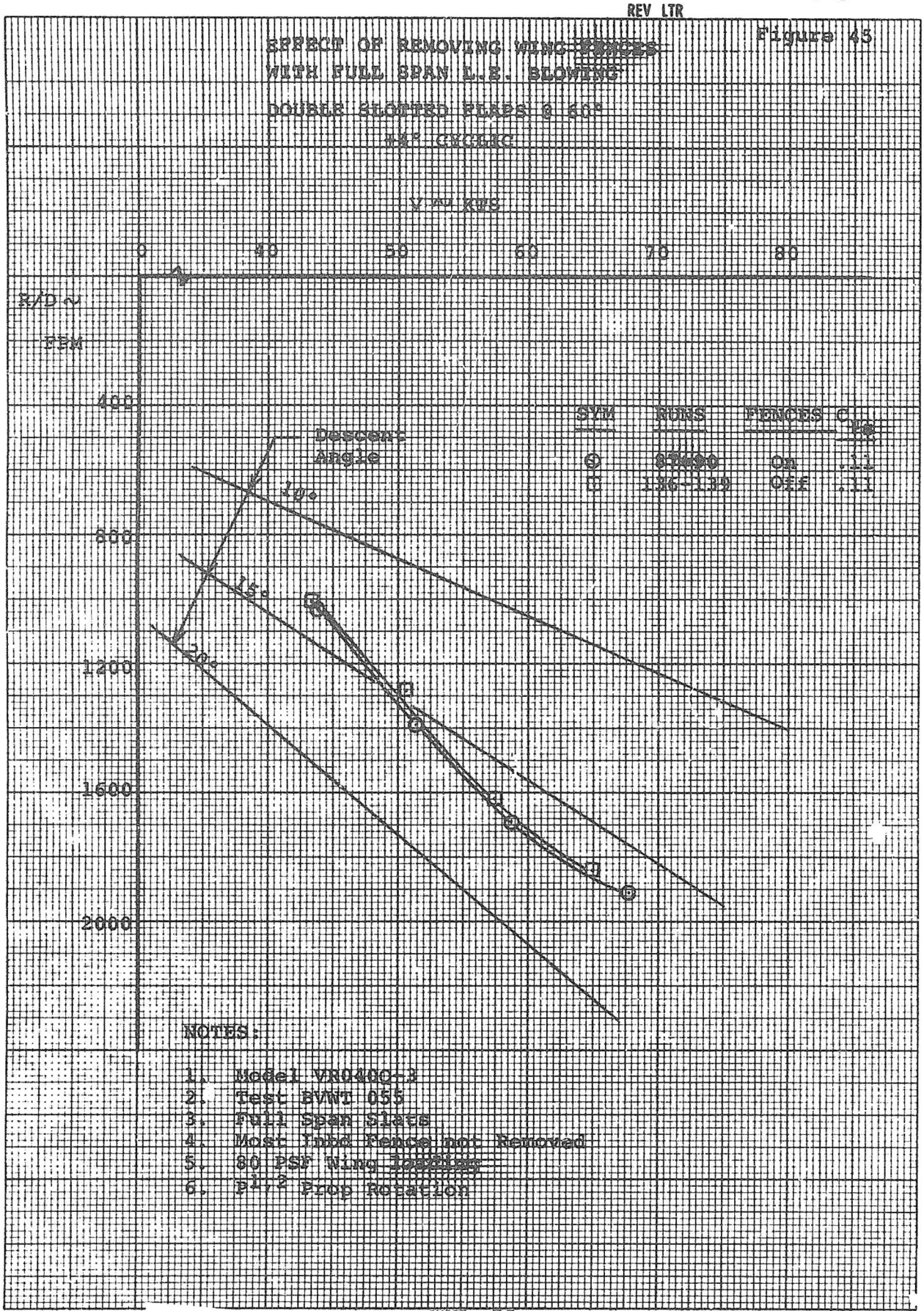

6.10 VARIATION OF BLOWN REGIONS AND BLOWING MAGNITUDE

During the first half of the subject test, the effect on descent performance of increasing the blown span of the wing was evaluated by conducting successive series of runs with the following blowing configurations (See Figure 2 for delineation of the blown wing areas).

a) Wing/body center section plus B region (A→B regions)

The A and B regions of the wing, not being immersed or completely immersed in the slipstream, are usually the first areas to show separation. Although this separation is not taken into consideration in evaluating buffet onset, because of the low q, separation of the center section can result in stall or buffet of the tail, so that delay or elimination of separation in this region is desirable.

b) Inboard panel (A→C region).

This blowing configuration extended leading edge blowing to include the wing area inboard of the inboard nacelle. The initial series of runs with no blowing showed that C region was the portion of the wing proper on which stall initially occurred. This result is, of course, valid only for the model configuration tested full span slats, 60° of double slotted flaps and the $P^{1,2}$ prop rotation (both-down-between nacelles).

c) Inboard panel plus tip panel (A→C and G regions)

During the runs with A→C region leading edge blowing, a tip corner stall was observed which was noted to be larger than the tip corner "separation" attributed to the wing tip vortex action at high wing incidence angles in the order of 30° to 45°.

d. Full span blowing (A→G regions)

The final blowing configuration evaluated was leading edge blowing extended over the full span of the wing, excluding the leading edge span encompassed by the nacelles.

Figure 46 compares the descent capability measured for the various blowing configurations when an average blowing coefficient ($C_{\mu s}$) of 0.11 was used. The corresponding buffet onset angle comparison is presented in Figure 47. Data in these plots show that either full span leading edge blowing or inboard panel plus tip panel blowing will provide an incremental improvement of 450 fpm in descent rate. The effect of the observed tip corner stall on descent capability and buffet onset angles, when the A→C region was blown, is noticeable. It is possible that this tip stall could be eliminated by minor redesign of the wing tip, without blowing. This was not investigated in this test.

The A→B region blowing configuration resulted in an early initial stall in the area immediately outboard of the B region at the highest speed tested.

During the investigation with full span leading edge blowing, the blowing coefficient (C_{μ_s}) was varied from .06 to .21. Figures 48 and 49 present the resultant effect on descent capability and buffet onset angle, respectively. Increasing the blowing coefficient increased descent capability at the lowest speeds tested, but not at the highest speed tested. The data also indicates that the effective wing stall angle increases with an increase in blowing coefficient. It should be pointed out that due to physical model limitations (minimum blowing slot that would be accurately set ~.005" and relatively low q_s), the .06 C_{μ_s} value was obtained with a pressure ratio of 1.70. This non-choked nozzle condition can result in spanwise flow distribution problems, that diminish BLC effectiveness.

Similar results were obtained for the partial span blowing configuration of inboard panel plus tip panel. Blowing magnitude was varied from .05 to .11 C_{μ_s}. Figures 50 and 51 depict the rate of descent capability and buffet onset angles, respectively.

Blowing magnitude was also varied for the A→C blown region case. The data shown in Figures 52 and 53 indicates only small measureable differences in descent capability for the C_{μ_s} range tested (.04 to .10C_{μ_s}).

In the fixed wing aircraft application, the primary objective of leading edge blowing is to increase lift. The tilt wing aircraft, however, requires a commensurate amount of drag to maintain the same rate of descent at a constant wing tilt angle.

Of concern in this test, since only relatively high values of C_{μ_s} could be obtained with a choked nozzle, was whether at these high C_{μ_s} values an increase in lift without a corresponding increase in drag would result and thus have an adverse effect on rate of descent.

Figure 54 illustrates that this was the case. The example was calculated from the data obtained during the full span leading edge blowing evaluation, at a constant wing tilt angle of 35 degrees. Increasing the blowing coefficient to a large value reduced the descent rate substantially at 60 knots. No loss occurred at a speed of 42 knots. Note that the above discussion relates to rate of descent <u>at constant wing angle</u>; thus with large amounts of blowing at the higher speeds, a higher wing angle would be needed for a given descent rate. The maximum rate of descent, as shown earlier in this report is improved by blowing.

Figure 46

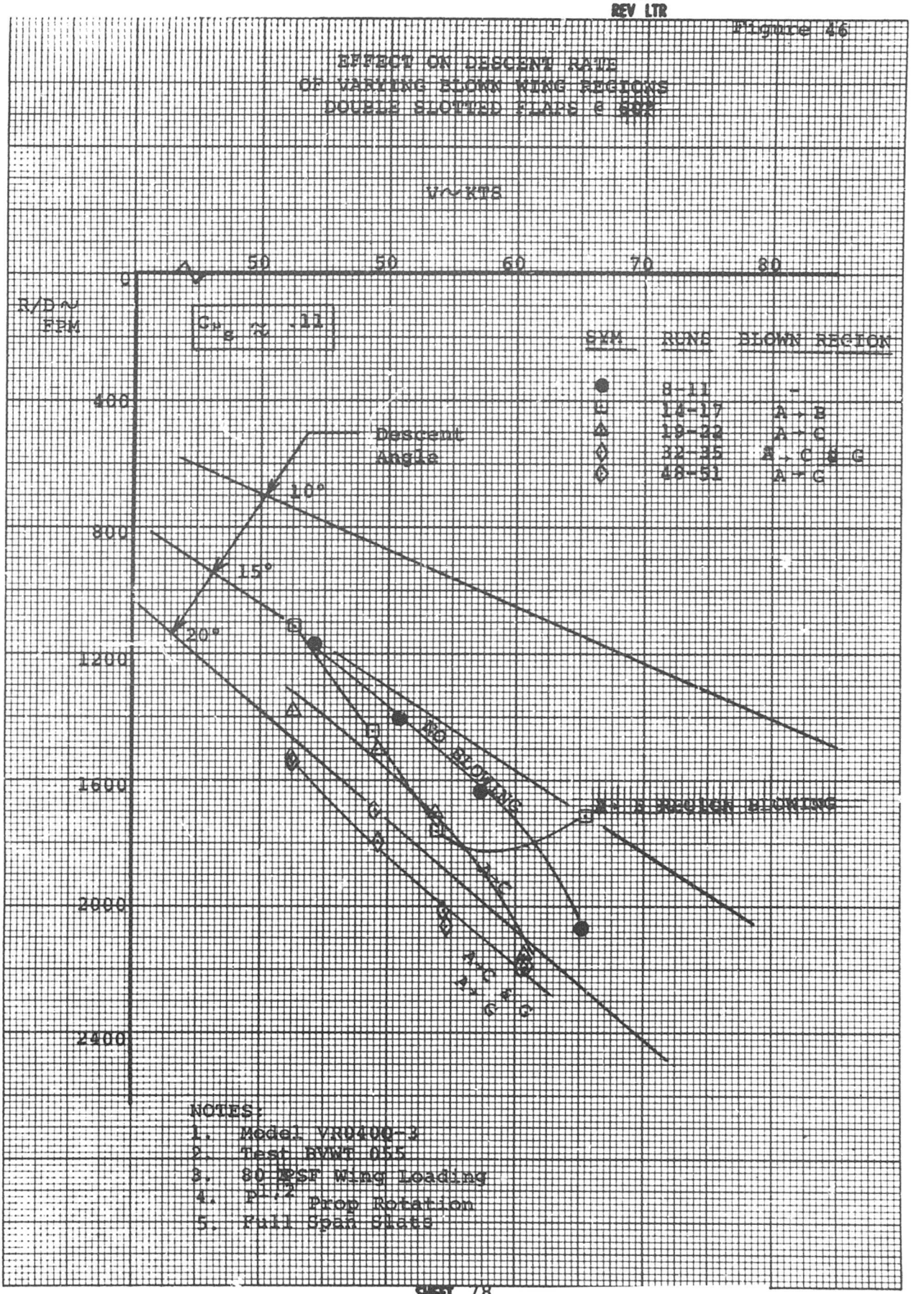

EFFECT ON BUFFET ONSET
OF VARYING BLOWN WING REGIONS
DOUBLE SLOTTED FLAPS @ 60°

Figure 47

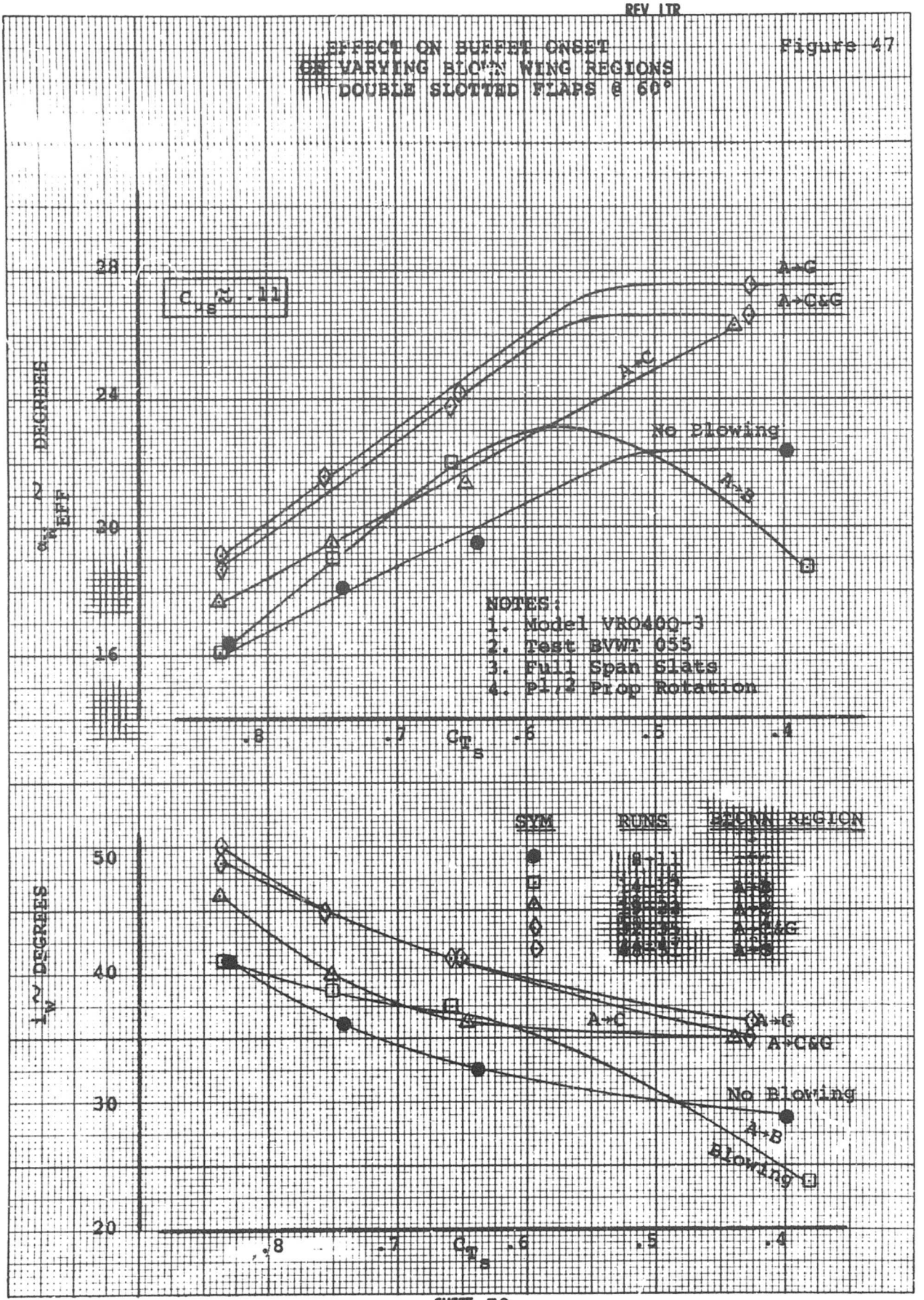

Figure 48

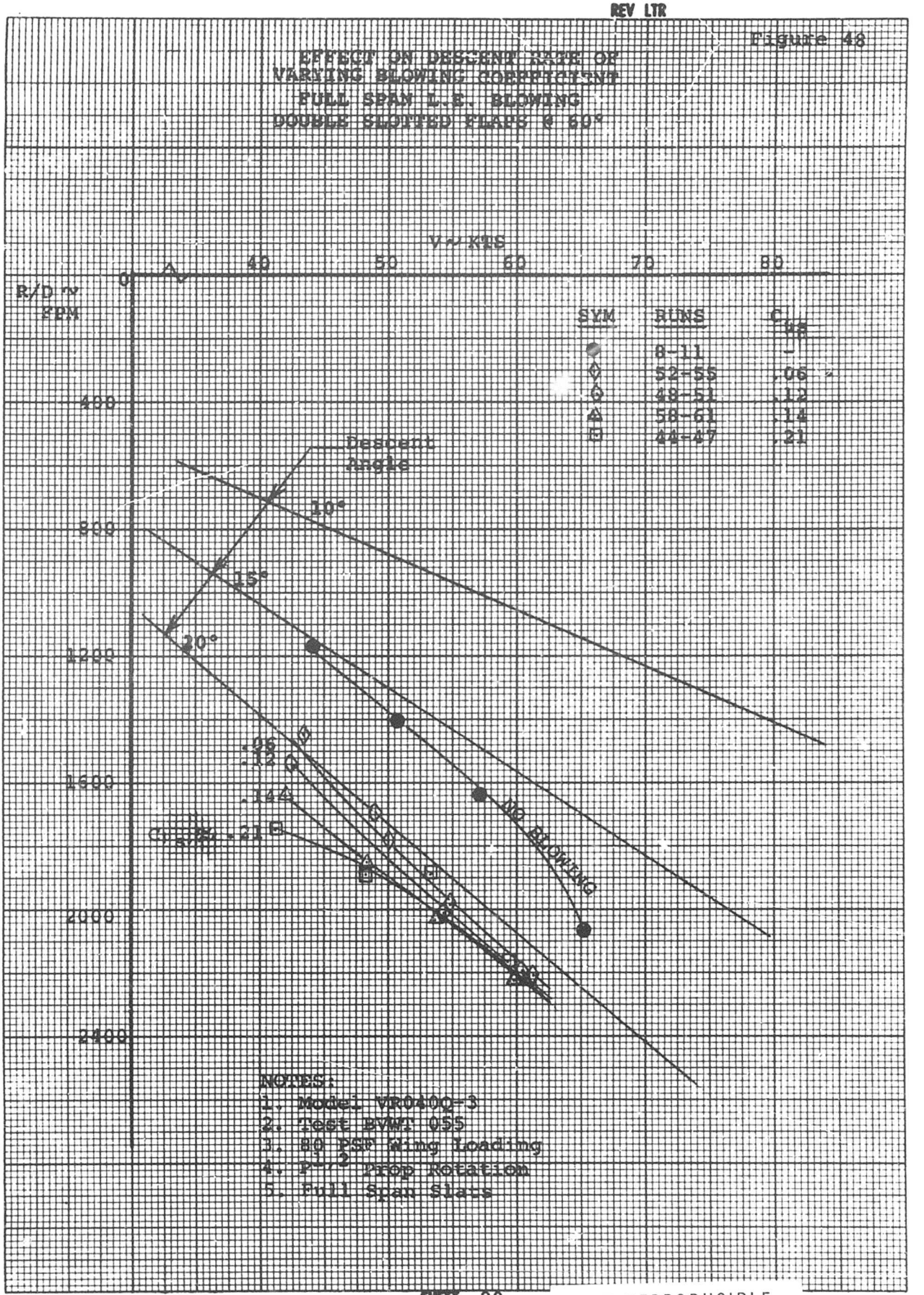

Figure 49

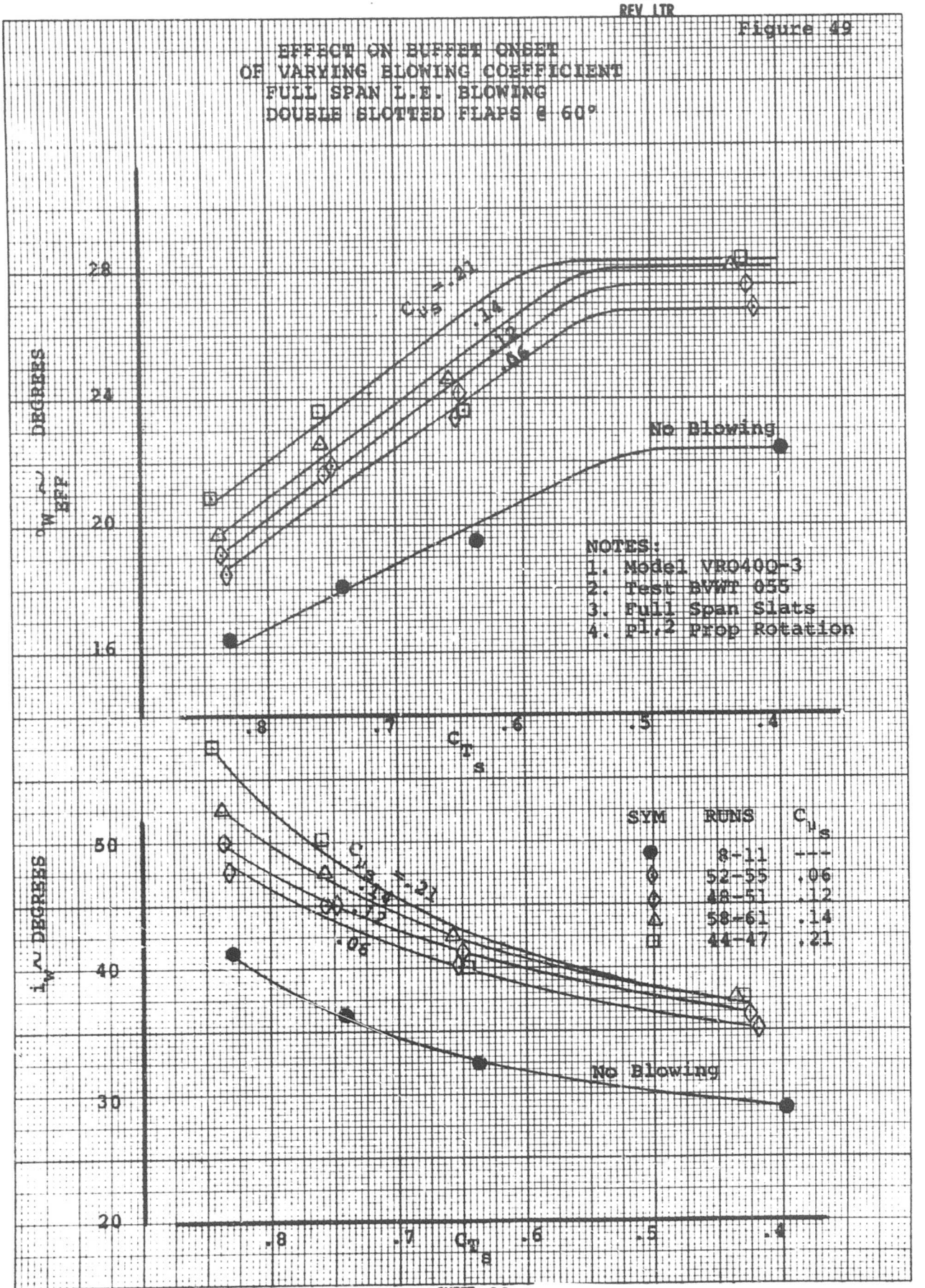

Figure 50

EFFECT ON DESCENT RATE
OF VARYING BLOWING COEFFICIENT
PARTIAL SPAN L.E. BLOWING (A, C, E, G REGIONS)
DOUBLE SLOTTED FLAPS @ 60°

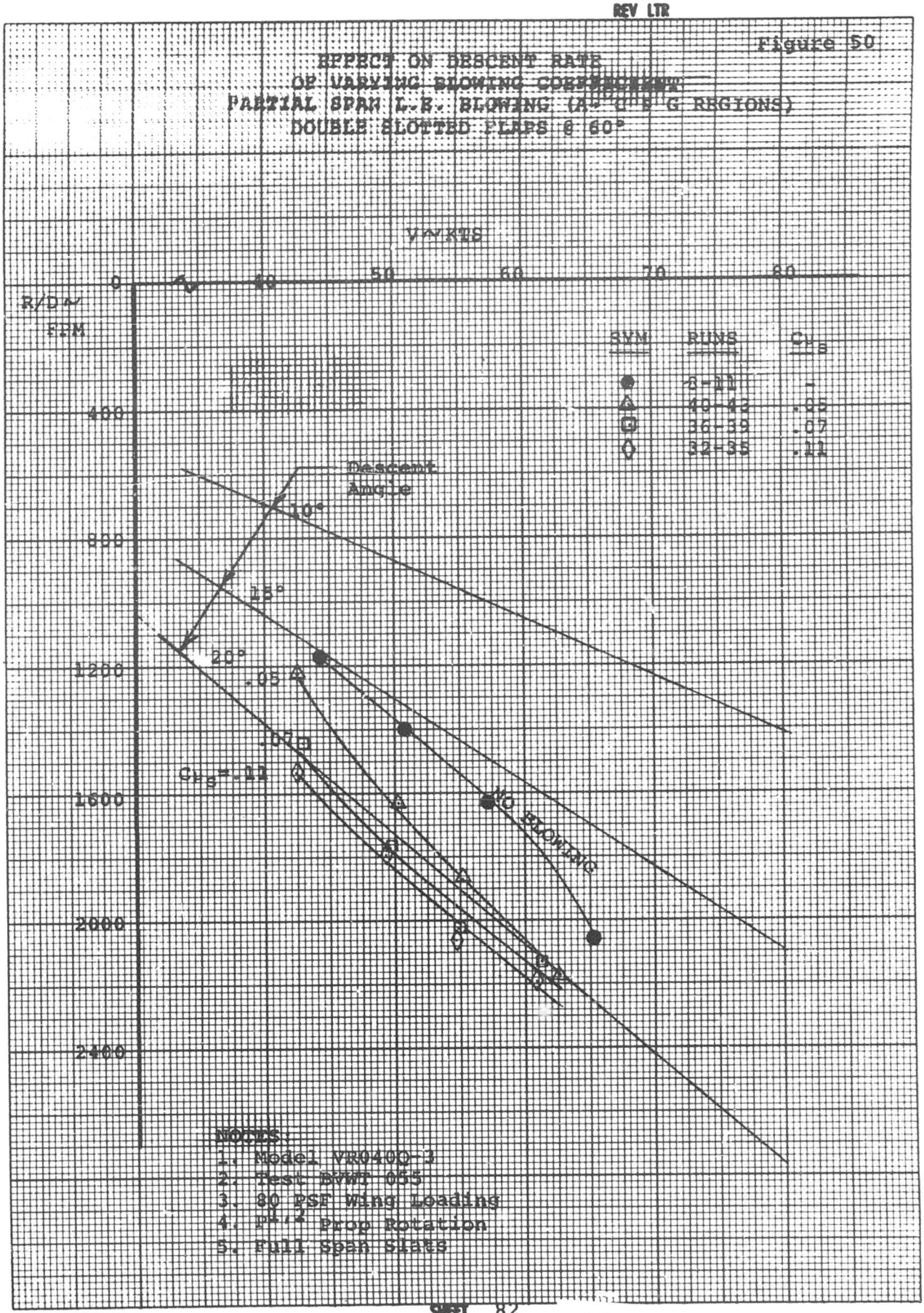

EFFECT ON BUFFET ONSET
OF VARYING BLOWING COEFFICIENT
PARTIAL SPAN L.E. BLOWING (A-CEG REGIONS)
DOUBLE SLOTTED FLAPS @ 60°

Figure 51

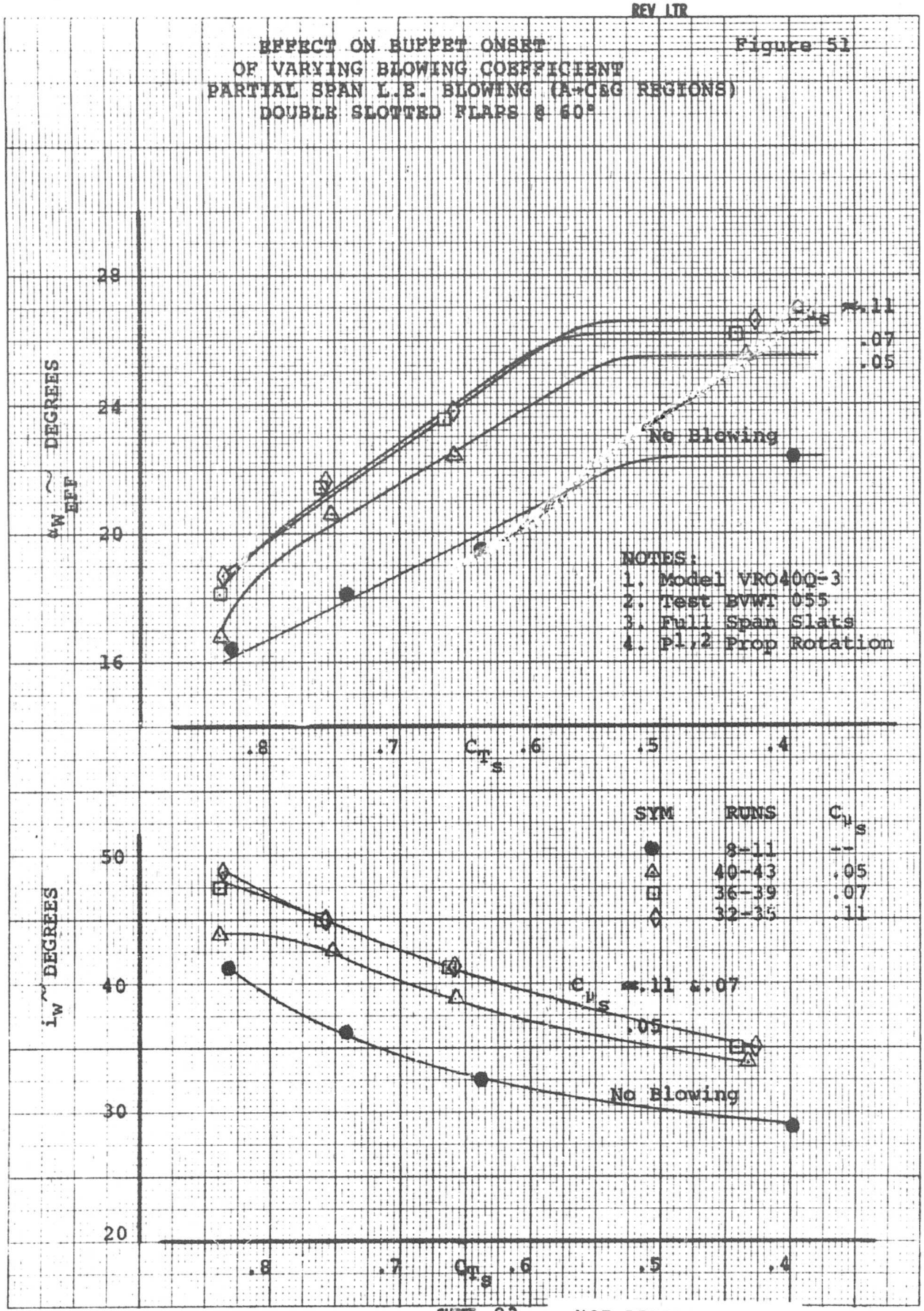

Figure 52

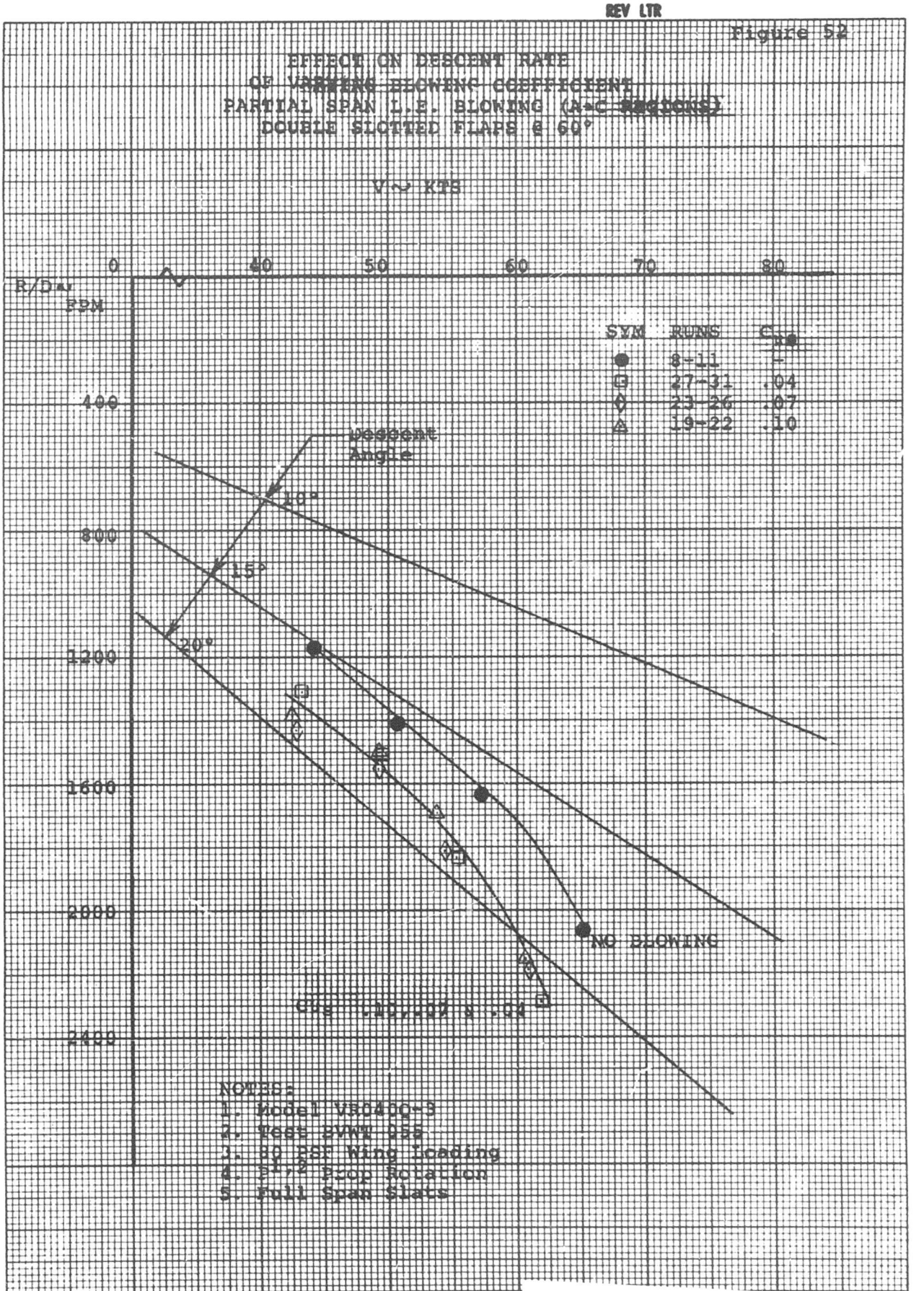

Figure 53

EFFECT OF BUFFER ONSET
OF VARYING BLOWING COEFFICIENT
PARTIAL SPAN L.E. BLOWING (A-C REGIONS)
DOUBLE SLOTTED FLAPS @ 60°

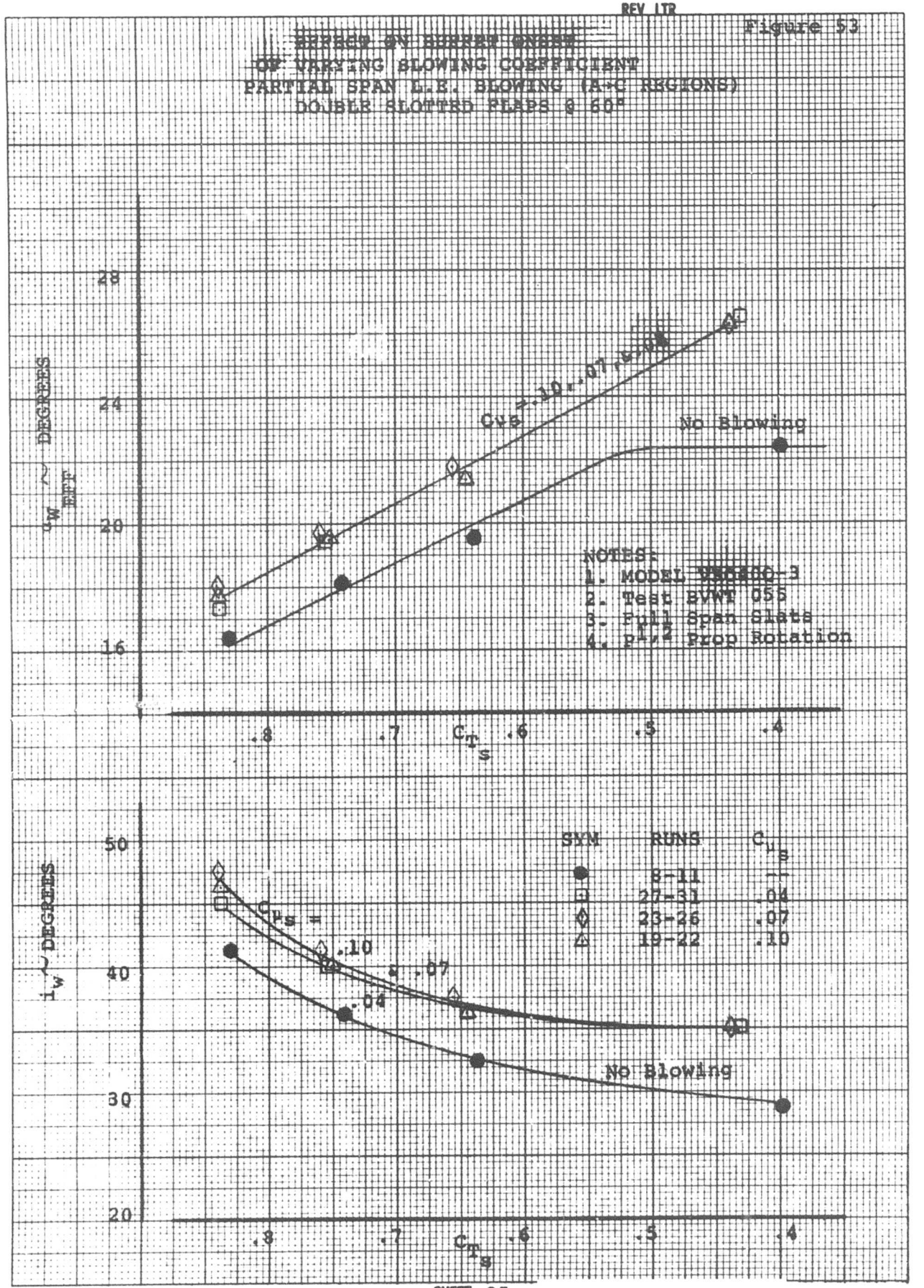

Figure 54

EFFECT OF BLOWING MAGNITUDE
ON DESCENT RATE OF A CONSTANT WING ANGLE
FULL SPAN L.E. BLOWING
DOUBLE SLOTTED FLAPS @ 60°

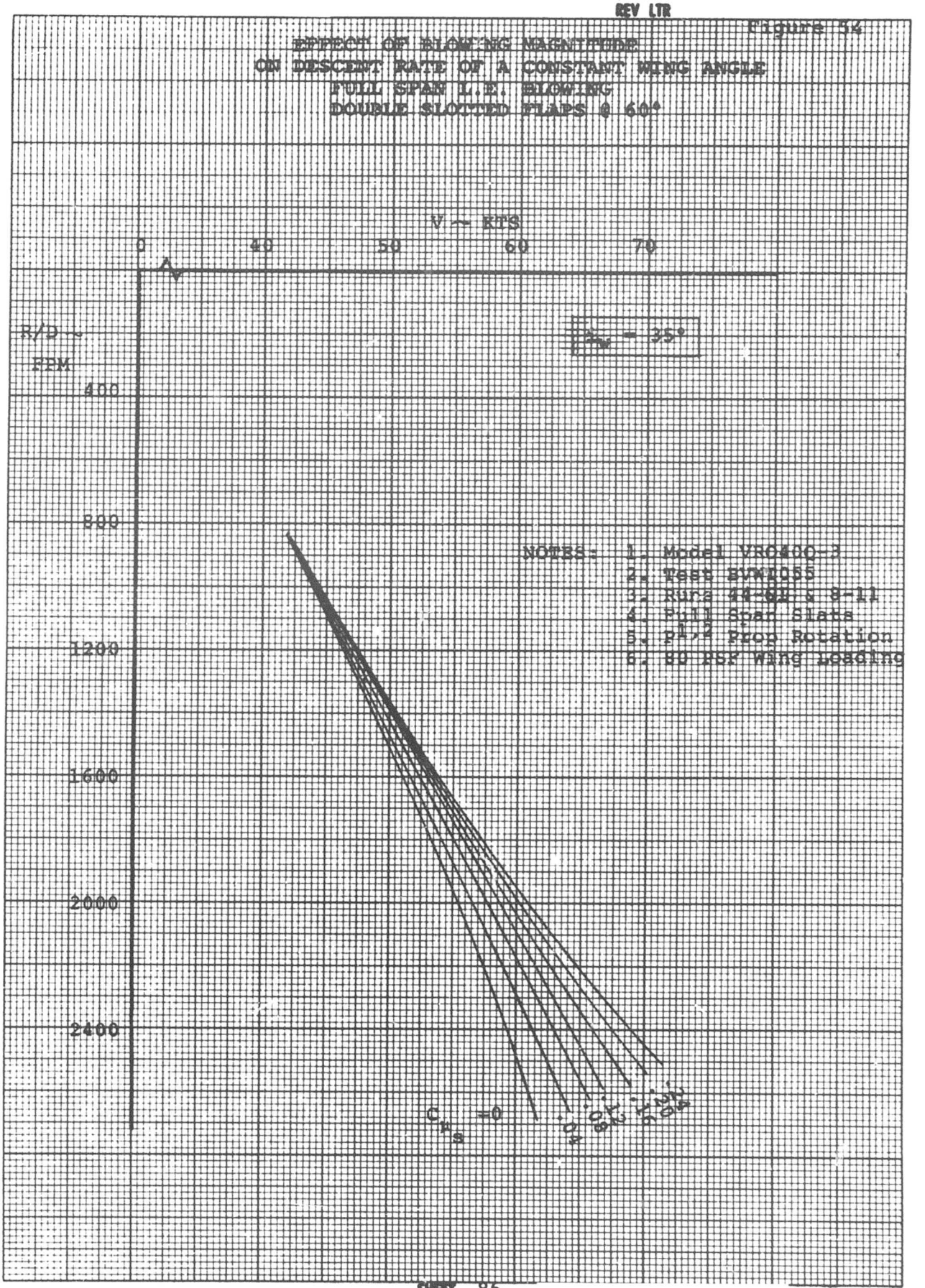

6.11 POWER REQUIRED FOR LEADING EDGE BLOWING

A four prop tilt wing aircraft with a wing area of 1390 ft^2 was chosen to illustrate the BLC system power requirement which is defined by the following equation.

$$HP = \frac{Q \Delta P_{tot}}{\eta\ 550}$$

where η = efficiency of the pump

Q = BLC air volume flux, ft^3/sec

ΔP_{tot} = total pressure rise through the BLC system

$= (P_{tot})_{jet} - (P_{tot})_{amb}$

In terms of C_{μ_s}, the equation for power reduces to

$$HP = \frac{C_{\mu_s} S_E\ q_s}{1100\eta} \sqrt{\frac{2\gamma g R T_D}{\gamma - 1} \left[\left(\frac{P_o}{P_D}\right)^{2/\gamma} - \left(\frac{P_o}{P_D}\right)^{\gamma+1/\gamma} \right]}$$

where q_s = slipstream q = q + T/A

γ = ratio of specific heats = C_p/C_v

R = universal gas constant = 53.3 ft/°F

T_D = absolute duct temperature, degrees Rankine

P_D = duct pressure, lbs/in^2

P_o = ambient pressure, lbs/in^2

Figure 55 depicts the power requirement for a range of blowing coefficients, a typical pressure ratio (P_D/P_o) of 5.0, and aircraft speeds of 40 and 70 knots. Two blowing configuration cases are shown: full span blowing and wing/body center section plus B region blowing. Calculations of power required were made at the following aircraft descent conditions:

V	Rate of Descent
40 knots	1200 fpm
70 knots	2050 fpm

Slipstream q's for these conditions were 36 and 15.5 lb/ft^2, respectively.

The power is shown to be from 1 to 4% of the 30,000 SHP which would be installed in an airplane of this size at a design condition of 40 knots and .06 C_{μ_s}.

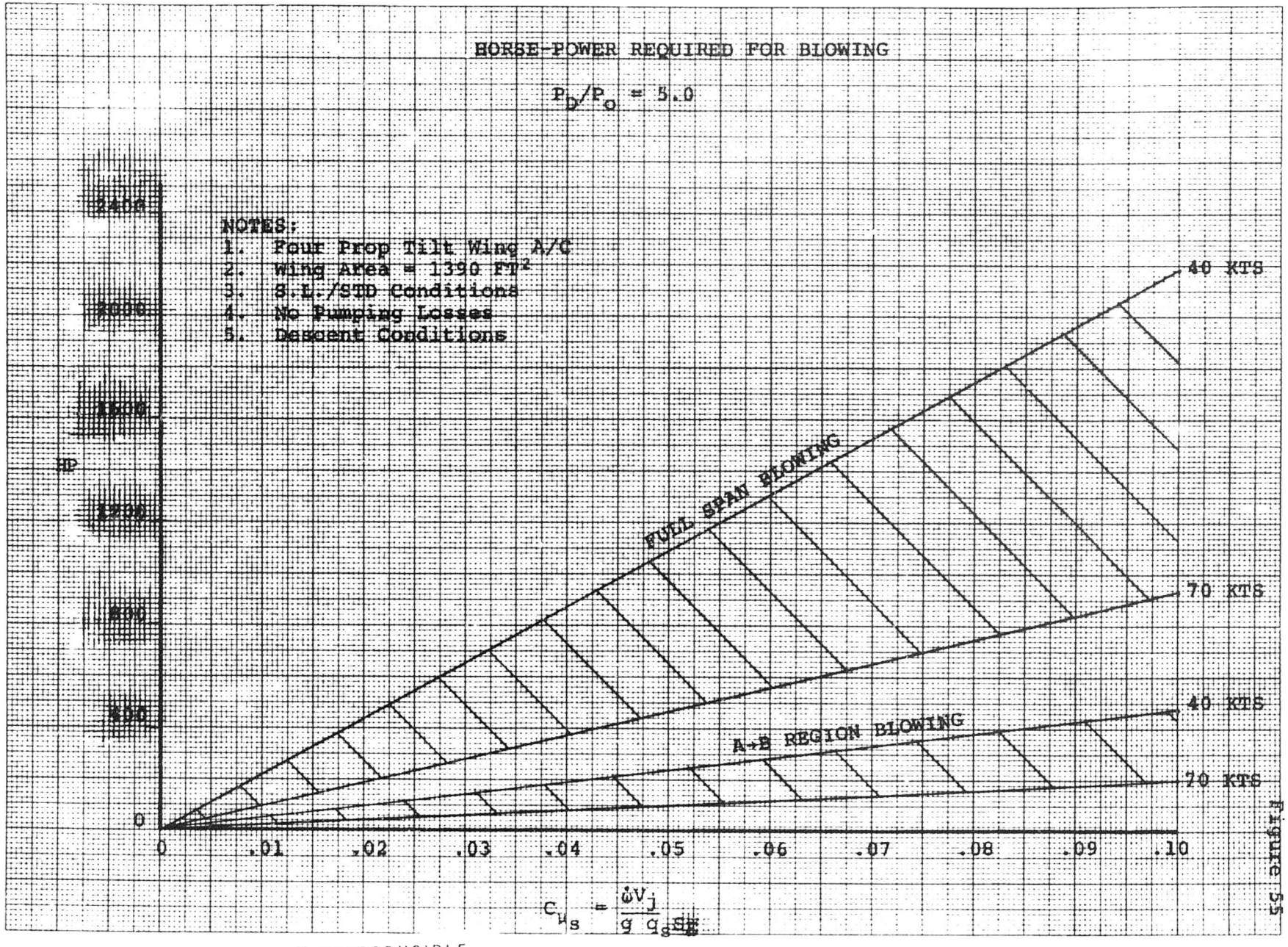

Figure 55

7.0 CONCLUSIONS

The primary conclusions derived from this test are listed below.

a. Full span leading edge BLC provided an average incremental improvement of 400 fpm in landing descent capability over the corresponding non-blown configuration with double slotted flaps set at 60° and full span slats (Figure 20). This increment is of the same order as the loss due to 4° of positive cyclic (Figure 26).

b. Leading edge blowing applied to the wing/body center section and the "B" region (See Figure 2 for definition) increased the stall angle in these areas by 18° and 10°, respectively (Figure 24).

c. The loss in descent capability due to positive cyclic coupled with either full span or partial span (excludes wing area between nacelles) L.E. blowing averages 100 fpm per degree of cyclic (Figures 26 and 29). Data from this test indicates that this loss is largely due to a decrease in turning effectiveness instead of a decrease in stall angle (Figure 28).

d. Previous tilt wing test data indicated that the "both-down-between-nacelles" prop rotation ($P^{1,2}$) resulted in substantially greater descent performance than with the opposite inboard prop rotation ($P^{1,1}$"both-down-inboard"). Full span leading blowing reduced this difference to approximately 100 fpm for the cases where 0°, 4°, and 6° of positive cyclic was employed (Figure 33).

e. Changing azimuth lead of cyclic angle input from 15°to 45°, reduced the descent capability by approximately 300 fpm.

f. The 60° double slotted flaps utilized provide an incremental improvement of 300 fpm descent capability over the 45° single slotted flap configuration. This comparison, performed with full span L.E. blowing coupled with +4° of cyclic is in agreement with conclusions derived from previous non-L.E. blowing tilt wing test data.

g. Leading edge blowing without full span slats results in an increase in descent capability at speeds less than 50 kts and a decrease (300 fpm) at higher speeds (Figure 43).

h. The two mid-span fences (between nacelles) can be removed with no deterioration in descent capability when full span leading edge blowing is employed (Figure 45).

i. Leading edge blowing was not incorporated on the nacelles. This did not detract from the ability of the leading edge blowing system to increase the wing stall angle over the non-blown case, i.e. wing stall did not initially occur over the nacelles.

j. No measureable difference in descent capability occurred between the full span leading edge blowing configuration and the partial span case (inboard panel plus tip panel). See Figure 46. However, when positive cyclic was coupled with the noted partial span L.E. blowing configuration, a premature stall was apparent at the highest speed tested (Figure 29).

APPENDIX A - 3-COMPONENT FORCE AND MOMENT DATA

Appendix A includes the on-line data plots obtained during the subject test. They are presented as sets of L/qb^2 vs D/qb^2, L/qb^2 vs i_w and C_{m_s} vs i_w graphs in the order in which they were discussed in Section 6.0. Each plot contains the series of runs (four tunnel q's) performed for each model configuration. The nominal slipstream thrust coefficient (C_{T_s}) corresponding to each noted tunnel q is presented on Figure 15 for collective hubs and Figure 18 for cyclic hubs. The Figure Index on the following page describes the major model configuration features applicable for each run.

Following is a discussion concerning Run 156 that has not been discussed previously. Sealing was thought to be necessary to assure that airflow did not leak through the wing root into the tunnel test section area below the ground board. To investigate this, the "added sealing" was removed for the last run of the test (Run 156). No difference could be detected between the data from Run 156 and the comparison run (Run152).

APPENDIX A ~ FIGURE INDEX

FIGURES	RUNS	PROP ROTATION	FLAP	δ_F	BLOWN REGION	C_{μ_s}	HUBS	CYCLIC ANGLE	REMARKS
56-58	8-11	$P^{1,2}$	Double Slotted	60°	None	-	Coll	-	
59-61	69-72	↓	↓	60°	A→G	.09	Coll	-	
62-64	148-151		Single Slotted	45°	A→G	.11	Cyclic	0°	(3)Outb. Fences Off
65-67	152-155		↓	45°	None	-	Cyclic	0°	(3)Outb. Fences Off
68-70	82-85		Double Slotted	60°	A→G	.11	Cyclic	0°	
71-73	87-90				A→G	.11		+4°	15° Lead On Cyclic
74-76	110-113				A→G	.12		+6°	↓
77-79	114-117				A→G	.12		-4°	
80-82	102-105				A→C&G	.11		0°	
83-85	93-96				A→C&G	.11		+4°	15° Lead on Cyclic
86-88	106-109				A→C&G	.11		+6°	↓
89-91	119-112	$P^{1,1}$			A→G	.11		0°	
92-94	123-126	↓			A→G	.11		+4°	15° Lead On Cyclic
95-97	127-130				A→G	.12		+6°	↓
98-100	65-68				A→G	.09	Coll	-	
101-103	97-100	$P^{1,2}$			A→C&G	.12	Cyclic	+4°	45° Lead On Cyclic
104-106	140-143		Single Slotted	45°	A→G	.11		+4°	(3)Outbd. Fences Off
107-109	144-147		↓	30°	A→G	.11		+4°	(3)Outbd. Fences Off
110-112	136-139		Double Slotted	60°	A→G	.11		+4°	(3)Outbd. Fences Off
113-115	132-135				A→G	.11		+4°	L.E. Slats Off
116-118	14-17				A→B	.10	Coll	-	
119-121	19-22				A→C	.10		-	
122-124	32-35				A→C&G	.11		-	
125-127	48-51				A→G	.12		-	
128-130	52-55				A→G	.06		-	
131-133	58-61				A→G	.14		-	
134-136	44-47				A→G	.21		-	
137-139	40-43				A→C&G	.05		-	
140-142	36-39				A→C&G	.07		-	
143-145	27-31				A→C	.04		-	
146-148	23-26				A→C	.07		-	
149-151	156		Single Slotted	45°	None	-	Cyclic	0°	Wing Root "Added Sealing" Removed

BASE RUNS - NO BLOWING

DOUBLE SLOTTED FLAPS @60°

COLLECTIVE HUBS

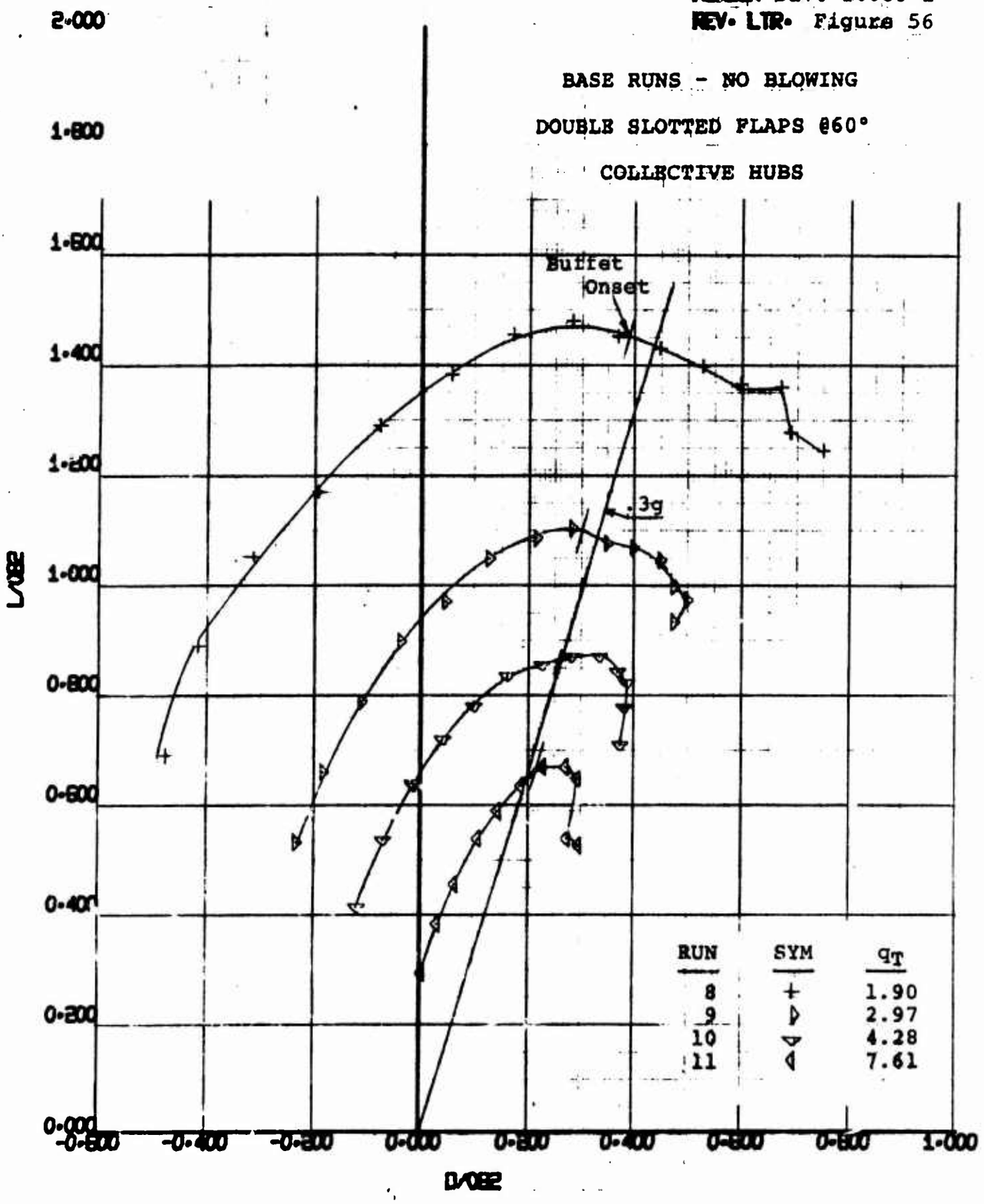

170 HALF SPAN MODEL WR 040 0-3 L/QR2 VS D/QR2	BMWT 55 4/ 3/70

NUMBER D170-10036-1
REV. LTR. Figure 57

BASE RUNS - NO BLOWING
DOUBLE SLOTTED FLAPS @60°
COLLECTIVE HUBS

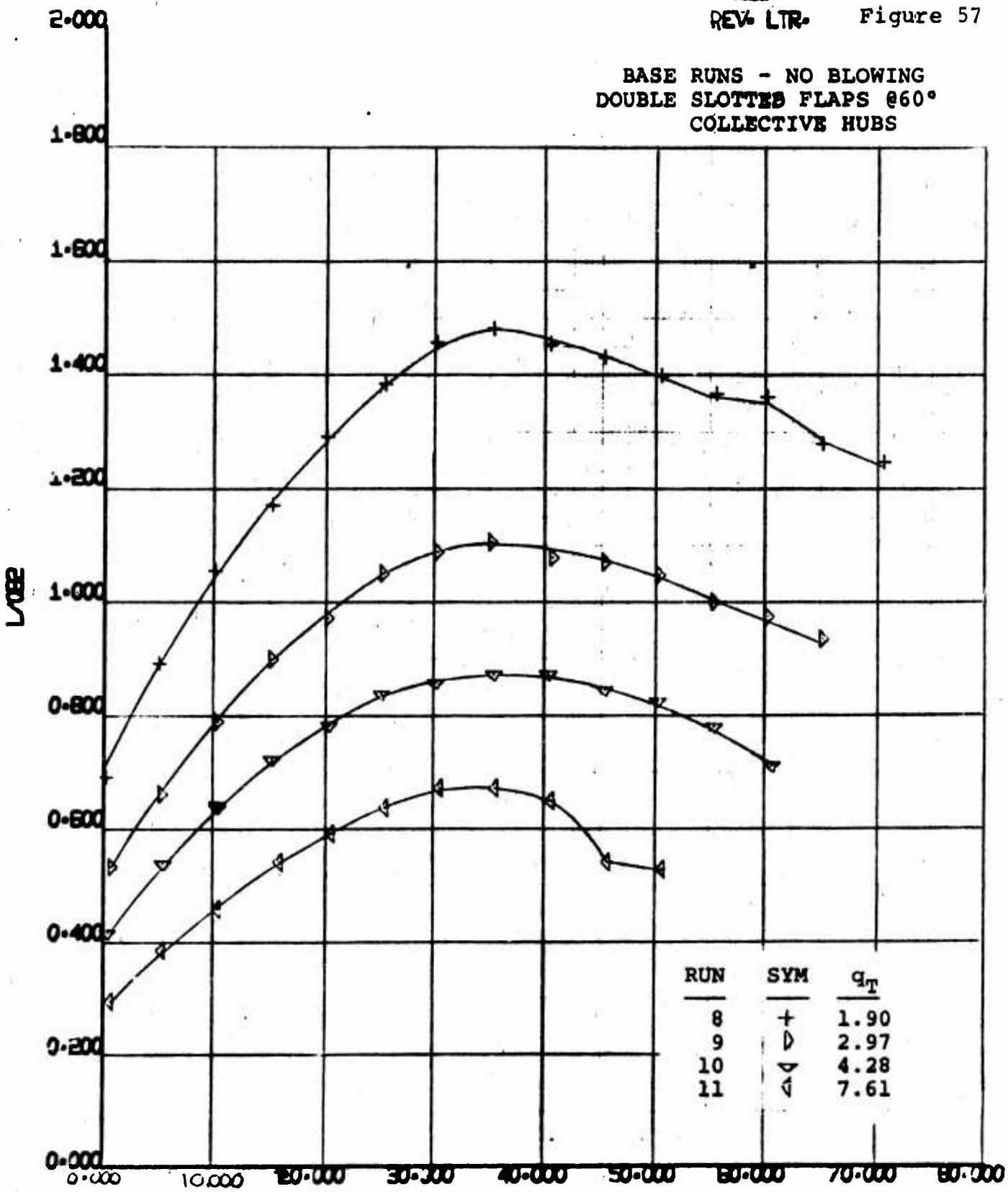

170 HALF SPAN MODEL	BMT 55
VR 40 0-3	
L/Q2 VS WING TILT ANGLE	4/ 3/70

SHEET 95

NUMBER D170-10036-1
REV. LIR-

Figure 58
BASE RUNS - NO BLOWING
DOUBLE SLOTTED FLAPS @60°
COLLECTIVE HUBS

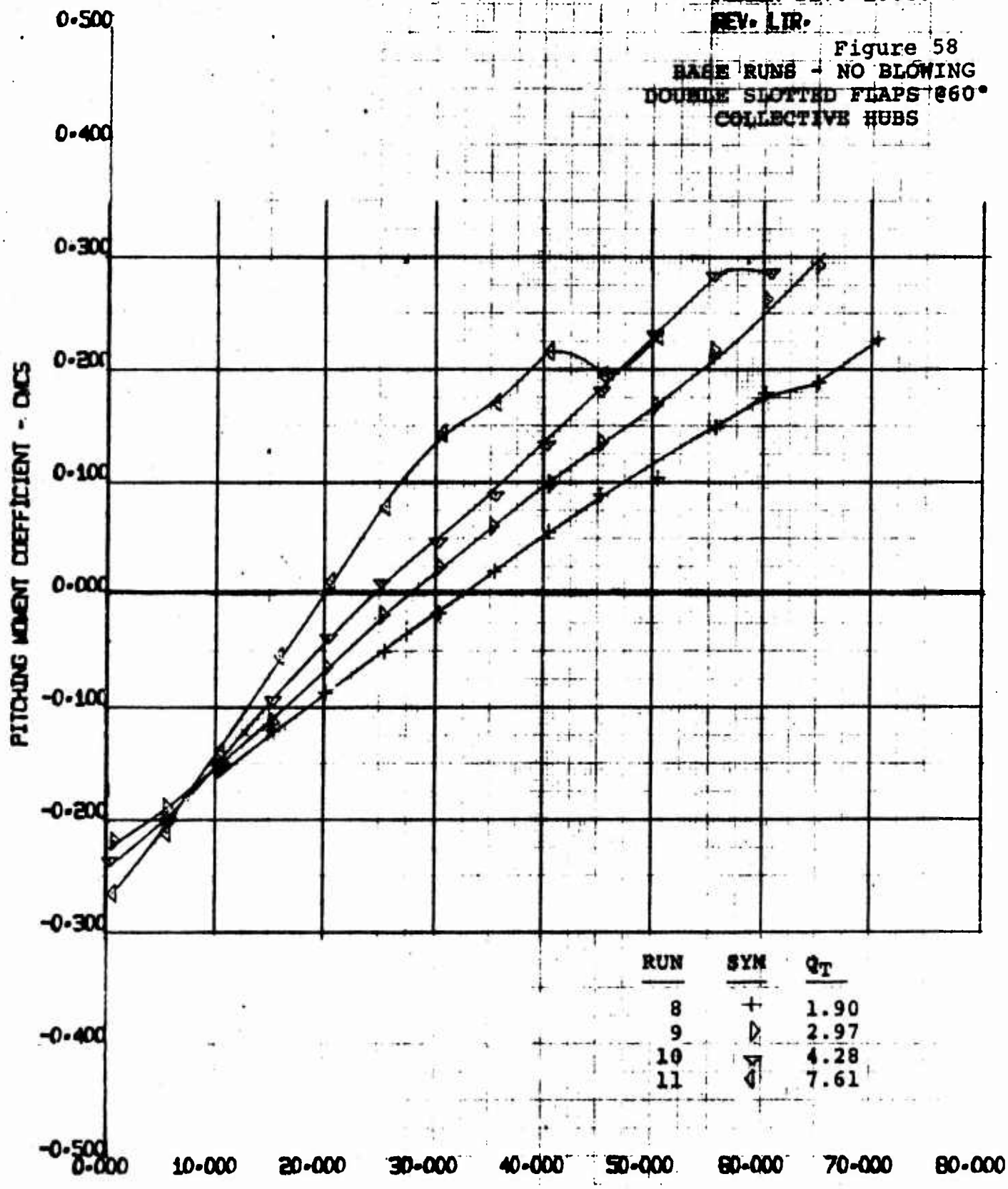

170 HALF SPAN MODEL WR 040 0-3 WING TILT ANGLE VS CMCS	BVWT 55 4/ 3/70

FULL SPAN BLOWING (A→G) $C_{\mu_s} \approx .09$

DOUBLE SLOTTED FLAPS @ 60°

COLLECTIVE HUBS

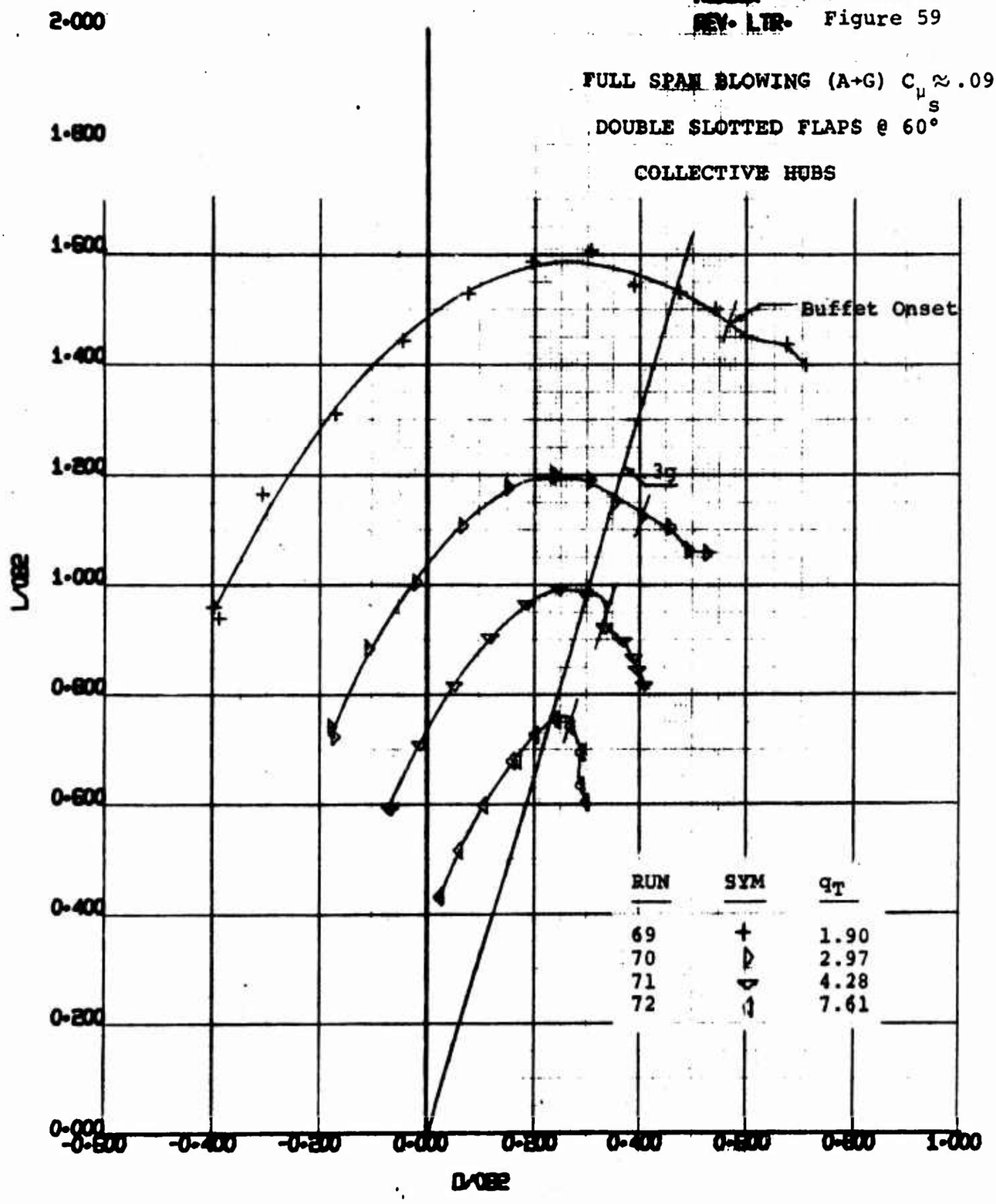

170 HALF SPAN MODEL VR 040 0-3 L/QS2 VS D/QS2	BMT 55 4/ 7/70

FULL SPAN BLOWING (A→G)$C_{\mu_s} \approx .09$

DOUBLE SLOTTED FLAPS @ 60°

COLLECTIVE HUBS

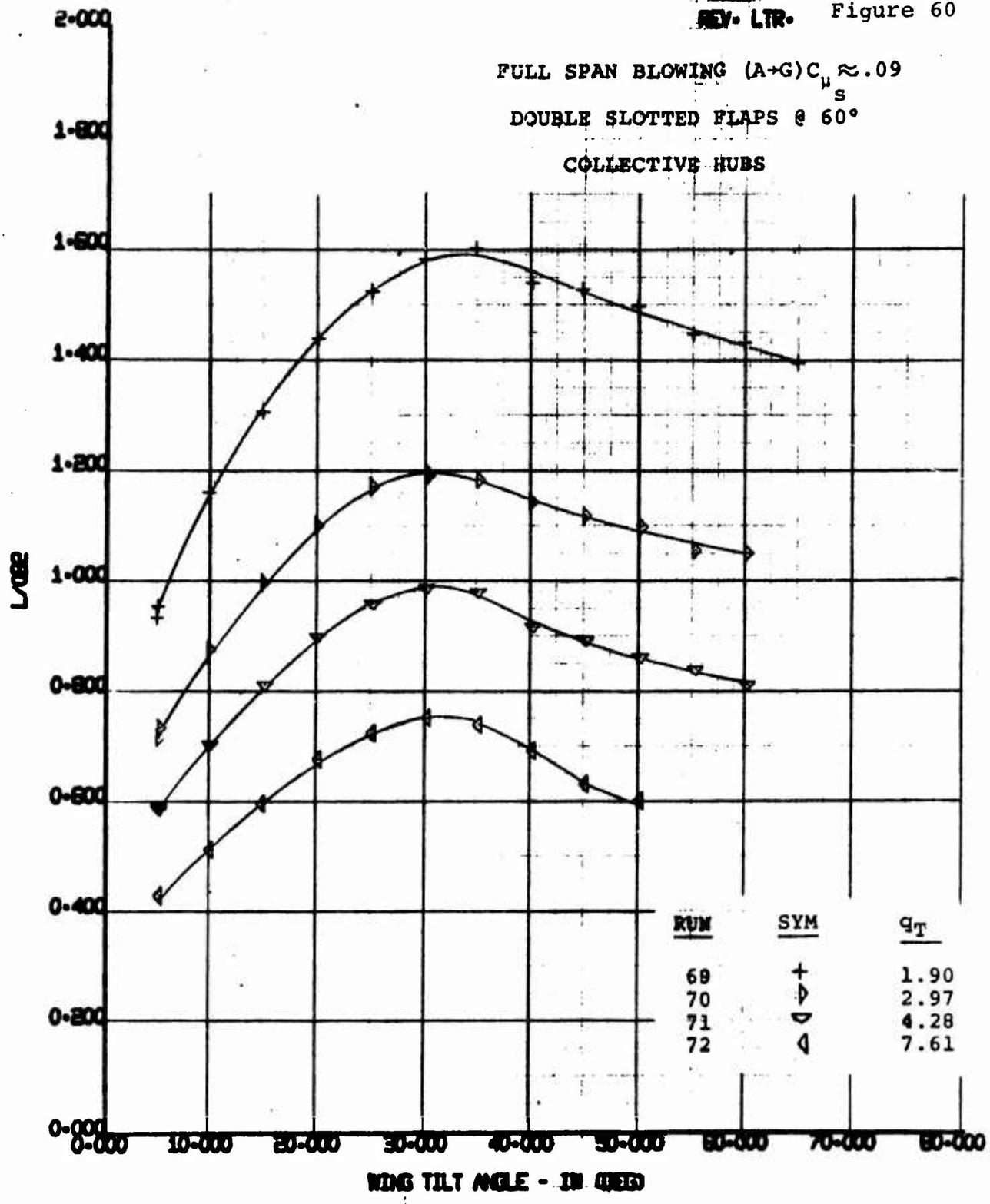

170 HALF SPAN MODEL VR 040 0-3 L/QR2 VS WING TILT ANGLE	BVWT 55 4/ 7/70

FULL SPAN BLOWING (A+G)$C_{\mu_s} \approx .09$

DOUBLE SLOTTED FLAPS @ 60°

COLLECTIVE HUBS

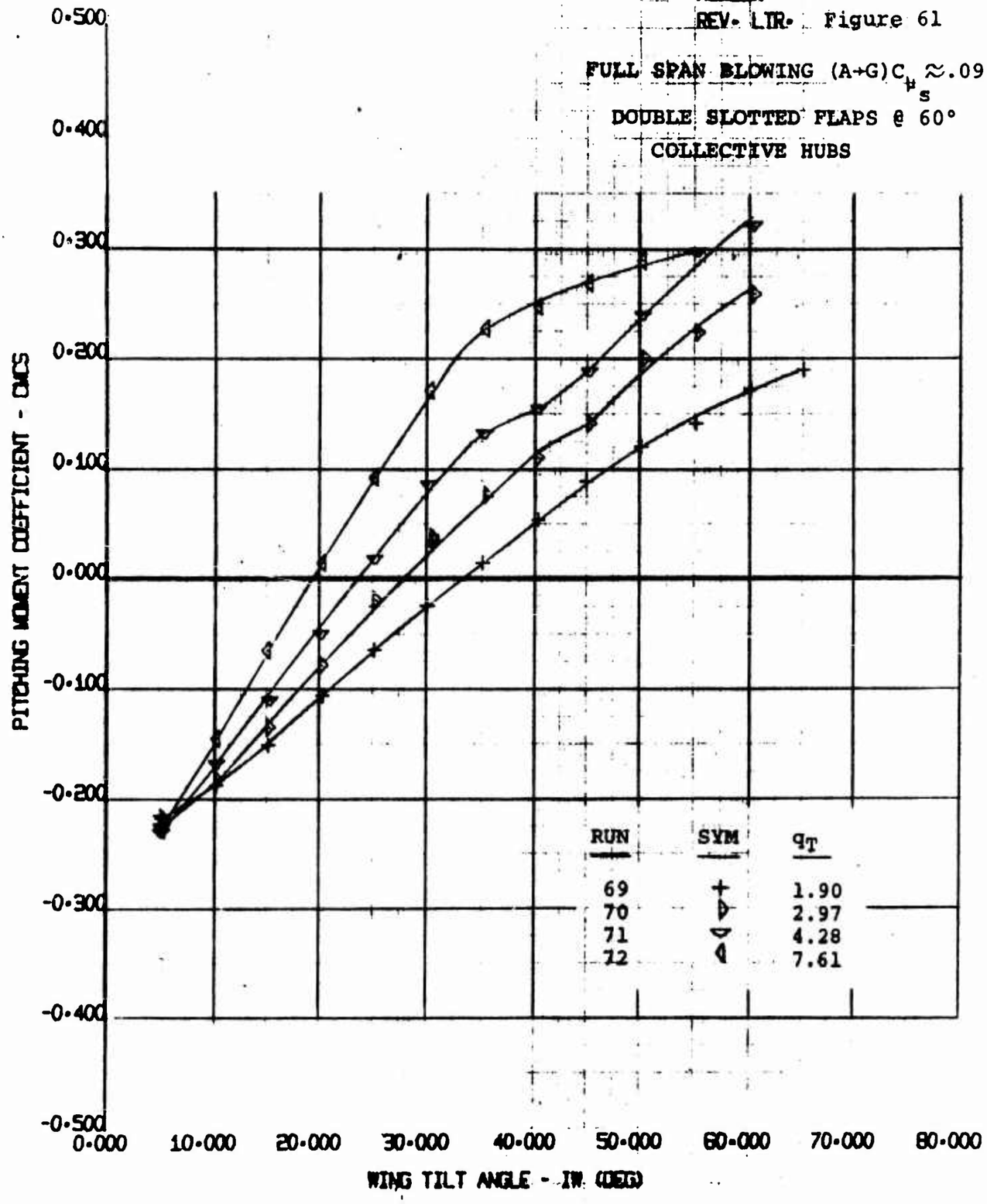

170 HALF SPAN MODEL VR 040 0-3 CMCS VS TILT WING ANGLE	BVWT 55 4/ 7/70

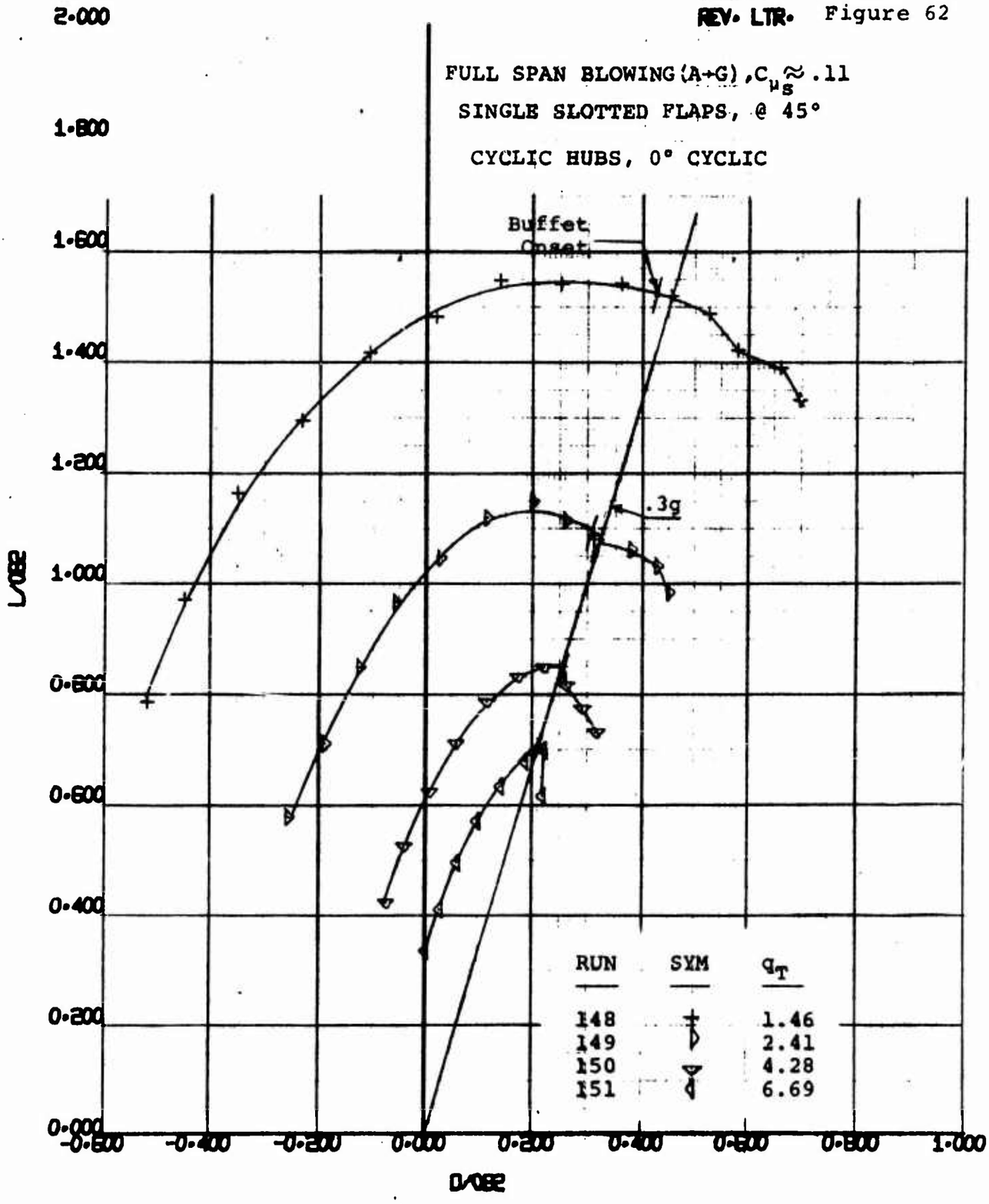

NOTE: (3) OUTBOARD FENCES OFF

170 HALF SPAN MODEL VR 040 0-3 L/QS2 VS D/QS2	BWT 55 4/ 8/70

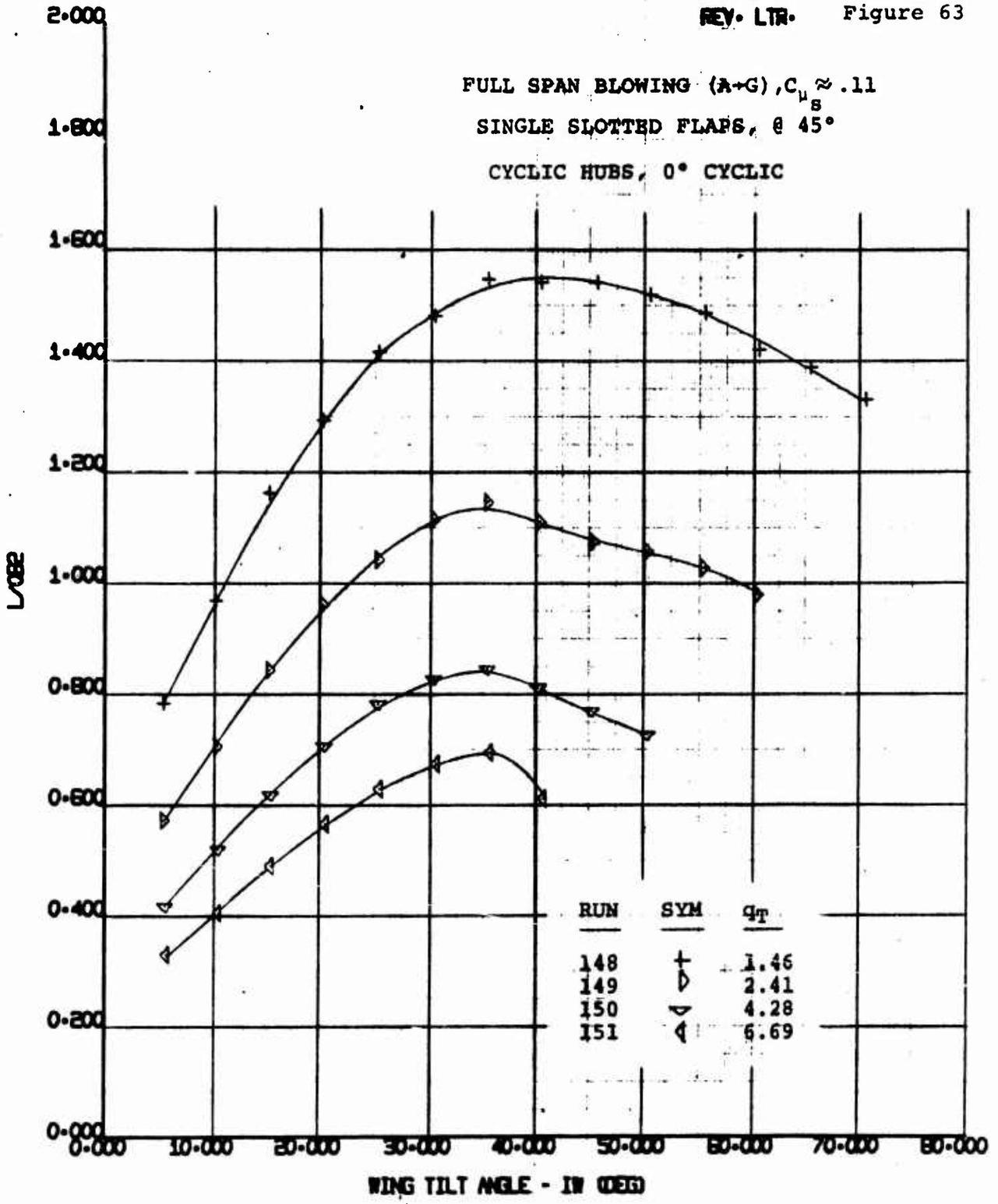

NOTE: (3) OUTBOARD FENCES OFF

170 HALF SPAN MODEL VR 040 0-3 L/QB2 VS WING TILT ANGLE	BWT 55 4/ 8/70

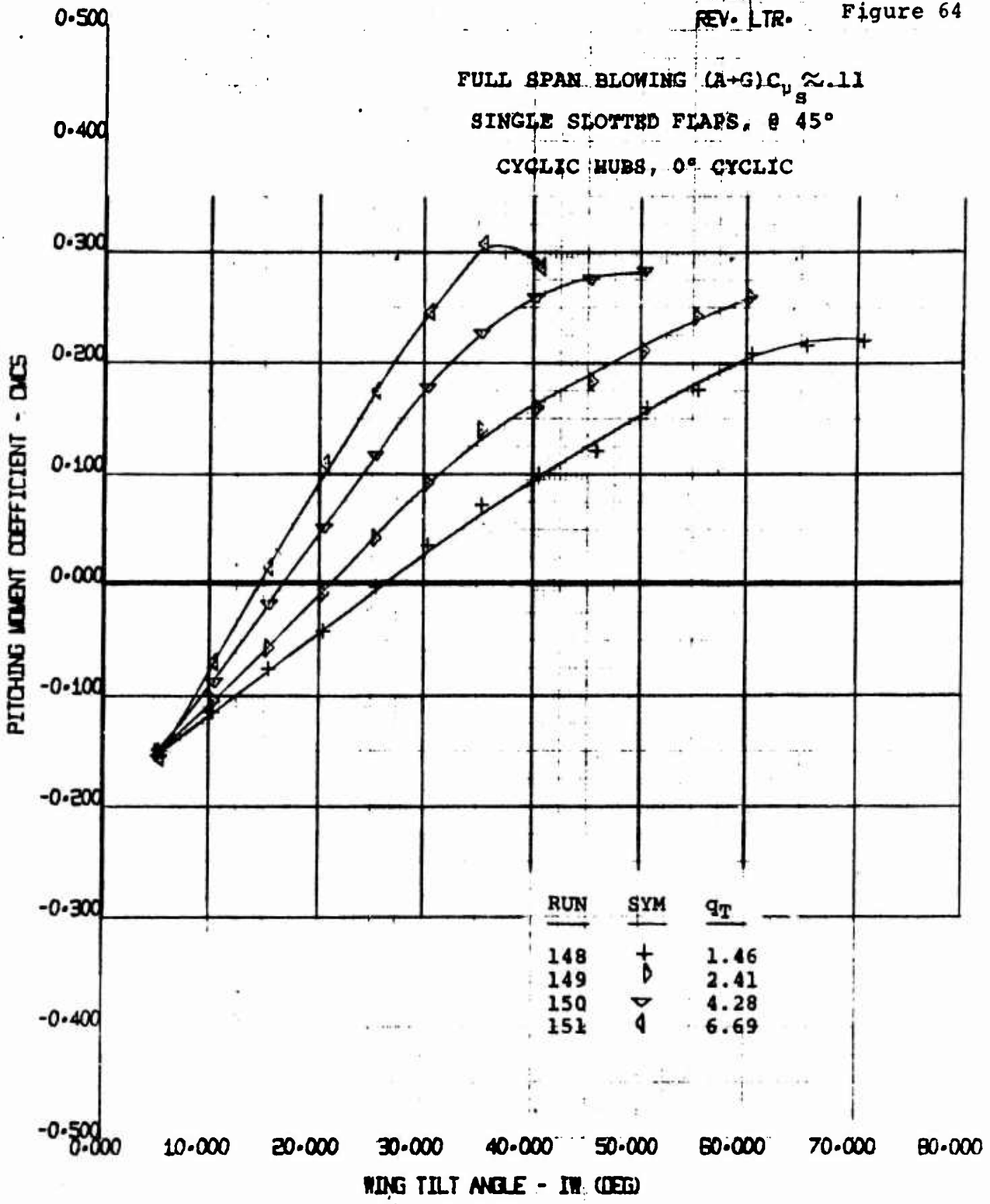

NOTE: (3) OUTBOARD FENCES OFF

170 HALF SPAN MODEL VR 040 0-3 CMCS VS TILT WING ANGLE	BVWT 55 4/ 8/70

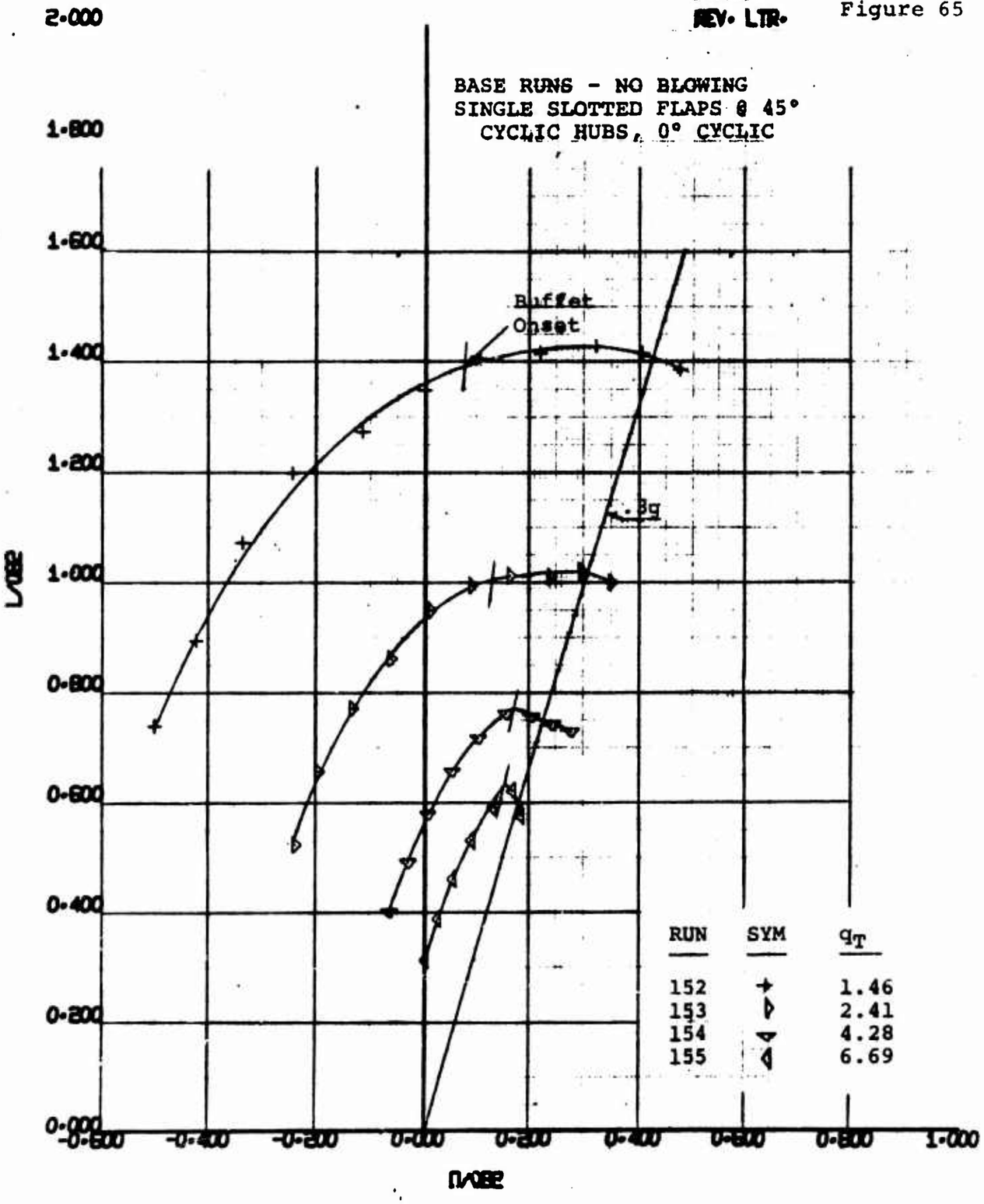

NOTE: (3) OUTBOARD FENCES OFF

170 HALF SPAN MODEL WR 040 0-3 L/QBZ VS D/QBZ	BMT 55 4/ 8/70

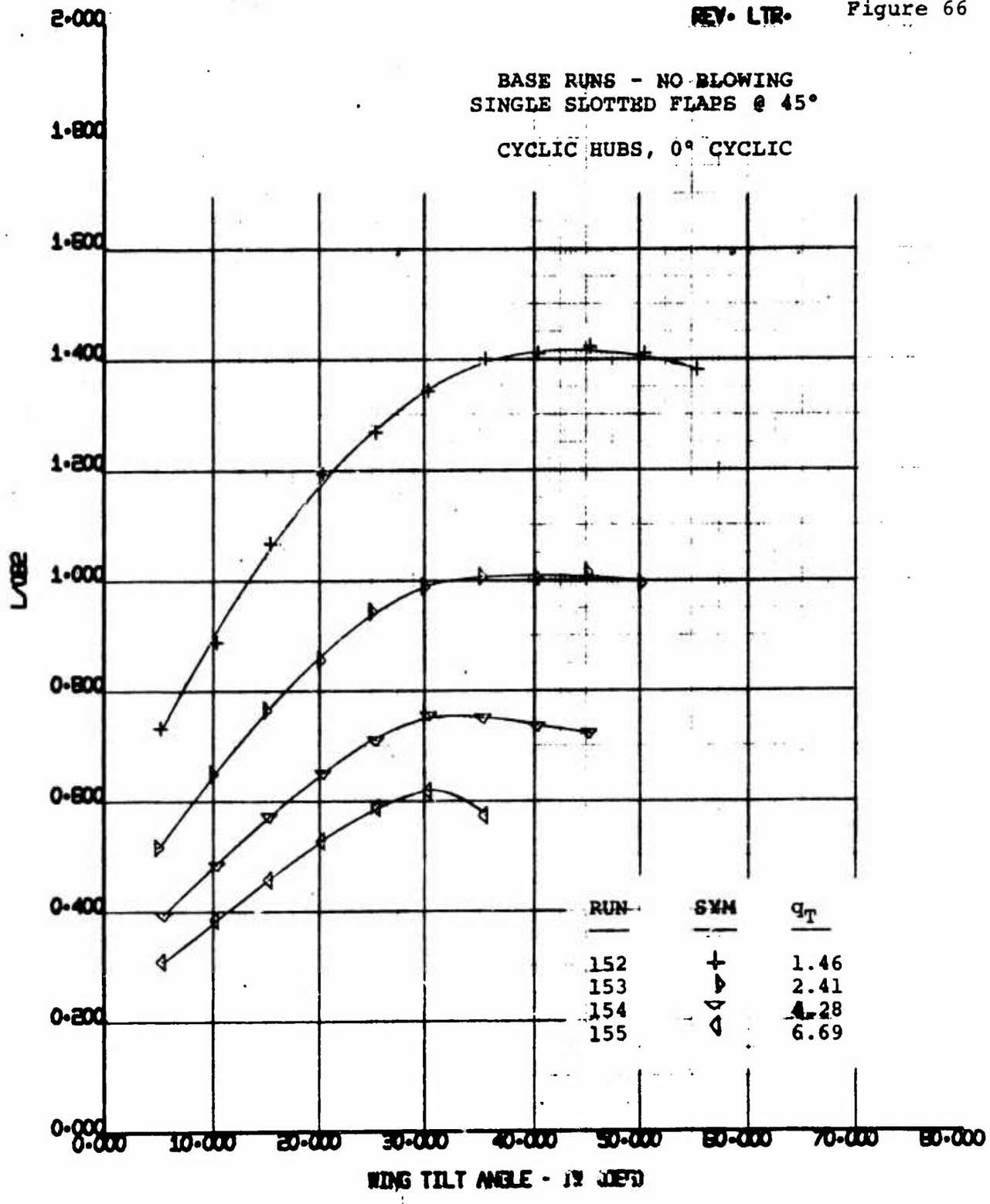

NOTE: (3) OUTBOARD FENCES OFF

170 HAL SPAN MODEL WR 040 0-3 L/QB2 VS WING TILT ANGLE	BWT 55 4/ B/70

BASE RUNS - NO BLOWING
SINGLE SLOTTED FLAPS @ 45°
CYCLIC HUBS, 0° CYCLIC

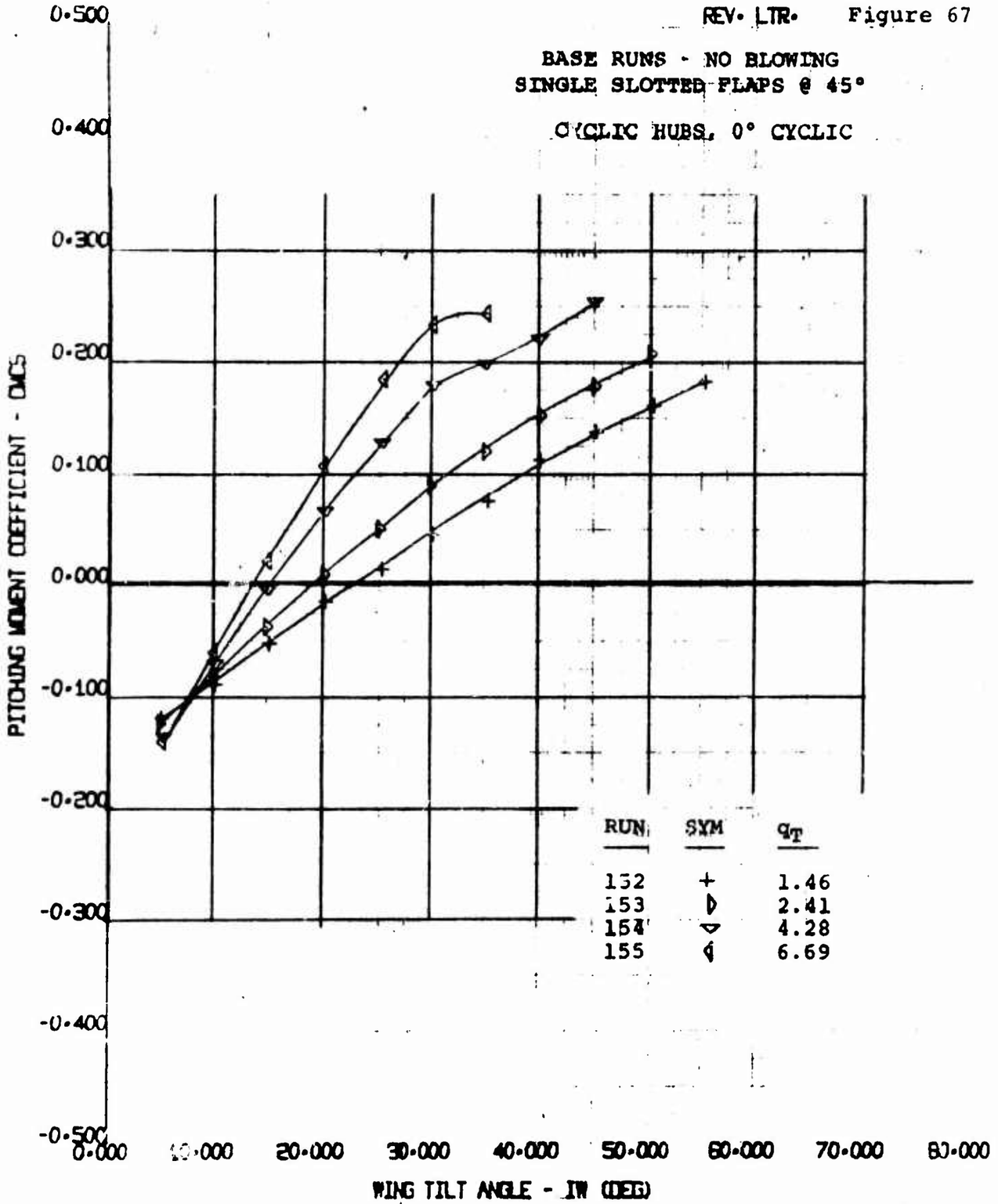

NOTE: (3) OUTBOARD FENCES OFF

170 HALF SPAN MODEL VR 040 0-3 CMCS VS TILT WING ANGLE	BWT 55 4/ 8/70

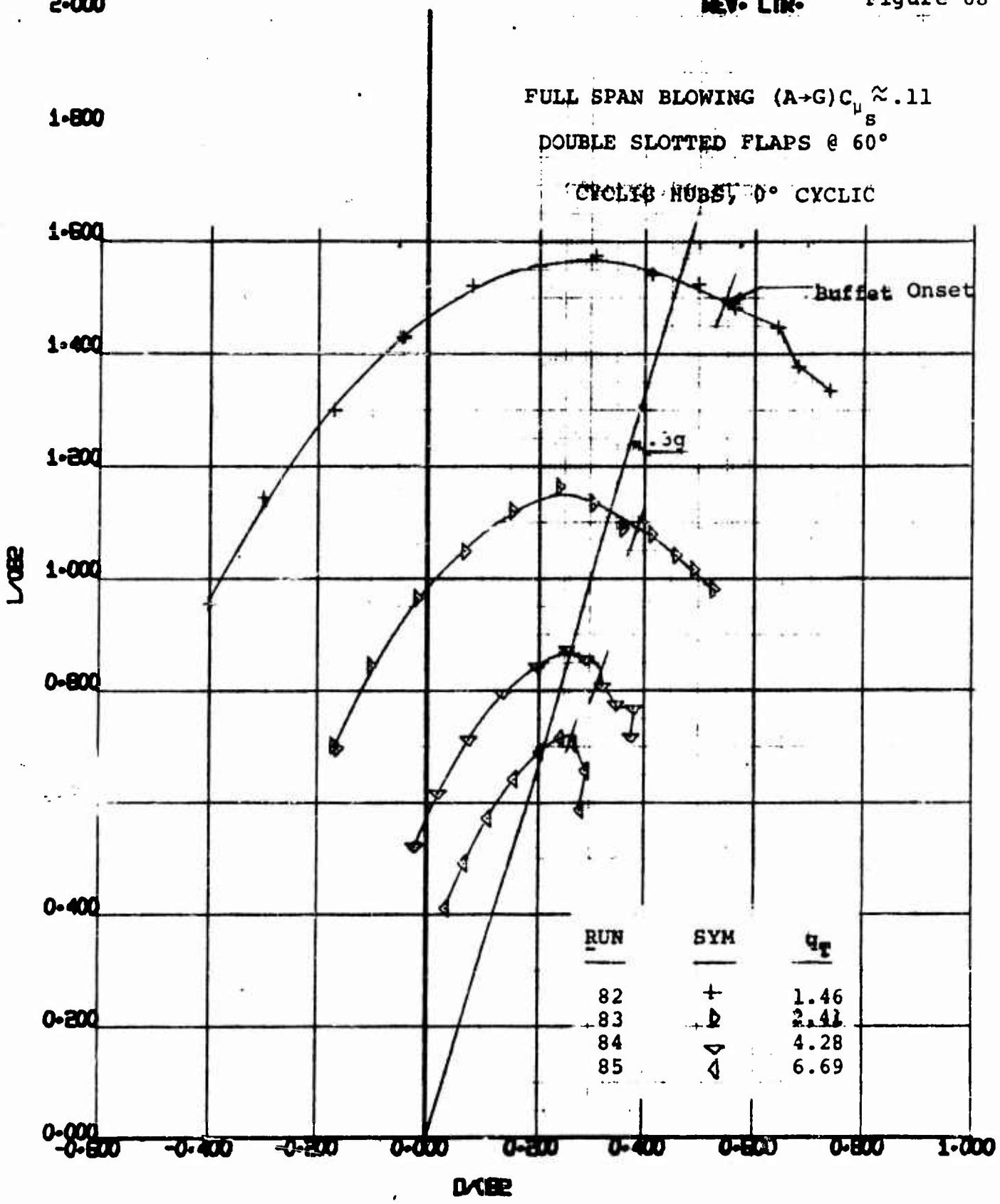

170 HALF SPAN MODEL VR 040 0-3 L/QBAR VS D/QBAR	BMWT 55 4/ 7/70

FULL SPAN BLOWING (A→G) $C_{\mu_s} \approx .11$

DOUBLE SLOTTED FLAPS @ 60°

CYCLIC HUBS, 0° CYCLIC

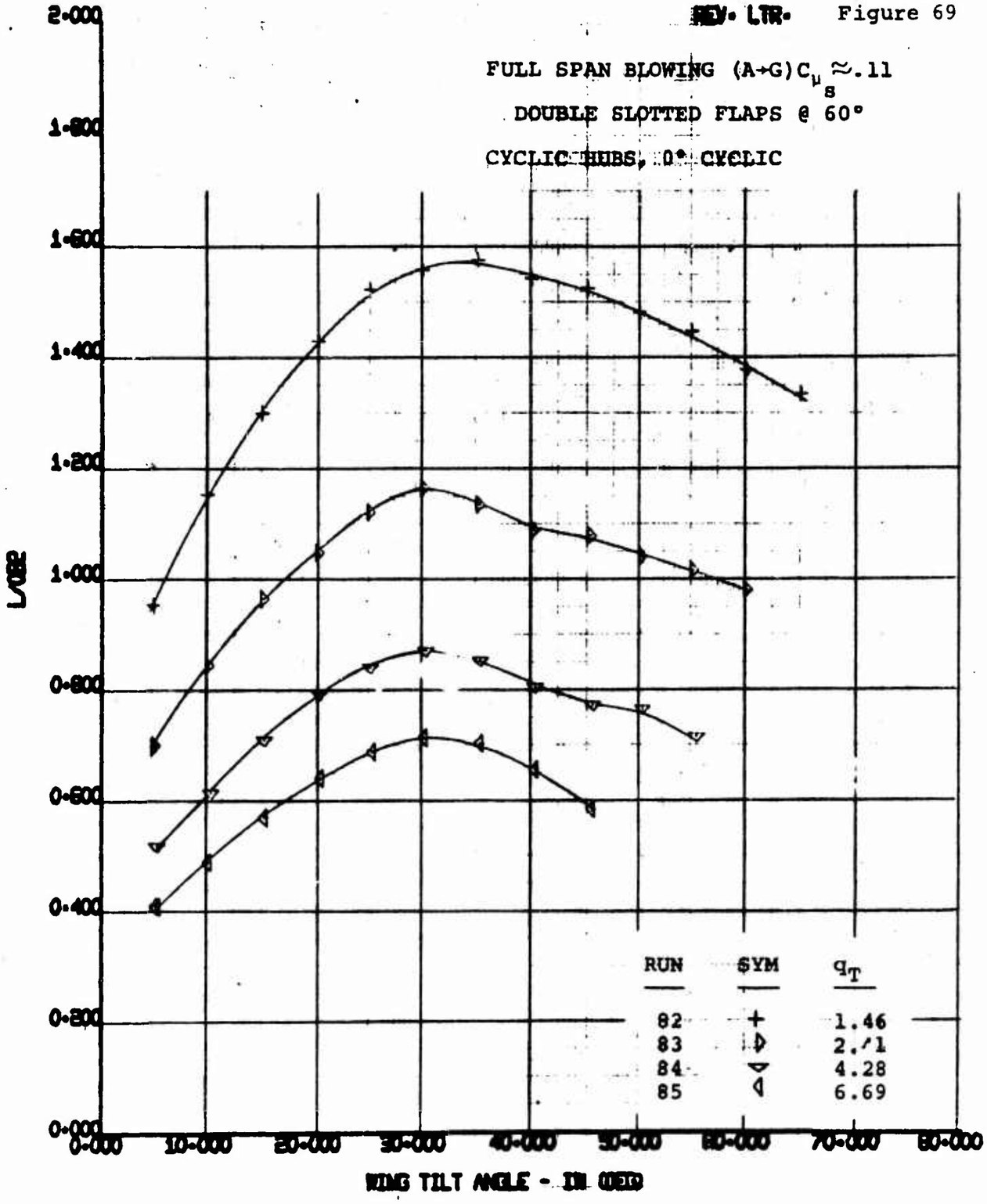

170 HALF SPAN MODEL VR 040 0-3 L/D2 VS WING TILT ANGLE	BWT 525 4/ 7/70

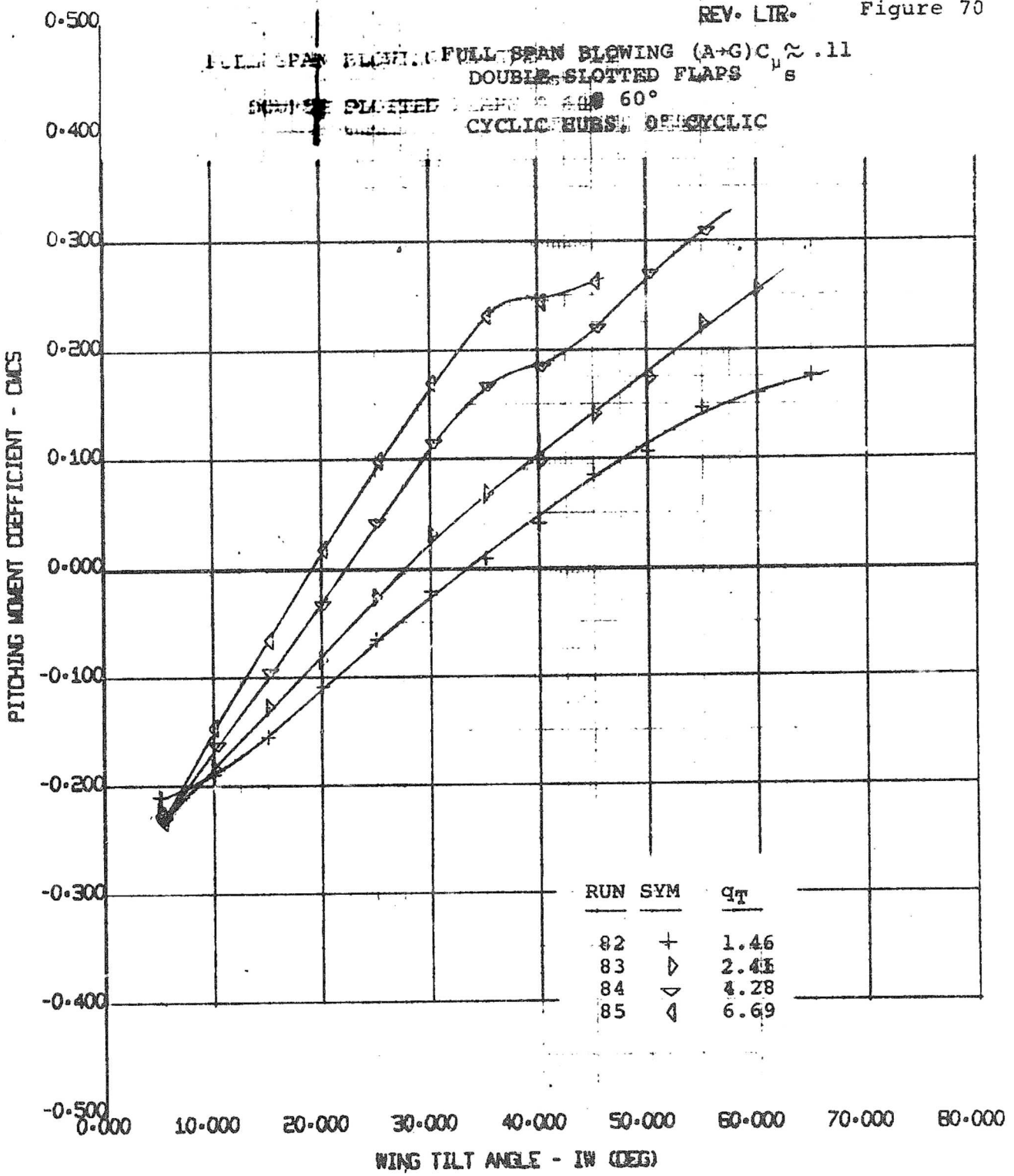

170 HALF SPAN MODEL VR 040 0-3 CMCS VS TILT WING ANGLE	BVWT 55 4/ 7/70

FULL SPAN BLOWING (A→G), $C_{\mu_s} \approx .11$

DOUBLE SLOTTED FLAPS @ 60°

CYCLIC HUBS, +4° CYCLIC

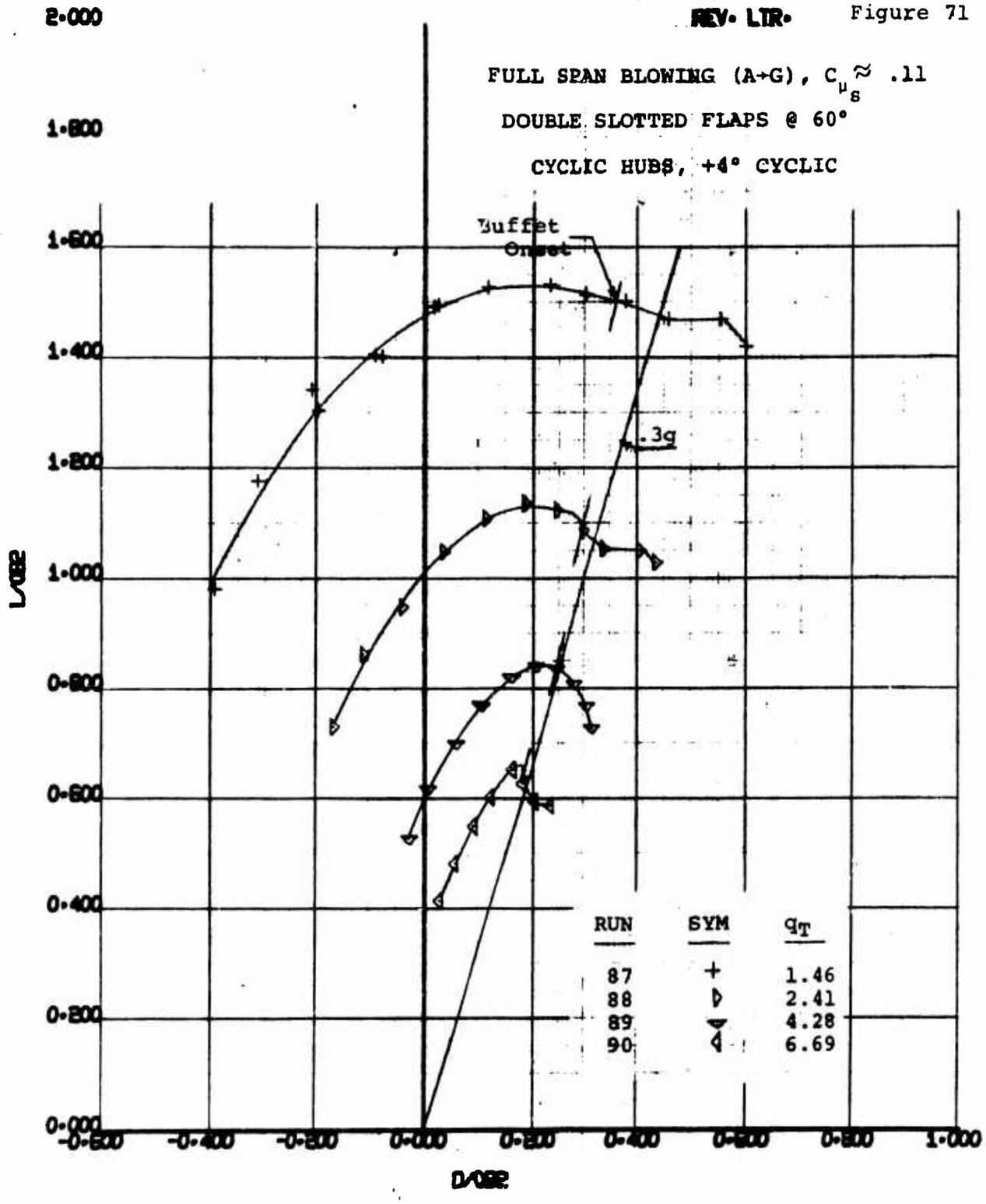

170 HALF SPAN MODEL VR 040 0-9 L/QS2 VS D/QS2	BMWT 55 4/ 7/70

Figure 72

FULL SPAN BLOWING (A+G), C_{μ_s} .11

DOUBLE SLOTTED FLAPS @ 60°

CYCLIC HUBS, +4° CYCLIC

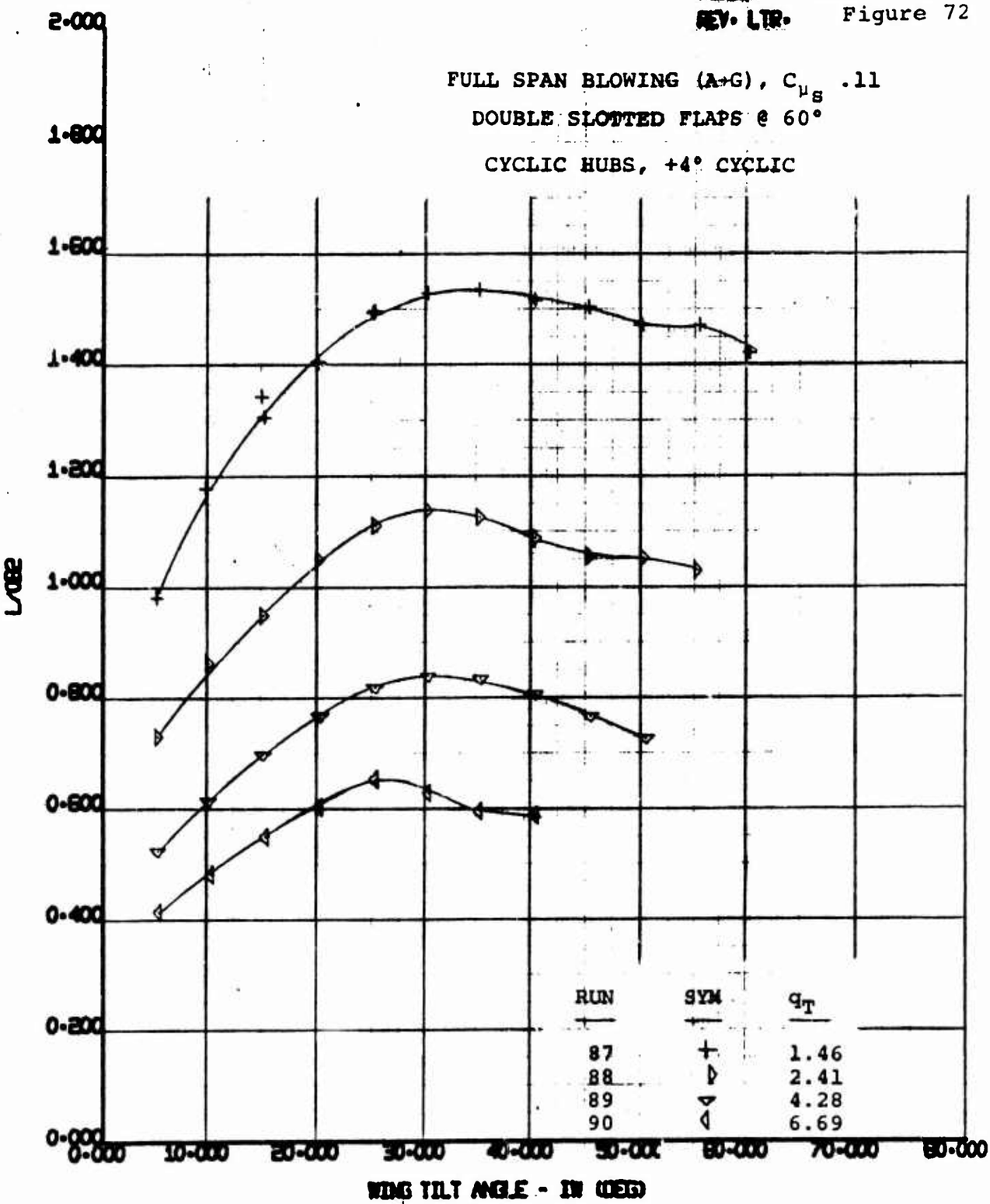

170 HALF SPAN MODEL WR 040 0-3 L/D82 VS WING TILT ANGLE	BWT 55 4/ 7/70

Figure 73

FULL SPAN BLOWING (A+G), $C_{\mu_s} \approx .11$

DOUBLE SLOTTED FLAPS @ 60°

CYCLIC HUBS, +4° CYCLIC

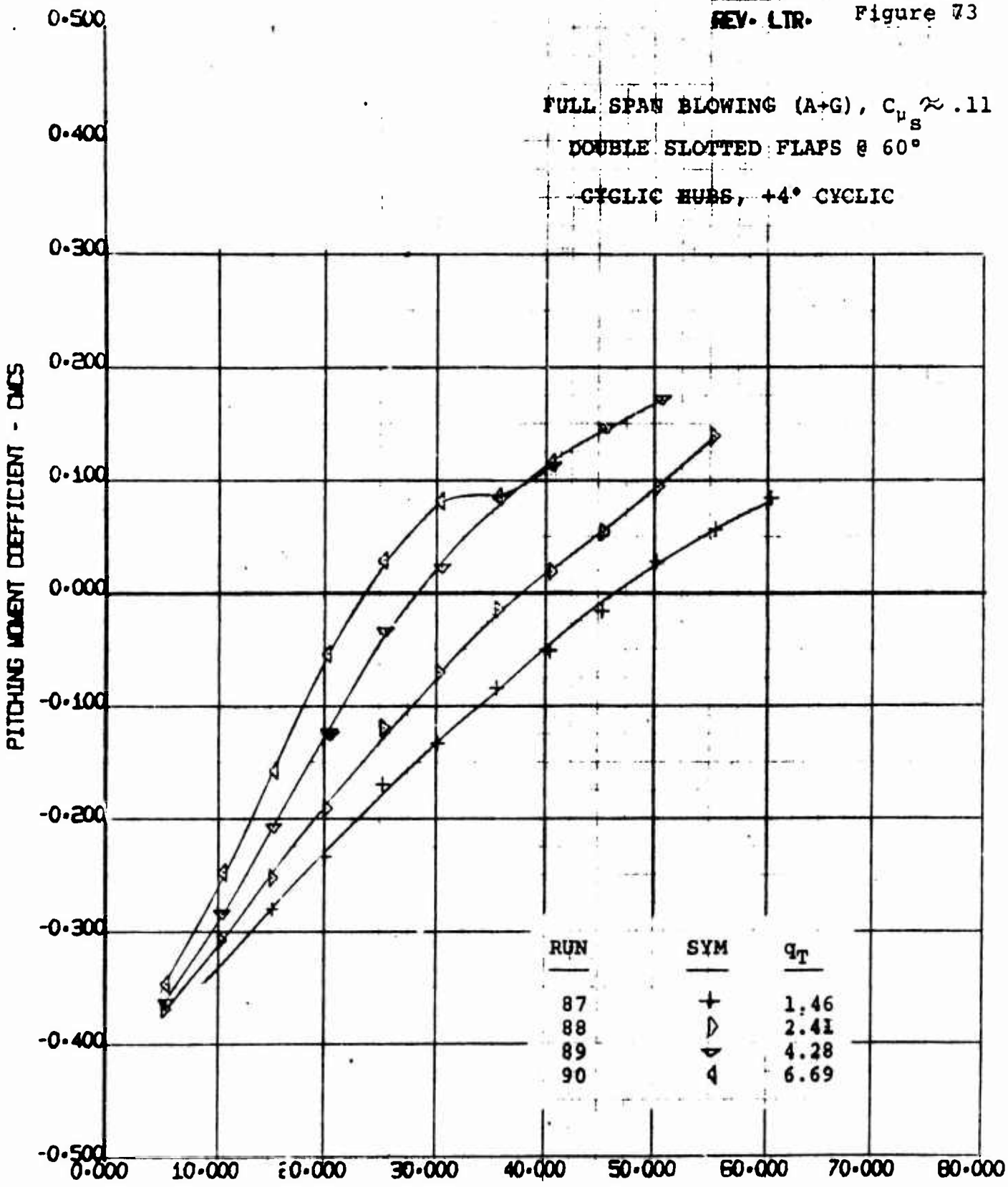

170 HALF SPAN MODEL VR 040 0-3 CMCS VS TILT WING ANGLE	BVWT SS 4/ 7/70

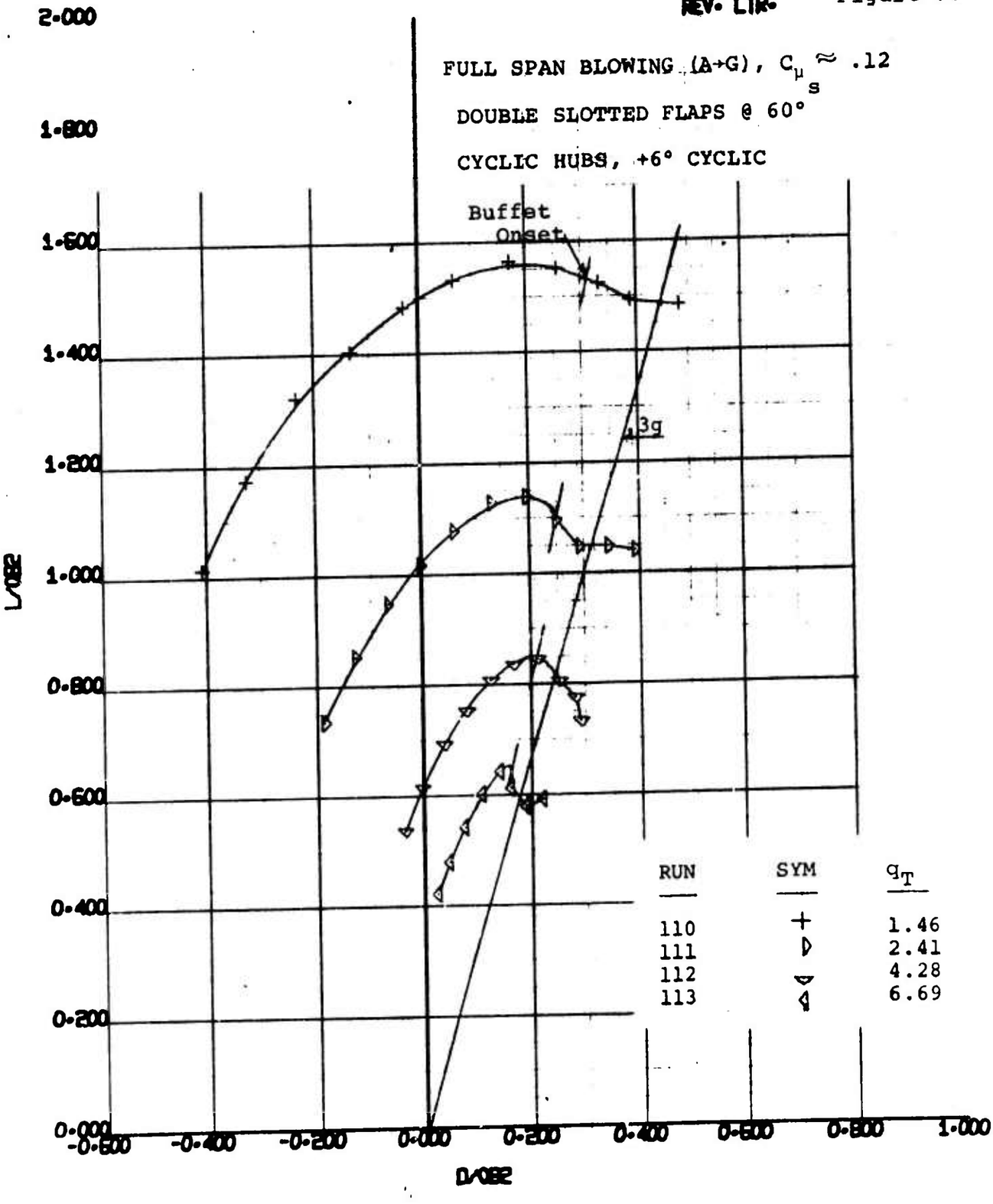

170 HALF SPAN MODEL VR 040 0-3 L/QB2 VS D/QB2	BMAT 55 4/ B-70

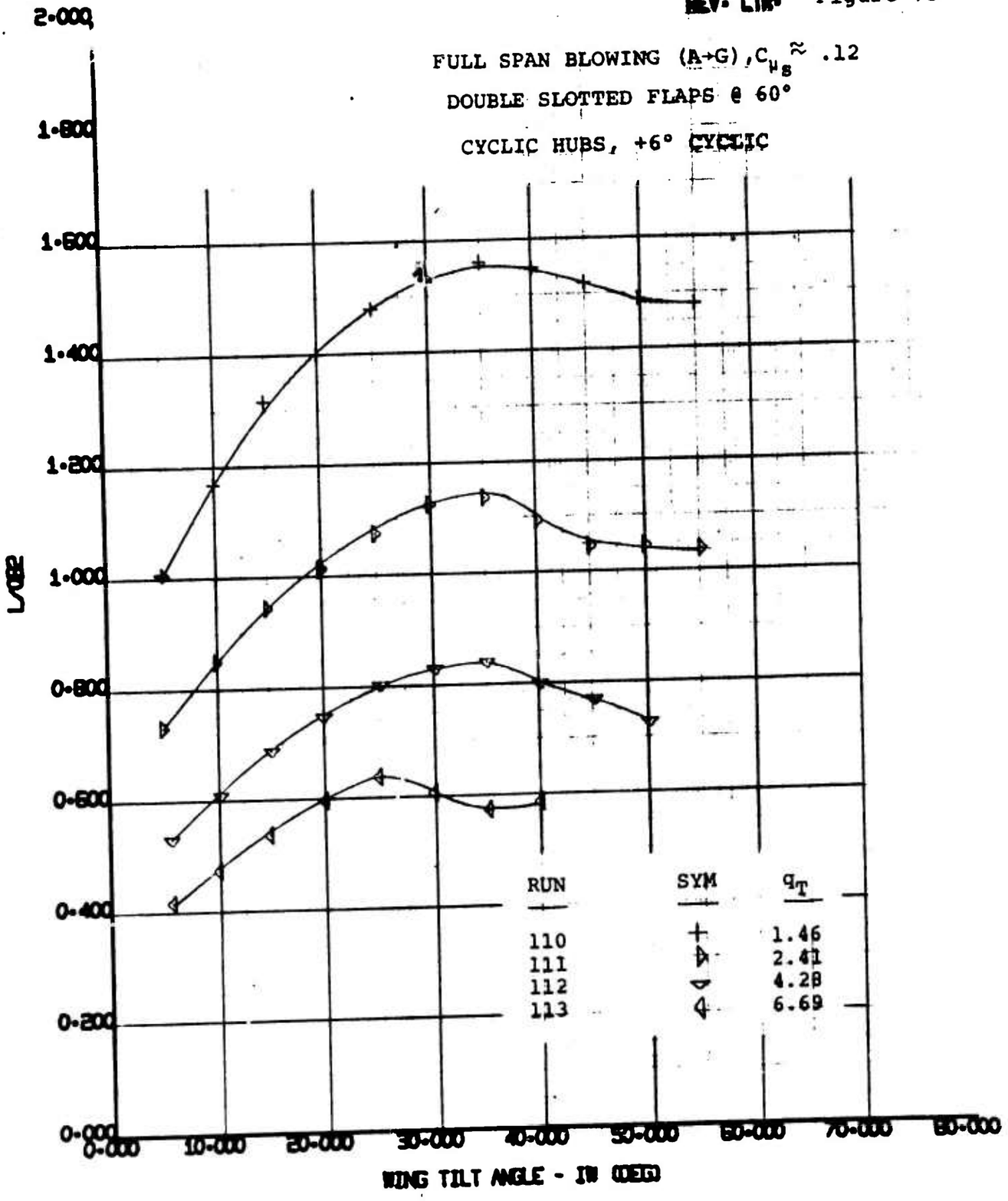

170 HALF SPAN MODEL VR 040 0-3 L/QB2 VS WING TILT ANGLE	BVWT 55 4/ 8/70

FULL SPAN BLOWING (A→G) $C_{\mu_S} \approx .12$

DOUBLE SLOTTED FLAPS @ 60°

CYCLIC HUBS, +6° CYCLIC

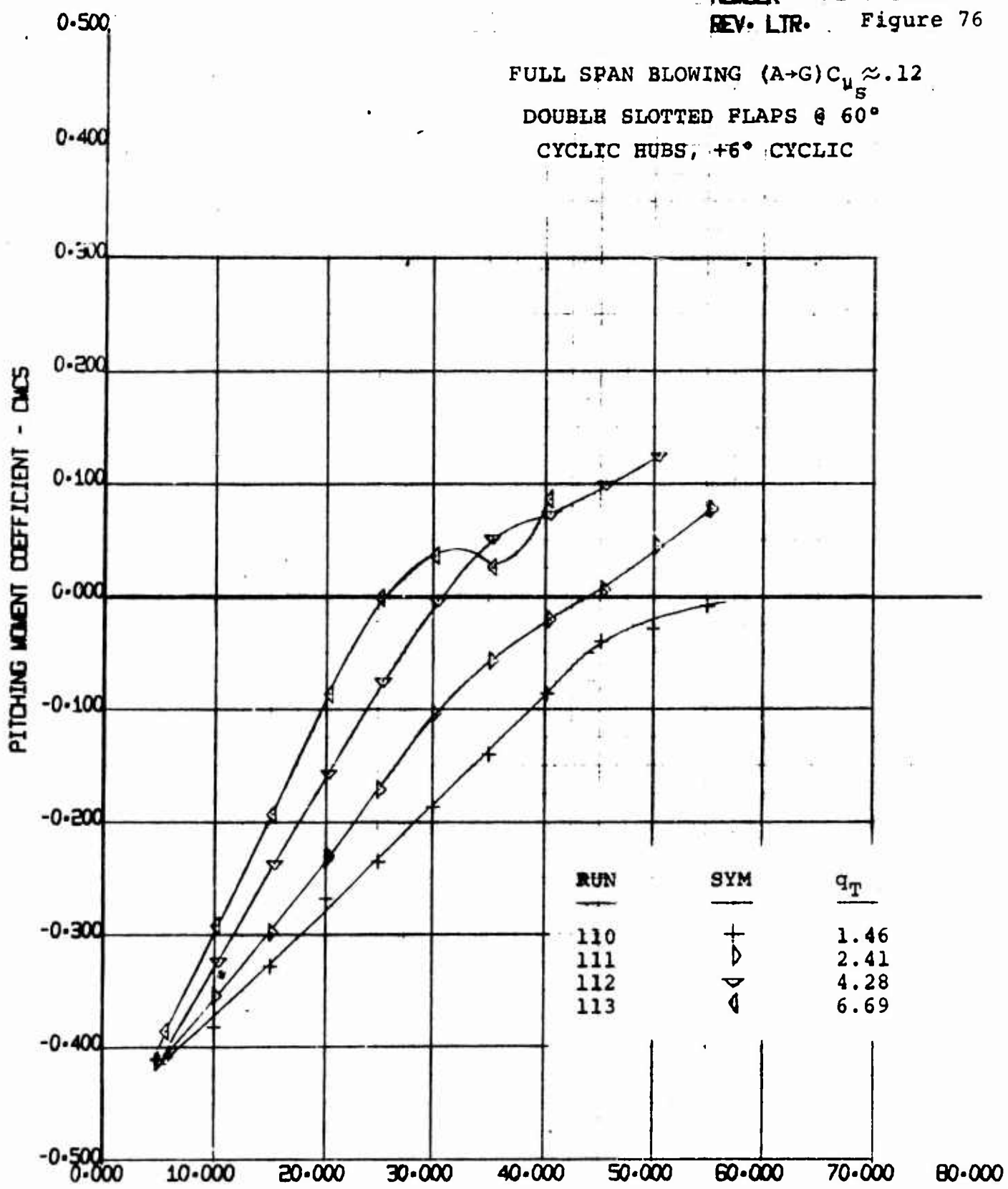

170 HALF SPAN MODEL VR 040 0-3 CMCS VS TILT WING ANGLE	BVWT 55 4/ 8/70

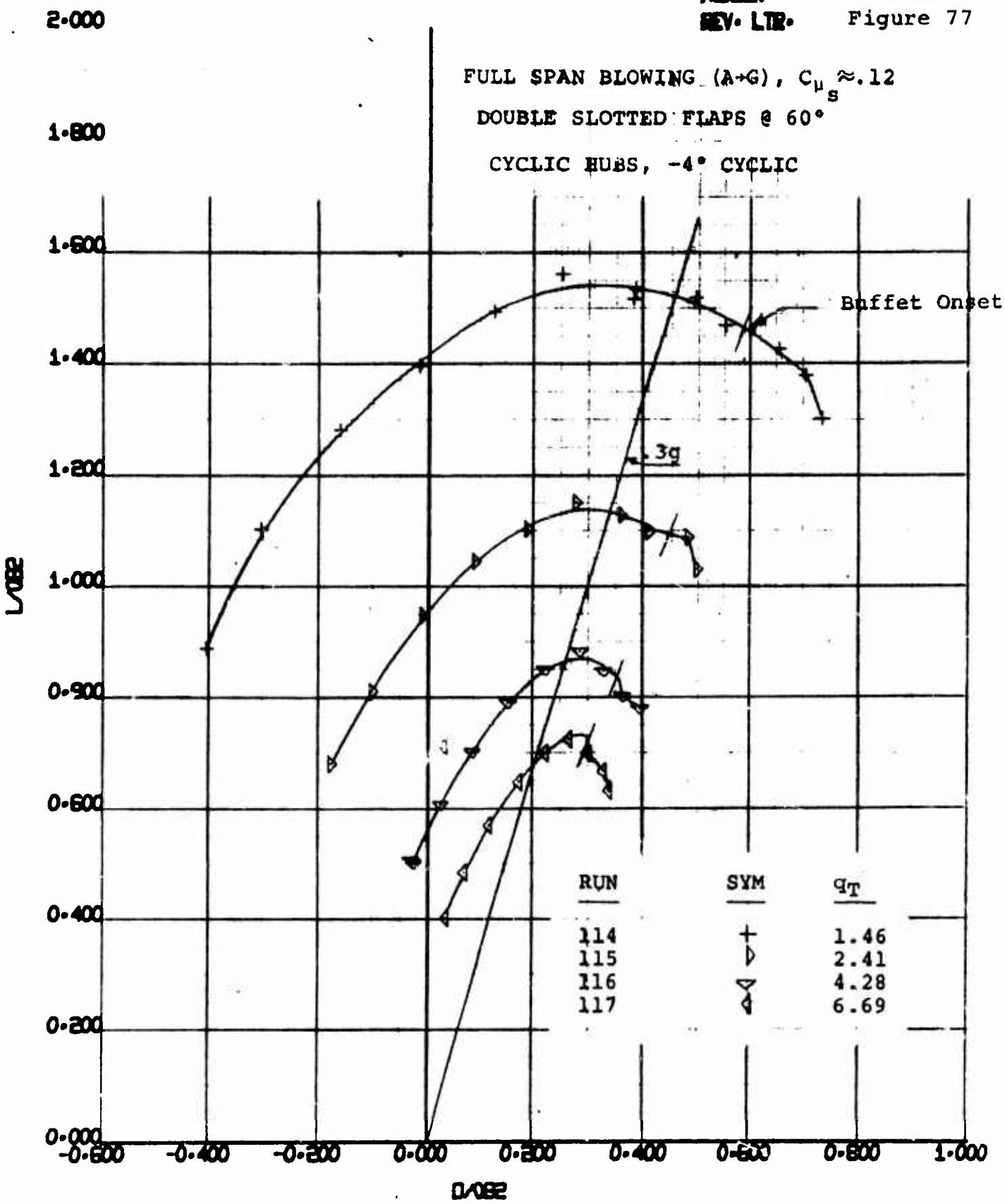

170 HALF SPAN MODEL VR 040 0-3 L/QBZ VS D/QBZ	BMT 55 4/ 7/70

FULL SPAN BLOWING (A→G), $C_{\mu_s} \approx .12$

DOUBLE SLOTTED FLAPS @ 60°

CYCLIC HUBS, -4° CYCLIC

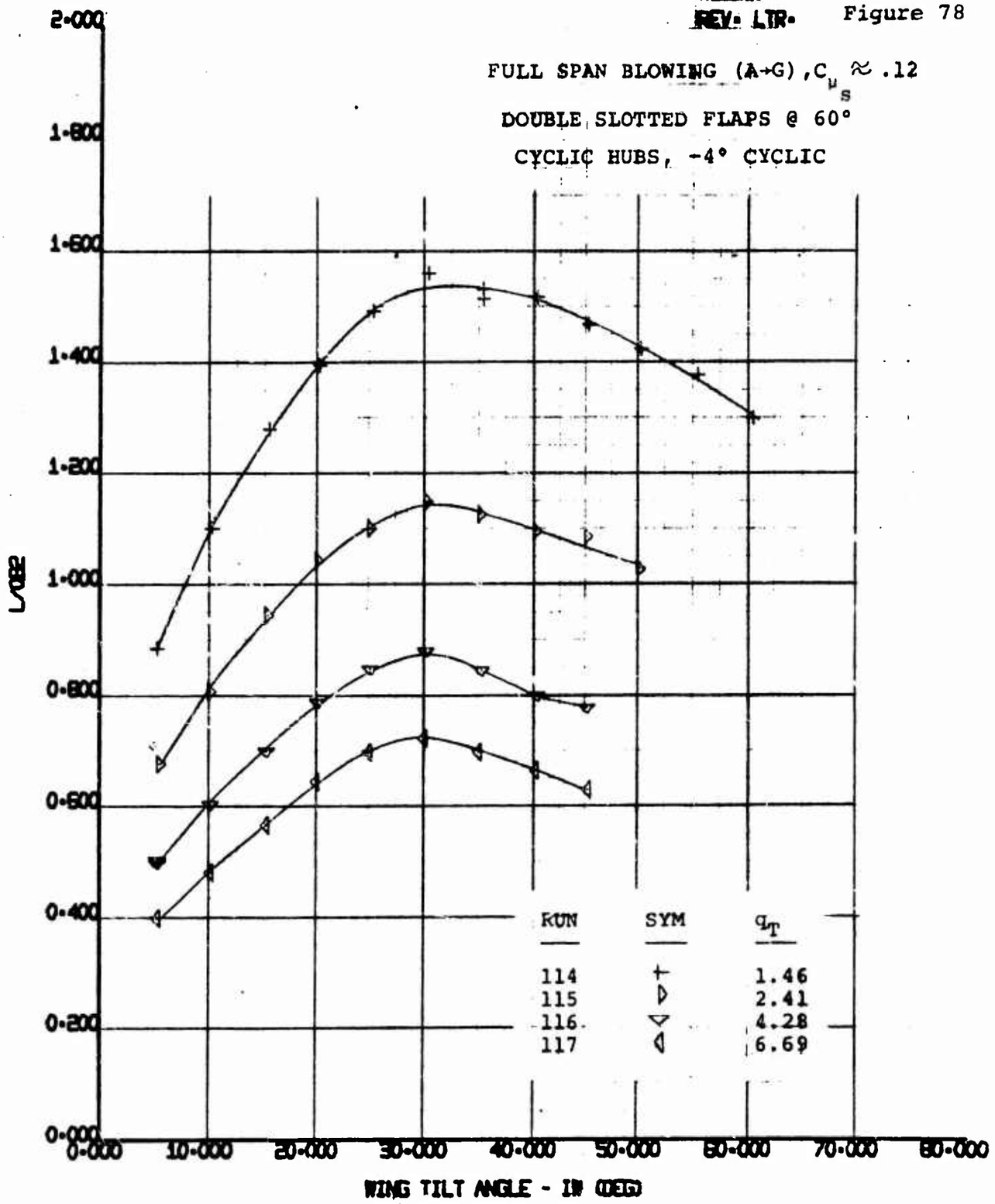

170 HALF SPAN MODEL VR 040 0-3 L/QB2 VS WING TILT ANGLE	BWT 55 4/ 7/70

FULL SPAN BLOWING (AUG), $C_{\mu_s} \approx .12$
DOUBLE SLOTTED FLAPS @ 60°
CYCLIC HUBS, -4° CYCLIC

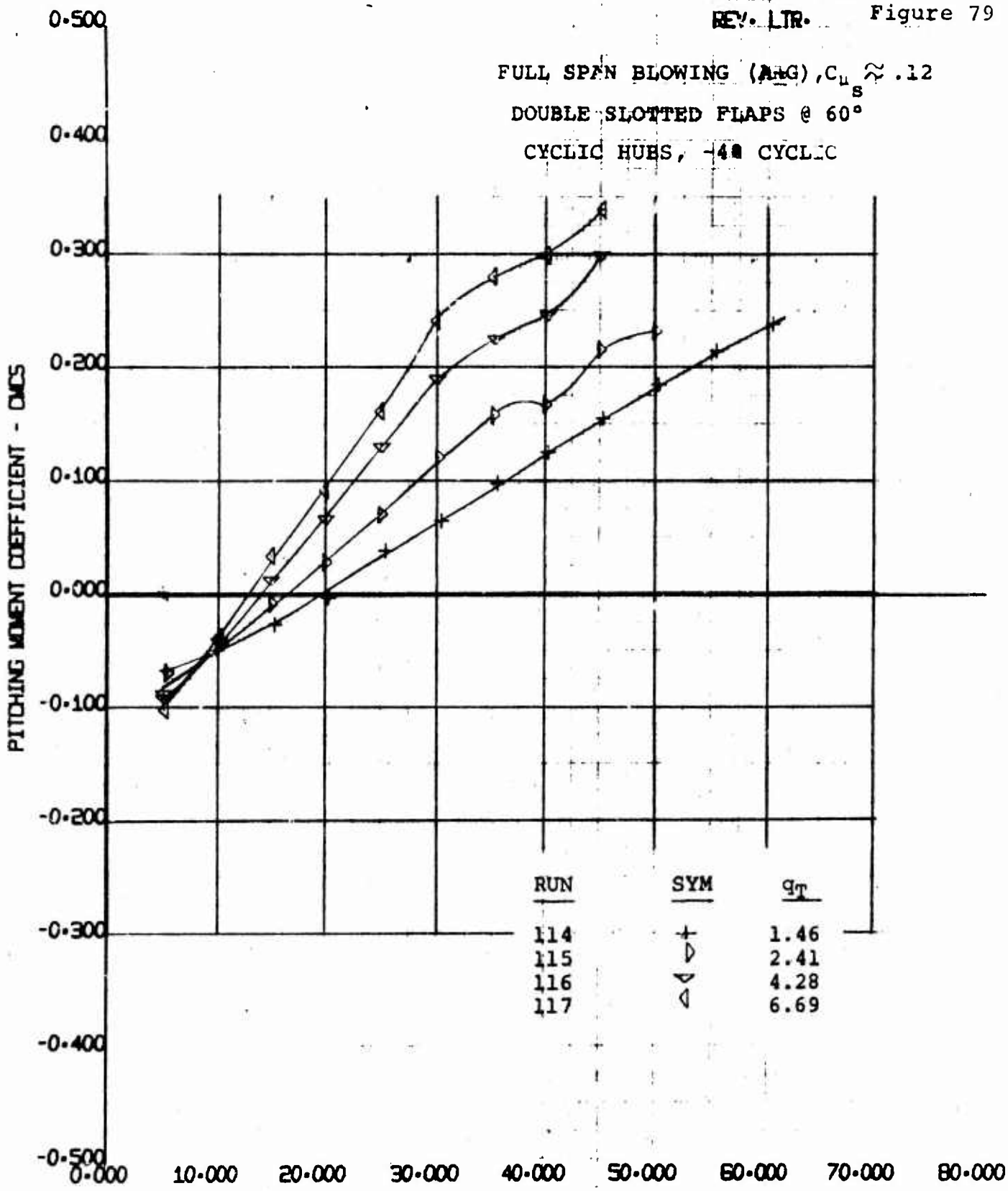

170 HALF SPAN MODEL VR 040 0-3 CMCS VS TILT WING ANGLE	BVWT 55 4/ 8/70

PARTIAL SPAN BLOWING $(A+C\&G)C_{\mu_S} \approx .11$

DOUBLE SLOTTED FLAPS @ 60°

CYCLIC HUBS, 0° CYCLIC

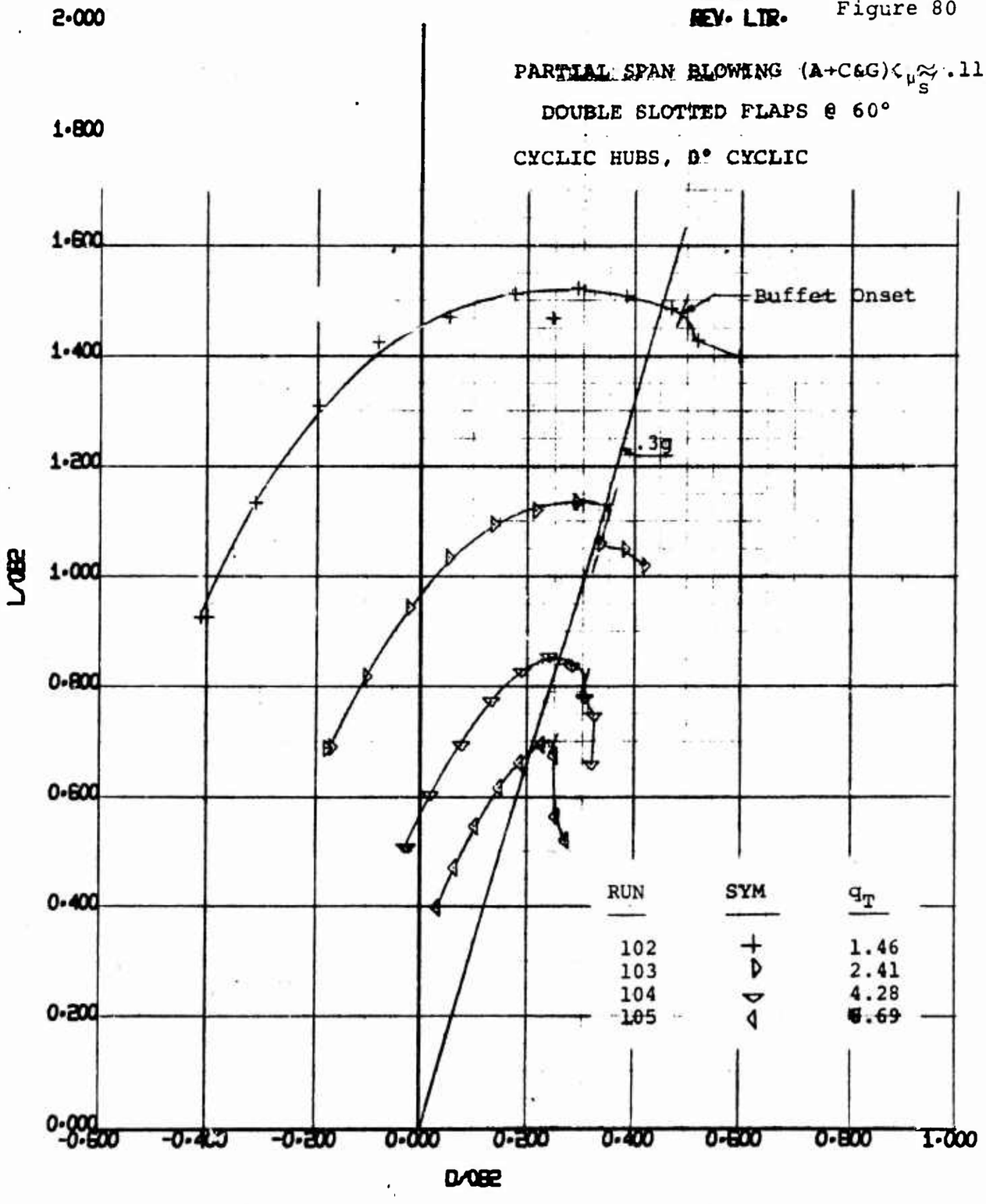

170 HALF SPAN MODEL VR 040 0-3 L/QBZ VS D/QBZ	BWT 55 4/ 7/70

PARTIAL SPAN BLOWING (A→C&G) $C_{\mu_s} \approx .11$

DOUBLE SLOTTED FLAPS @ 60°

CYCLIC HUBS, 0° CYCLIC

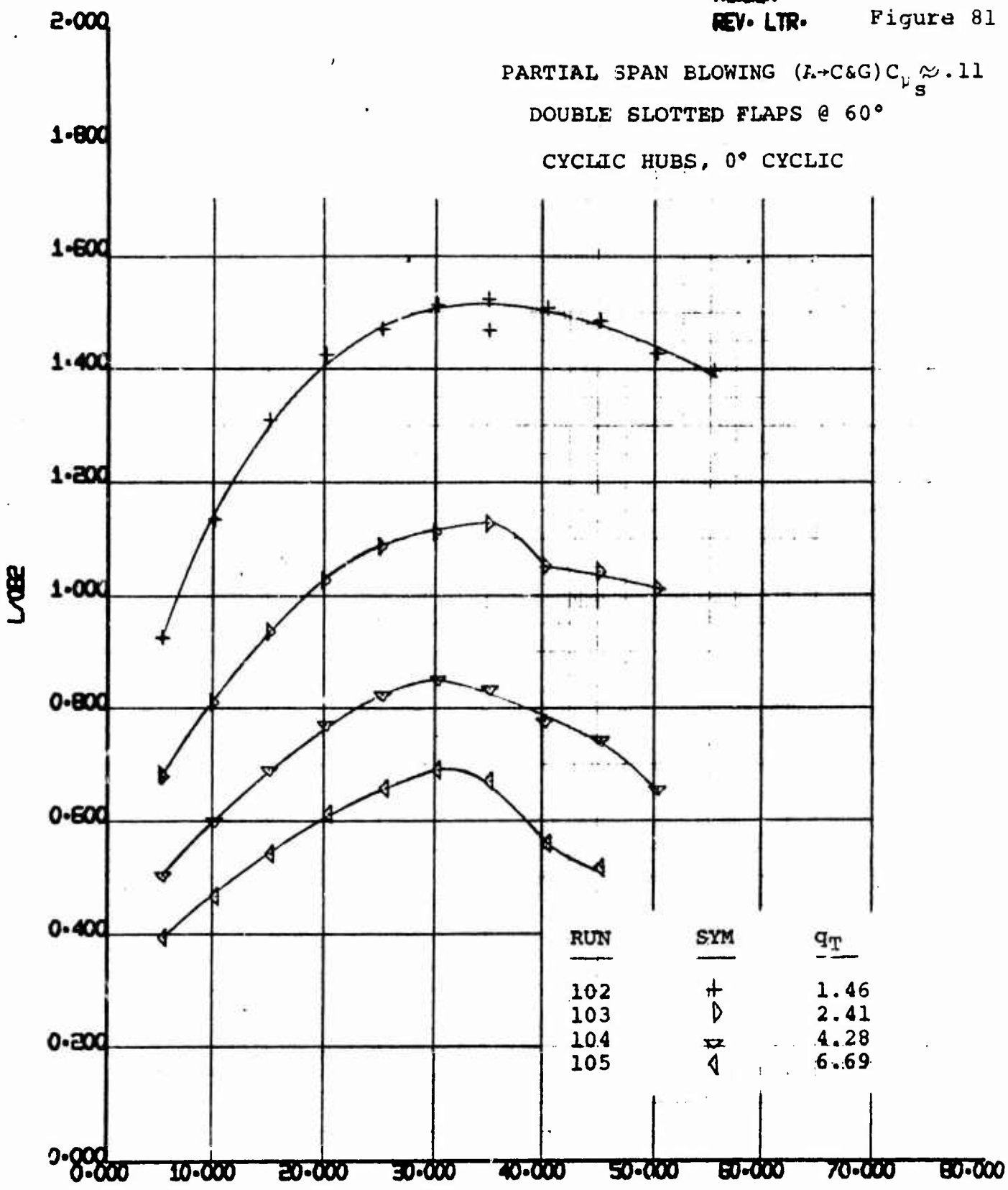

D70 HALF SPAN MODEL WT 040 0-3 L/D82 VS WING TILT ANGLE	BWT 55 4/ 7/70

PARTIAL SPAN BLOWING (A→C&G) $C_{\mu_s} \approx .11$

DOUBLE SLOTTED FLAPS @ 60°

CYCLIC HUBS, 0° CYCLIC

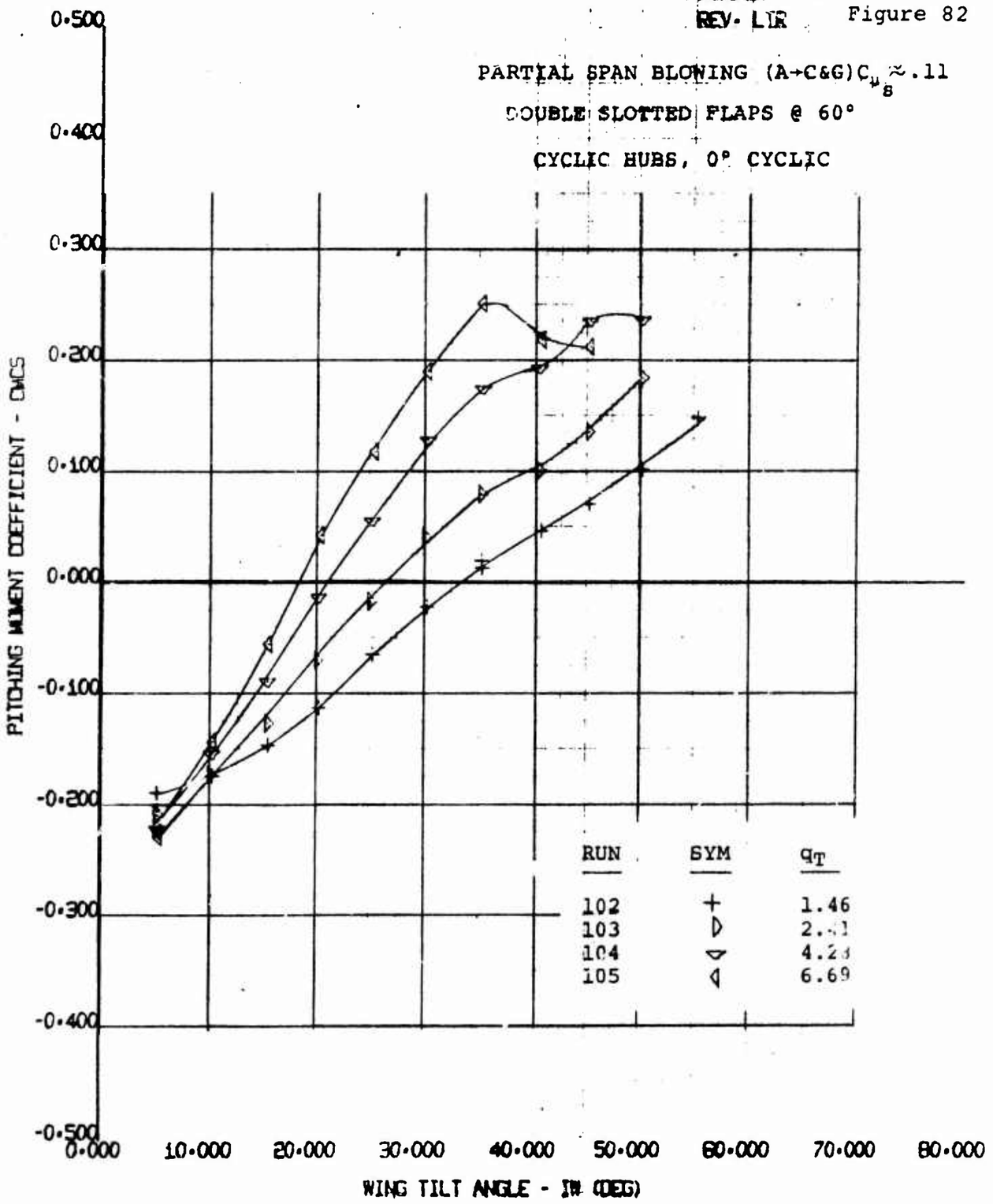

170 HALF SPAN MODEL VR 040 0-3 CMCS VS TILT WING ANGLE	BVWT 55 4/ 7/70

PARTIAL SPAN BLOWING (A+C&G) $C_{\mu_s} \approx .11$

DOUBLE SLOTTED FLAPS @ 60°

CYCLIC HUBS, +4° CYCLIC

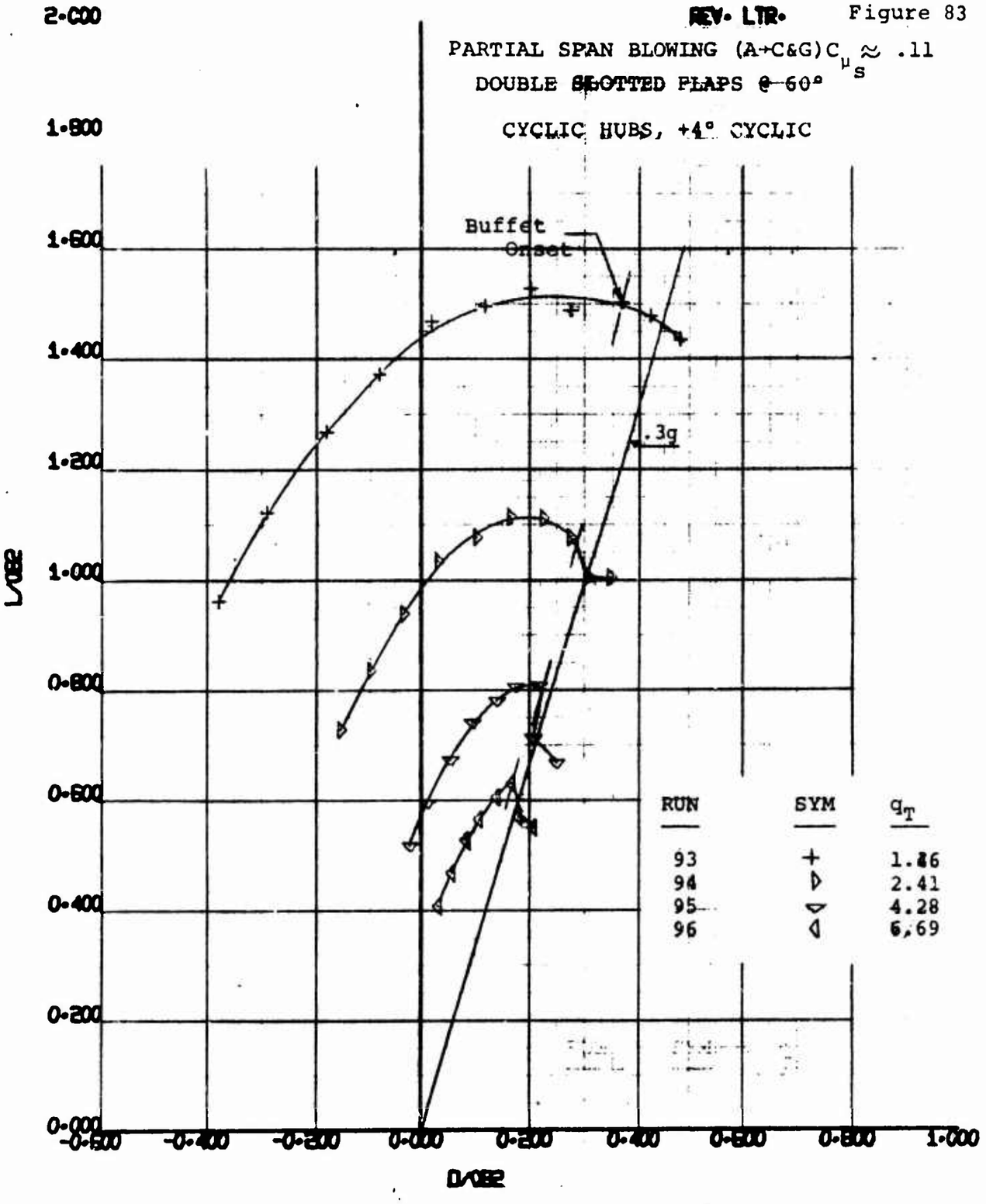

170 HALF SPAN MODEL WR 040 0-3 L/QS2 VS D/QS2	BMT 55 4/ 7/70

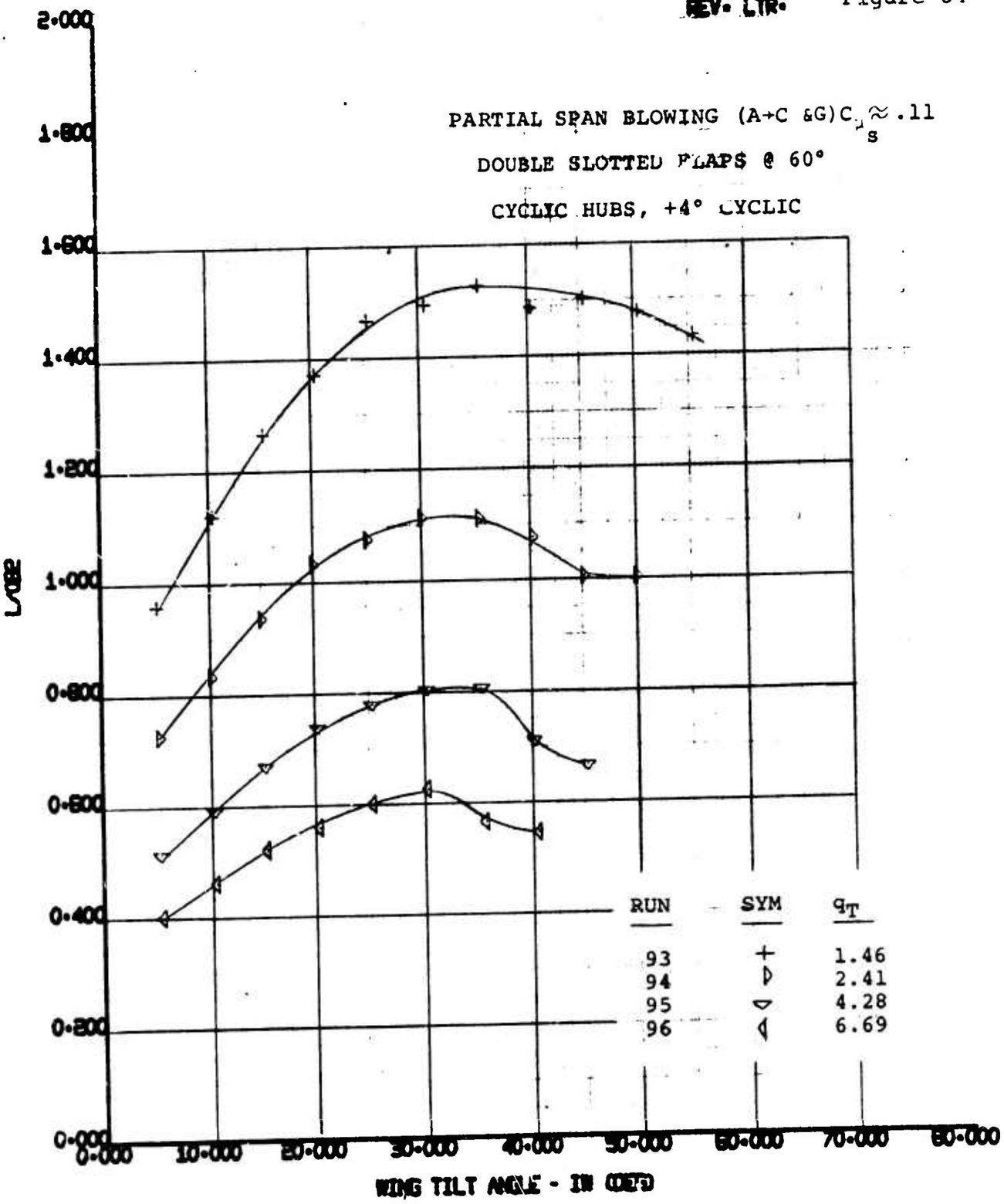

170 HALF SPAN MODEL WR 040 0-3 L/QB2 VS WING TILT ANGLE	BVWT 55 4/ 7/70

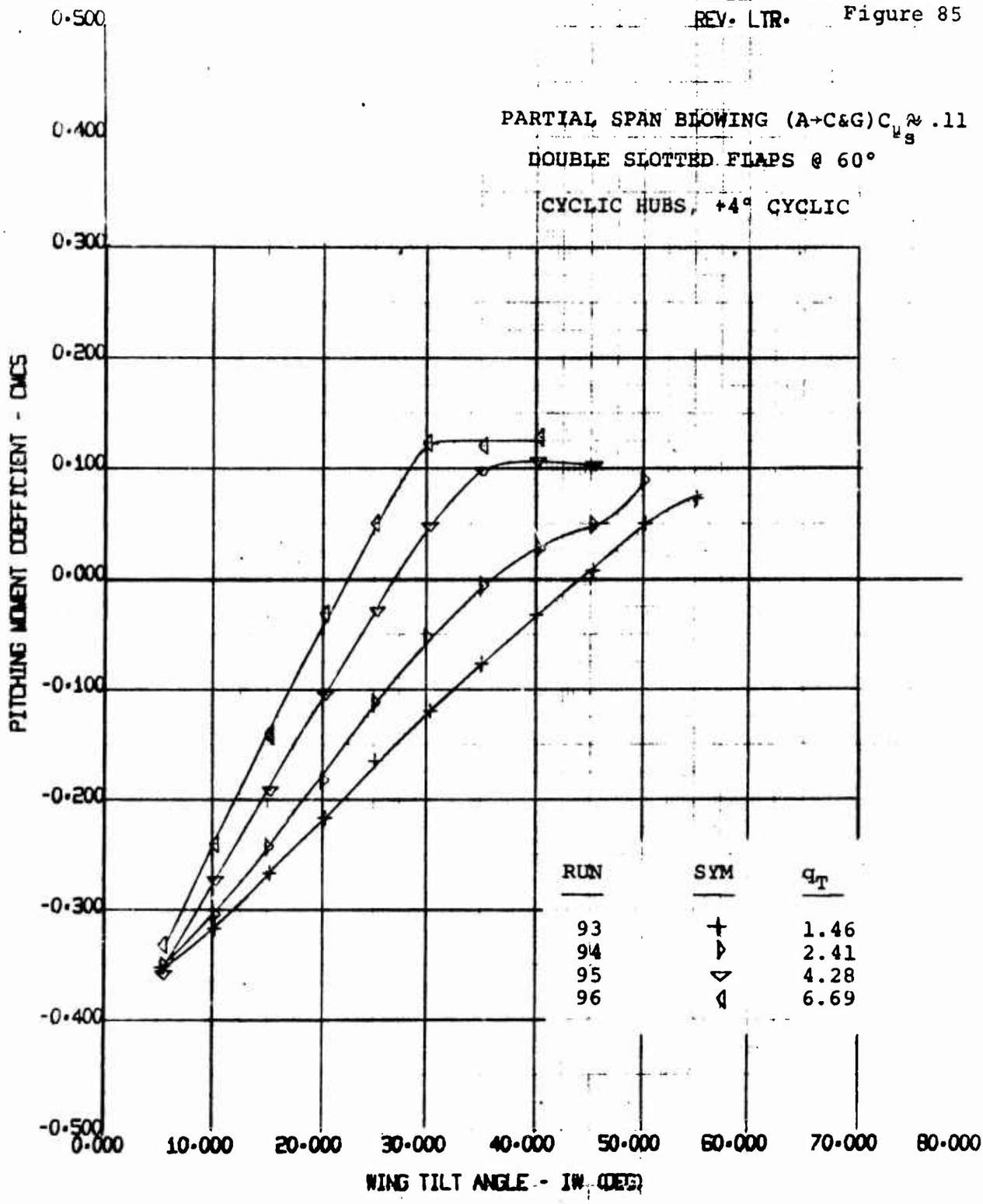

170 HALF SPAN MODEL VR 040 0-3 CMCS VS TILT WING ANGLE	BVWT 55 4/ 7/70

Figure 86

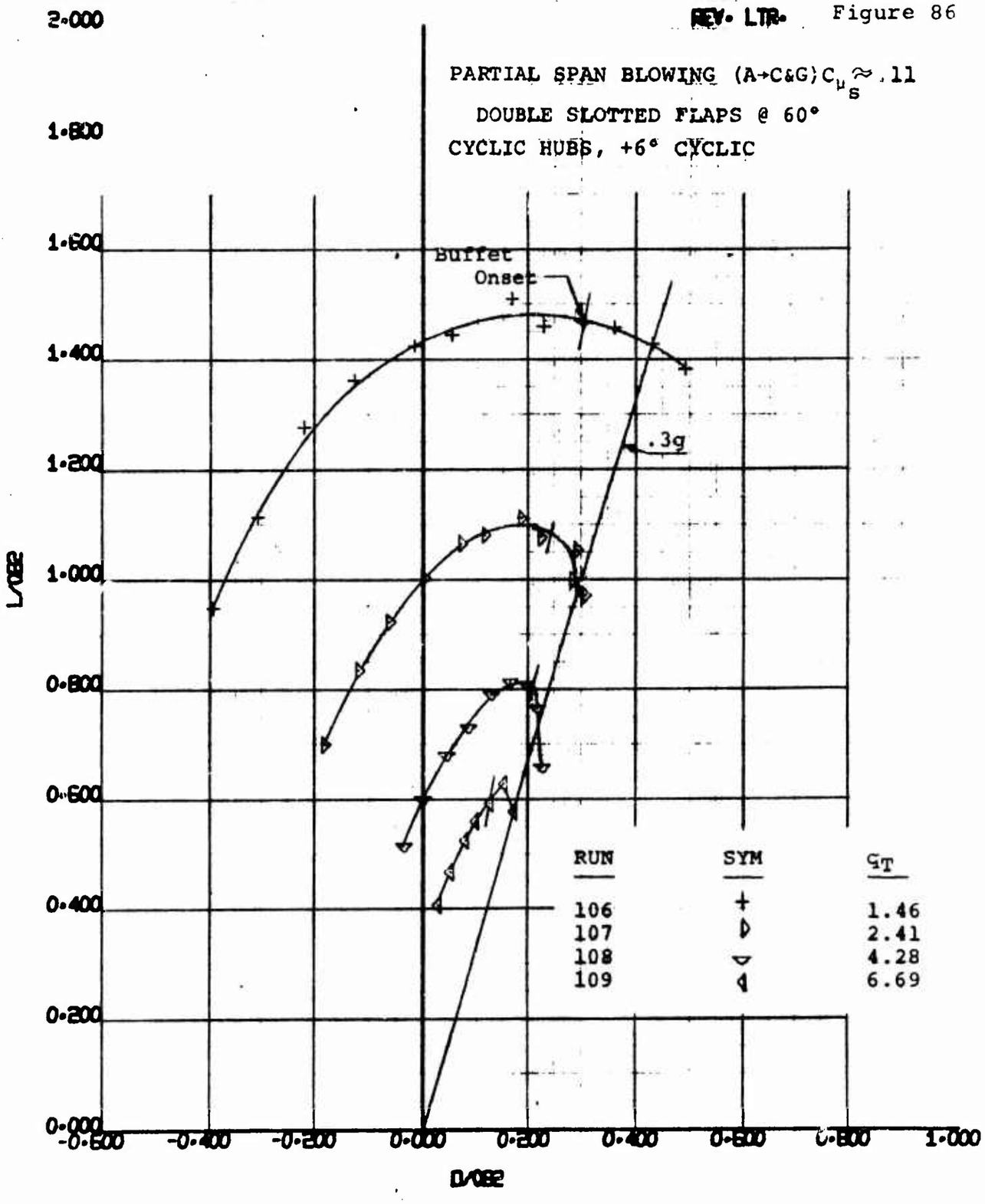

170 HALF SPAN MODEL WR 040 0-3 L/QS2 VS D/QS2	BMWT 55 4/ 8/70

PARTIAL SPAN BLOWING (A+C&G)$C_{\mu_s} \approx .11$

DOUBLE SLOTTED FLAPS @ 60°

CYCLIC HUBS, +6° CYCLIC

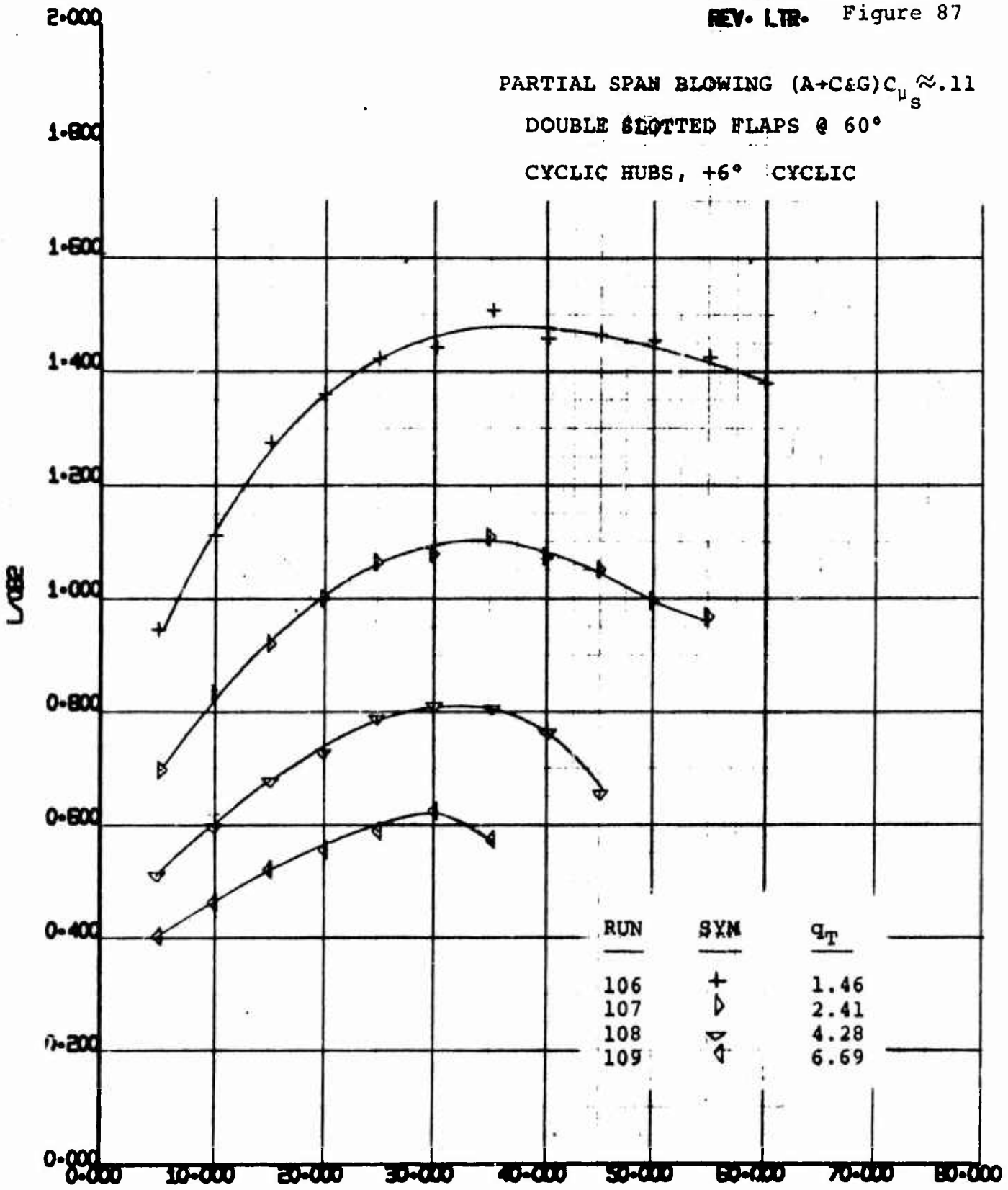

170 HALF SPAN MODEL WR 040 0-3 L/DBE VS WING TILT ANGLE	BWT 55 4/ 8/70

PARTIAL SPAN BLOWING (A→C&G) $C_{\mu_s} \approx .11$

DOUBLE SLOTTED FLAPS @ 60°

CYCLIC HUBS, +6° CYCLIC

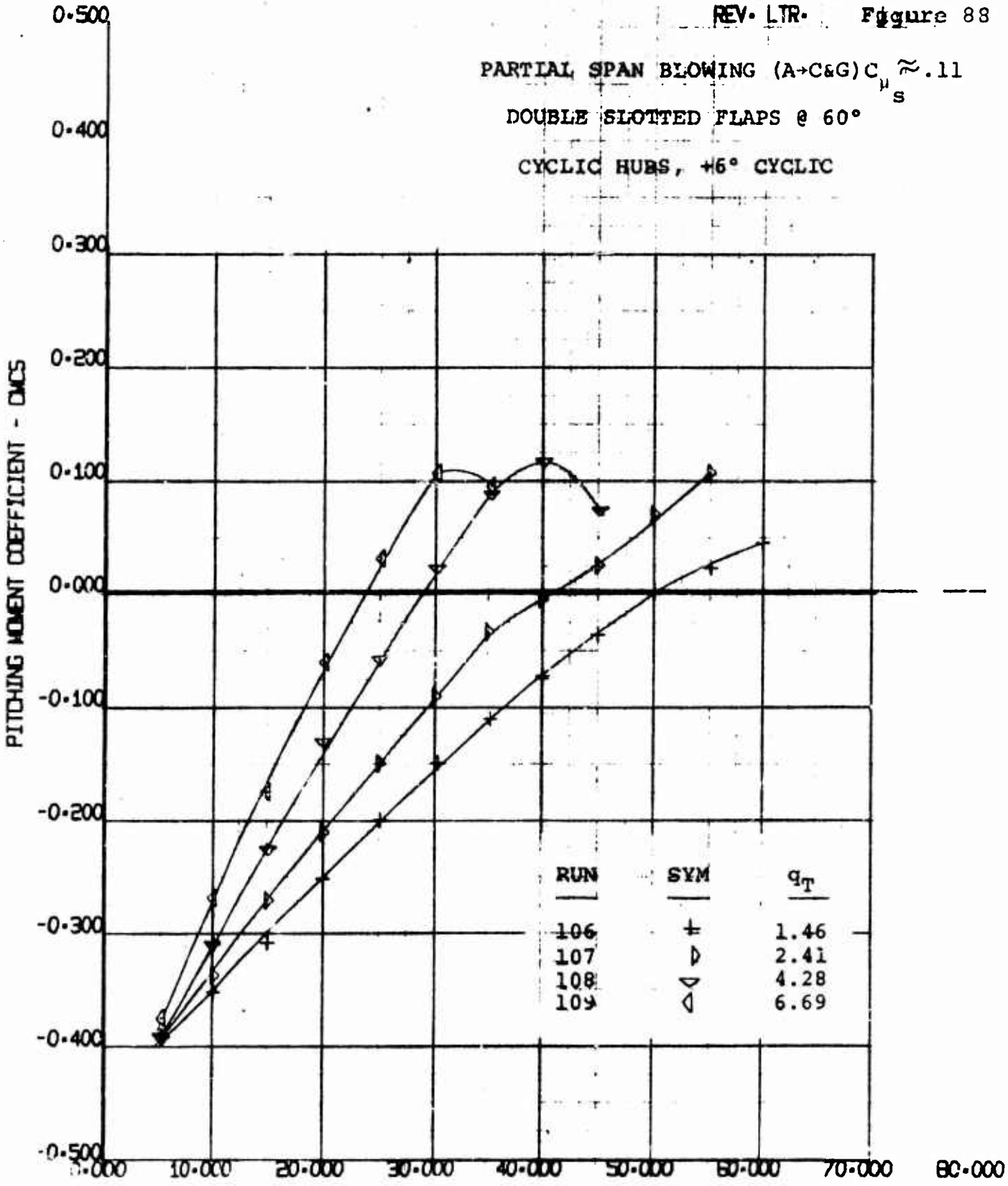

170 HALF SPAN MODEL VR 040 0-3 CMCS VS TILT WING ANGLE	BOEING 4/ 8/70

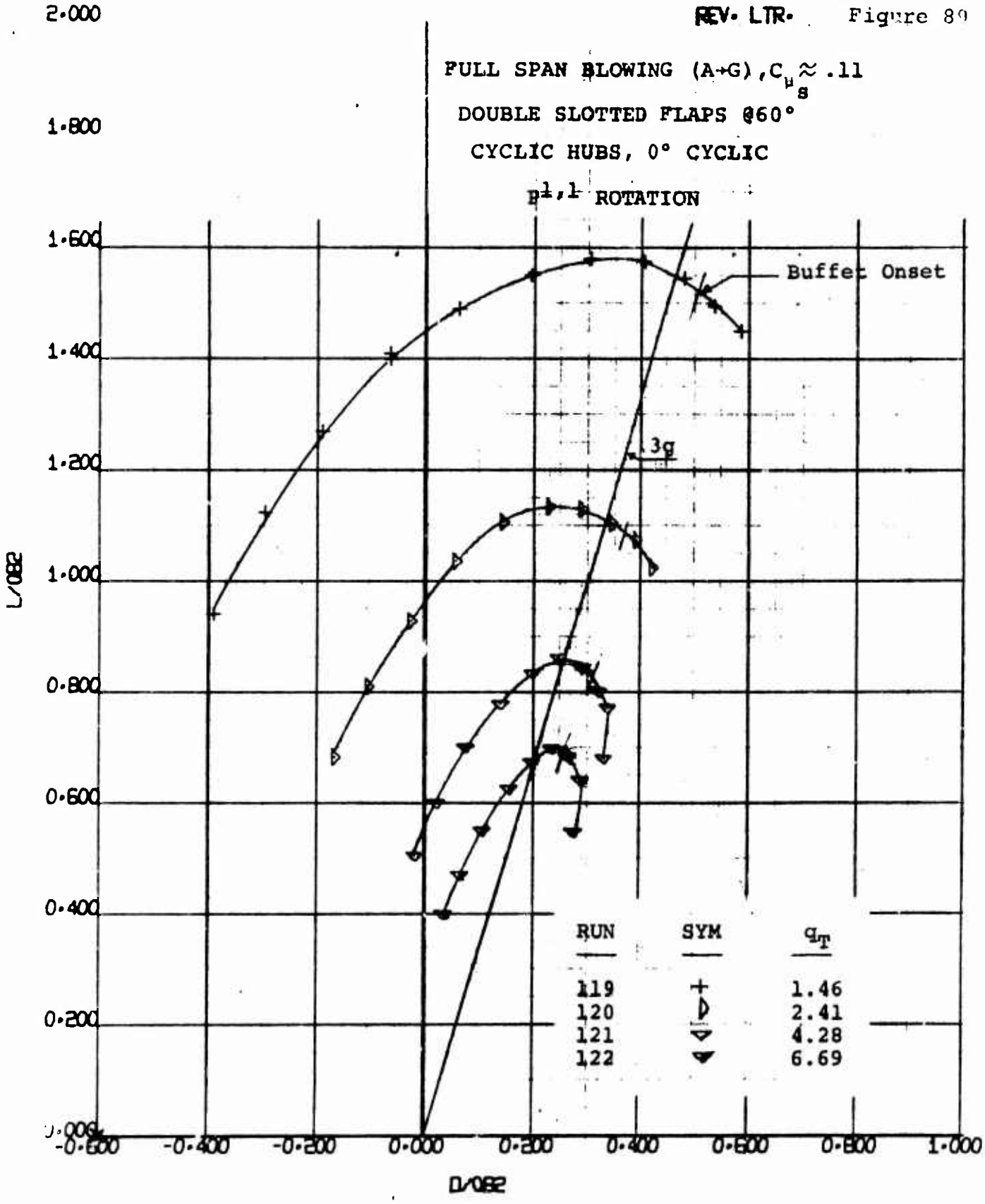

170 HALF SPAN MODEL VR 040 0-3 L/Q82 VS D/Q82	BVWT 55 4/ 8/70

FULL SPAN BLOWING (A→G), $C_{\mu_s} \approx .11$

DOUBLE SLOTTED FLAPS @60°

CYCLIC HUBS, 0° CYCLIC

$p^{1.1}$ ROTATION

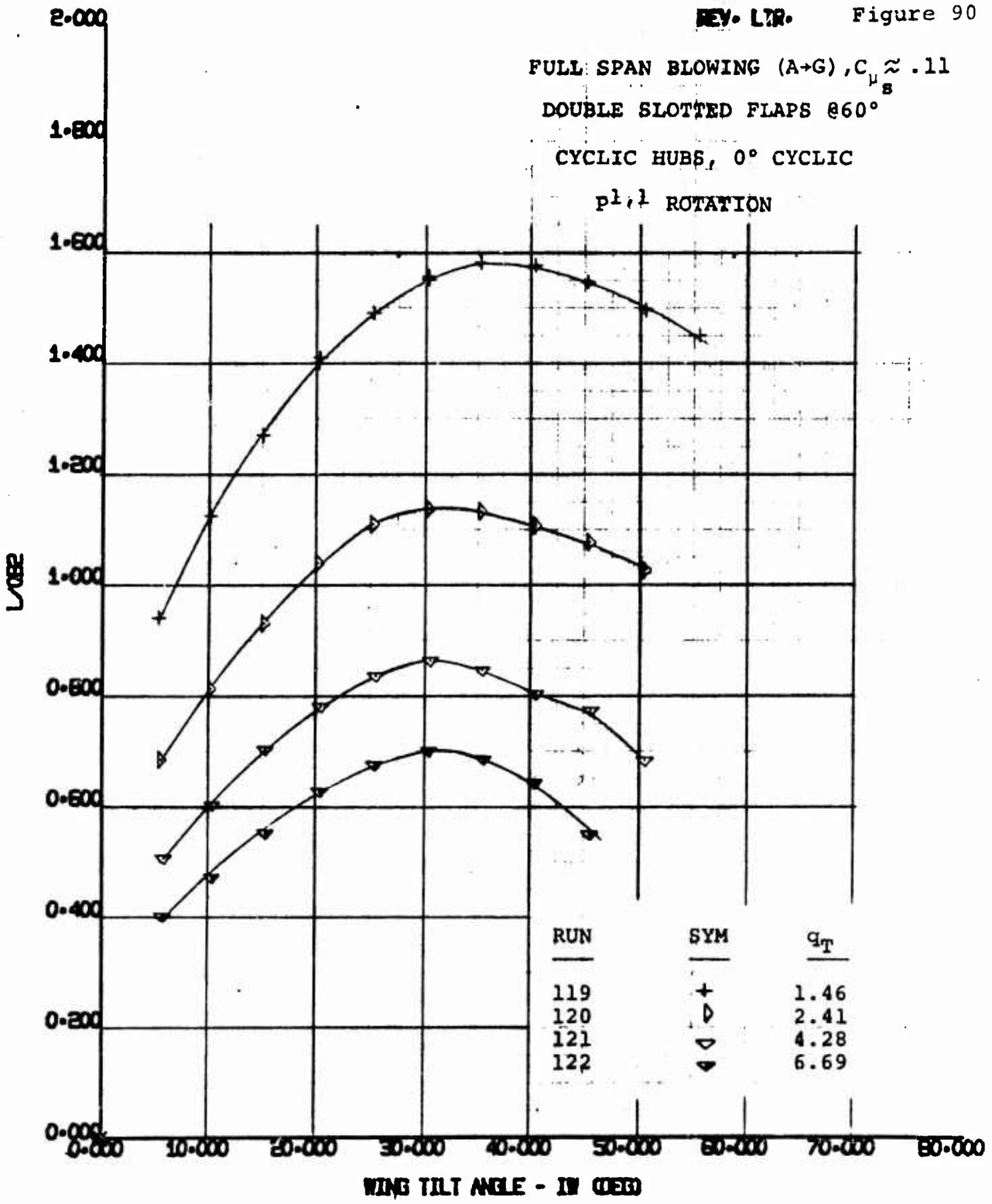

170 HALF SPAN MODEL VR 040 0-3 L/QB2 VS WING TILT ANGLE	BWT 55 4/ 8/70

FULL SPAN BLOWING (A→G), $C_{\mu_s} \approx .11$

DOUBLE SLOTTED FLAPS @60°

CYCLIC HUBS, 0° CYCLIC

p1,1 ROTATION

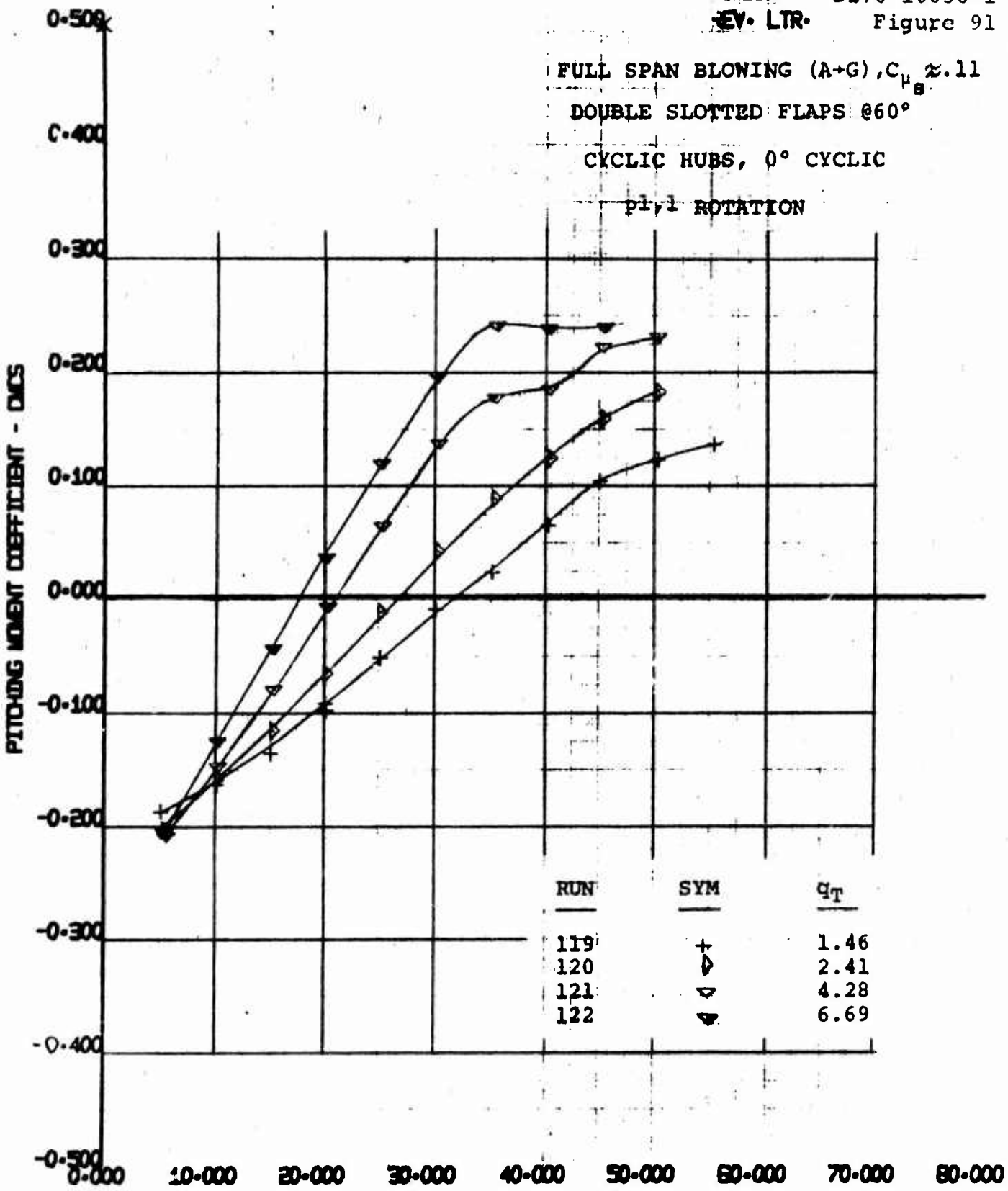

170 HALF SPAN MODEL VR 040 0-3 CMCS VS TILT WING ANGLE	BWT 55 4/ 8/70

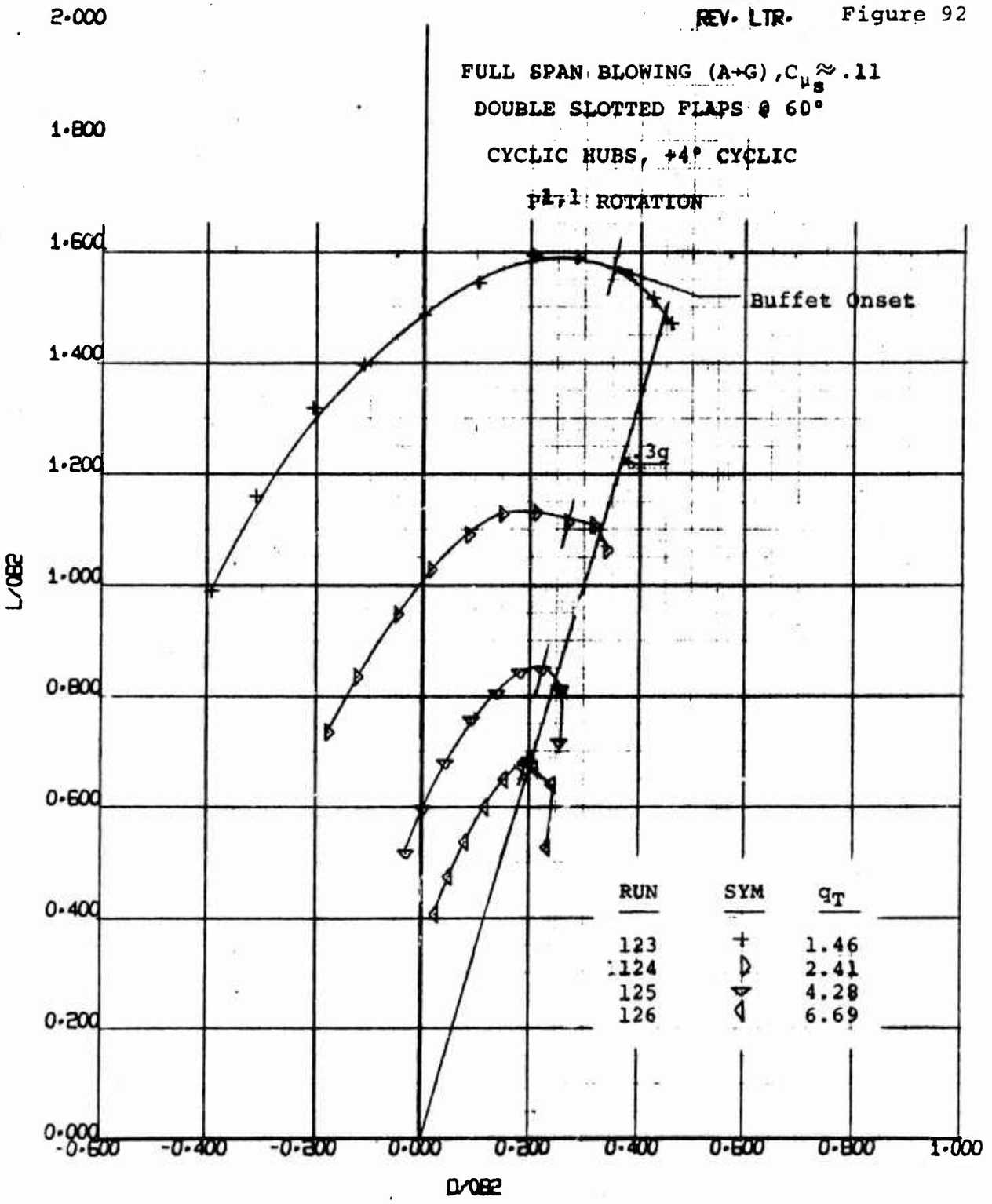

170 HALF SPAN MODEL VR 040 0-3 L/QB2 VS D/QB2	BVWT SS 4/ 8/70

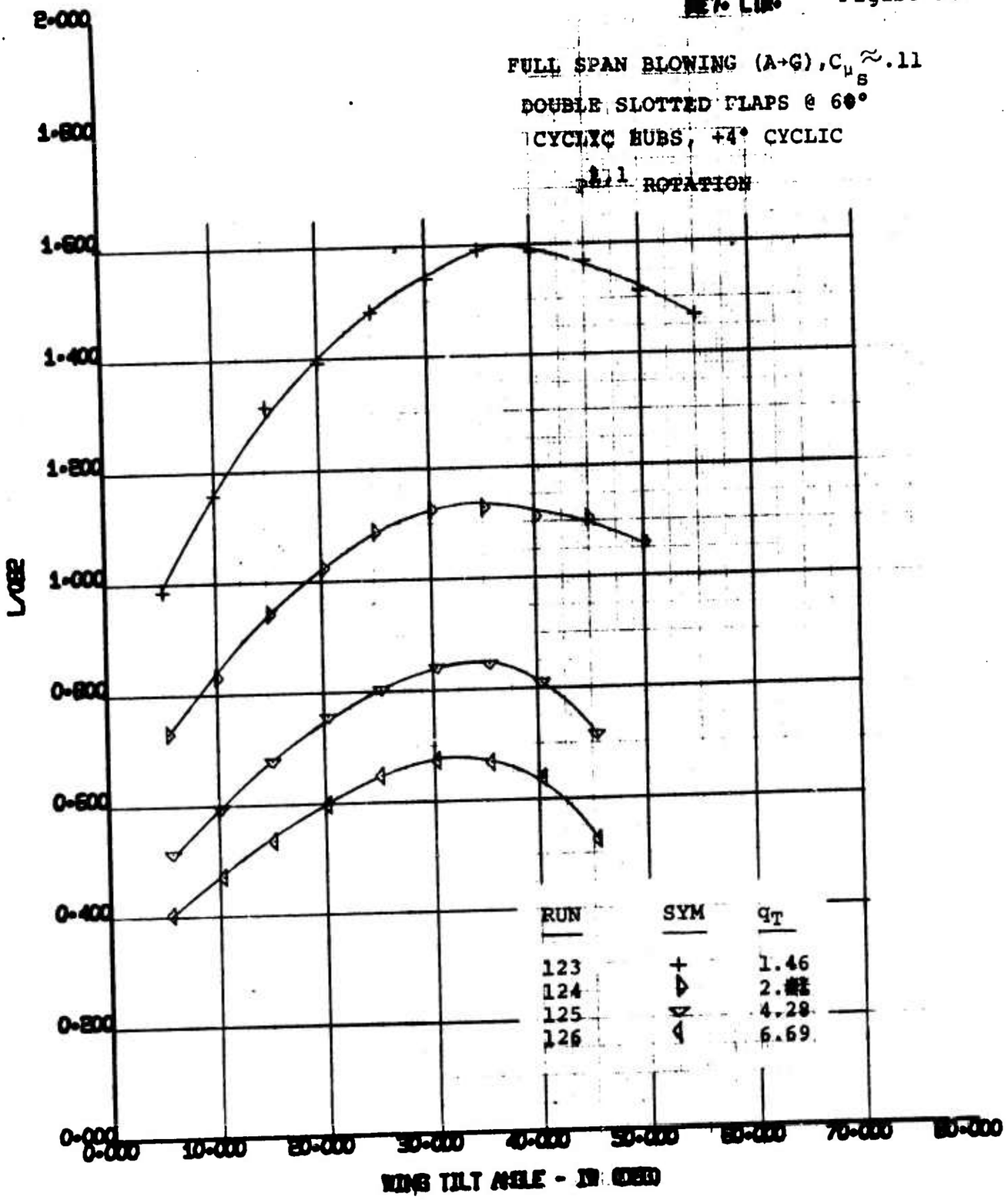

170 HALF SPAN MODEL VR 040 0-9 L/QS2 VS WING TILT ANGLE	BMWT 55 4/ 8/70

Figure 94

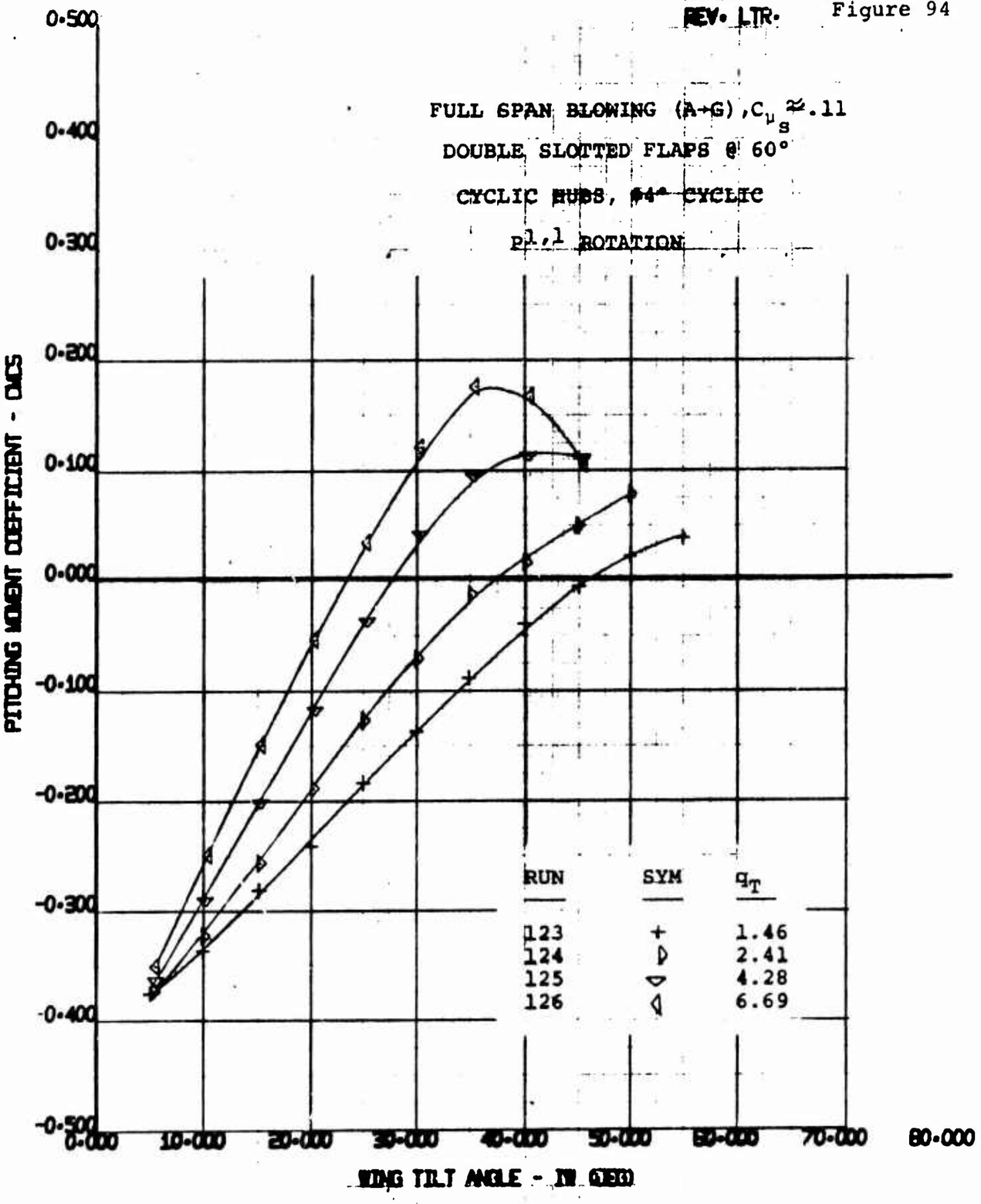

170 HALF SPAN MODEL VR 040 0-3 CMCS VS TILT WING ANGLE	BVWT 55 4/ 8/70

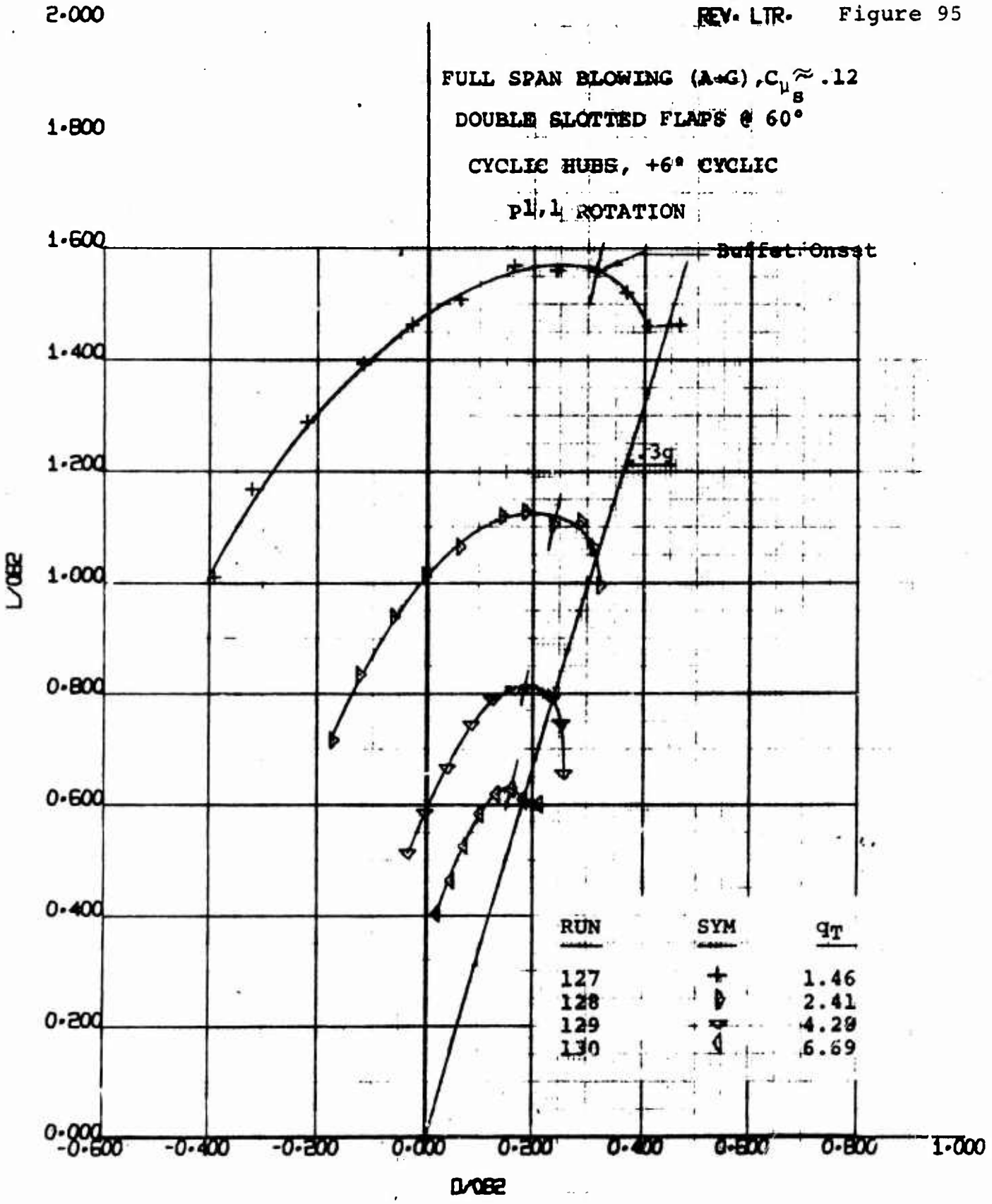

170 HALF SPAN MODEL VR 040 0-3 L/QB2 VS D/QB2	BVWT 55 4/ 8/70

FULL SPAN BLOWING (A→G), $C_{\mu_s} \approx .12$

DOUBLE SLOTTED FLAPS @ 60°

CYCLIC HUBS, +6° CYCLIC

$p_{1,1}$ ROTATION

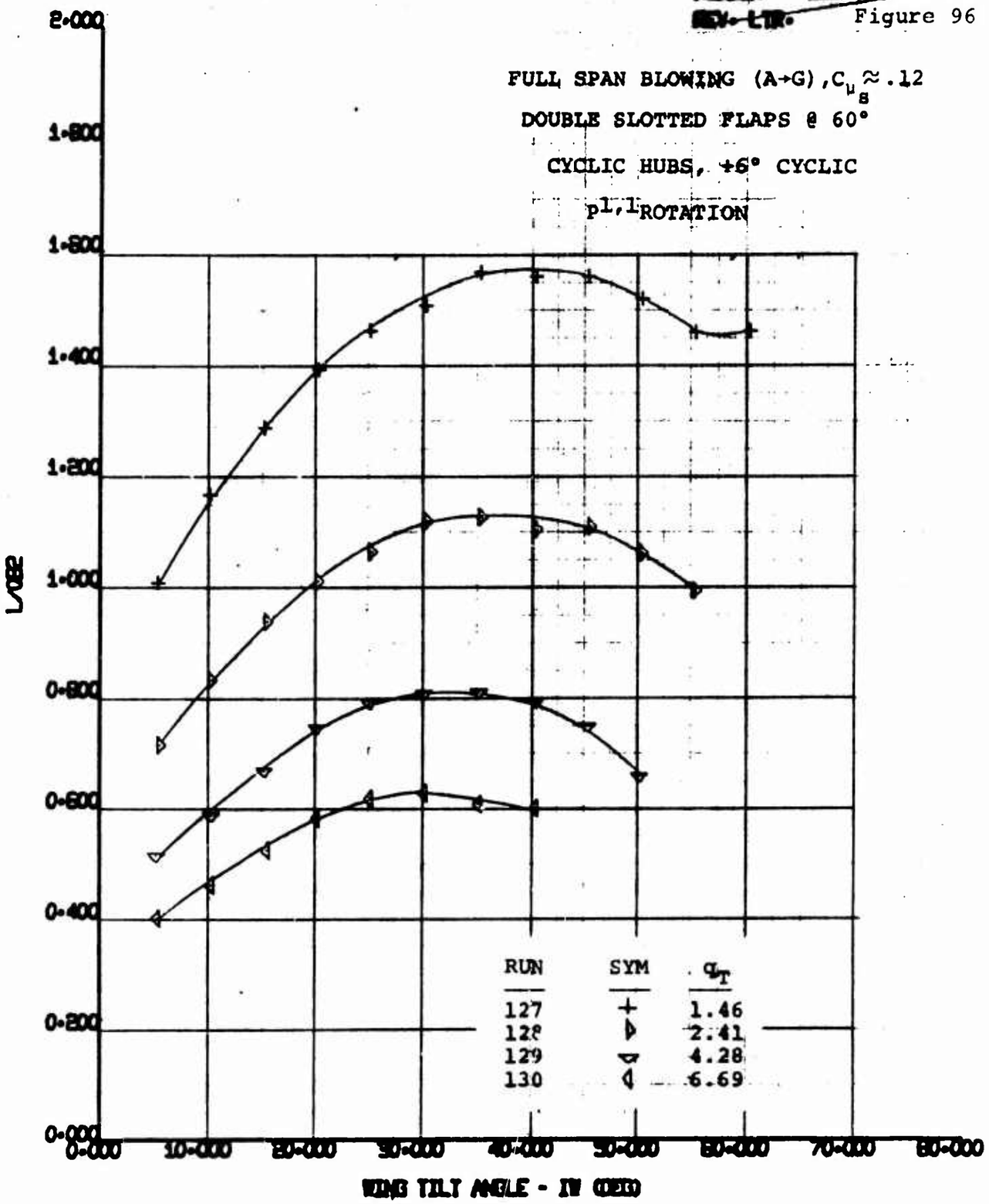

170 HALF SPAN MODEL WT 040 0-3 L/QB2 VS WING TILT ANGLE	BWT 55 4/ 8/70

FULL SPAN BLOWING (A→G), $C_{\mu_s} \approx .12$

DOUBLE SLOTTED FLAPS @ 60°

CYCLIC HUBS, +6° CYCLIC

$P_{1,1}$ ROTATION

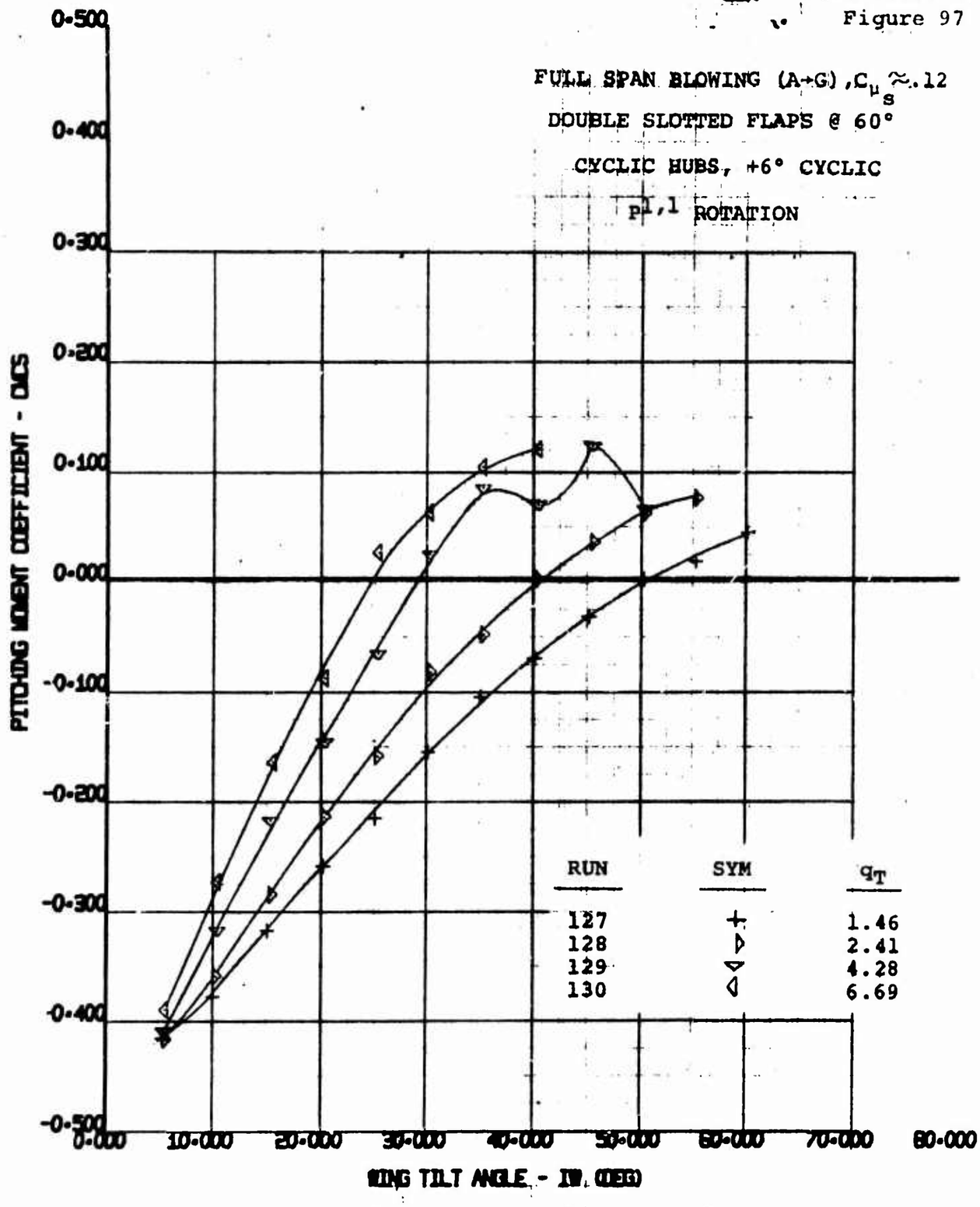

170 HALF SPAN MODEL VR 040 0-3 CMCS VS TILT WING ANGLE	BWT 55 4/ 8/70

FULL SPAN BLOWING (A→G) $C_{\mu_s} \approx .09$

DOUBLE SLOTTED FLAPS @60°

COLLECTIVE HUBS
p1,1 ROTATION

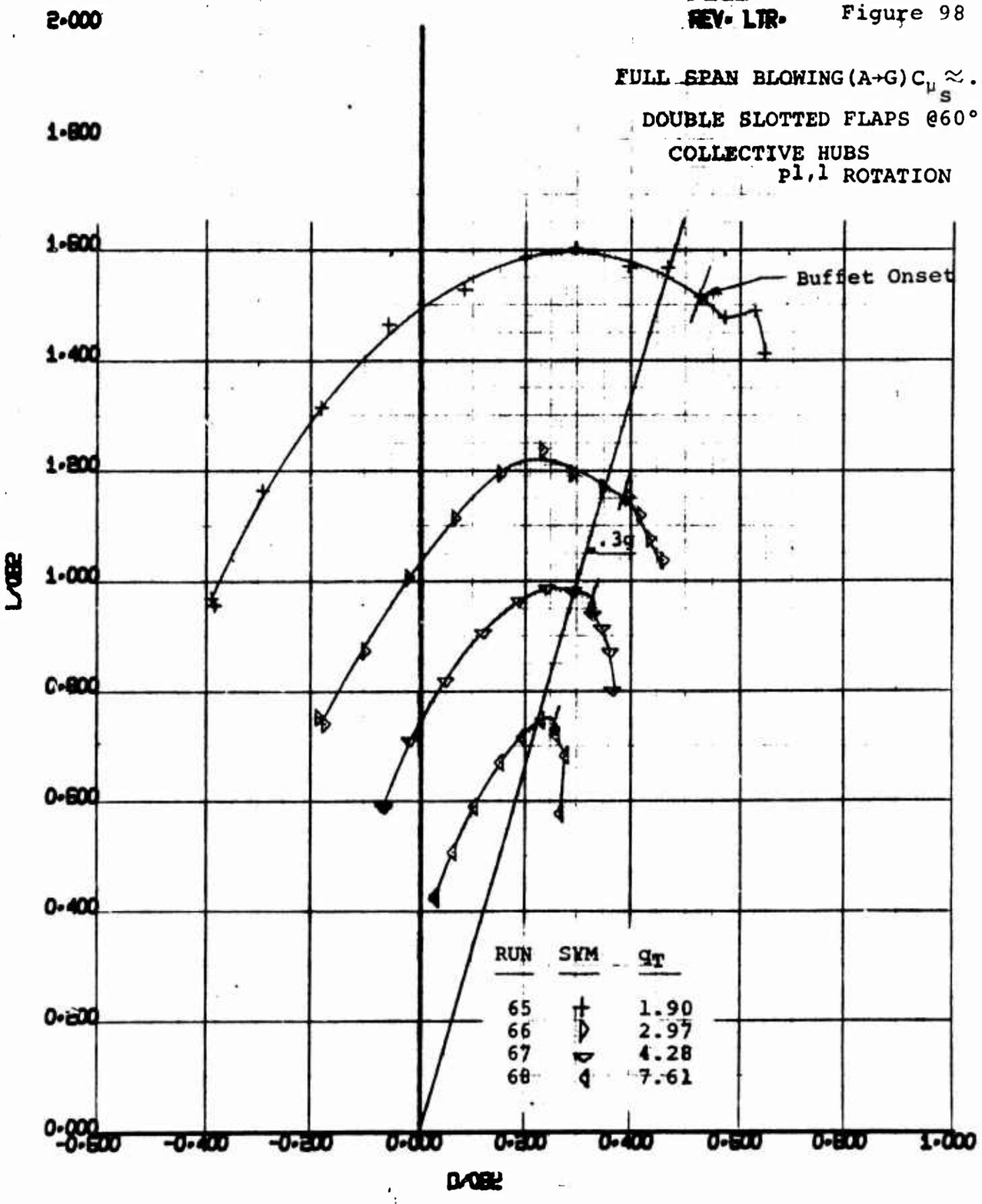

170 HALF SPAN MODEL VR 040 0-9 L/QS2 VS D/QS2	BMT 55 4/ 7/70

FULL SPAN BLOWING (A+G) $C_{\mu_s} \approx .09$
DOUBLE SLOTTED FLAPS @60°
COLLECTIVE HUBS, pl.1 ROTATION

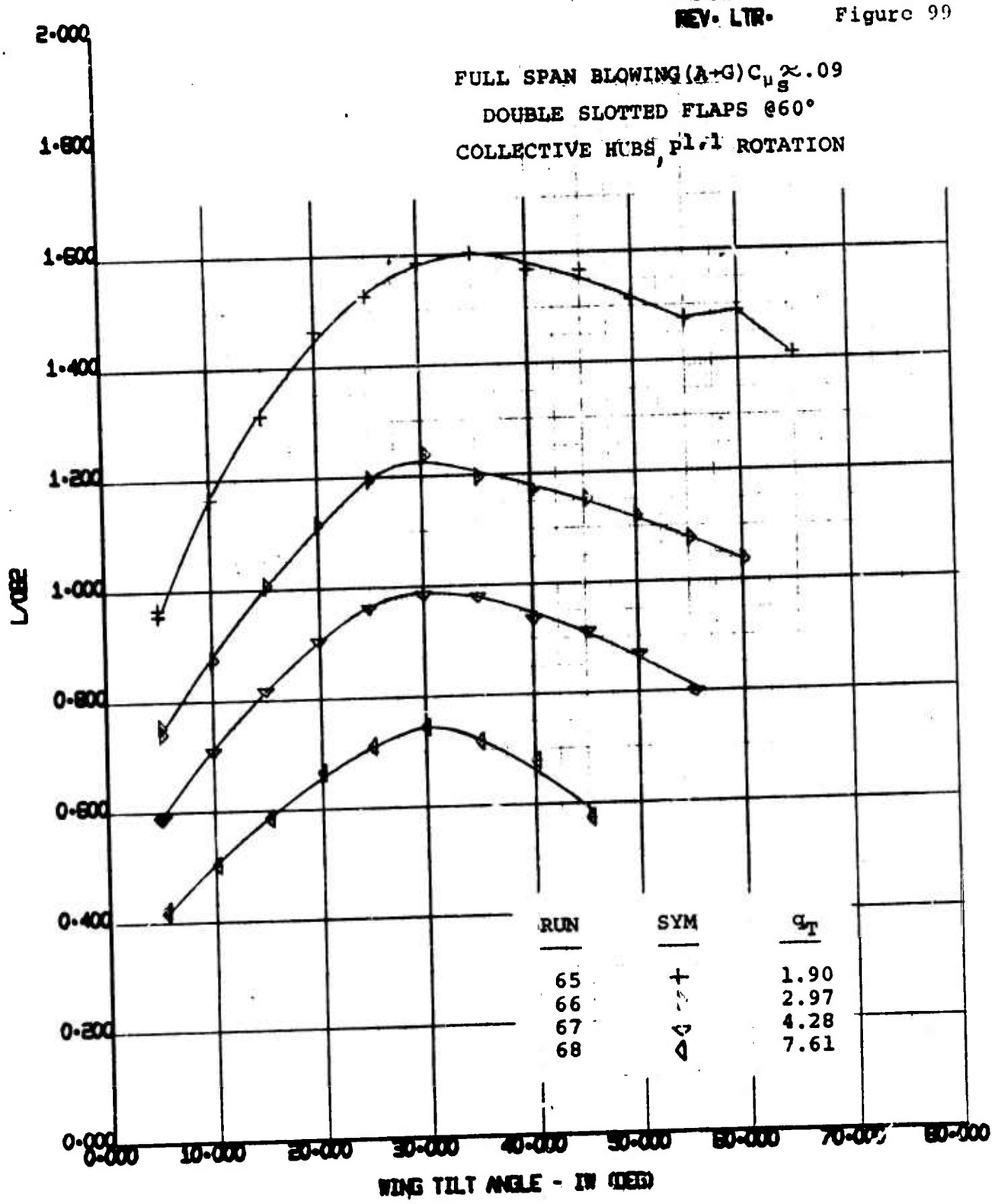

170 HALF SPAN MODEL WR 040 0-3 L/QS2 VS WING TILT ANGLE	BVWT 55 4/ 7/70

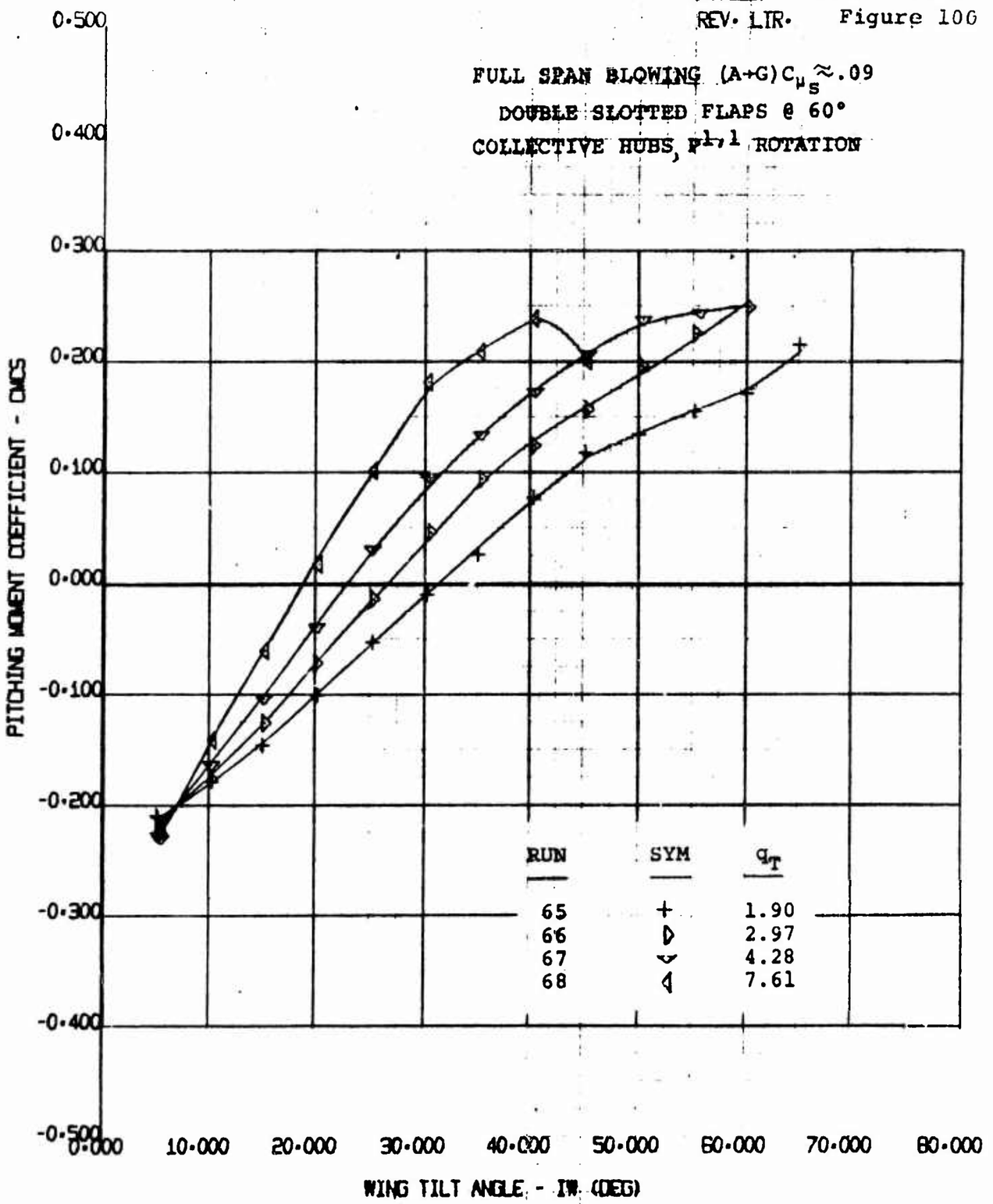

170 HALF SPAN MODEL VR 040 0-3 CMCS VS TILT WING ANGLE	BVWT 55 4/ 7/70

PARTIAL SPAN BLOWING (A→C&G) $C_{\mu_s} \approx .12$

DOUBLE SLOTTED FLAPS @ 60°

CYCLIC HUBS, +4° CYCLIC, 45° LEAD

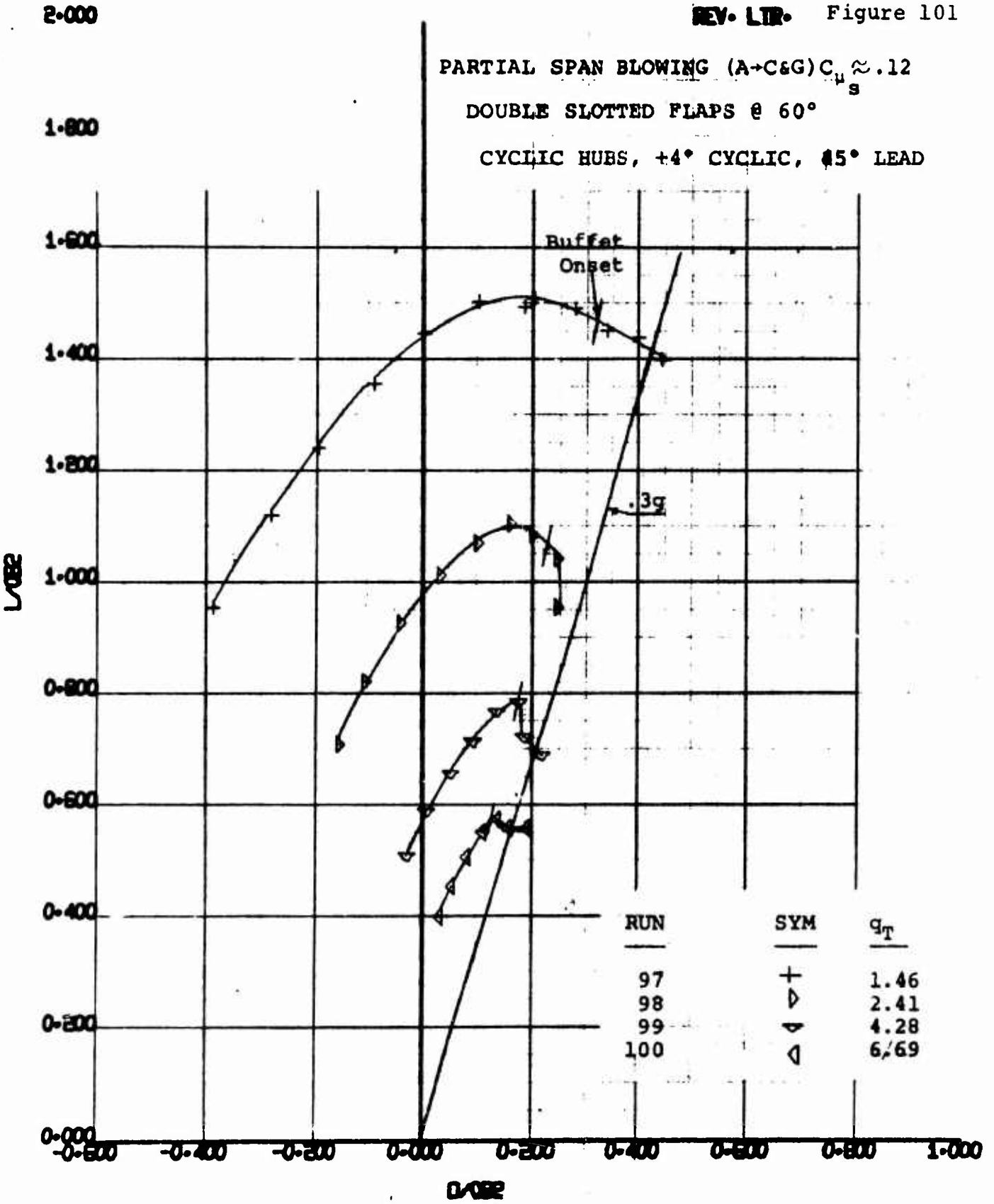

170 HALF SPAN MODEL WR 040 0-3 L/QS2 VS D/QS2	BMIT 55 4/ 7/70

PARTIAL SPAN BLOWING (A→C&G) $C_{\mu_s} \approx .12$
DOUBLE SLOTTED FLAPS @ 60°
CYCLIC HUBS, +4° CYCLIC, 45° LEAD

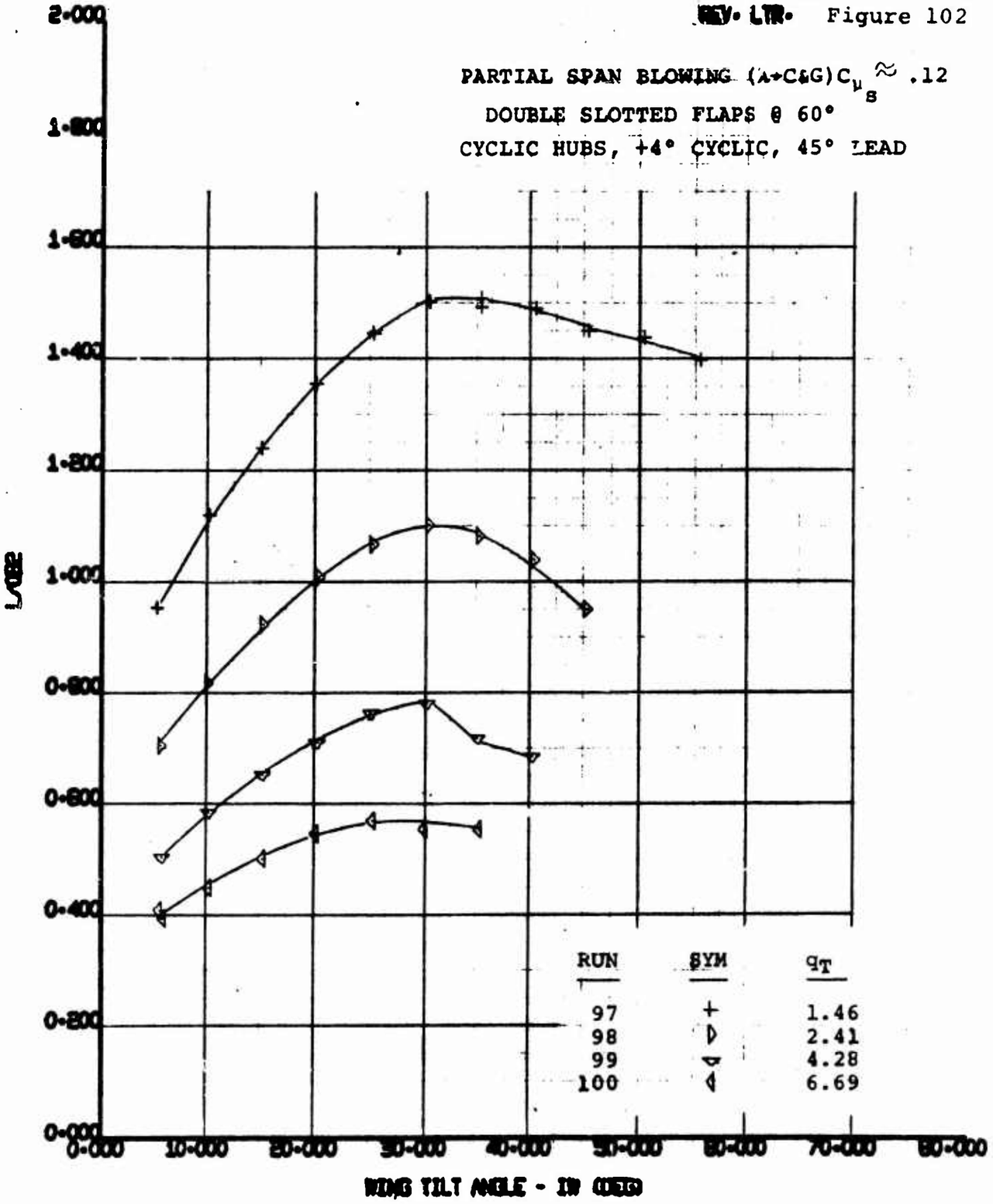

170 HALF SPAN MODEL VR 040 0-3 L/QE2 VS WING TILT ANGLE	BWT 95 4/ 7/70

PARTIAL SPAN BLOWING (A+C&G) $C_{\mu_s} \approx .12$

DOUBLE SLOTTED FLAPS @ 60°

CYCLIC HUB$, +4° CYCLIC, 45° LEAD

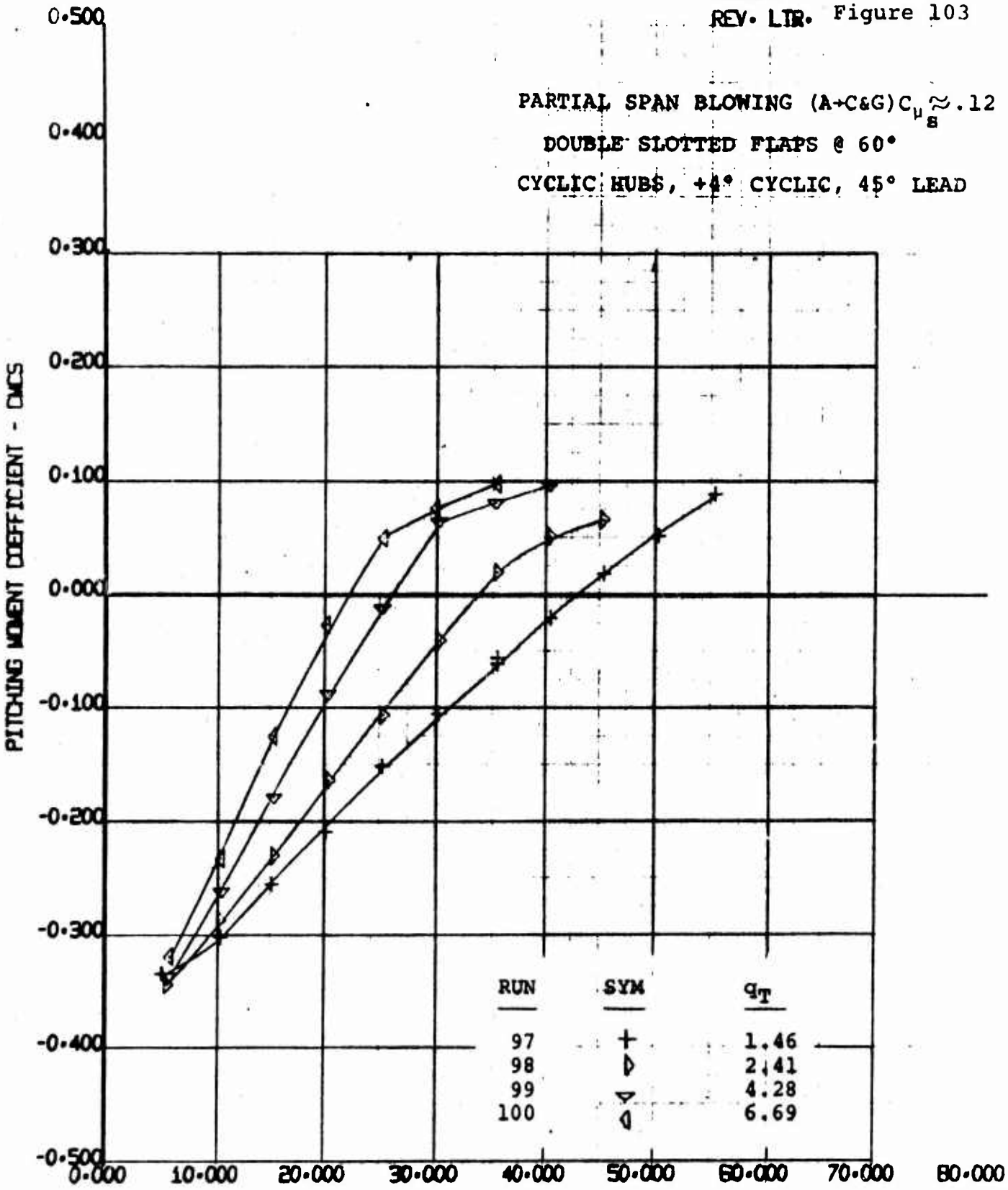

170 HALF SPAN MODEL VR 240 0-3 CMCS VS TILT WING ANGLE	BVWT 55 4/ 7/70

Figure 104

FULL SPAN BLOWING (A→G), $C_{\mu_s} \approx .11$

SINGLE SLOTTED FLAPS @ 45°

CYCLIC HUBS, +4° CYCLIC

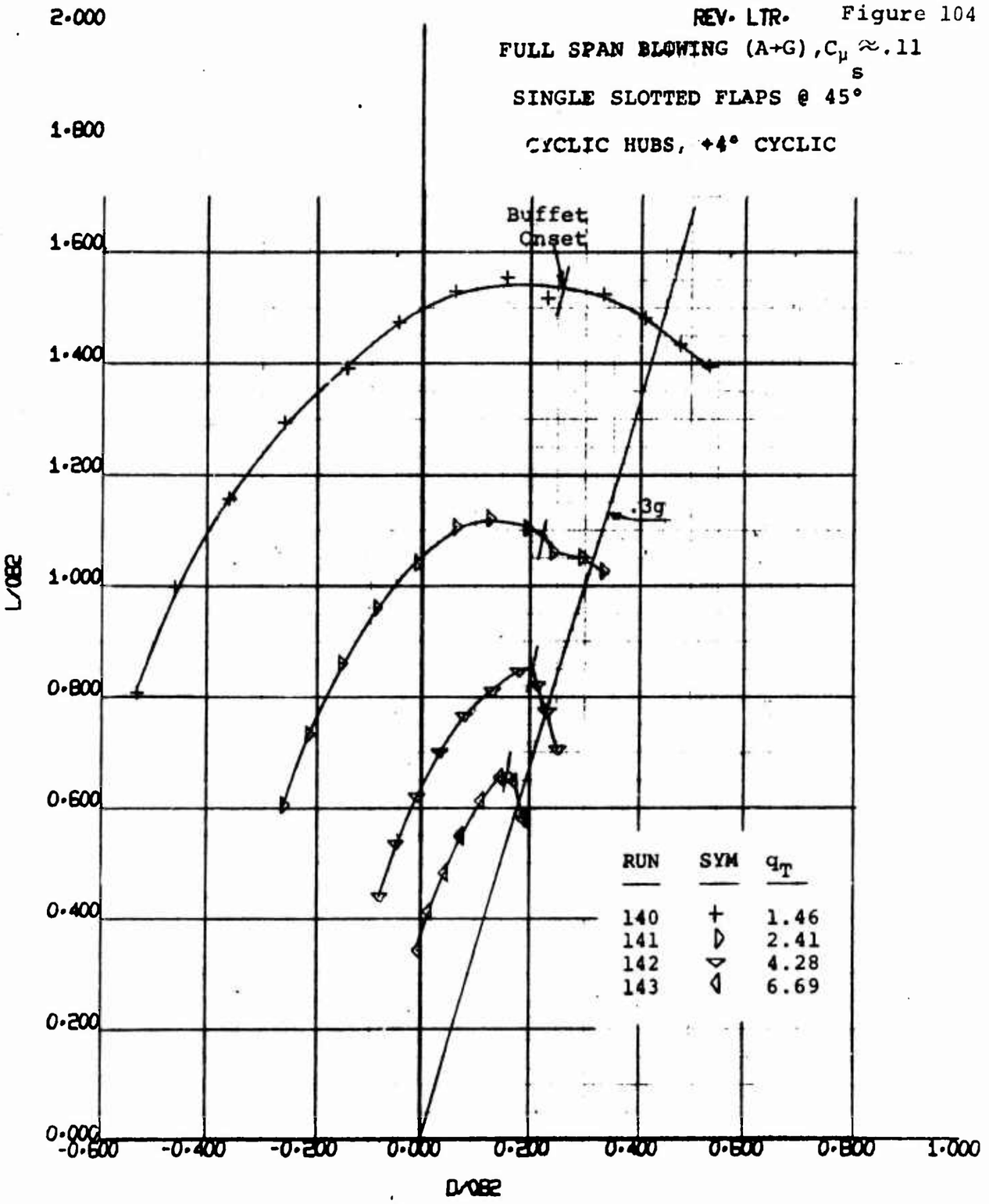

NOTE: (3) OUTBOARD FENCES OFF

170 HALF SPAN MODEL VR 040 0-3 L/QS2 VS D/QS2	BVWT 55 4/ 8/70

FULL SPAN BLOWING (A+G), $C_{\mu_s} \approx .11$

SINGLE SLOTTED FLAPS @ 45°

CYCLIC HUBS, +4° CYCLIC

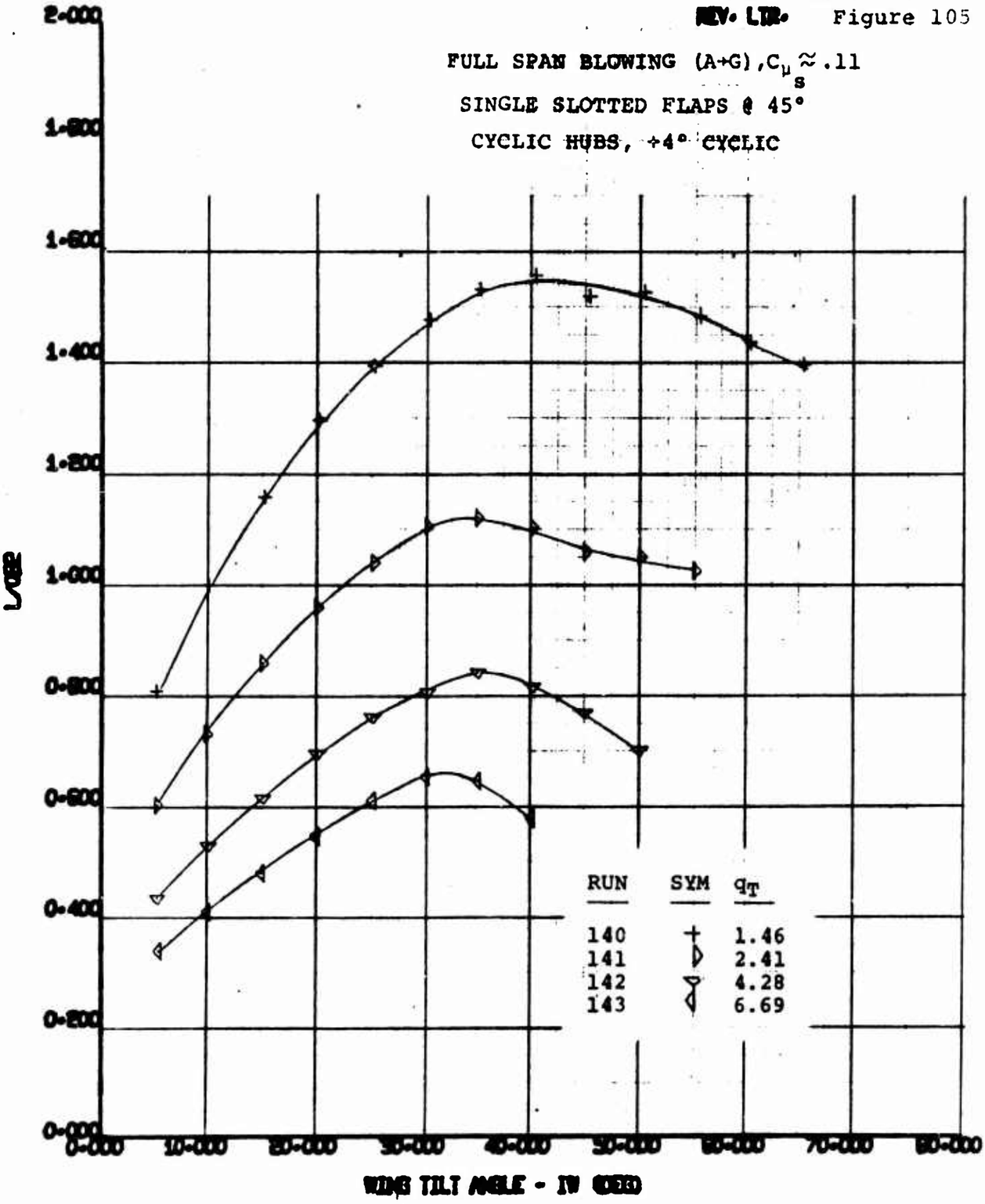

NOTE: (3) OUTBOARD FENCES OFF

170 HALF SPAN MODEL VR 040 0-9 L/QR2 VS WING TILT ANGLE	BMT 55 4/ 8/70

FULL SPAN BLOWING (A→G), $C_{\mu_s} \approx .11$
SINGLE SLOTTED FLAPS @ 45°
CYCLIC HUBS, 44° CYCLIC

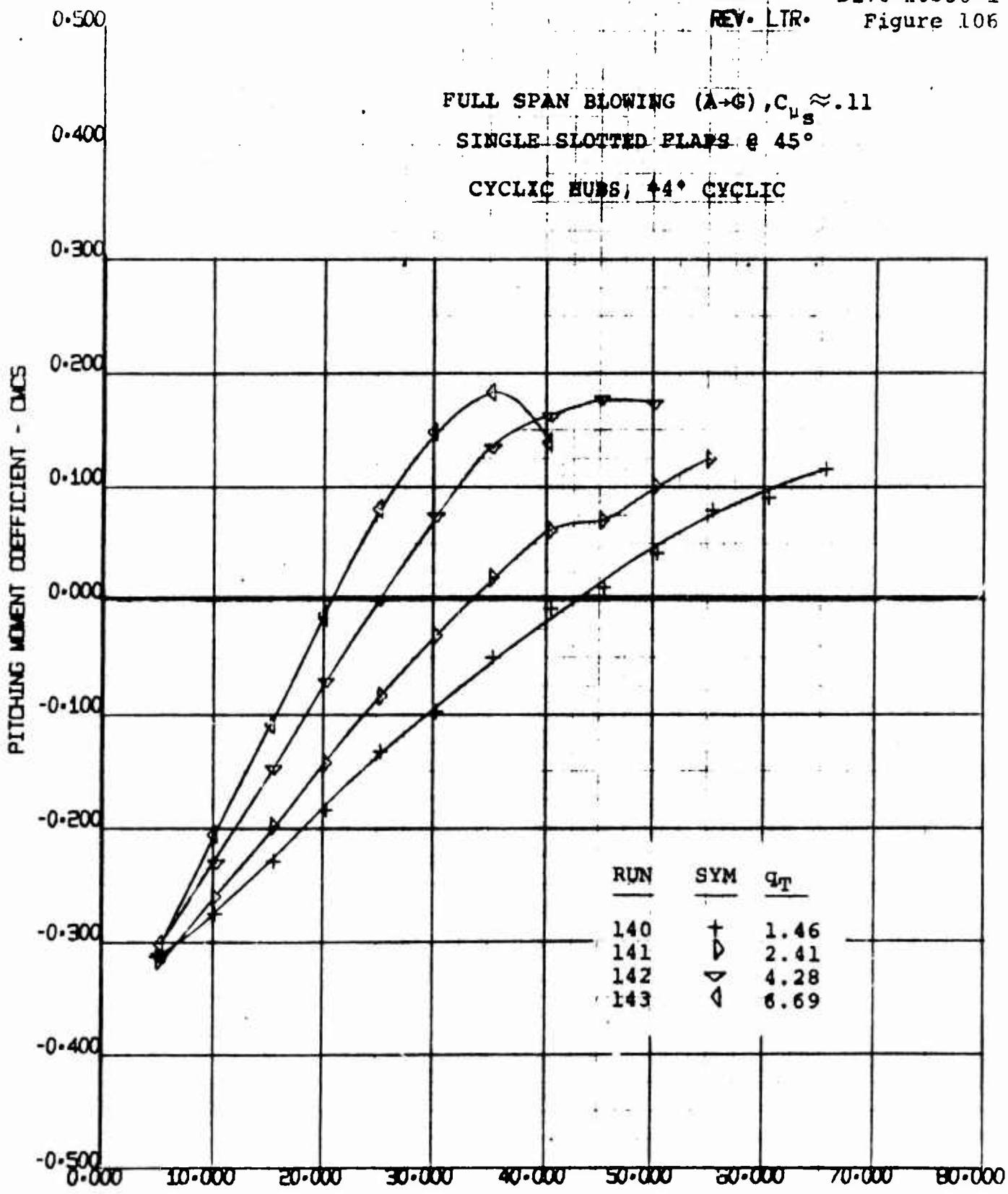

NOTE: (3) OUTBOARD FENCES OFF

170 HALF SPAN MODEL VR 040 0-3 CMCS VS TILT WING ANGLE	BVWT 55 4/ 8/70

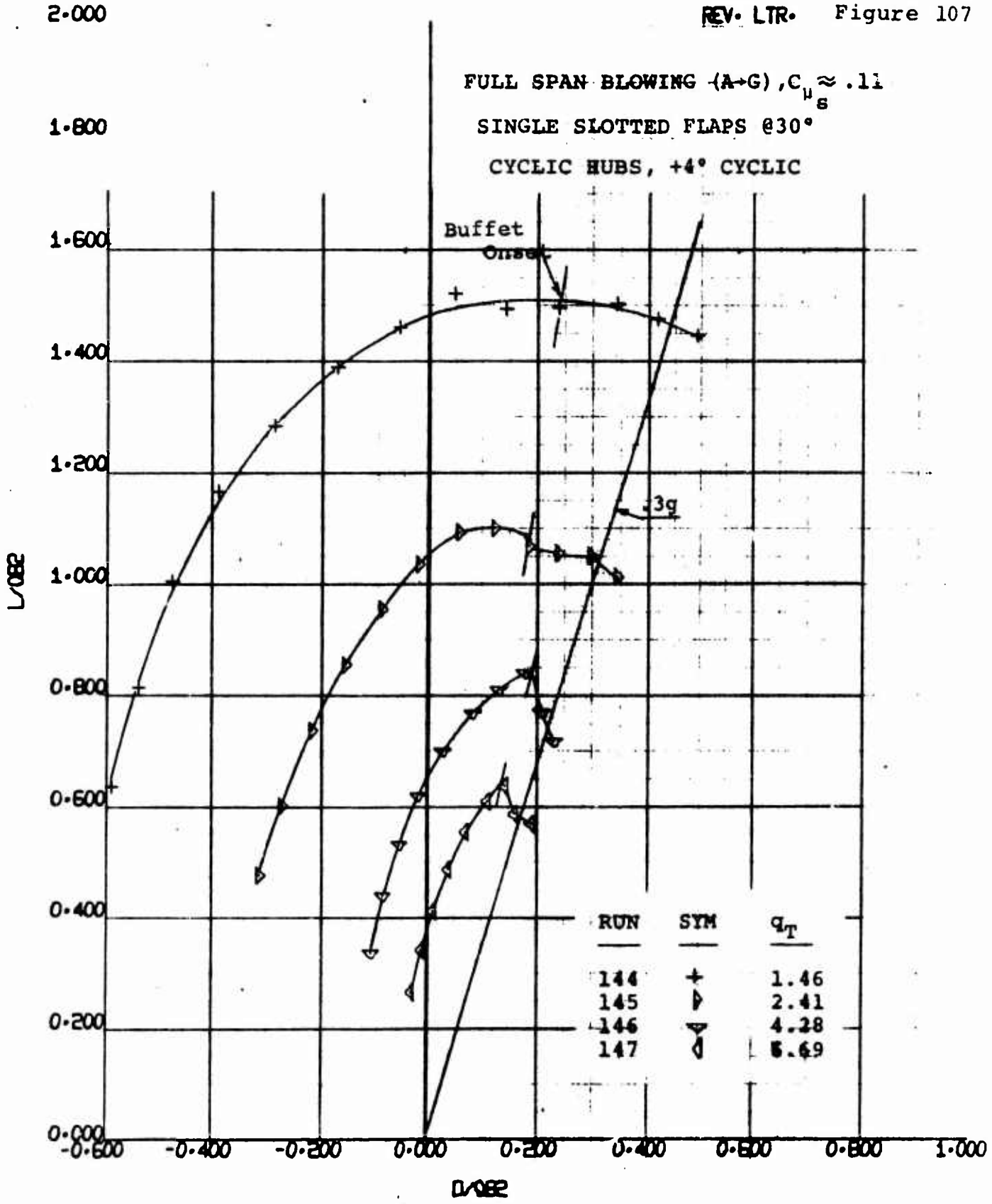

NOTE: (3) OUTBOARD FENCES OFF

170 HALF SPAN MODEL VR 040 0-3 L/QBZ VS D/QBZ	BVWT 55 4/ 8/70

FULL SPAN BLOWING (A+G) $C_{\mu_s} \approx .11$

SINGLE SLOTTED FLAPS @30°

CYCLIC HUBS, +4° CYCLIC

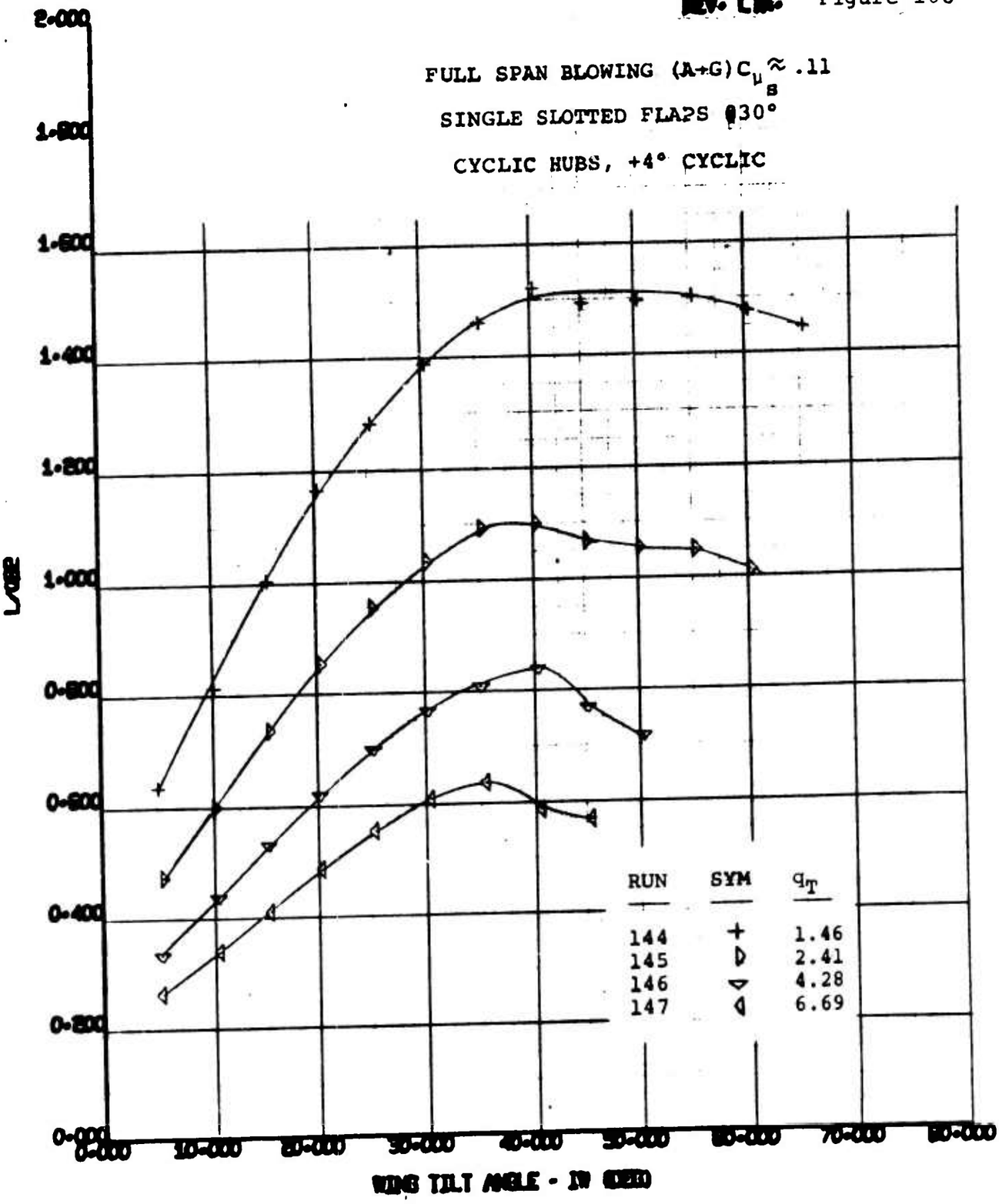

NOTE: (3) OUTBOARD FENCES OFF

170 HALF SPAN MODEL VR 040 0-3 L/QR2 VS WING TILT ANGLE	BWT 55 4/ 8/70

FULL SPAN BLOWING (A+C), $C_{\mu_s} \approx .11$

SINGLE SLOTTED FLAPS @30°

CYCLIC HUBS, +4° CYCLIC

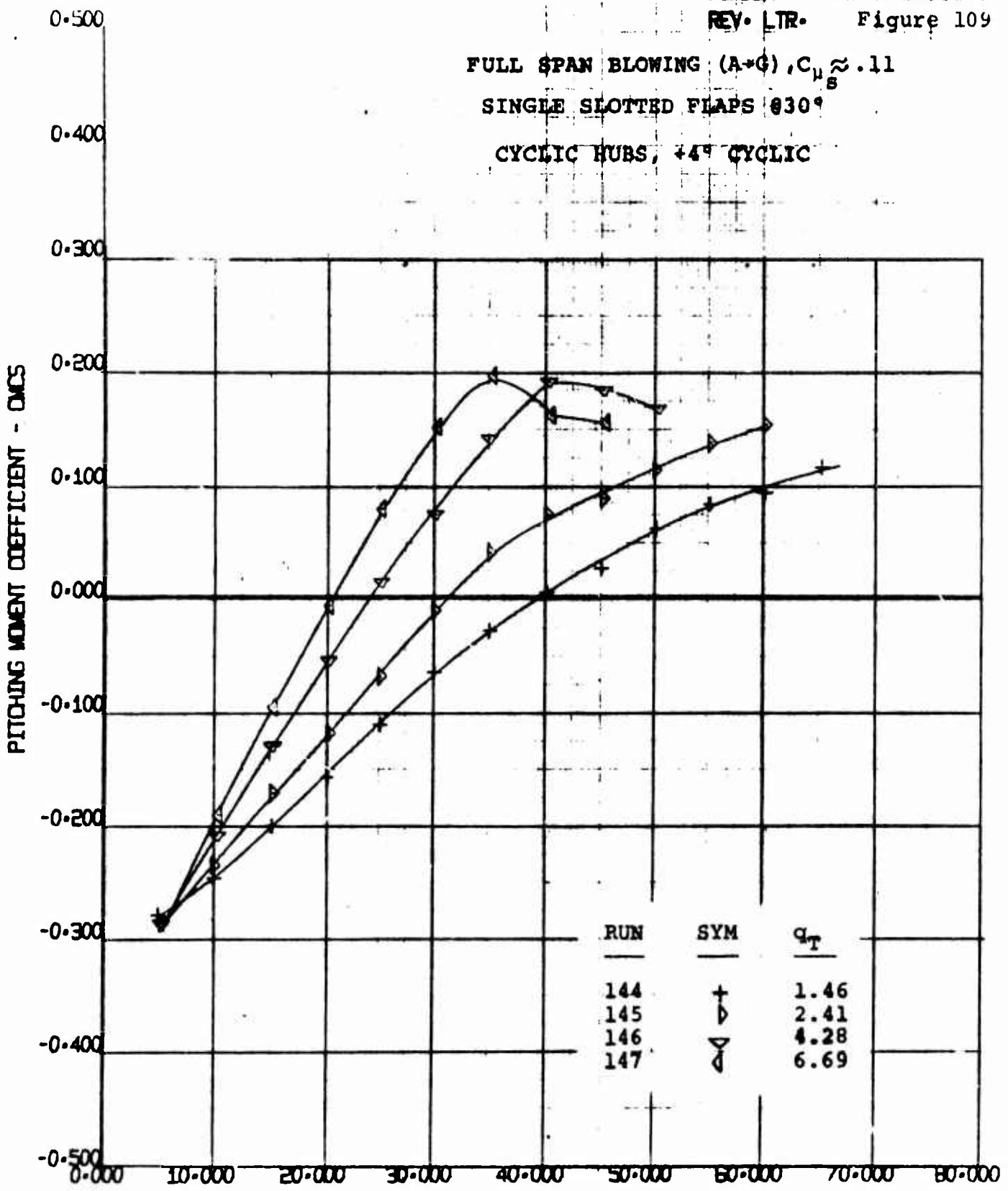

NOTE: (3) OUTBOARD FENCES OFF

170 HALF SPAN MODEL VR 040 0-3 CMCS VS TILT WING ANGLE	BVWT 55 4/ 8/70

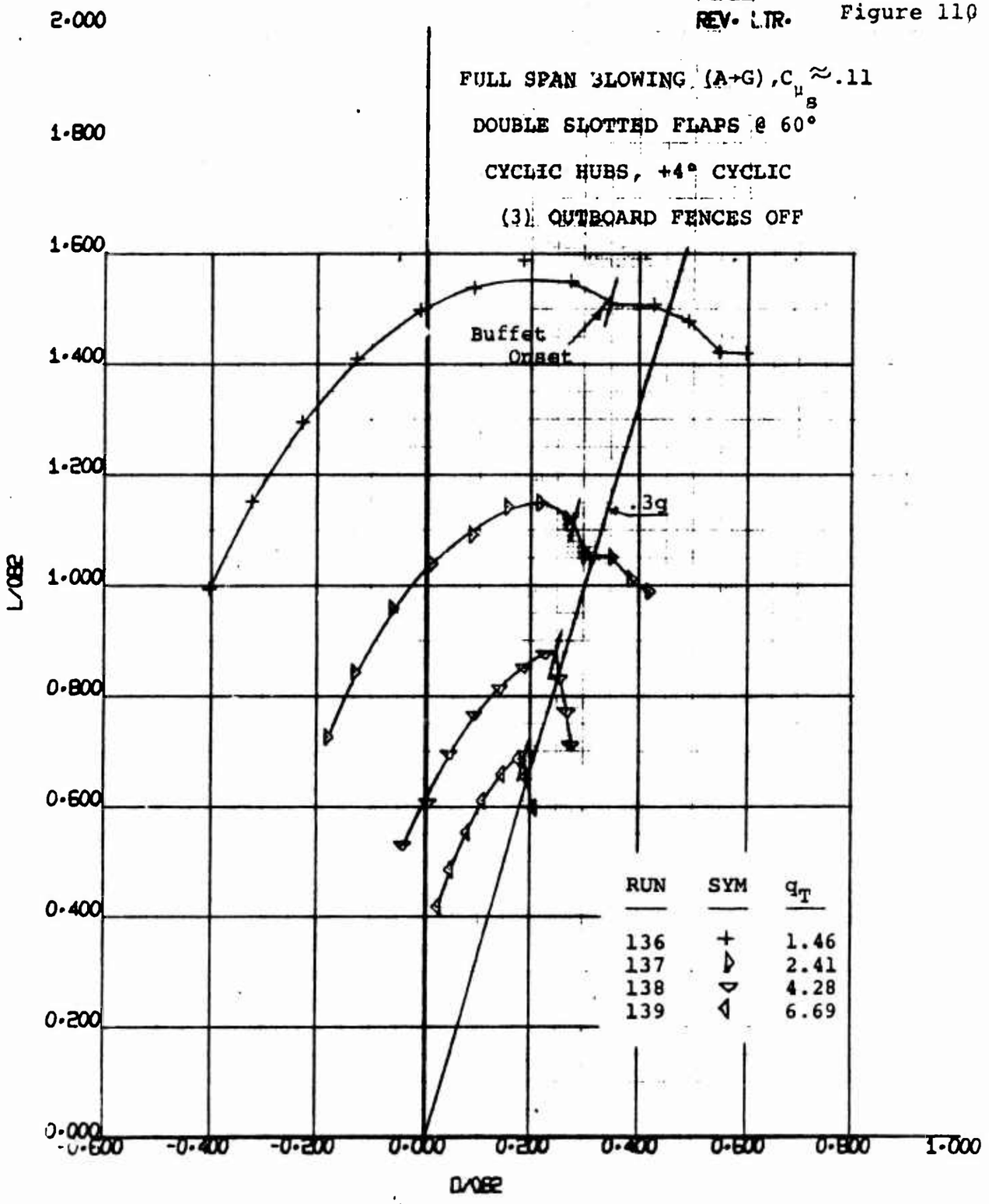

170 HALF SPAN MODEL VR 040 0-3 L/QS2 VS D/QS2	BVWT 55 4/ 8/70

FULL SPAN BLOWING (A→G), $C_{\mu_s} \approx .11$

DOUBLE SLOTTED FLAPS @ 60°

CYCLIC HUBS, +4° CYCLIC

(3) OUTBOARD FENCES OFF

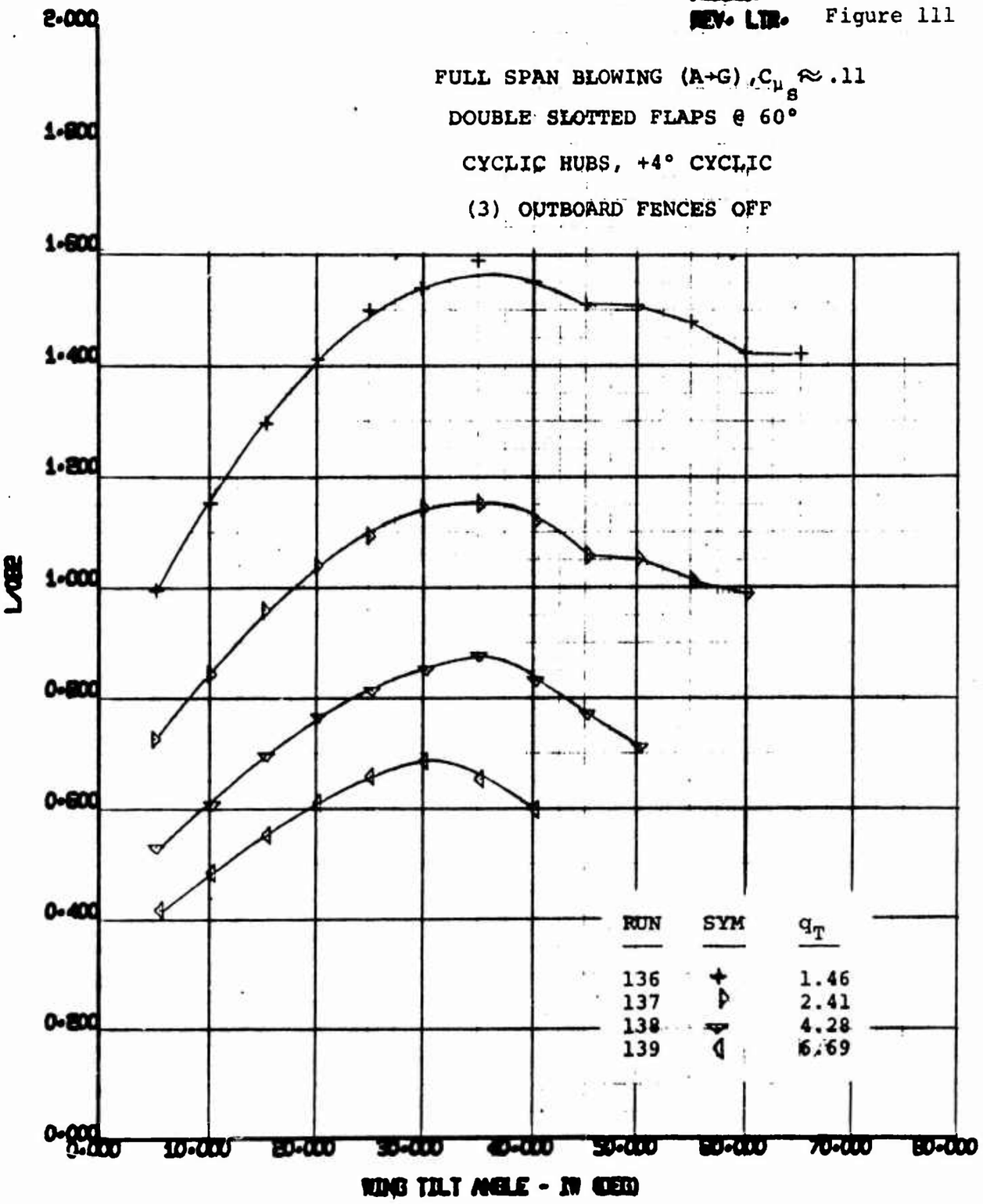

170 HALF SPAN MODEL VR 040 0-9 L/QS2 VS WING TILT ANGLE	BWT 55 4/ 8/70

NUMBER
REV. LTR.

FULL SPAN BLOWING (A+G), $C_{\mu_s} \approx .11$

DOUBLE SLOTTED FLAPS @ 60°

CYCLIC HUBS, +4° CYCLIC

(3) OUTBOARD FENCES OFF

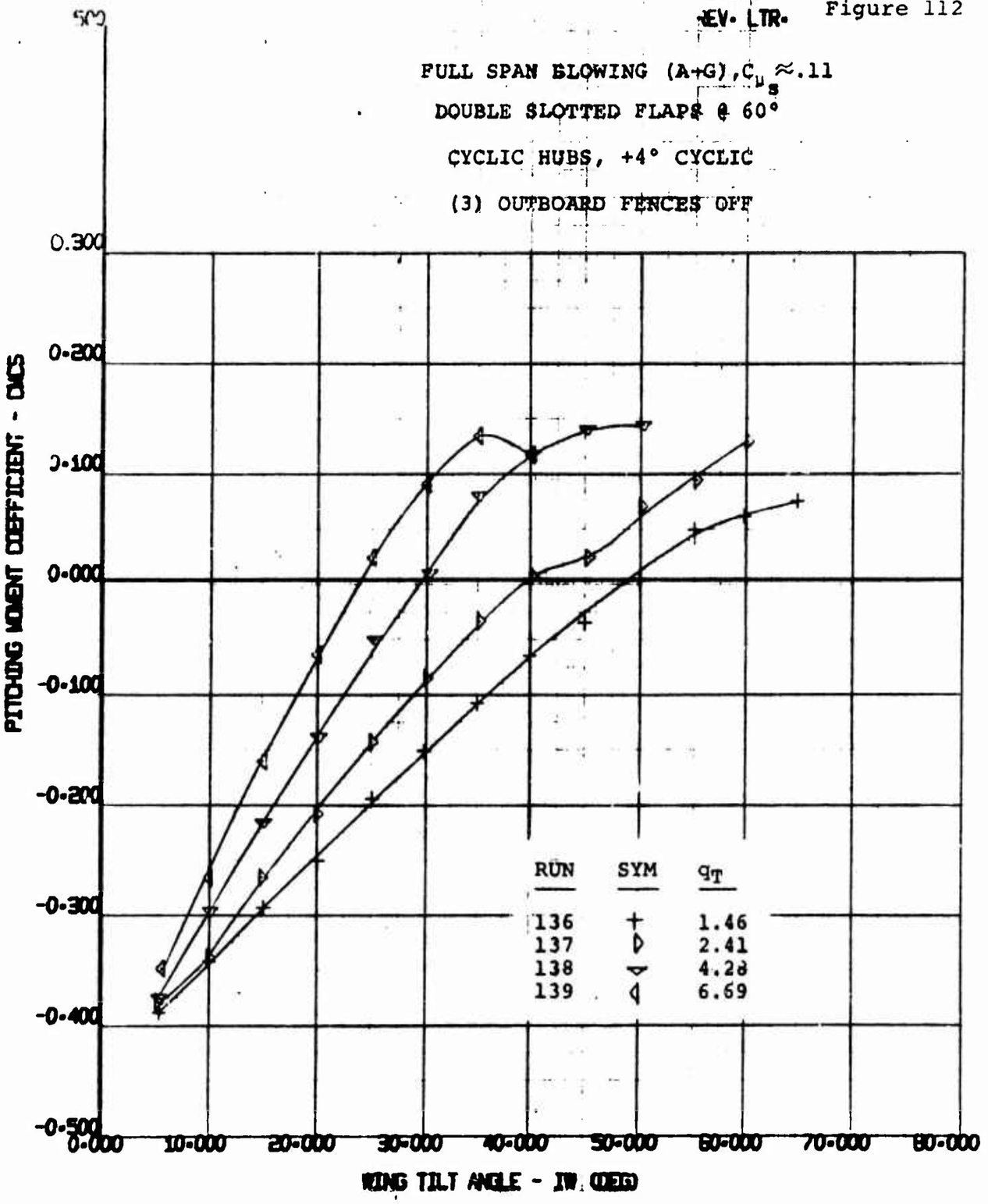

170 HALF SPAN MODEL VR 040 0-3 CMCS VS TILT WING ANGLE	BWT 55 4/ 8/70

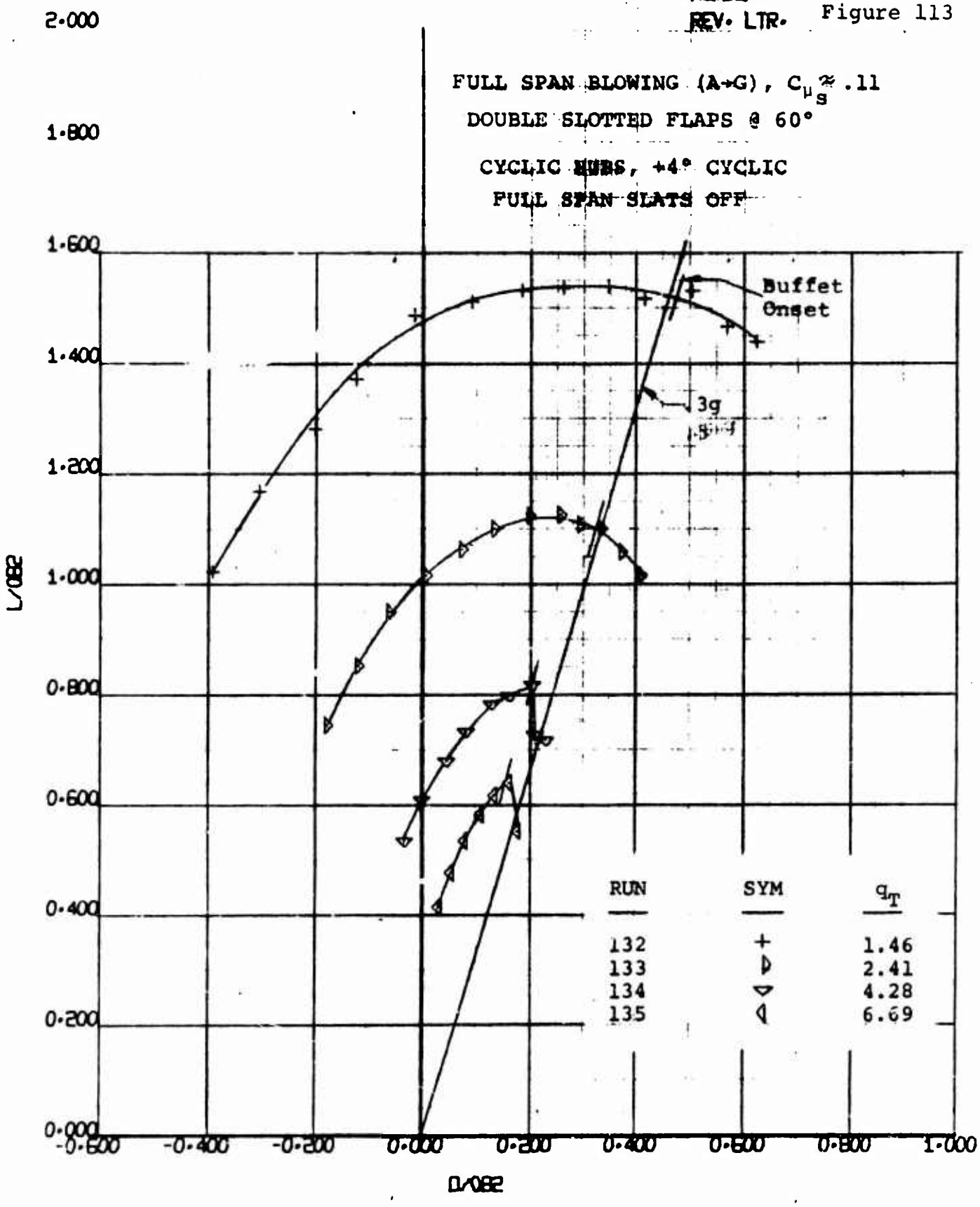

170 HALF SPAN MODEL WR 040 0-3 L/QBZ VS D/QBZ	BWT 55 4/ 8/70

FULL SPAN BLOWING (A+G), $C_{\mu_s} \approx .11$

DOUBLE SLOTTED FLAPS @ 60°

CYCLIC HUBS, +4° CYCLIC

FULL SPAN SLATS OFF

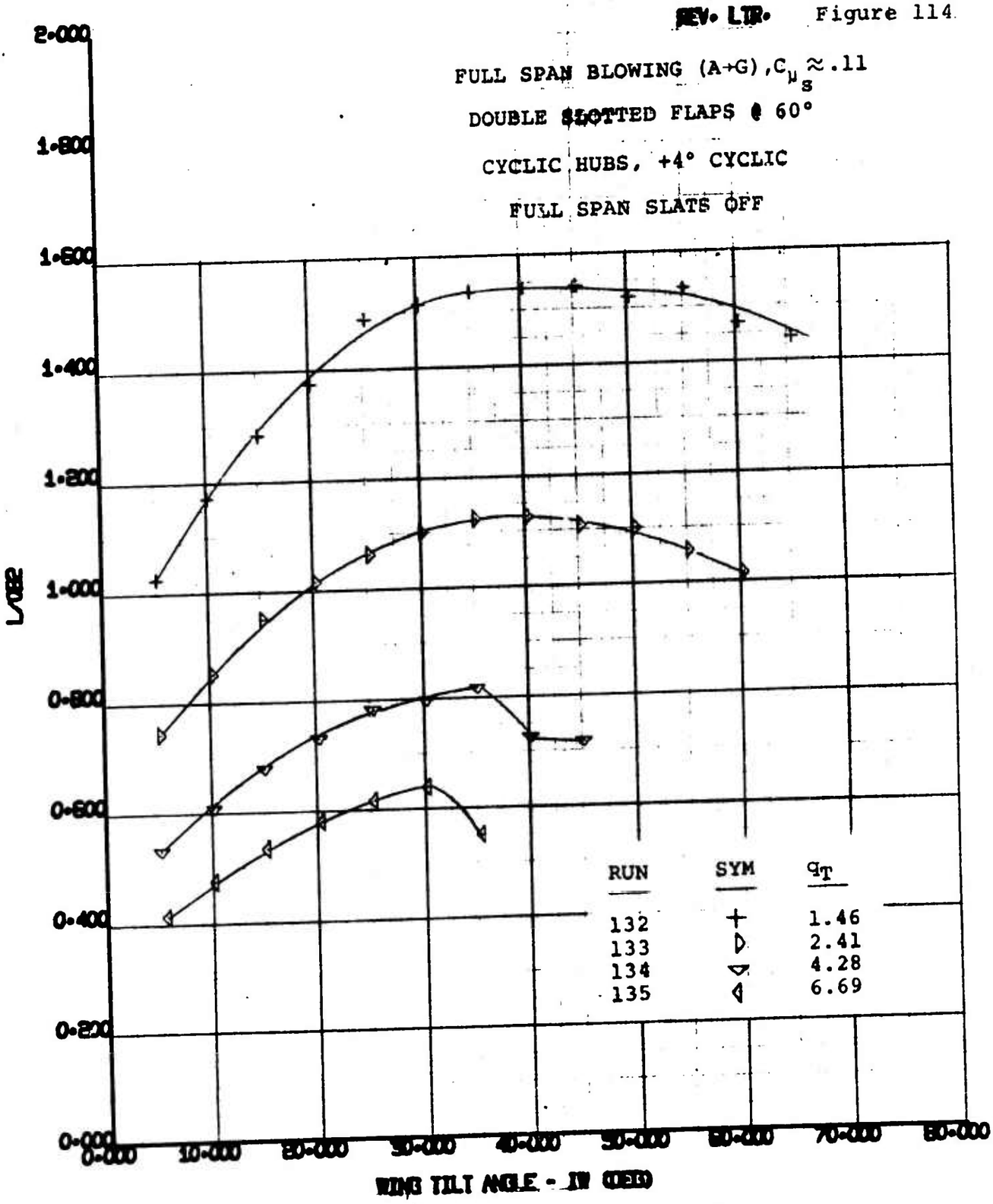

170 HALF SPAN MODEL VR 040 0-9 L/QB2 VS WING TILT ANGLE	BMT 55 4/ 8/70

FULL SPAN BLOWING (A→G), $C_{\mu_s} \approx .11$

DOUBLE SLOTTED FLAPS @ 60°

CYCLIC HUBS, +4° CYCLIC

FULL SPAN SLATS OFF

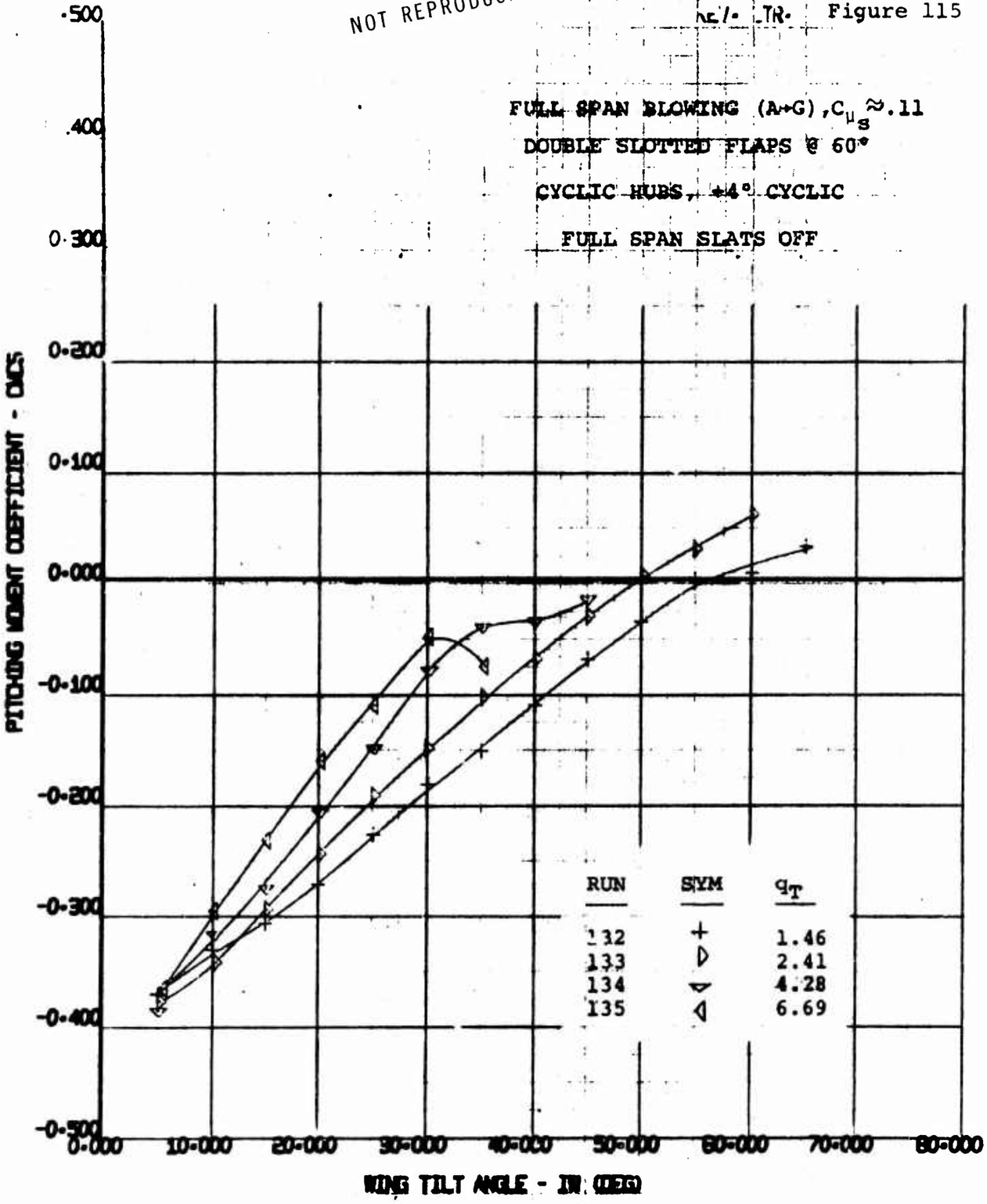

170 HALF SPAN MODEL VR 040 0-3 CMCS VS TILT WING ANGLE	BWT 55 4/ 8/70

Figure 116

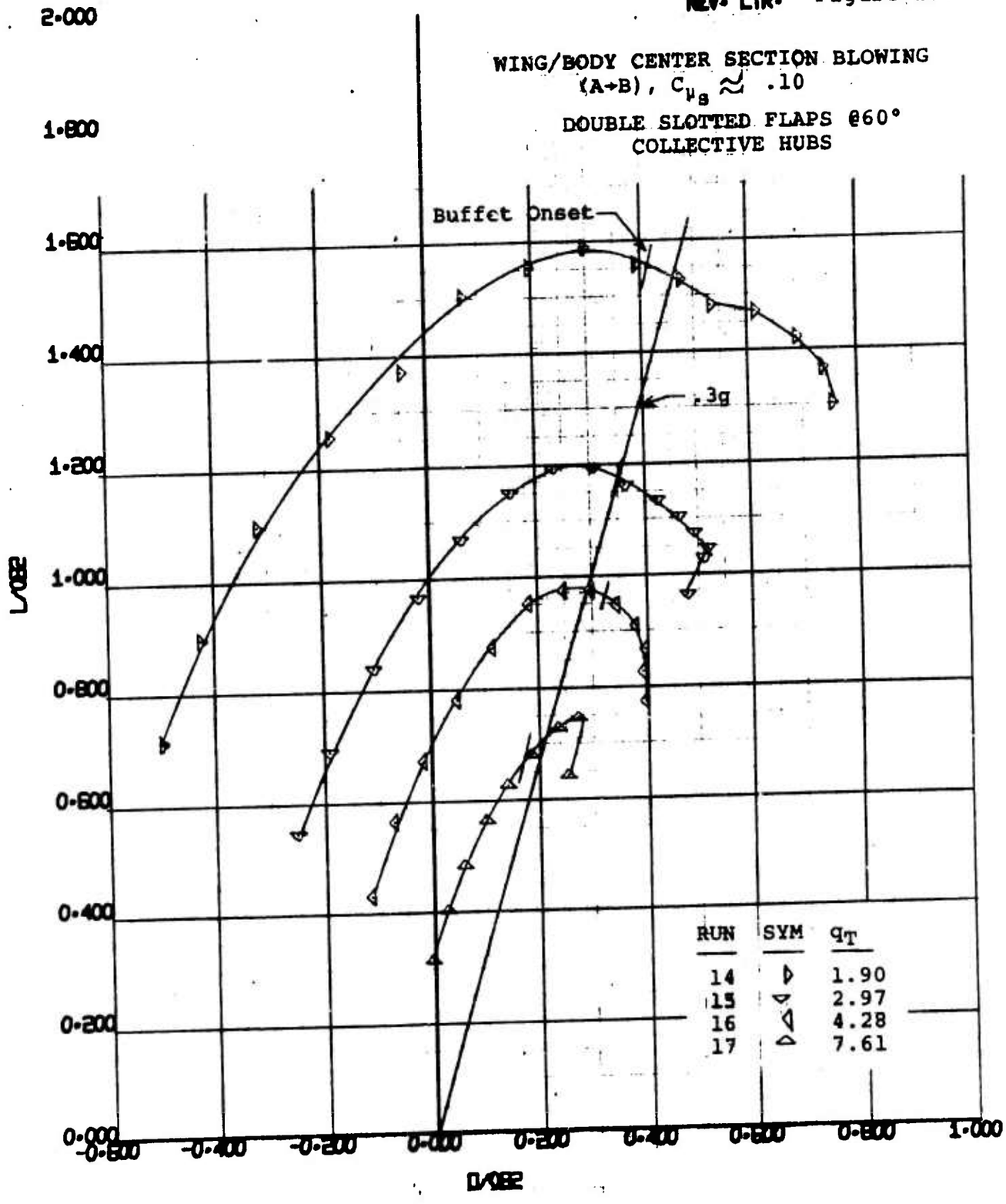

170 HALF SPAN MODEL VR 040 0-3 L/QB2 VS D/QB2	BMIT 55 4/ 3/70

WING/BODY CENTER SECTION BLOWING
(A→B), $C_{\mu_s} \approx .10$
DOUBLE SLOTTED FLAPS @60°
COLLECTIVE HUBS

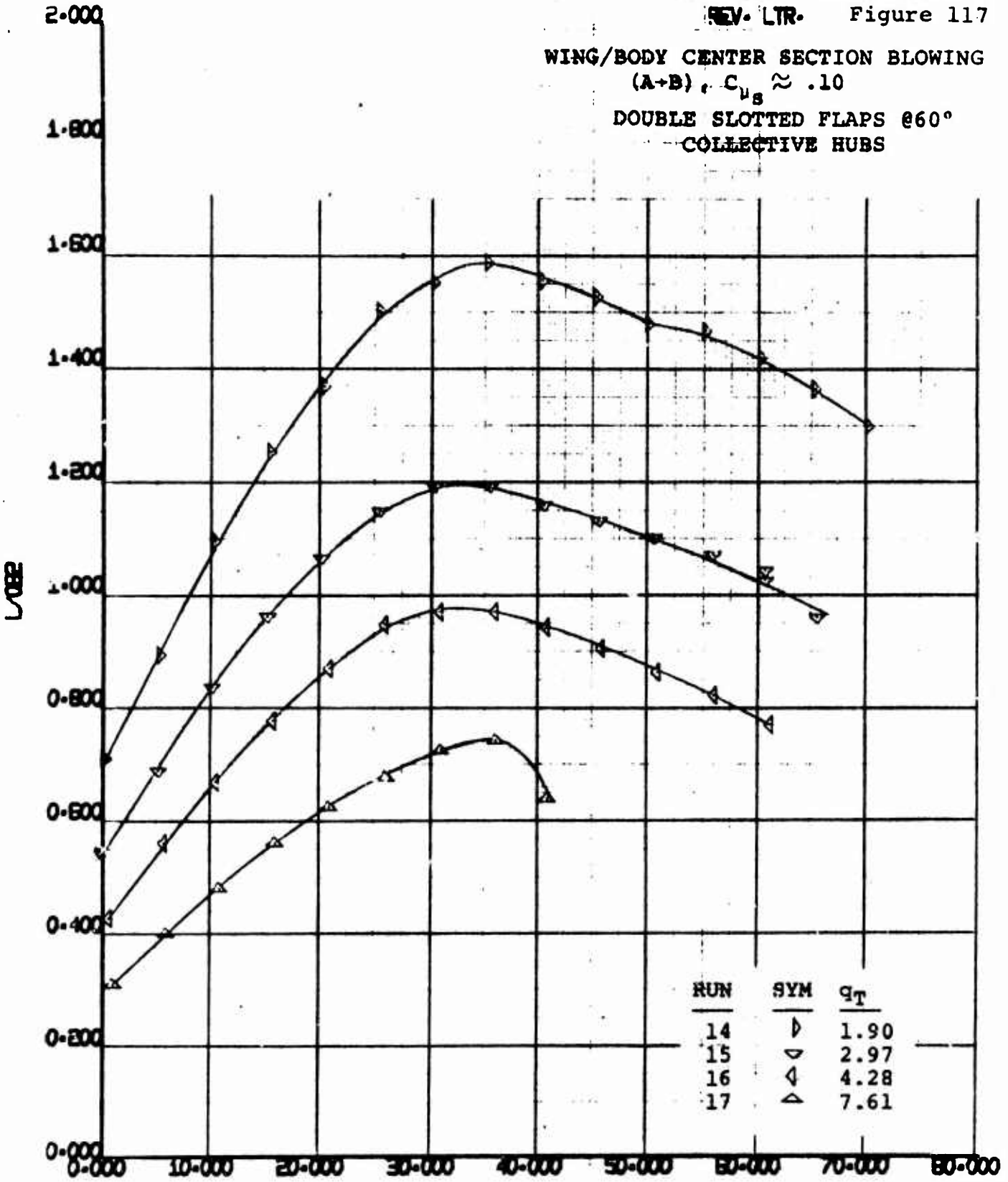

WING TILT ANGLE - IN DEG

170 HALF SPAN MODEL VR 040 0-3 L/QB2 VS WING TILT ANGLE	BMAT 55 4/ 3/70

WING/BODY CENTER SECTION BLOWING
(A+B), $C_{\mu_s} \approx .10$
DOUBLE SLOTTED FLAPS @60°
COLLECTIVE HUBS

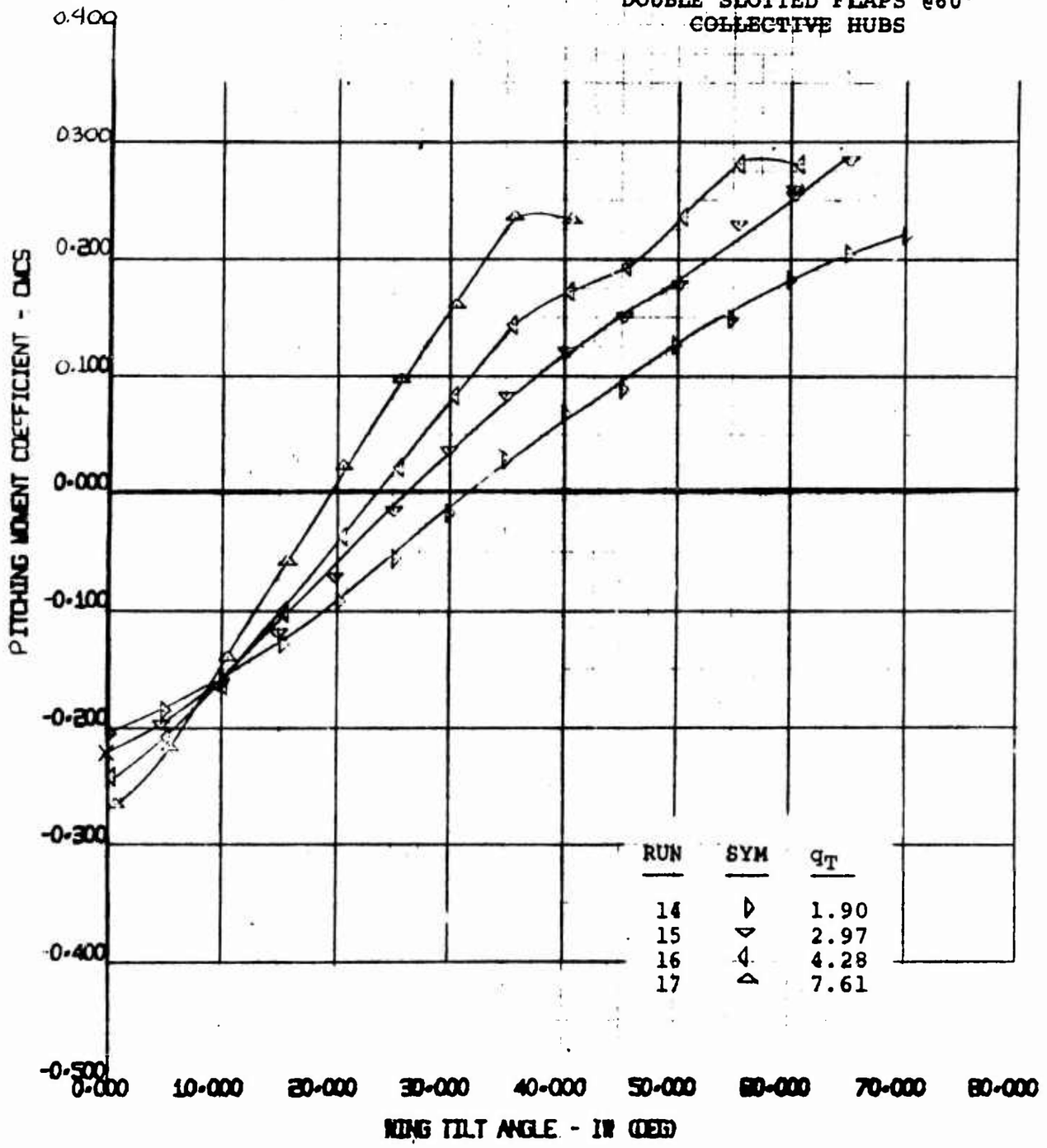

170 HALF SPAN MODEL R 040 0-3 MCS VS TILT WING ANGLE	BMHT 55 4/ 3/70

PARTIAL SPAN BLOWING (A+C) $C_{\mu_s} \approx .10$

DOUBLE SLOTTED FLAPS @60°
COLLECTIVE HUBS

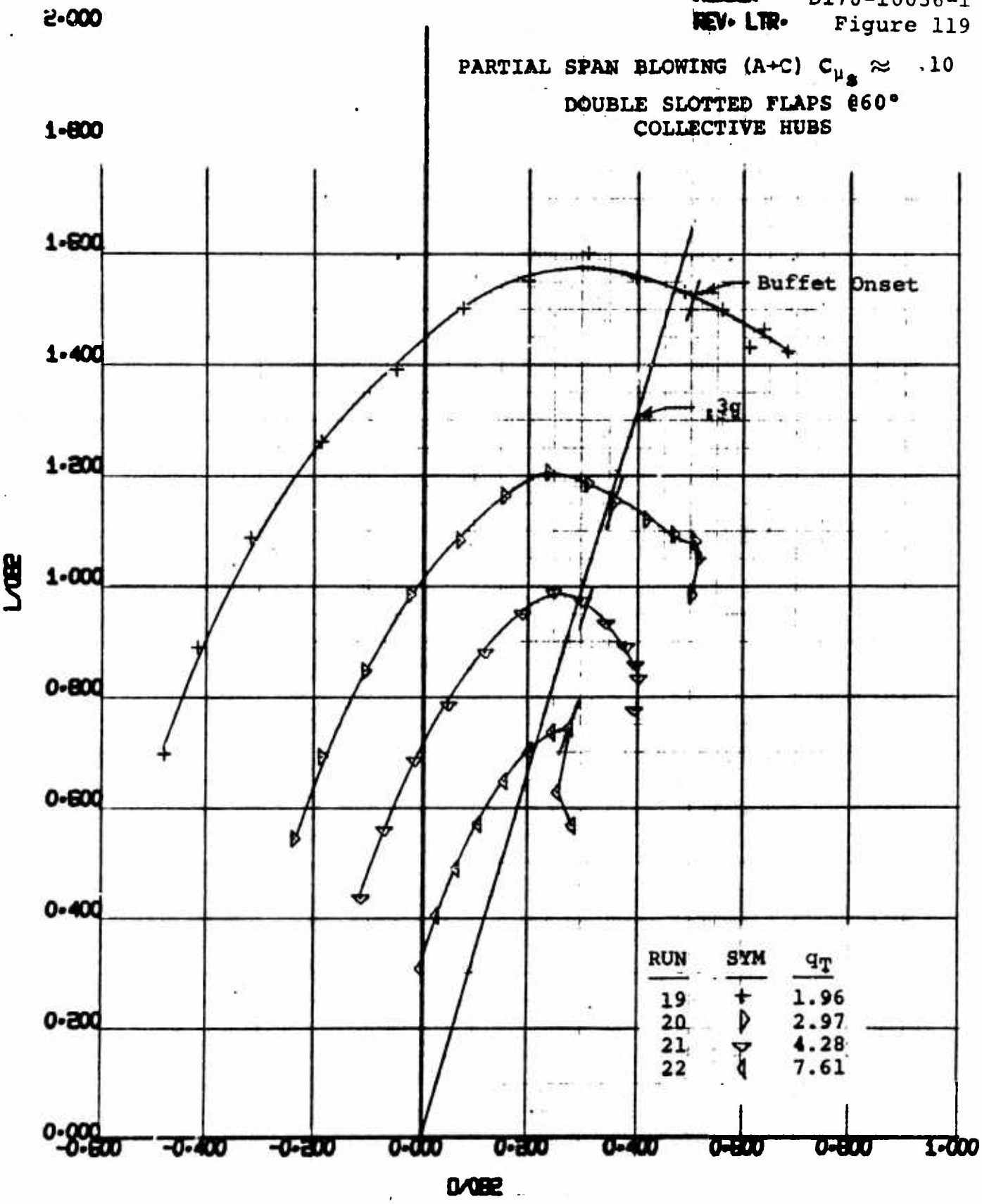

170 HALF SPAN MODEL WR 040 0-3 L/QBZ VS D/QBZ	BWT 55 4/ 3/70

PARTIAL SPAN BLOWING (A→C) $C_{\mu_s} \approx .10$

DOUBLE SLOTTED FLAPS @60°
COLLECTIVE HUBS

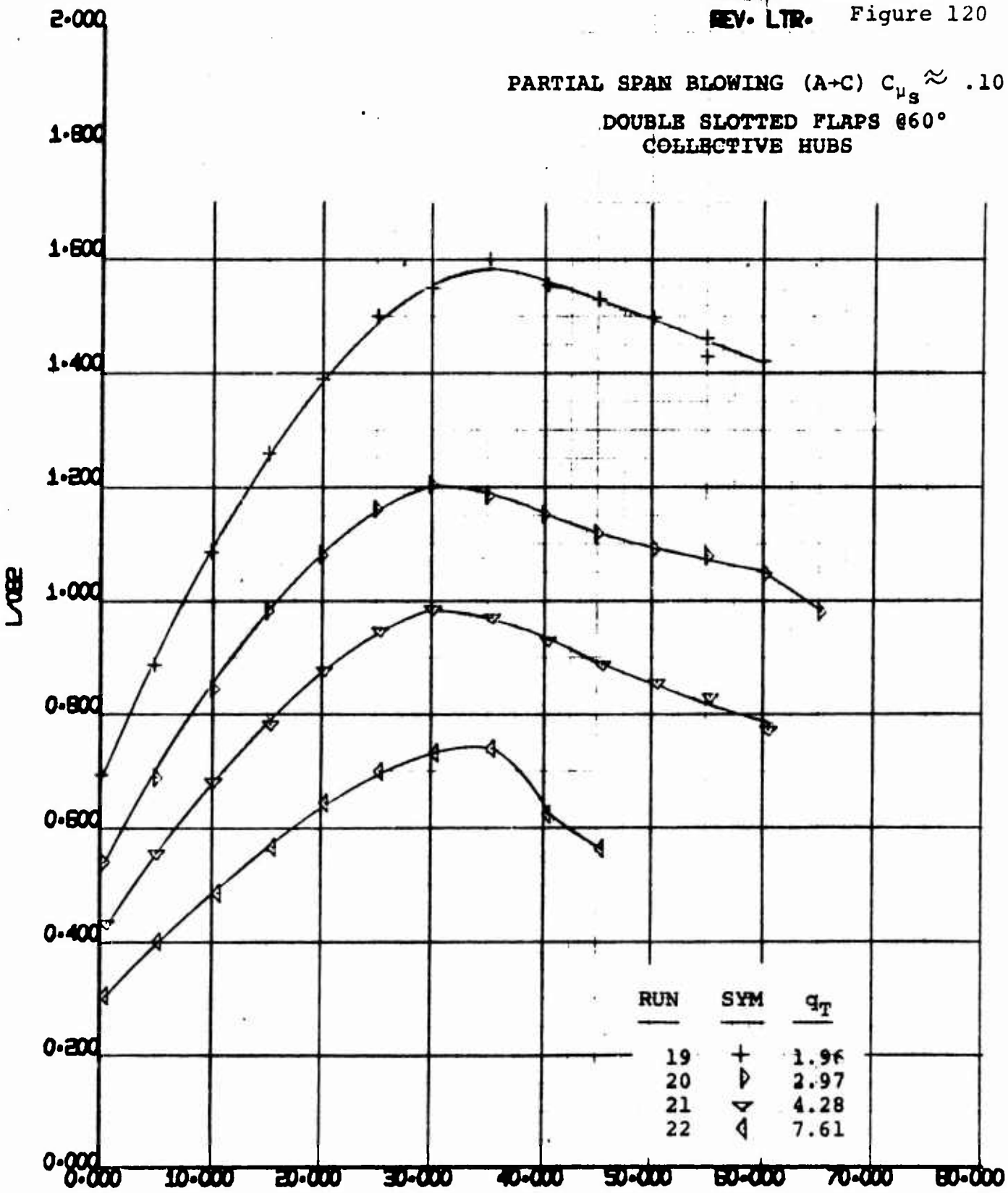

WING TILT ANGLE - IW (DEG)

170 HALF SPAN MODEL WR 040 0-3 L/QBZ VS WING TILT ANGLE	BWT 55 4/ 3/70

PARTIAL SPAN BLOWING (A+C) $C_{\mu_s} \approx .10$

DOUBLE SLOTTED FLAPS @60°
COLLECTIVE HUBS

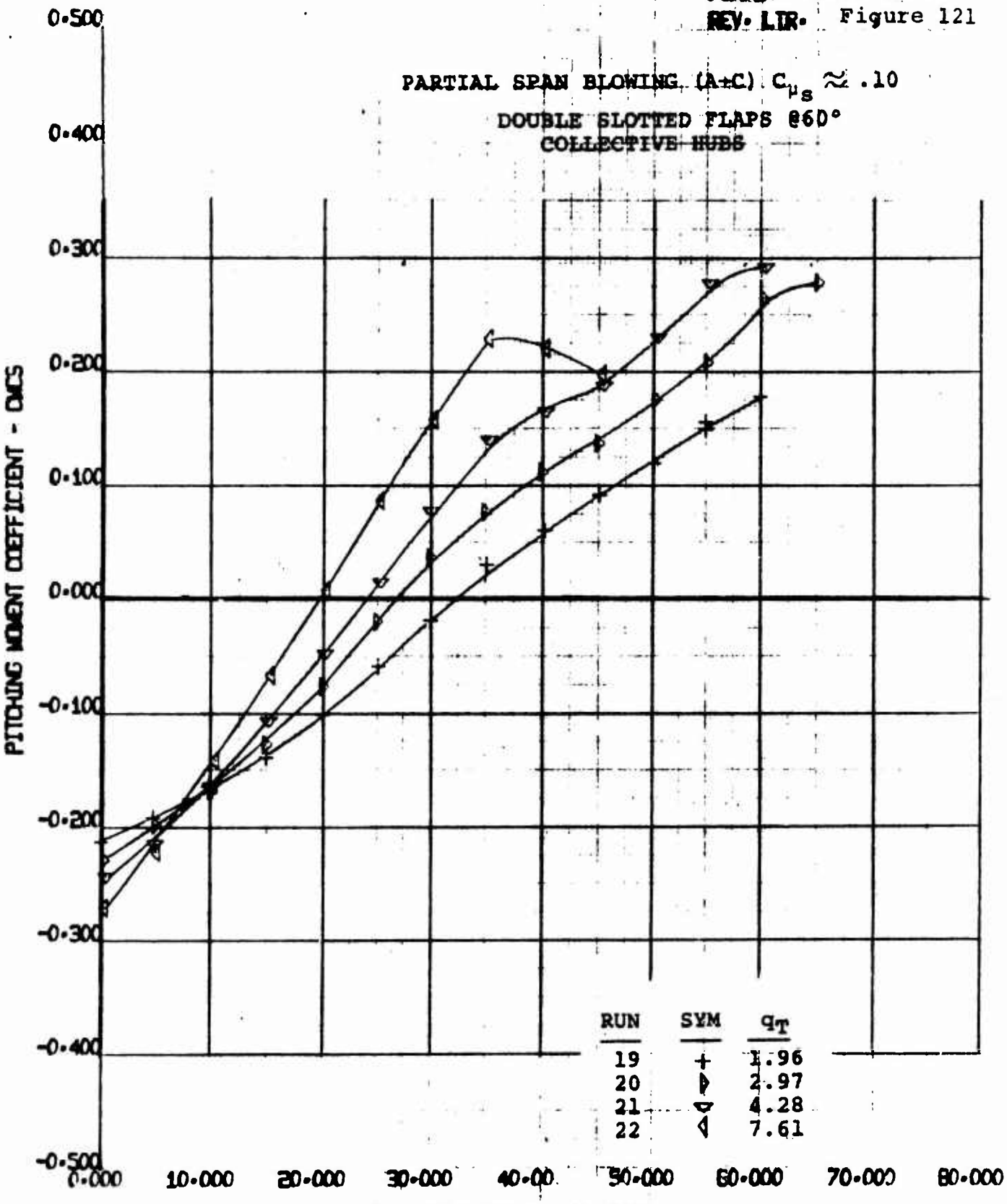

170 HALF SPAN MODEL VR 040 0-3 WING TILT ANGLE VS CMCS	BVWT 55 4/ 3/70

PARTIAL SPAN BLOWING (A→C&G) $C_{\mu_S} \approx .11$

DOUBLE SLOTTED FLAPS @ 60°

COLLECTIVE HUBS

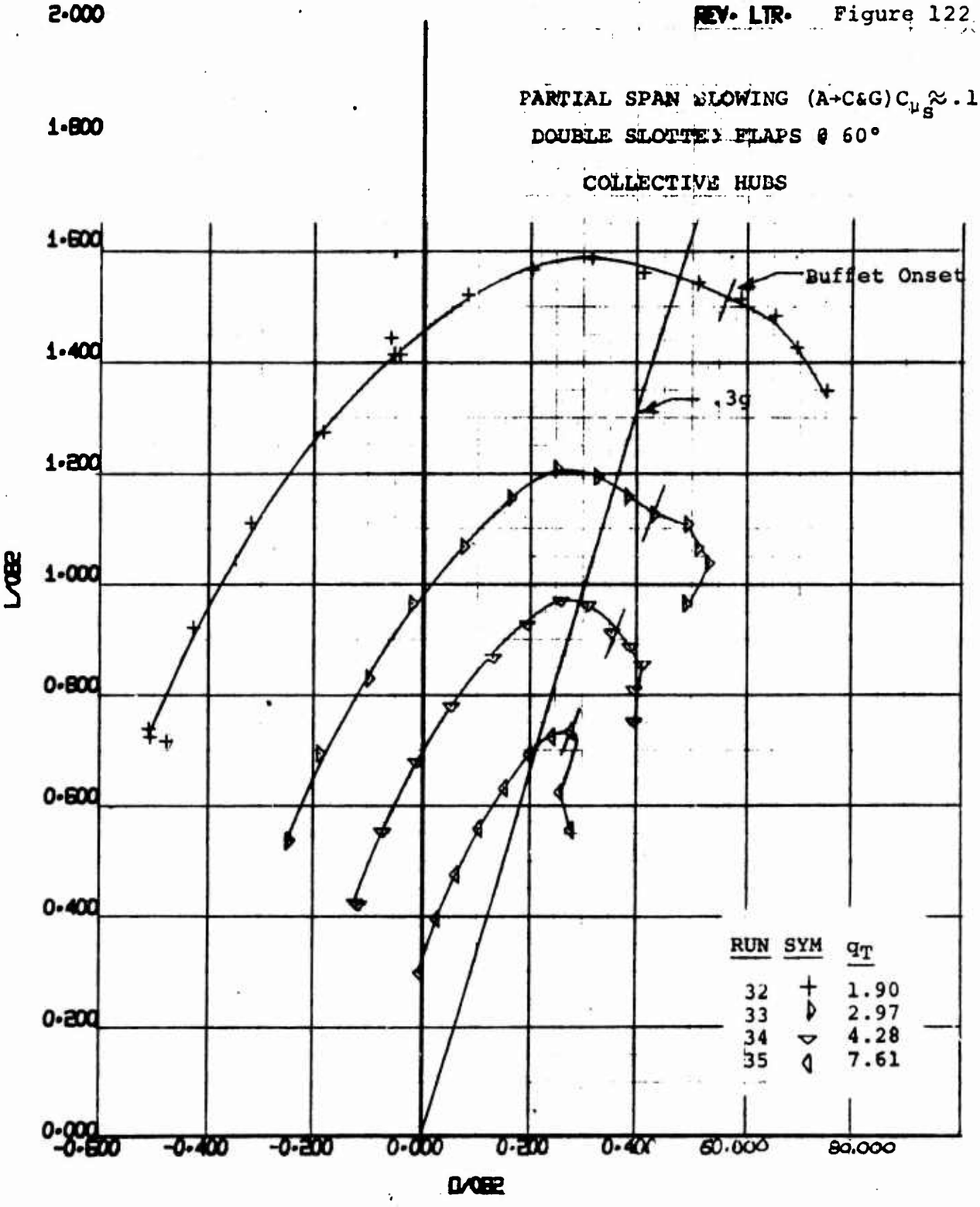

MODEL
VR 040 0-3
L/QBZ VS D/QBZ

4/ 3/70

PARTIAL SPAN BLOWING (A→C&G) $C_{\mu_s} \approx .11$

DOUBLE SLOTTED FLAPS @ 60°

COLLECTIVE HUBS

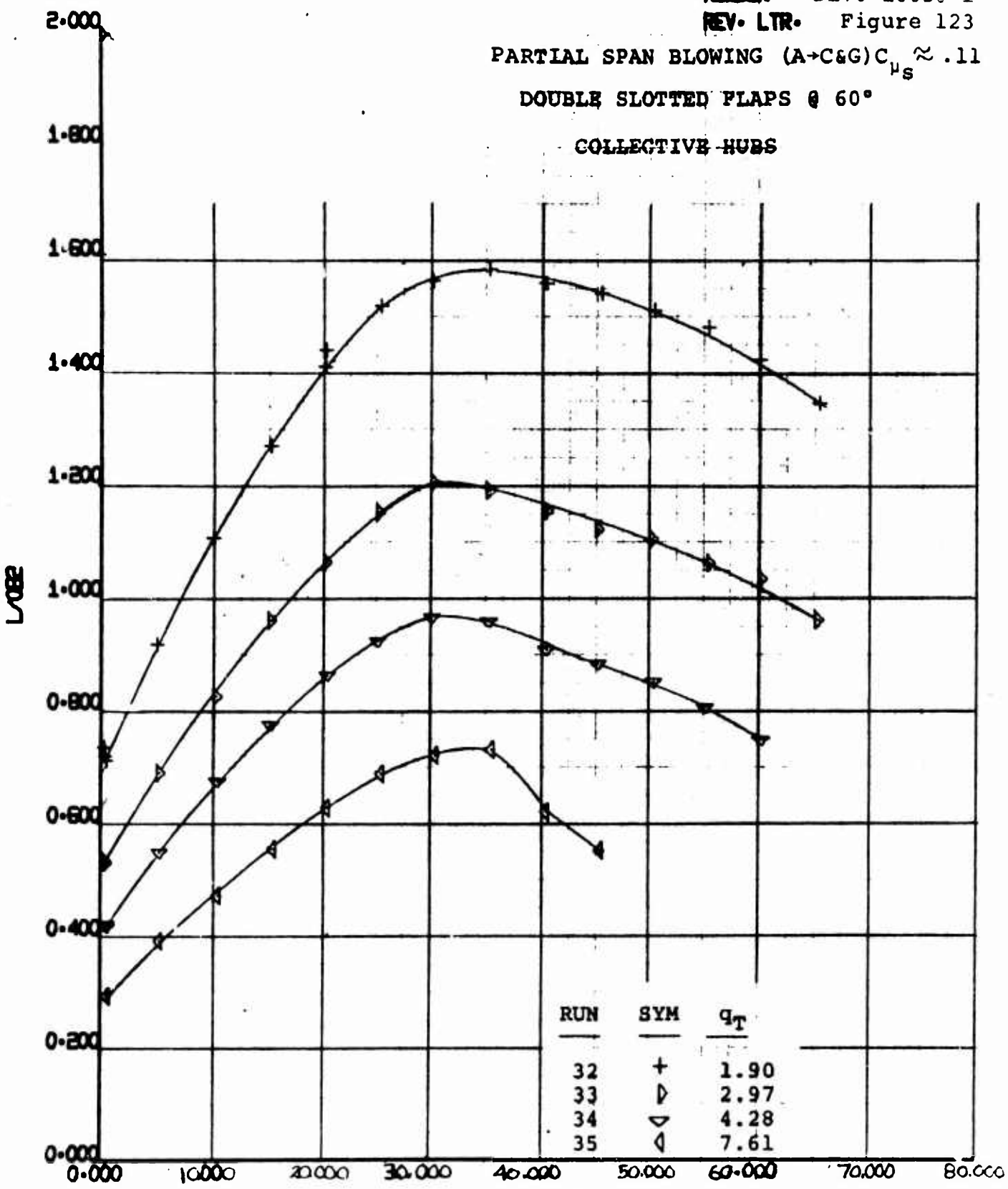

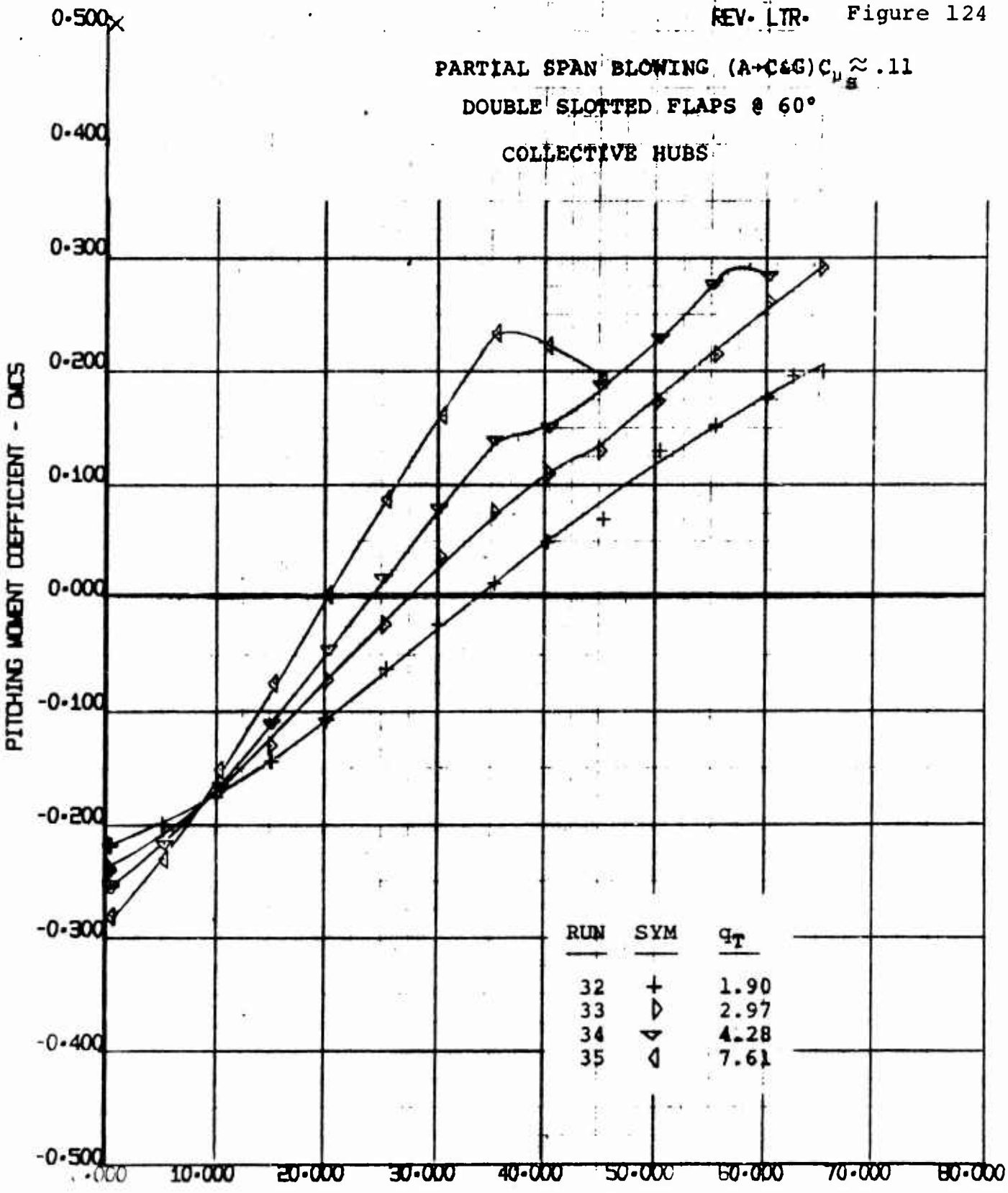

170 HALF SPAN MODEL WR 040 0-3 CMCS VS TILT WING ANGLE	BVWT 55 4/ 3/70

FULL SPAN BLOWING (A→G) $C_{\mu_s} \approx .12$

DOUBLE SLOTTED FLAPS @ 60°
COLLECTIVE HUBS

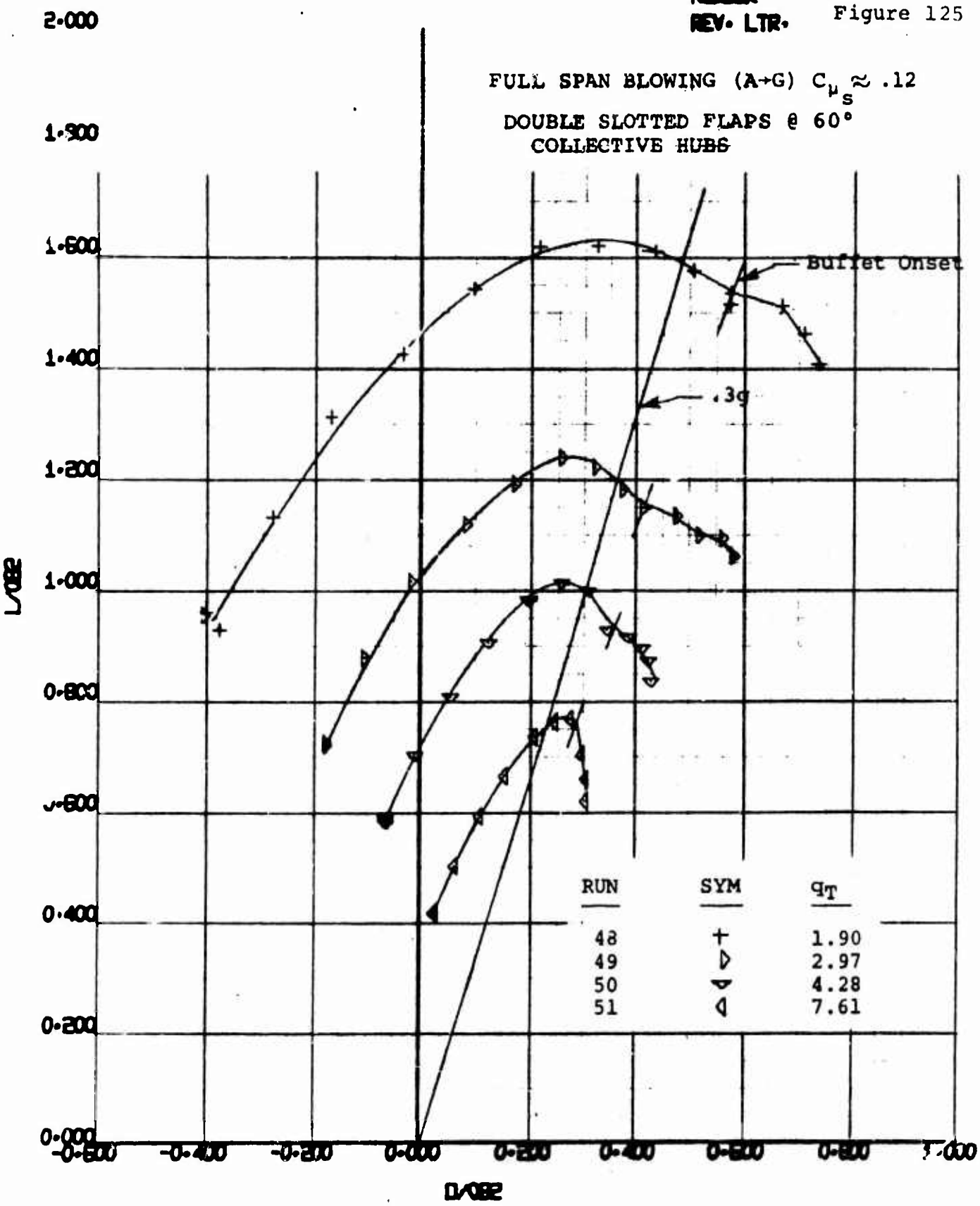

170 HALF SPAN MODEL VR 040 0-3 L/Q̄S2 VS D/Q̄S2	BMAT 55 4/ 3/70

FULL SPAN BLOWING (A→G) $C_{\mu_s} \approx .12$

DOUBLE SLOTTED FLAPS @ 60°

COLLECTIVE HUBS

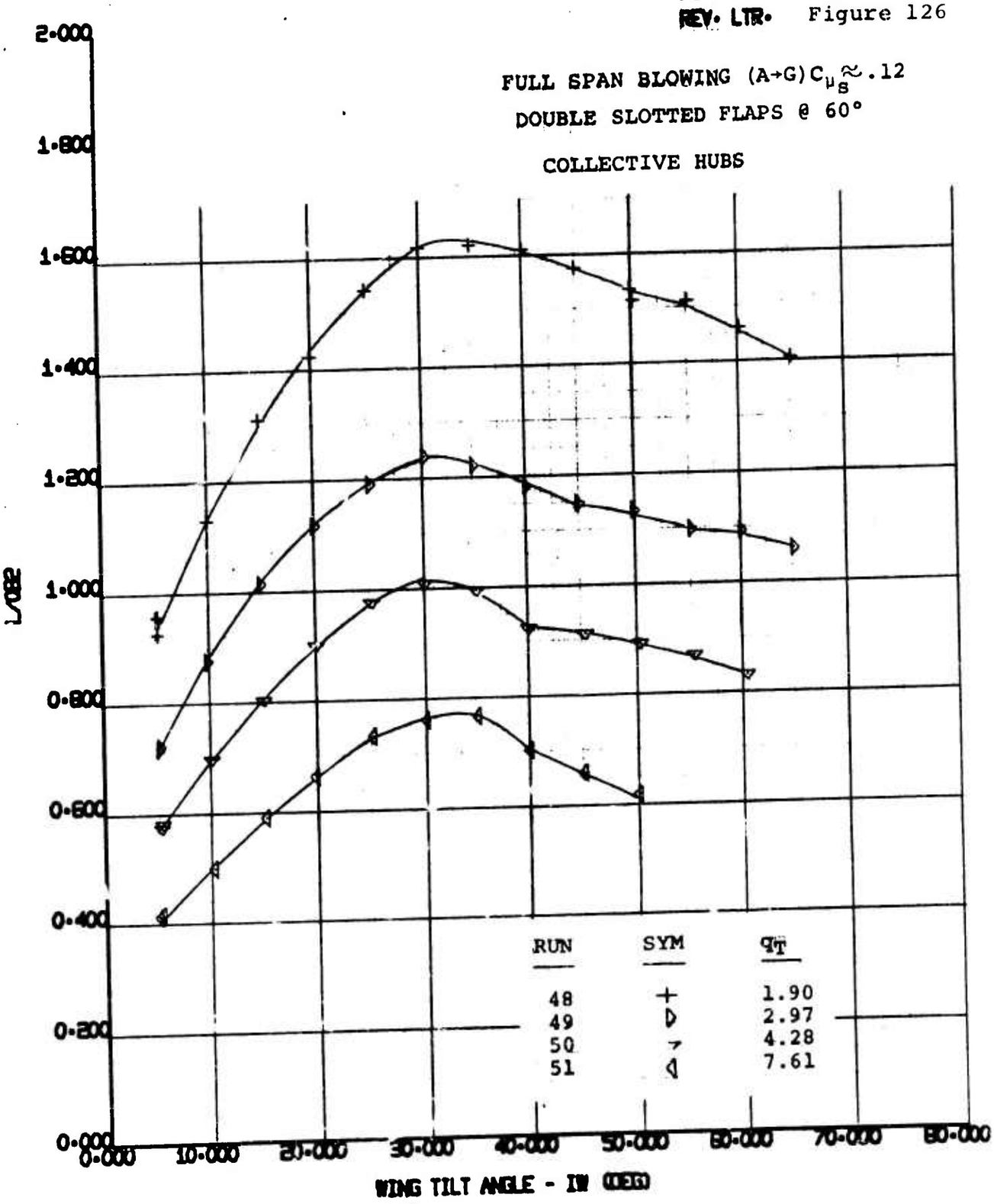

170 HALF SPAN MODEL WR 040 0-3 L/QB2 VS WING TILT ANGLE	BWT 55 4/ 3/70

NUMBER D170-10036-1
REV. LTR. Figure 127

FULL SPAN BLOWING (A→G) $C_{\mu_s} \approx .12$

DOUBLE SLOTTED FLAPS @ 60°

COLLECTIVE HUBS

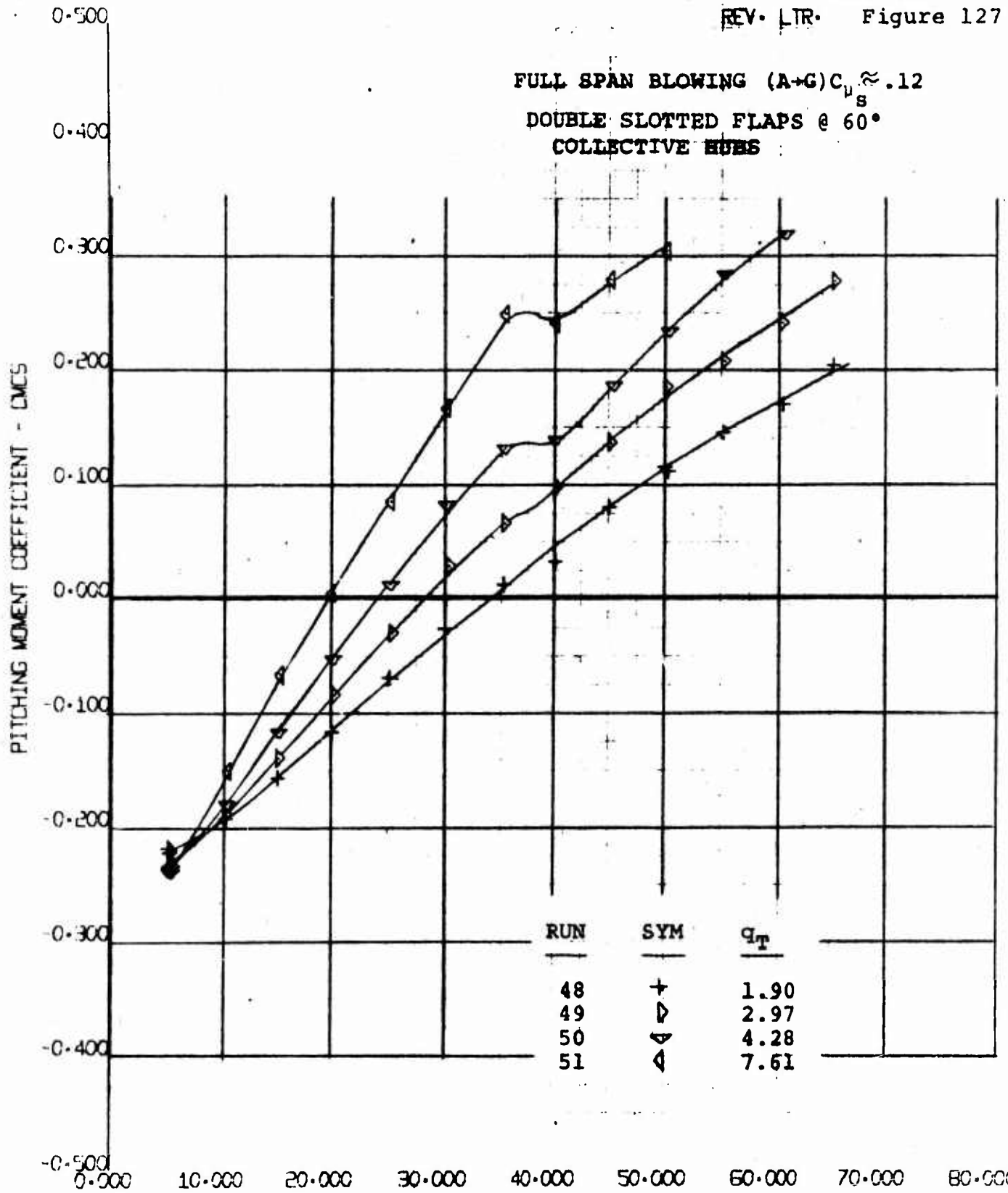

170 HALF SPAN MODEL VR 040 0-3 WING TILT ANGLE VS CMCS	BVWT 55 4/ 2/70

FULL SPAN BLOWING (A→G) $C_{\mu_S} \approx .06$
DOUBLE SLOTTED FLAPS @ 60°
COLLECTIVE HUBS

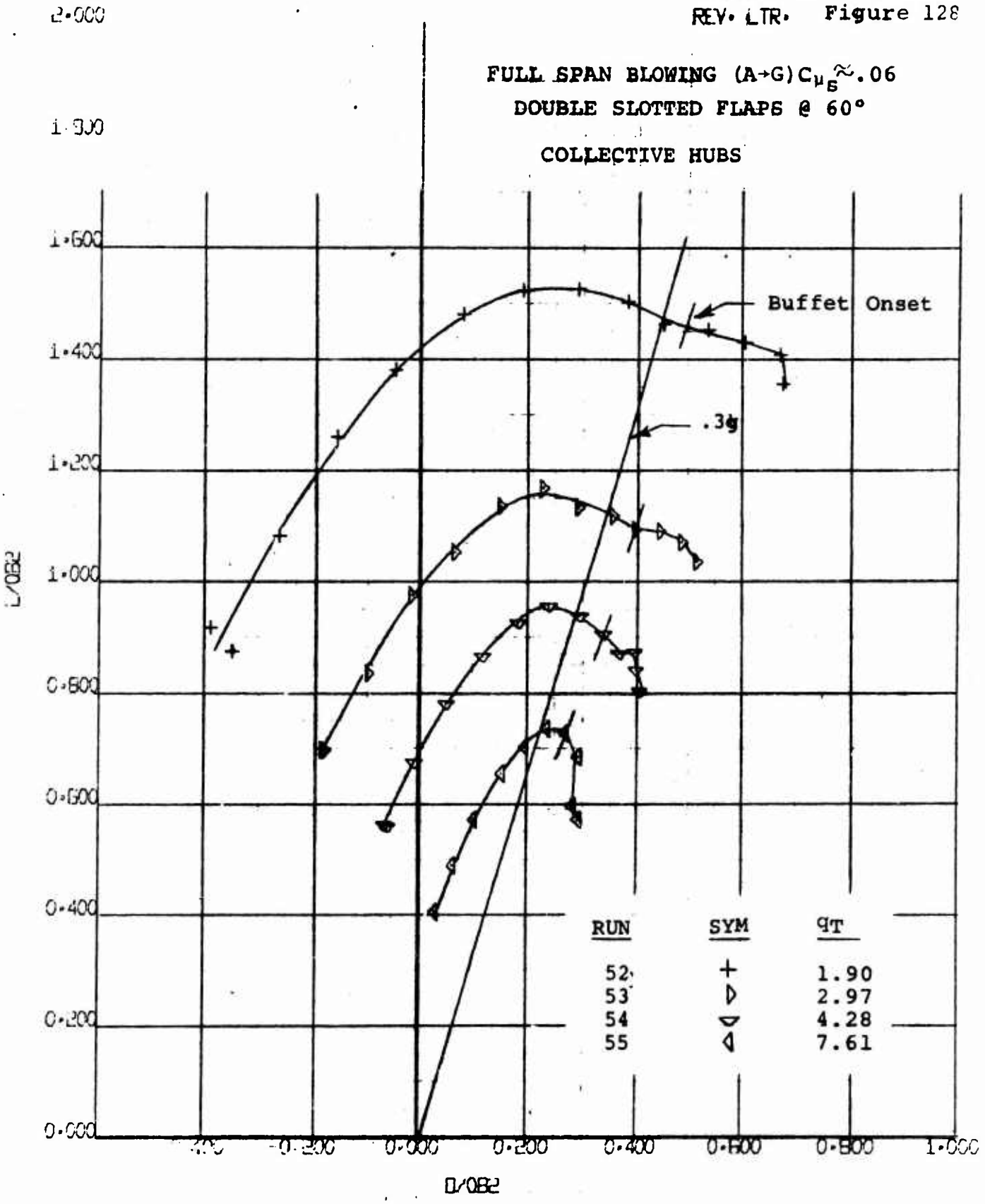

170 HALF SPAN MODEL VR 040 0-3 L/QB2 VS D/QB2	BVWT 55 4/ 2470

FULL SPAN BLOWING (A+G) $C_{\mu_s} \approx .06$

DOUBLE SLOTTED FLAPS @ 60°
COLLECTIVE HUBS

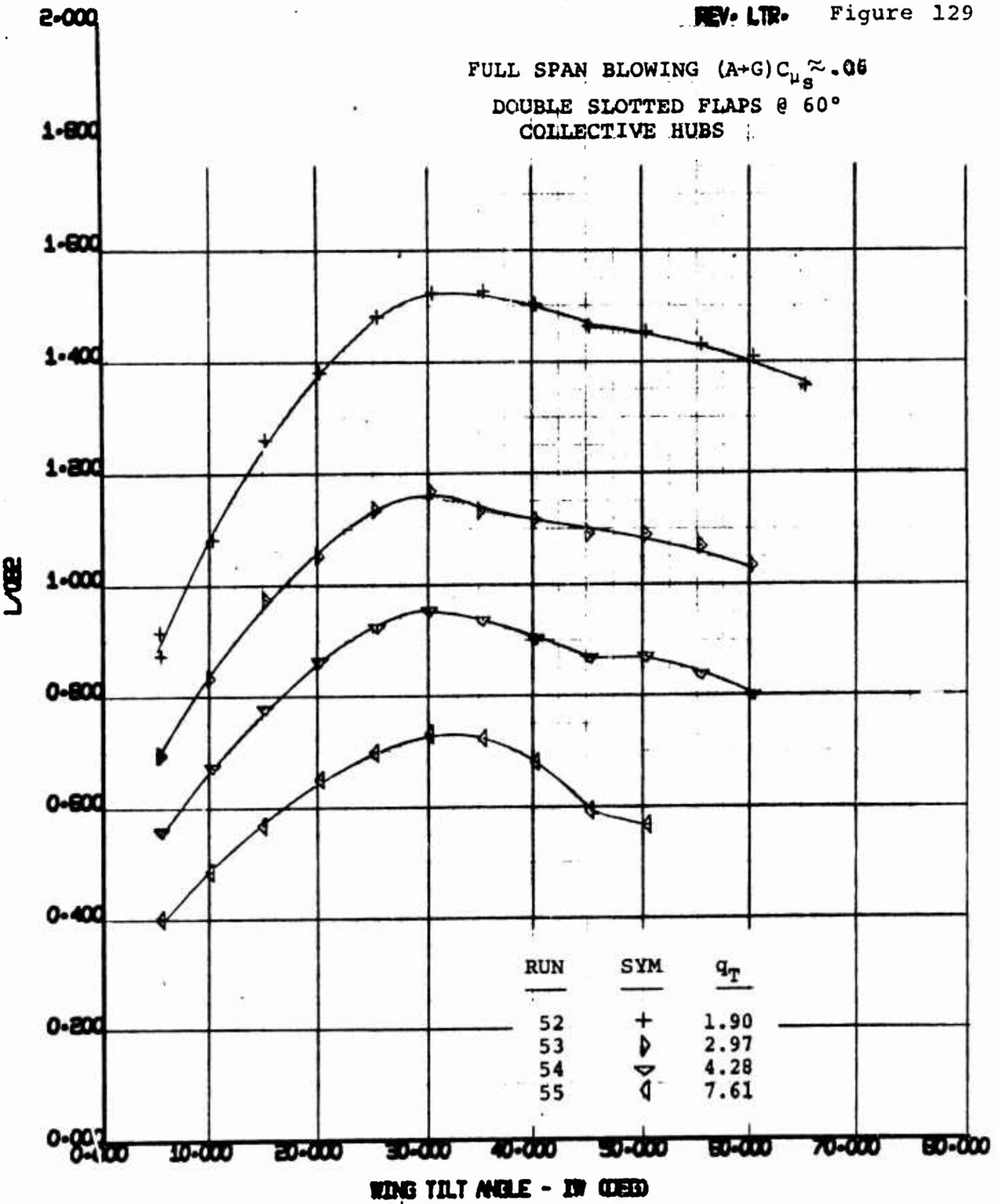

170 HALF SPAN MODEL WR 040 0-3 L/QB2 VS WING TILT ANGLE	BWT 55 4/ 3/70

FULL SPAN BLOWING (A→G) $C_{\mu_s} \approx .06$

DOUBLE SLOTTED FLAPS @ 60°

COLLECTIVE HUBS

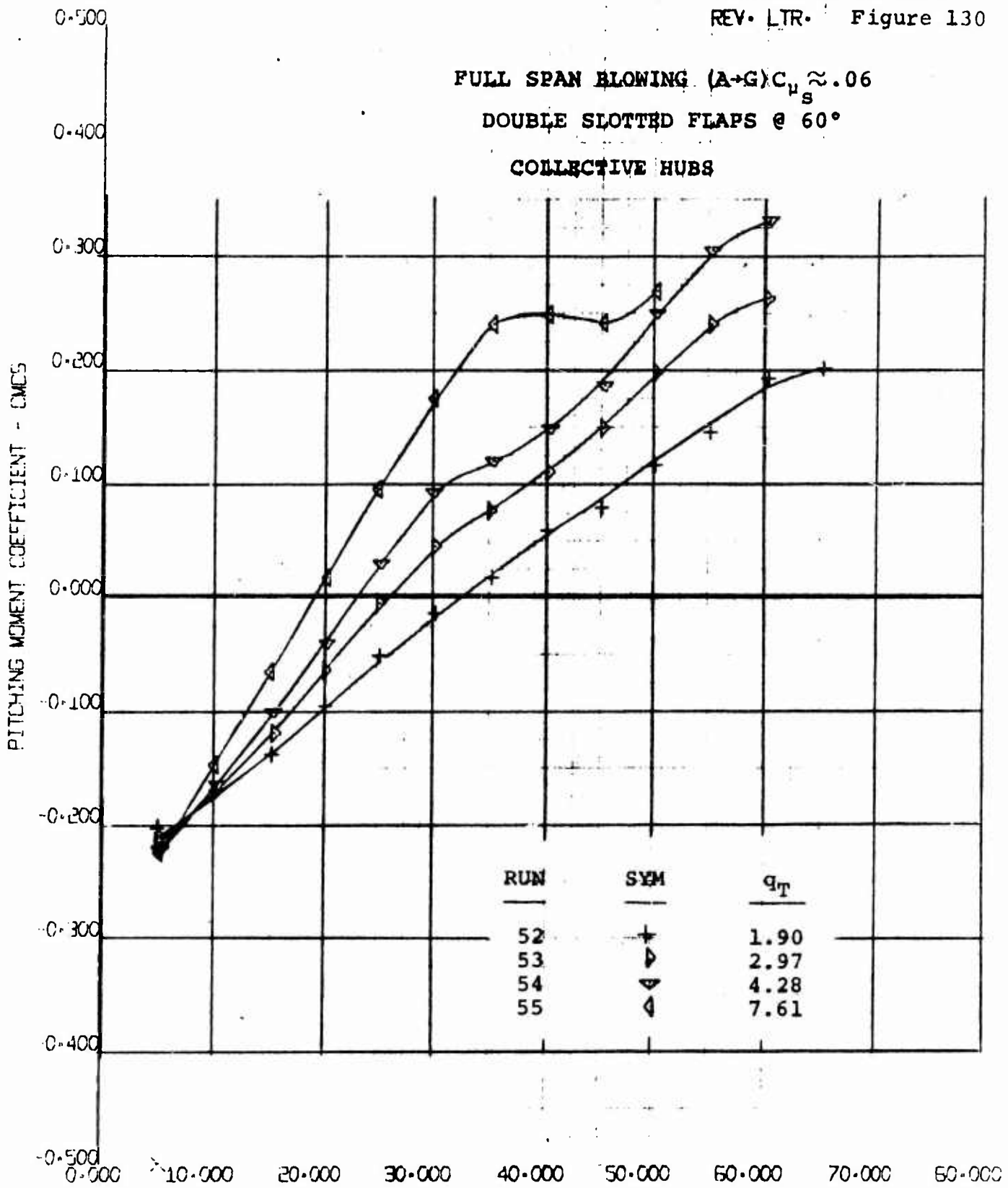

170 HALF SPAN MODEL VR 040 0-3 WING TILT ANGLE VS LMCS	BVWT 55 4/ 2470

FULL SPAN BLOWING (A→G) $C_{\mu_S} \approx .14$
DOUBLE SLOTTED FLAPS @ 60°
COLLECTIVE HUBS

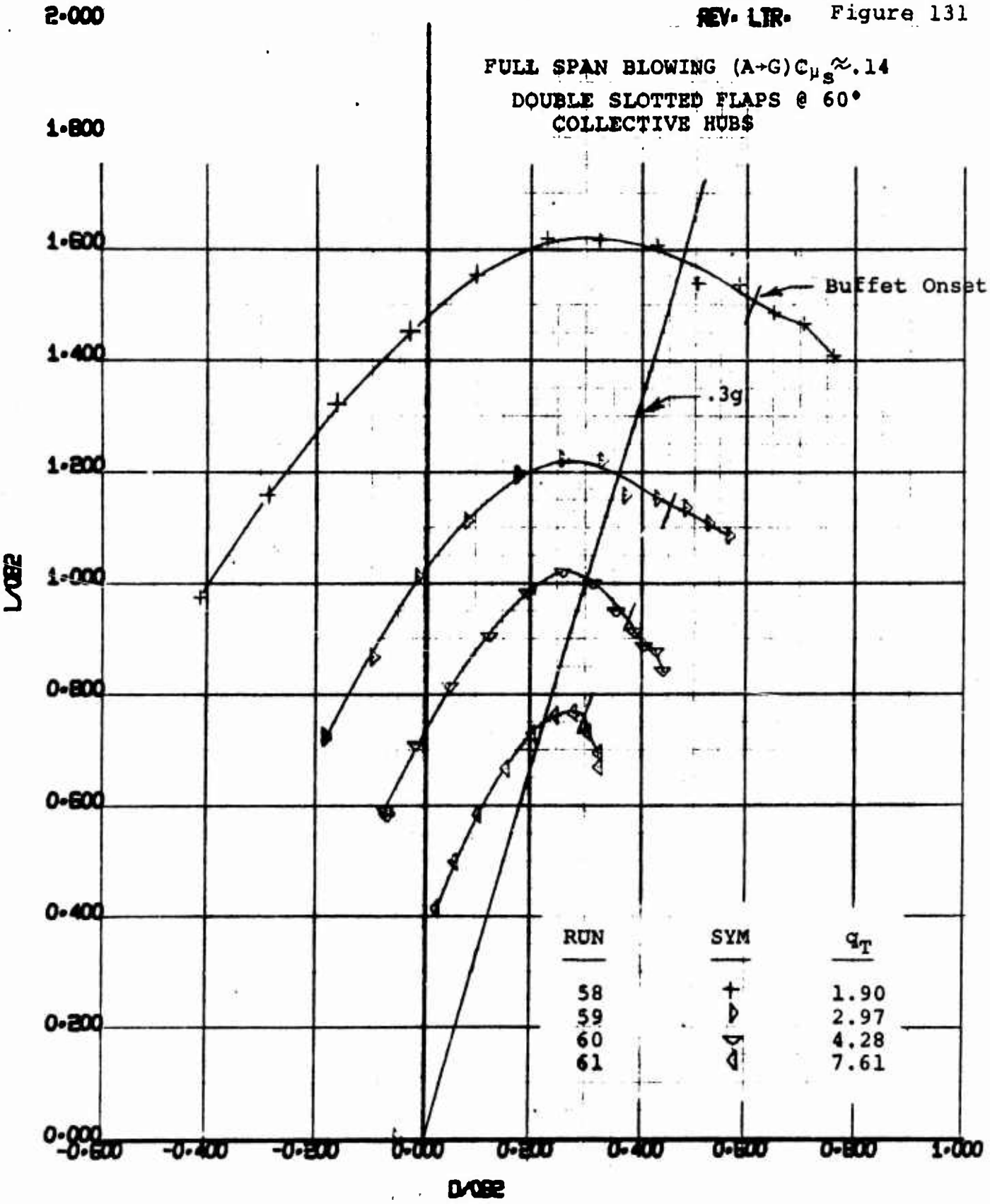

170 HALF SPAN MODEL WR 040 0-9 L/QB2 VS D/QB2	BMT 55 4/ 7/70

FULL SPAN BLOWING (A→G)$C_{\mu_s} \approx .14$

DOUBLE SLOTTED FLAPS @ 60°
COLLECTIVE HUBS

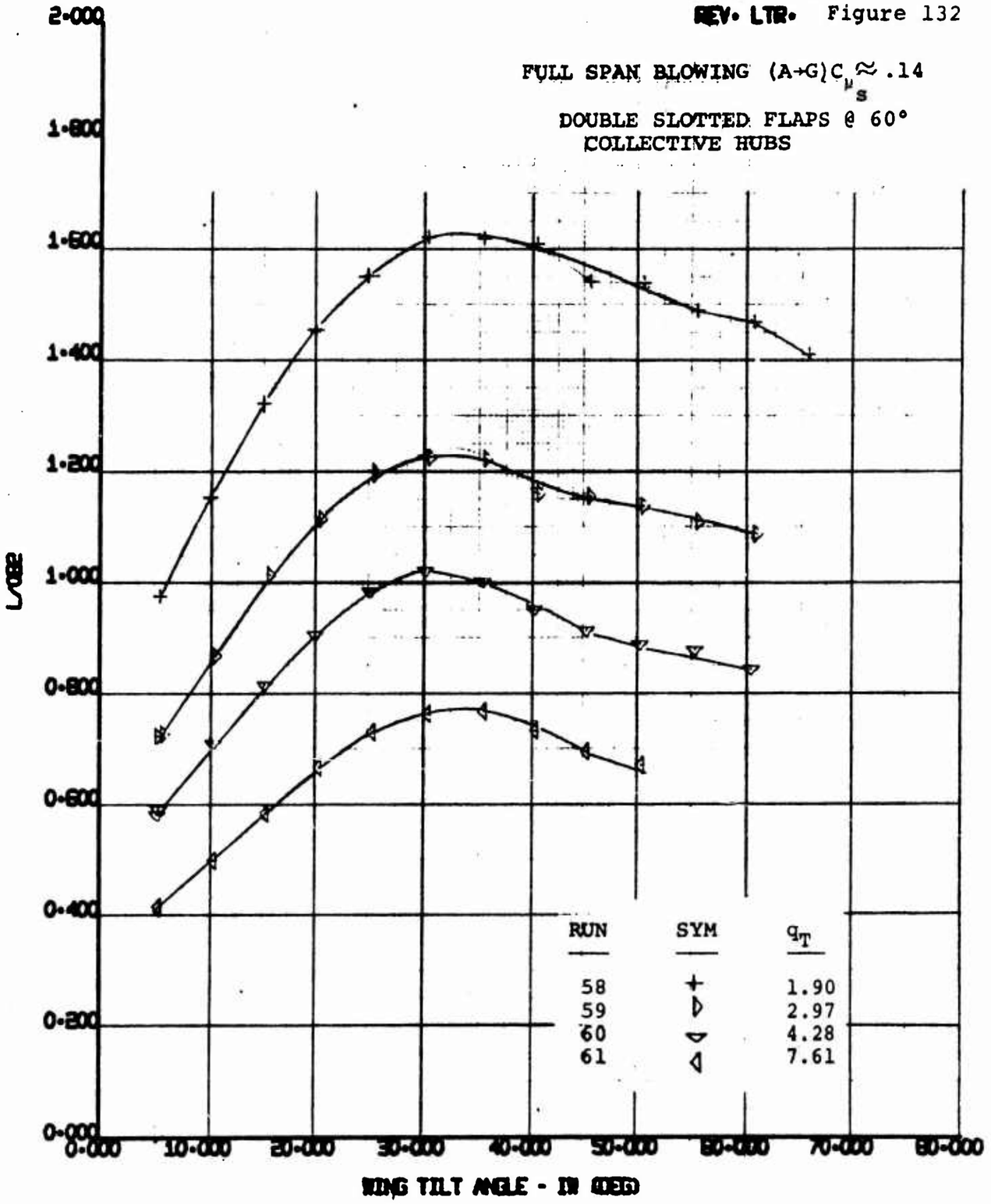

170 HALF SPAN MODEL WR 040 0-3 L/QB2 VS WING TILT ANGLE	BMWT 55 4/ 7/70

NUMBER D170-10036-1
REV. LTR. Figure 133

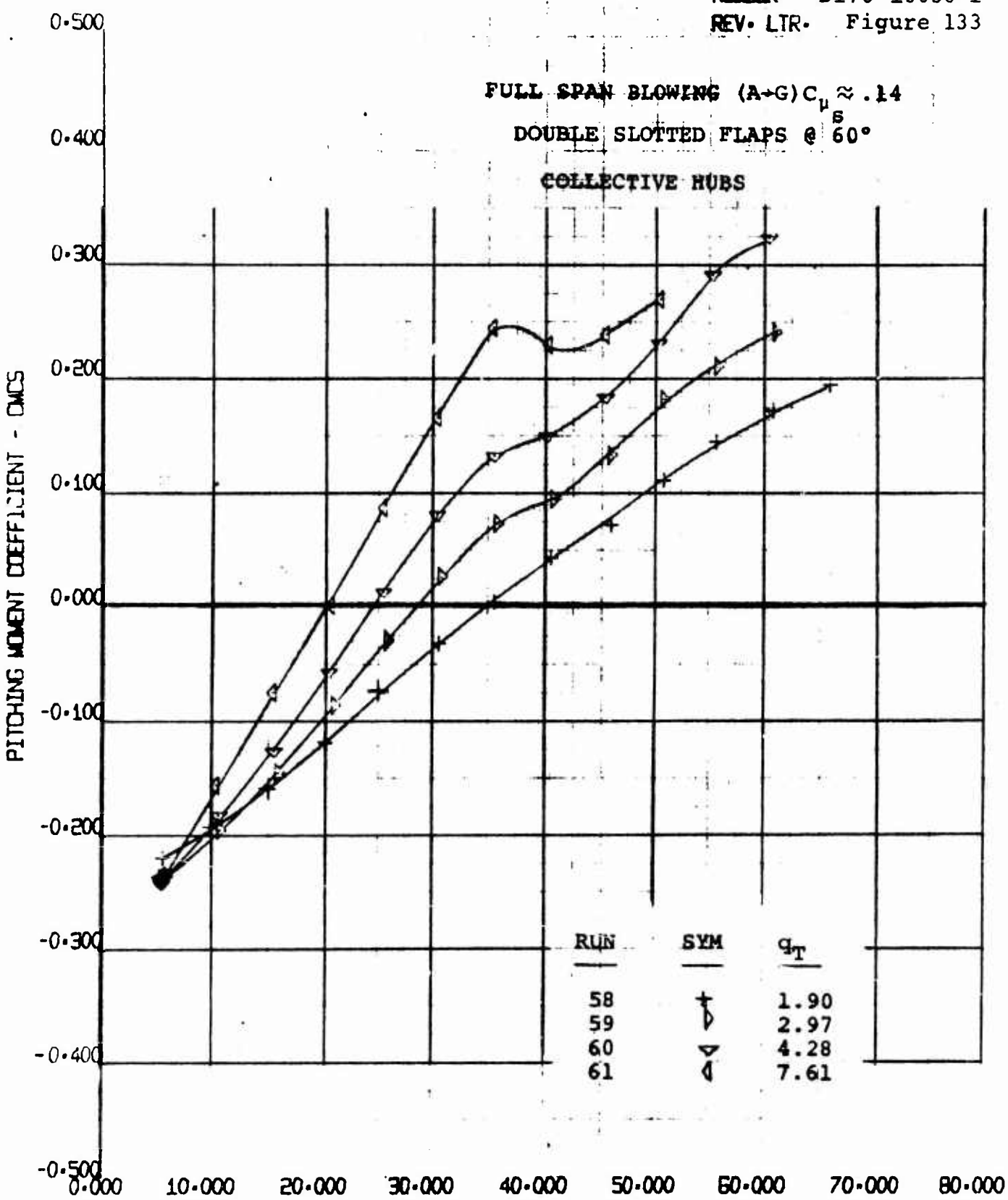

170 HALF SPAN MODEL VR 040 0-3 CMCS VS TILT WING ANGLE	BVWT 55 4/ 7/70

FULL SPAN BLOWING (A+G)$C_\mu \approx .21$

DOUBLE SLOTTED FLAPS @ δ_s 60°
COLLECTIVE HUBS

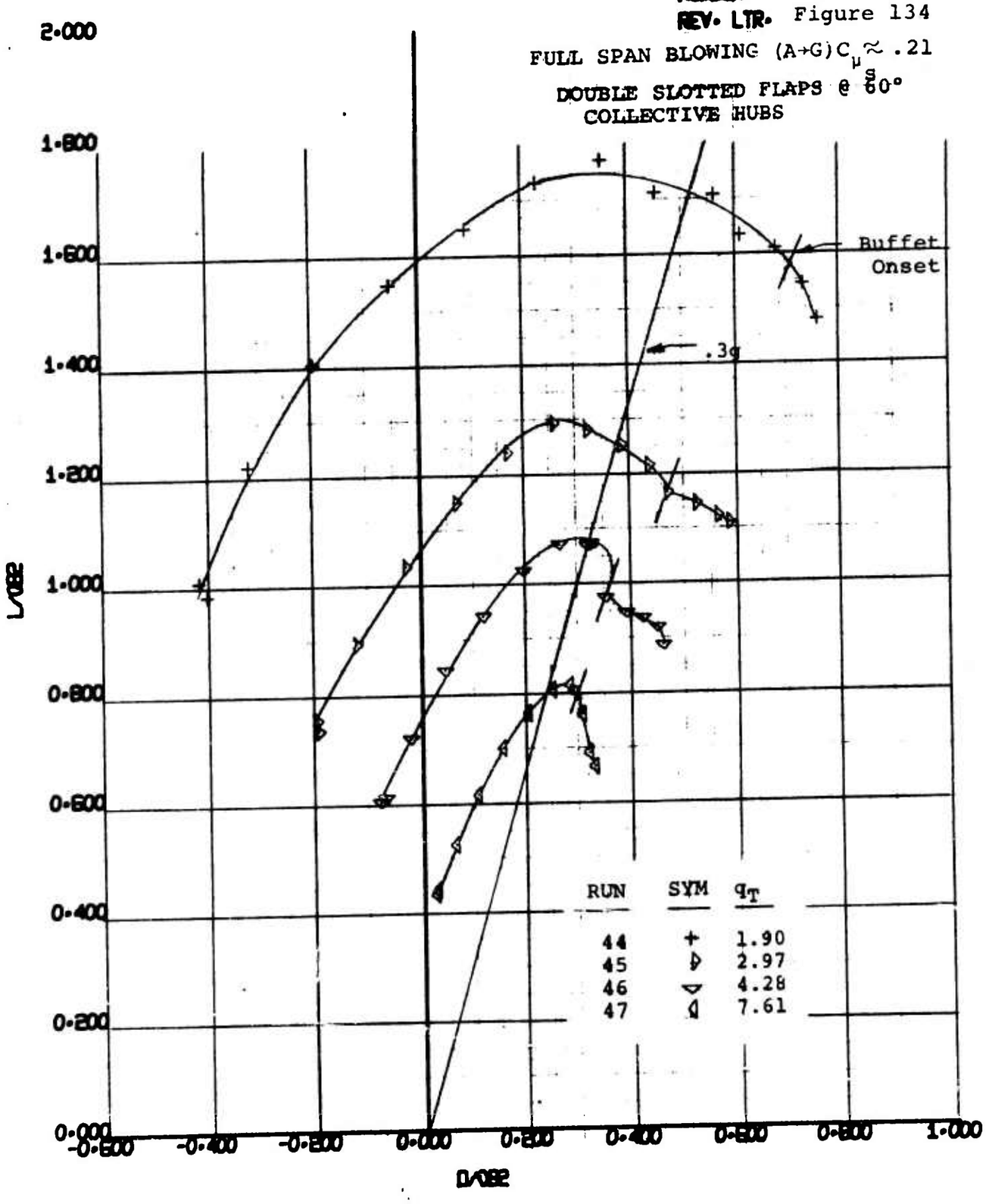

170 HALF SPAN MODEL WR 040 0-3 L/QS2 VS D/QS2	BMAT 55 4/ 3/70

FULL SPAN BLOWING (A→G)$C_{\mu_s} \approx .21$

DOUBLE SLOTTED FLAPS @ 60°
COLLECTIVE HUBS

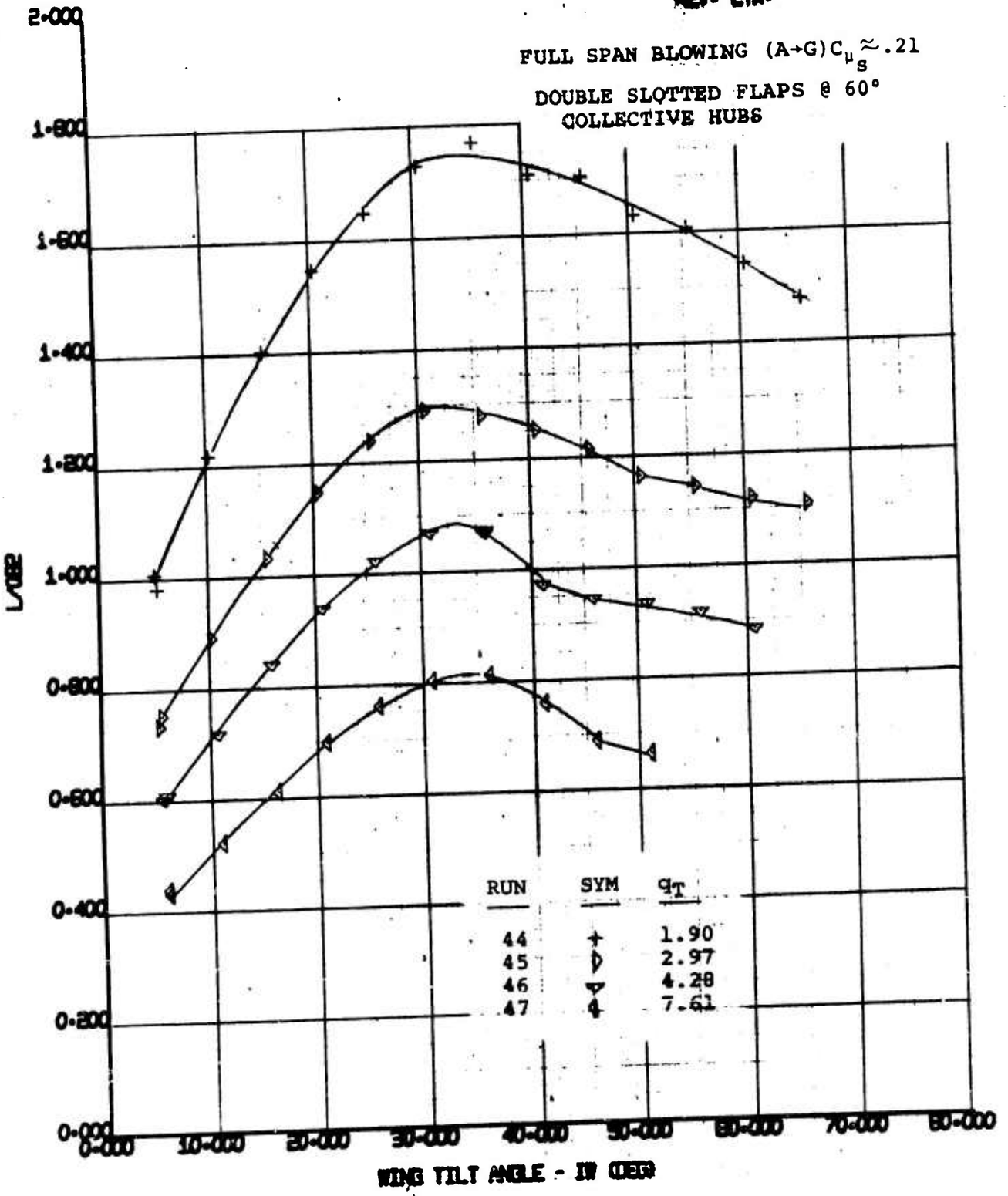

170 HALF SPAN MODEL AR 040 0-3 L/QE2 VS WING TILT ANGLE	BMT 55 4/ 3/70

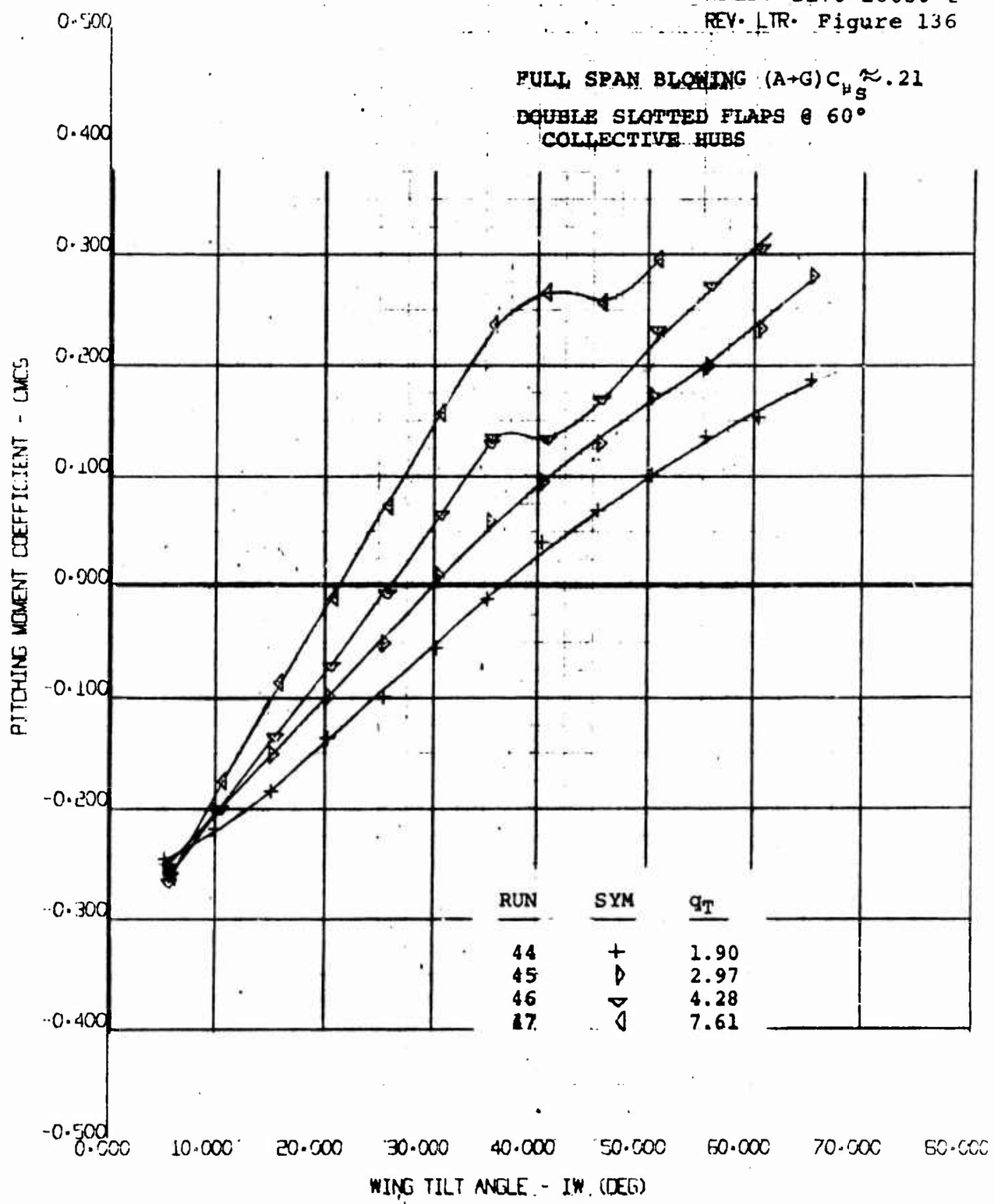

170 HALF SPAN [illegible]	BVWT
VR 040 0-3	55
WING TILT ANGLE VS [illegible]	47 [illegible]

PARTIAL SPAN BLOWING (A+C&G) $C_{\mu_s} \approx .05$

DOUBLE SLOTTED FLAPS @ 60°

COLLECTIVE HUBS

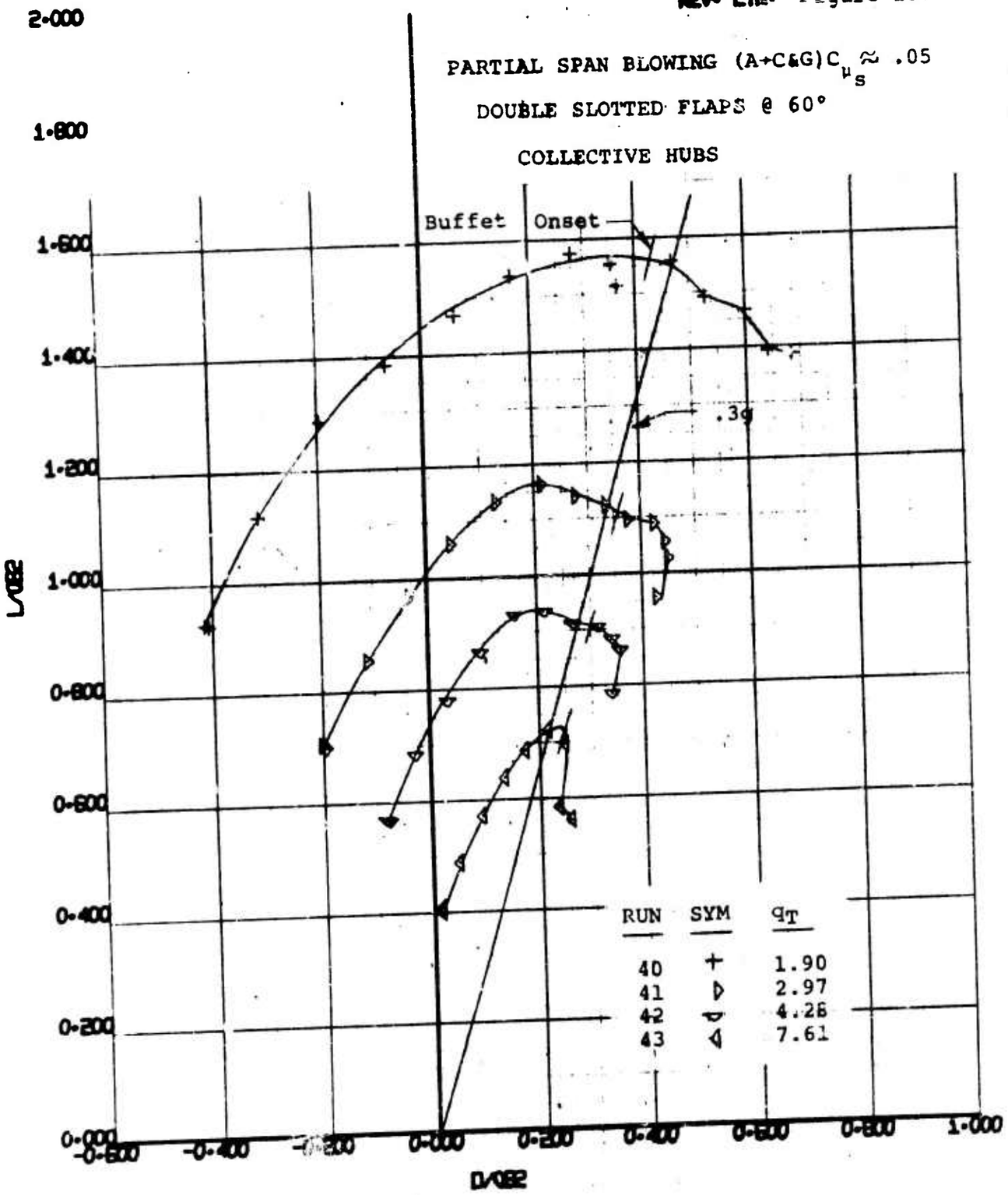

170 HALF SPAN MODEL VR 040 0-3 L/QB2 VS D/QB2	BMAT 55 4/ 3/70

PARTIAL SPAN BLOWING (A→C&G) $C_{\mu_s} \approx .05$

DOUBLE SLOTTED FLAPS AT 60°

COLLECTIVE HUBS

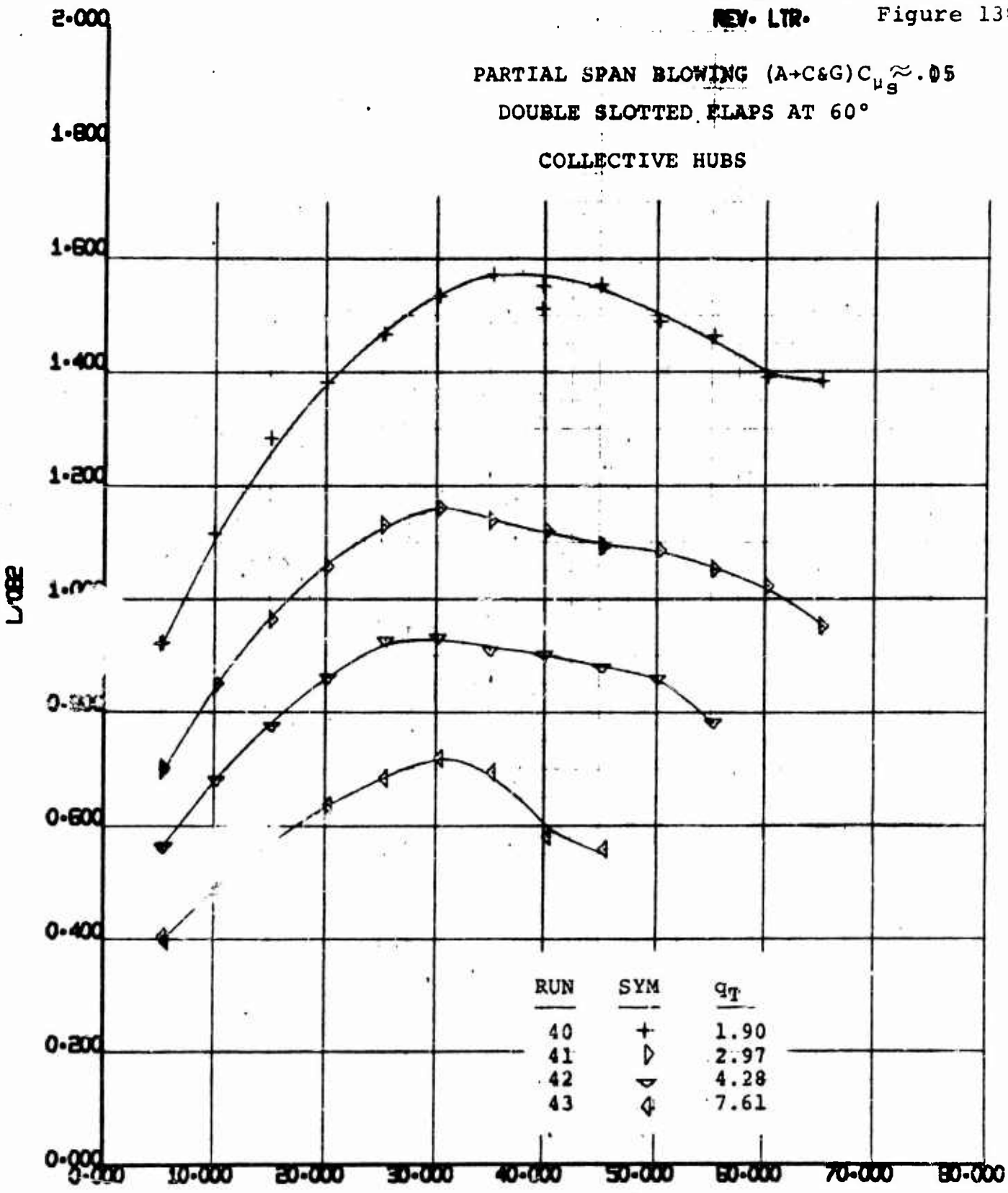

WING TILT ANGLE - IW (DEG)

170 HALF SPAN MODEL VR 040 0-3 L/QBZ VS WING TILT ANGLE	BVWT 55 4/ 3/70

PARTIAL SPAN BLOWING (A→C&G) $C_{\mu_s} \approx .05$

DOUBLE SLOTTED FLAPS AT 60°

COLLECTIVE HUBS

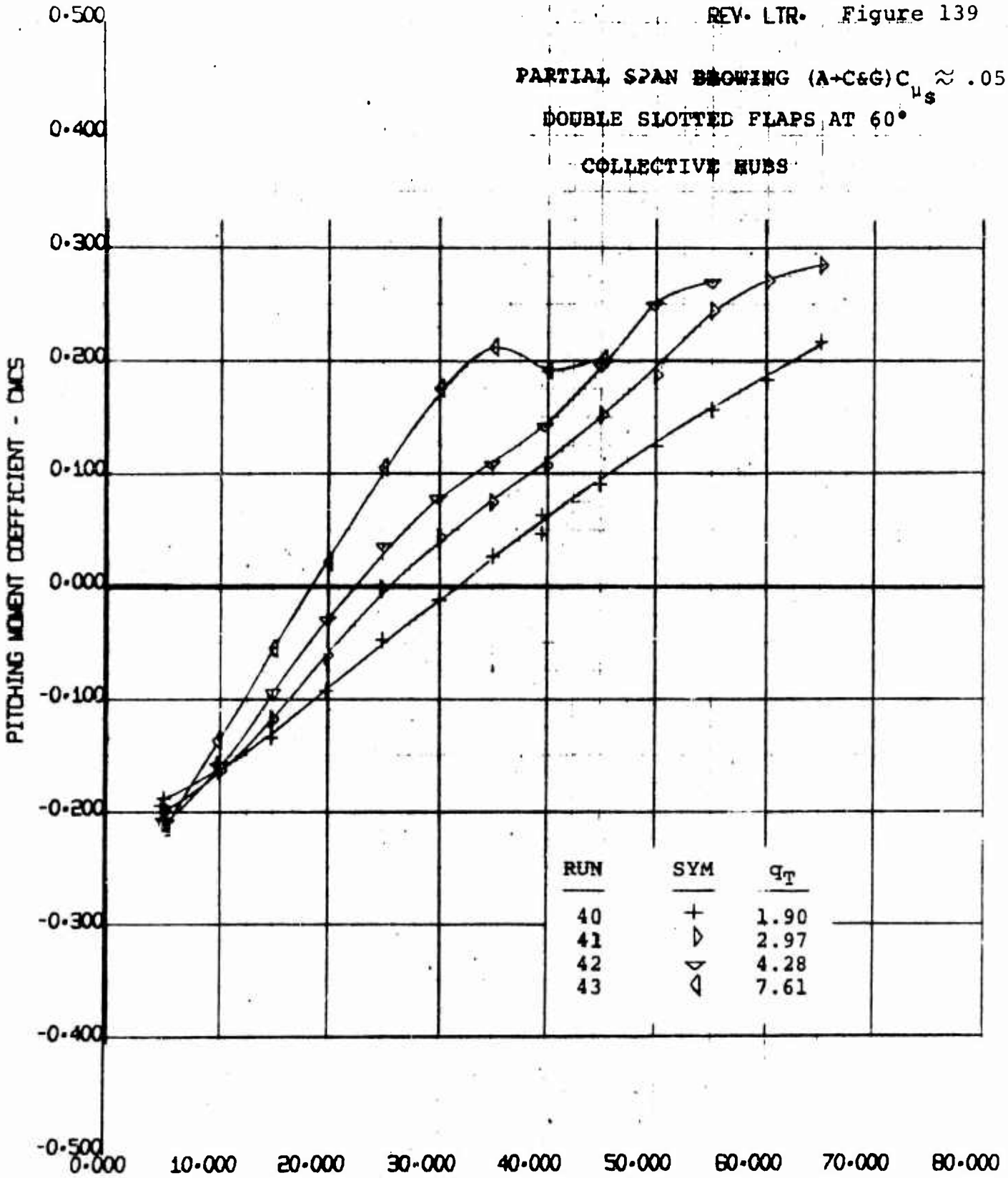

170 HALF SPAN MODEL VR 040 0-3 CMCS VS TILT WING ANGLE	BVWT 55 4/ 3/70

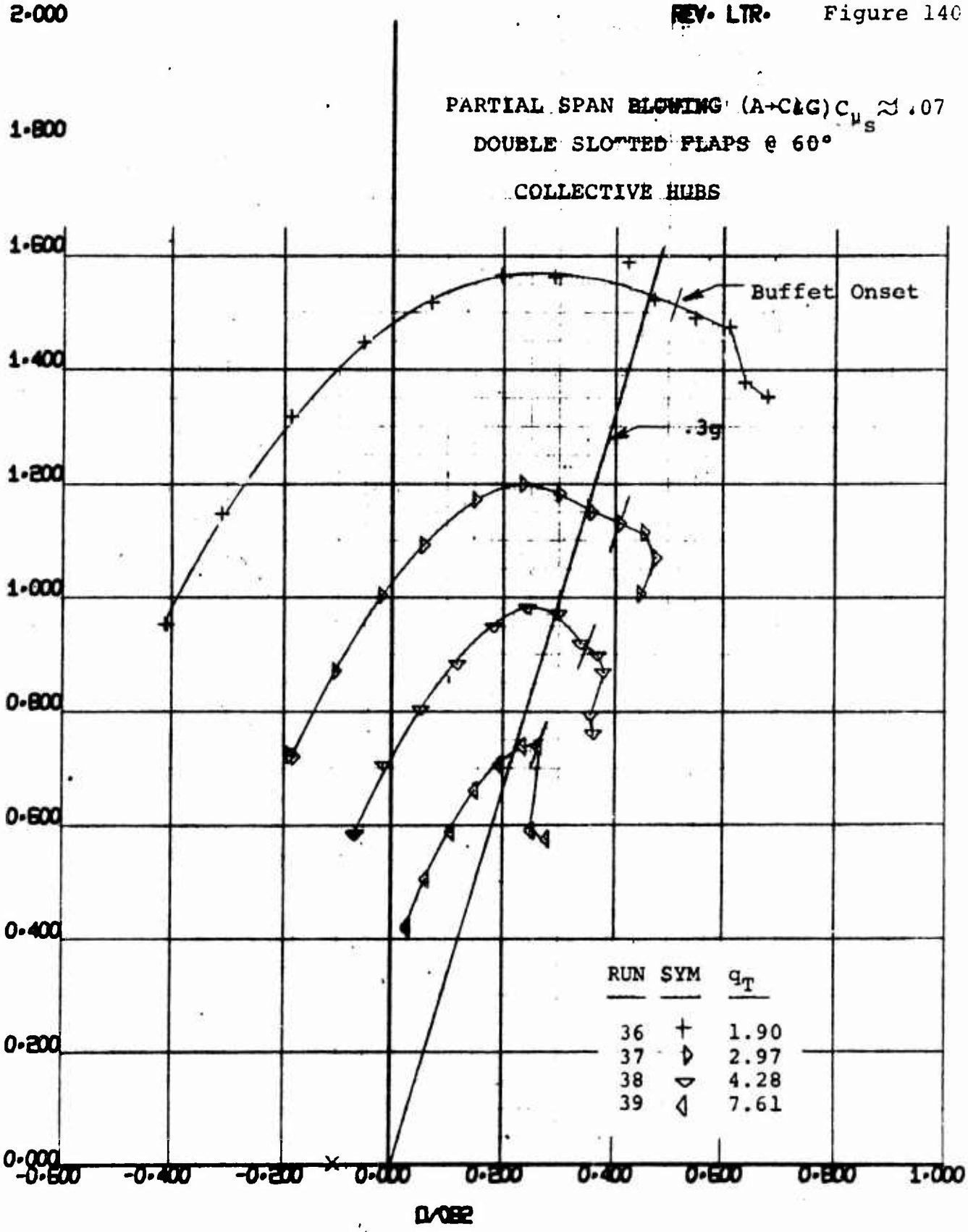

170 HALF SPAN MODEL VR 040 0-3 L/QBZ VS D/QBZ	BMT 55 4/ 3/70

PARTIAL SPAN BLOWING (A→C&G) $C_{\mu_s} \approx .07$

DOUBLE SLOTTED FLAPS @ 60°

COLLECTIVE HUBS

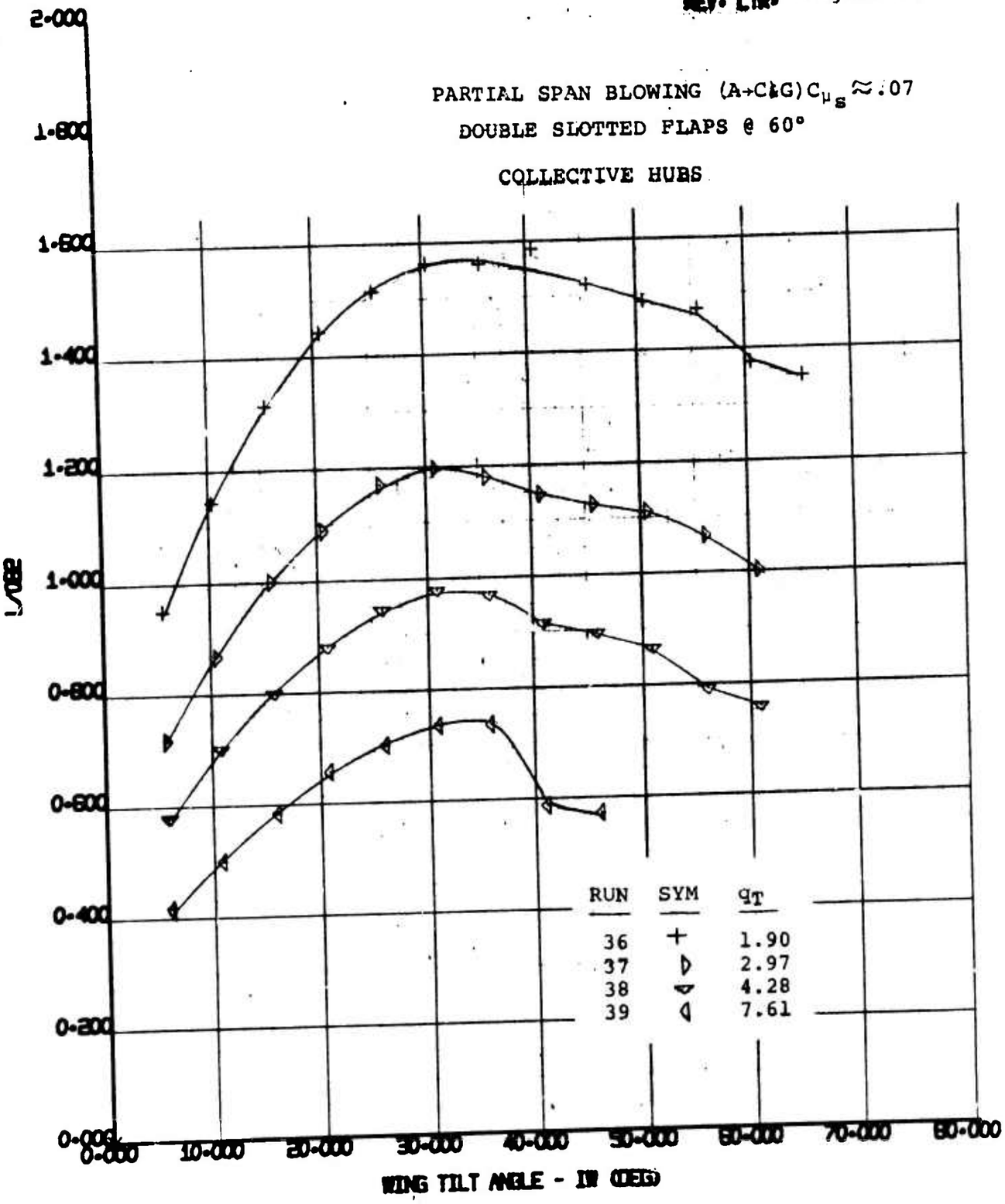

170 HALF SPAN MODEL VR 040 0-3 L/DB2 VS WING TILT ANGLE	BMT 55 4/ 3/70

PARTIAL SPAN BLOWING (A→C&G) $C_{\mu_s} \approx .07$

DOUBLE SLOTTED FLAPS @ 60°

COLLECTIVE HUBS

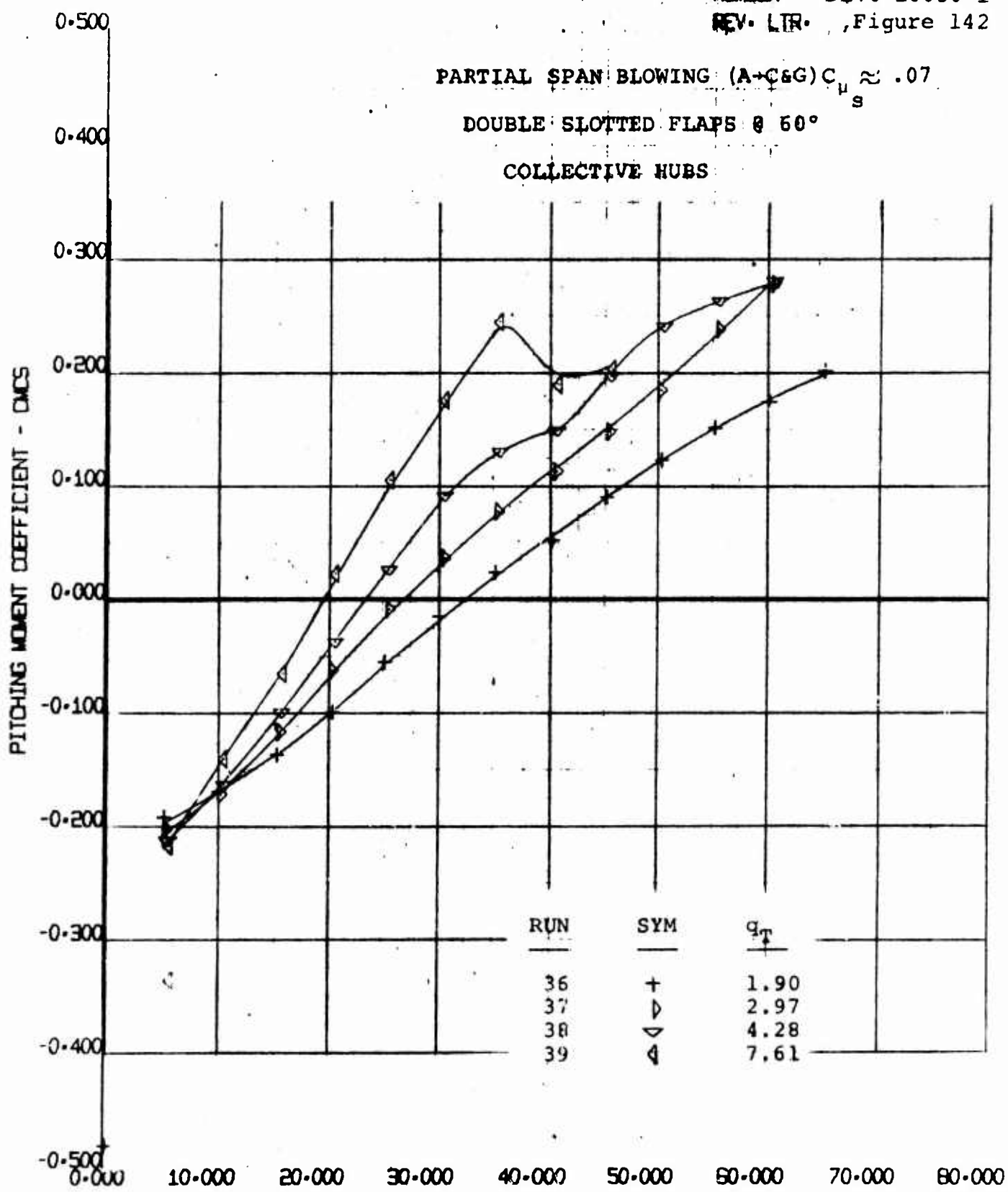

170 HALF SPAN MODEL VR 040 0-3 CMCS VS TILT WING ANGLE	BVWT 55 4/ 3/70

PARTIAL SPAN BLOWING (A→C), $C_{\mu_s} \approx .04$

DOUBLE SLOTTED FLAPS @ 60°
COLLECTIVE HUBS

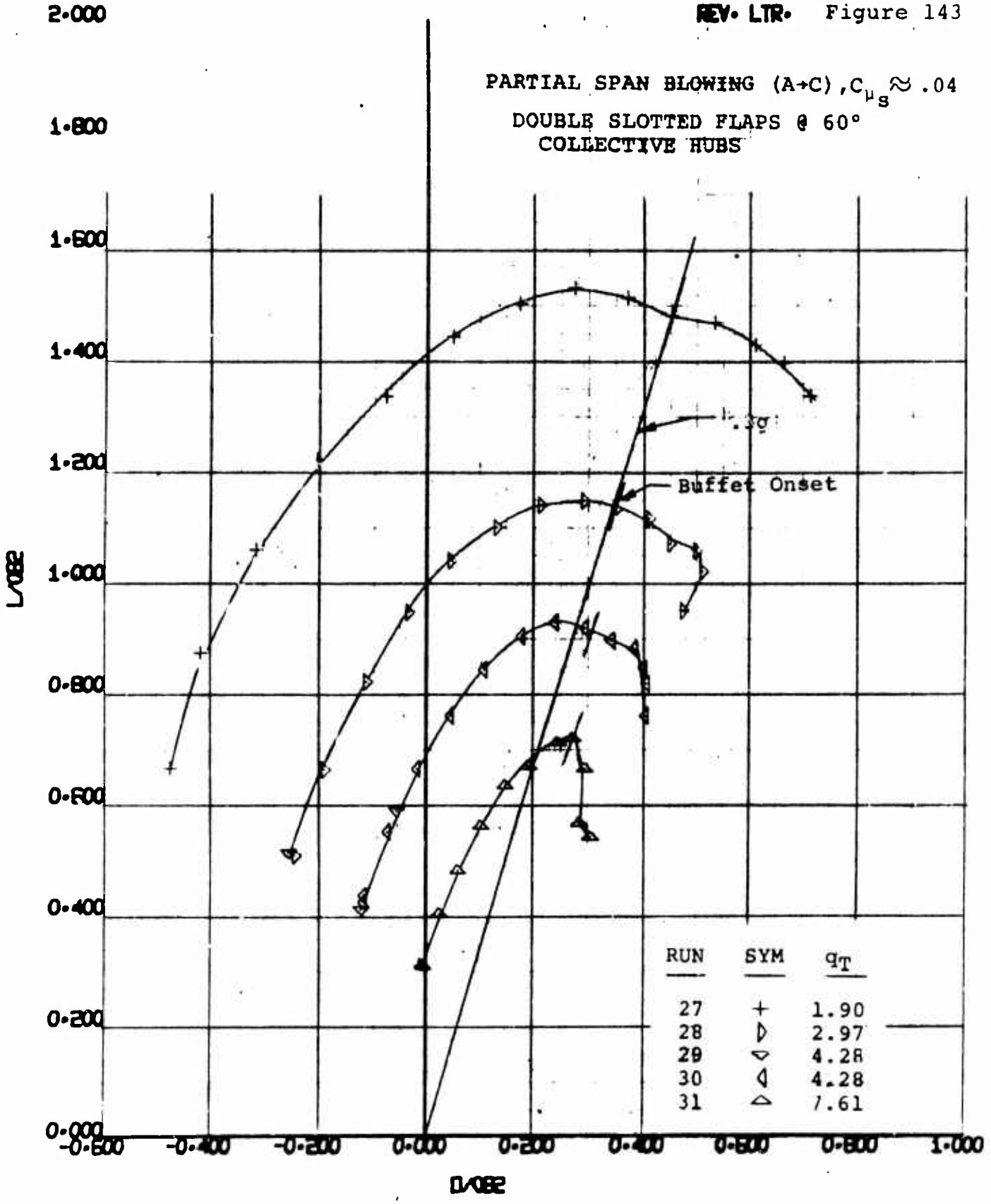

170 HALF SPAN MODEL WR 040 0-3 L/QBZ VS D/QBZ	BMWT 55 4/ 3/70

PARTIAL SPAN BLOWING (A→C), $C_{\mu_s} \approx .04$

DOUBLE SLOTTED FLAPS @ 60°
COLLECTIVE HUBS

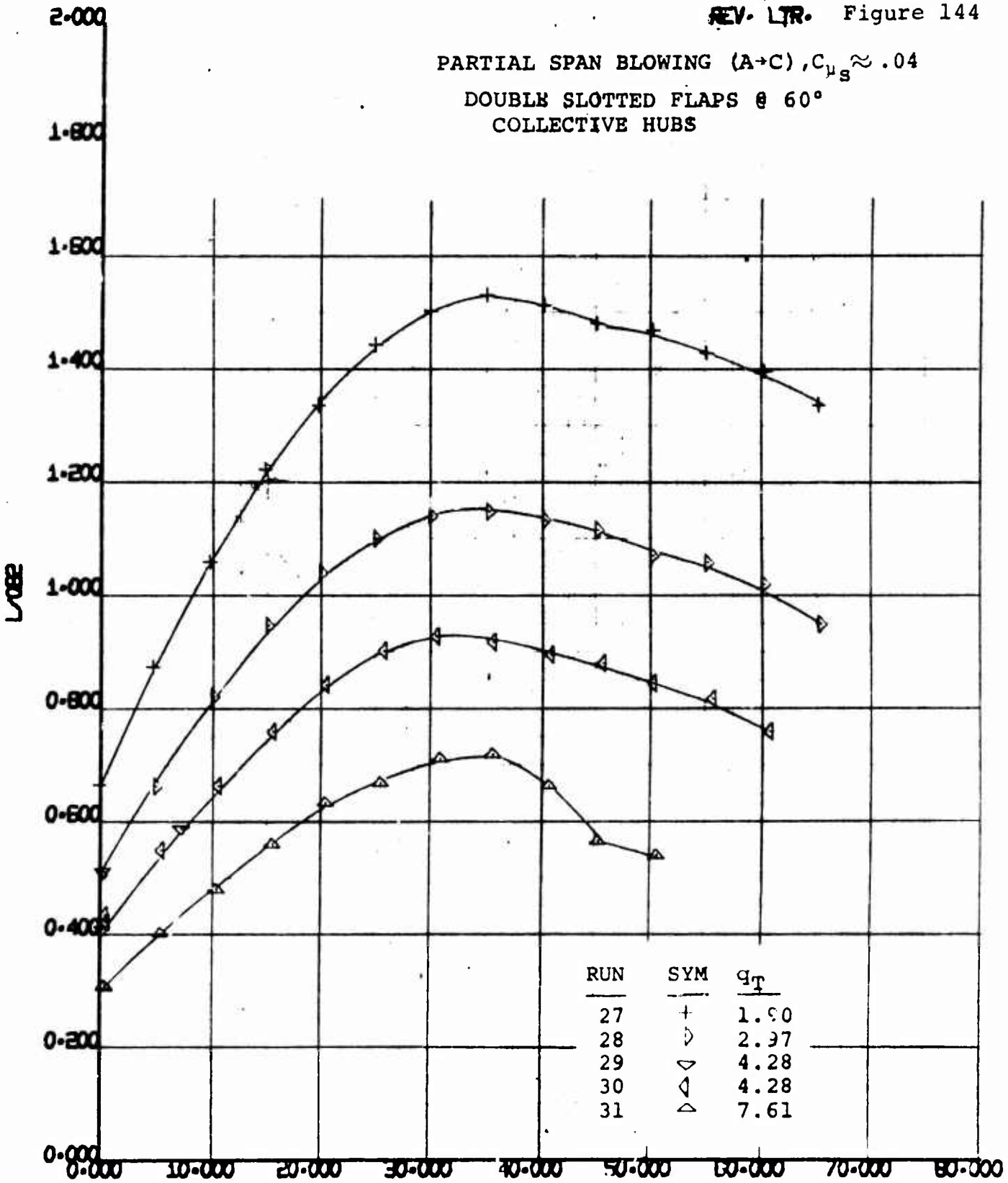

170 HALF SPAN MODEL VR 040 Q-3 L/QBS VS WING TILT ANGLE	BMT 55 4/ 3/10

NUMBER
REV. LTR.

PARTIAL SPAN BLOWING (A→C) $C_{\mu_B} \approx .04$

DOUBLE SLOTTED FLAPS @ 60°
COLLECTIVE HUBS

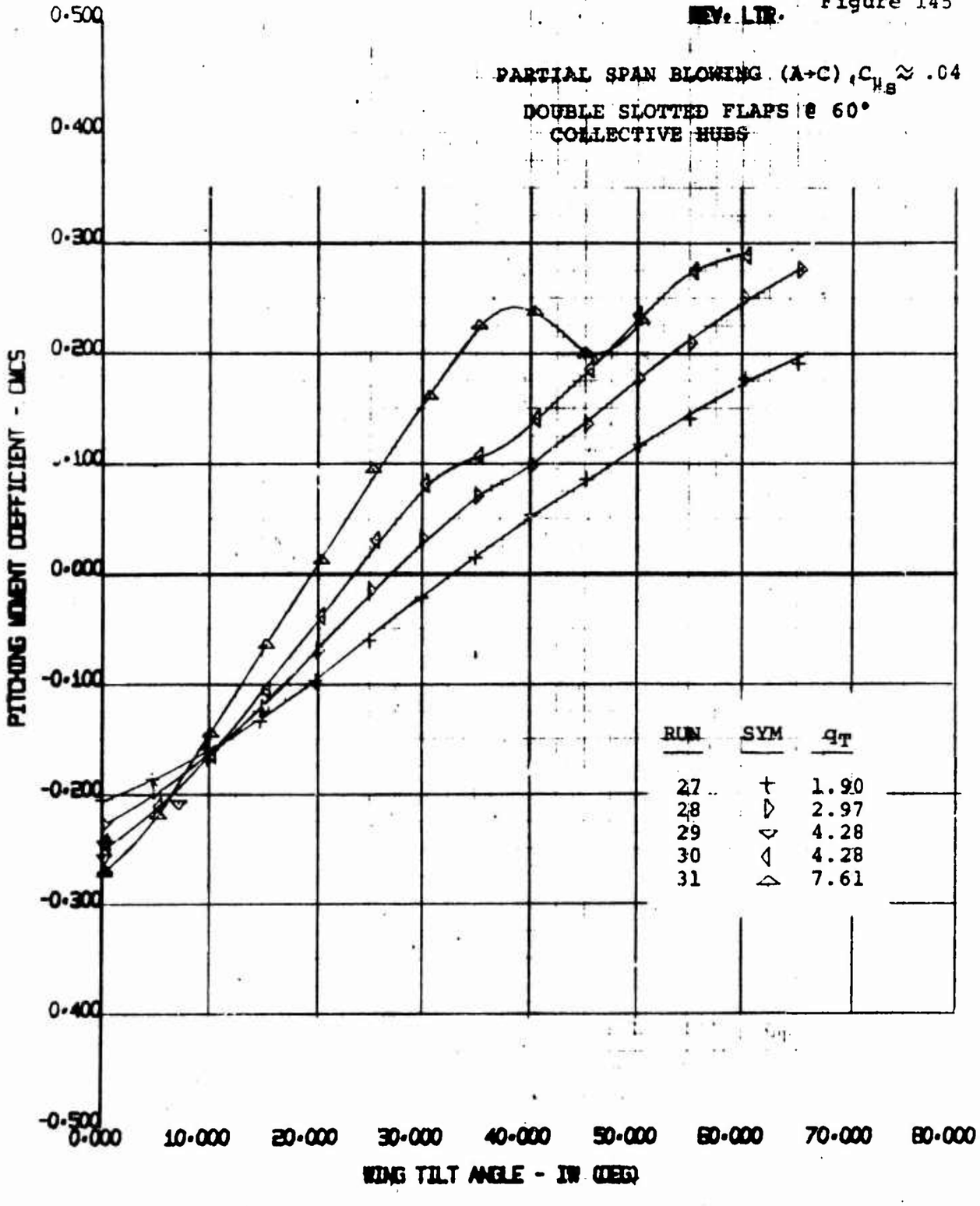

170 HALF SPAN MODEL VR 040 0-3 CMCS VS TILT WING ANGLE	BWT 55 4/ 3/70

PARTIAL SPAN BLOWING (A-C) $C_{\mu_{TS}} \approx .07$

DOUBLE SLOTTED FLAP @ 60°

COLLECTIVE HUBS

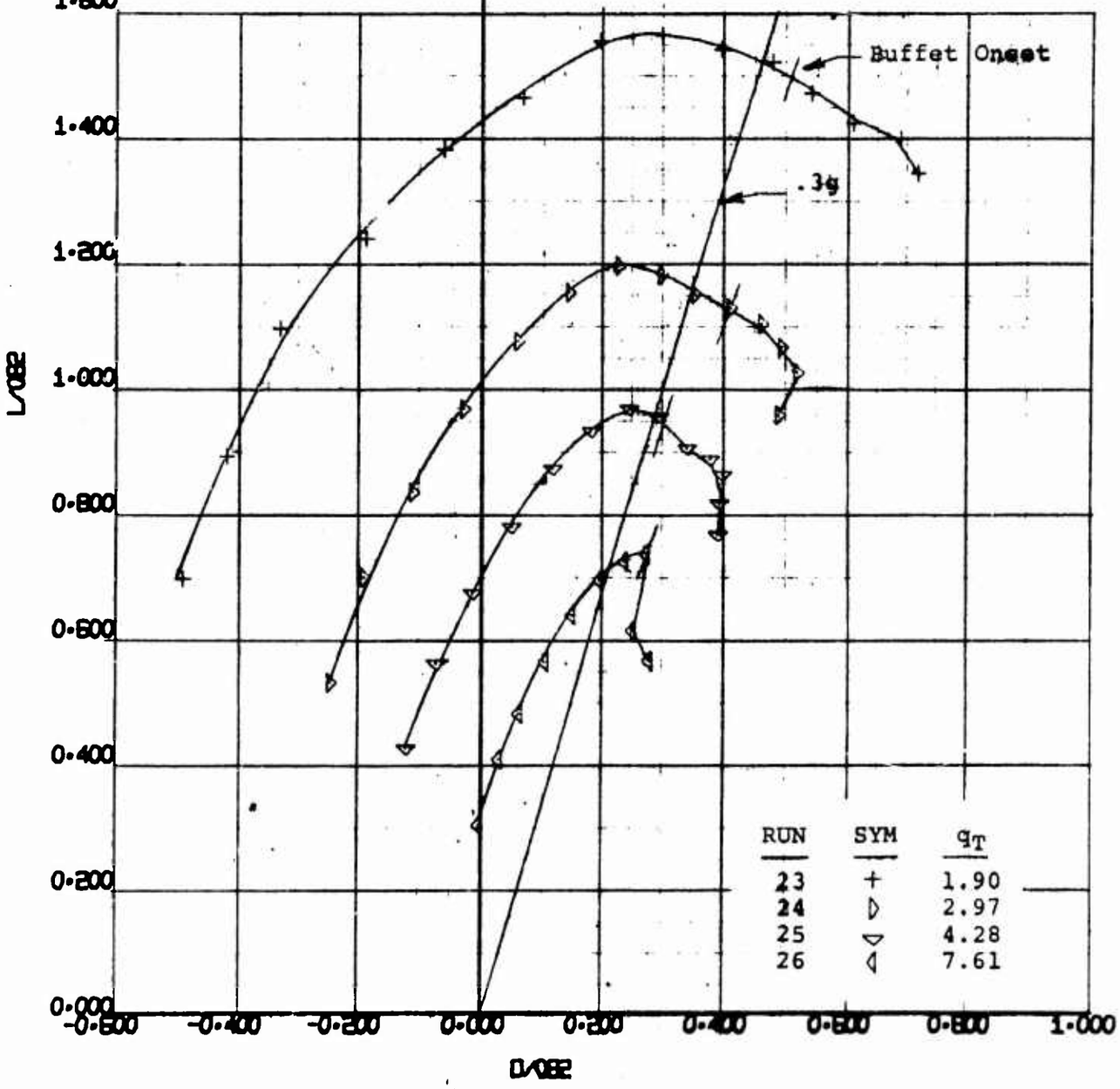

170 HALF SPAN MODEL VR 040 0-3 L/QS2 VS D/QS2	BMWT 55 4/ 3/70

PARTIAL SPAN BLOWING (A-C) $C_{\mu_s} \approx .07$

DOUBLE SLOTTED FLAP @ 60°

COLLECTIVE HUBS

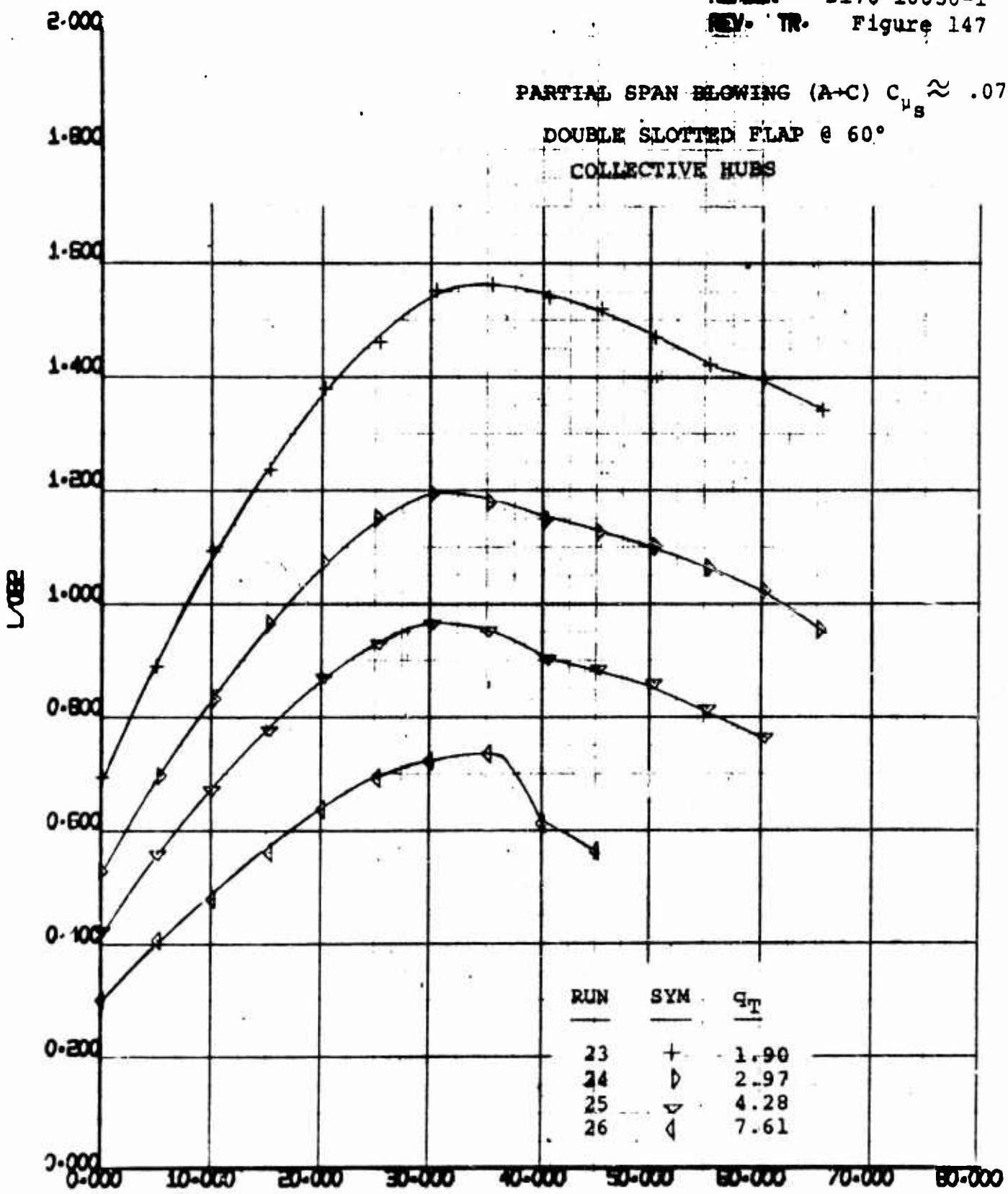

WING TILT ANGLE - i_W (DEG)

170 HALF SPAN MODEL AR 040 0-3 L/QB2 VS WING TILT ANGLE	BWT 55 4/ 3/70

PARTIAL SPAN BLOWING $(A+C)C_{\mu_s} \approx .07$
DOUBLE SLOTTED FLAP @60°
COLLECTIVE HUBS

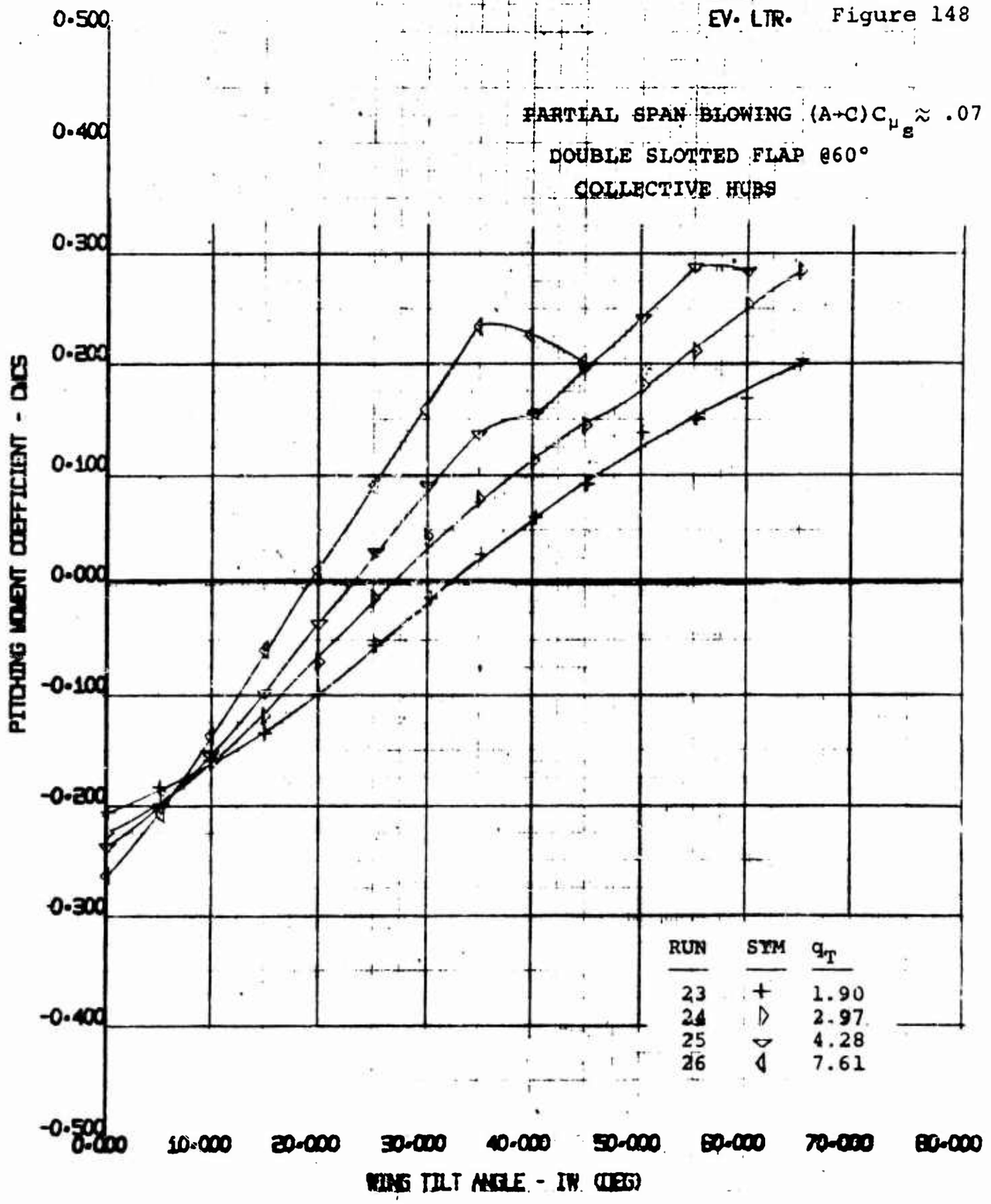

170 HALF SPAN MODEL VR 040 0-3 CMCS VS TILT WING ANGLE	BWT 55 4/ 3/70

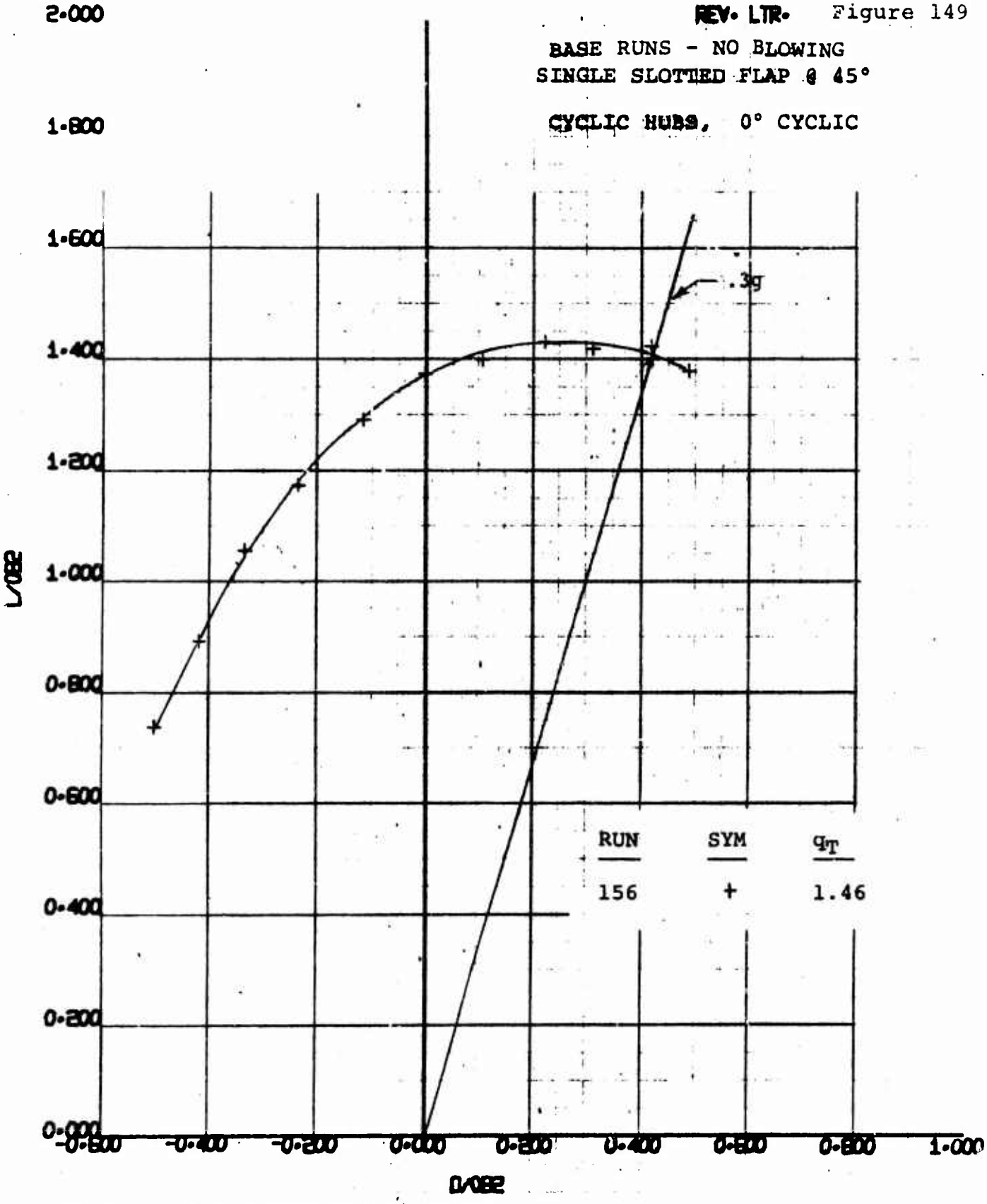

NOTES: (3) OUTBOARD FENCES OFF

170 HALF SPAN MODEL WR 040 0-3 L/Q82 VS D/Q82	BMT 55 4/ 8/70

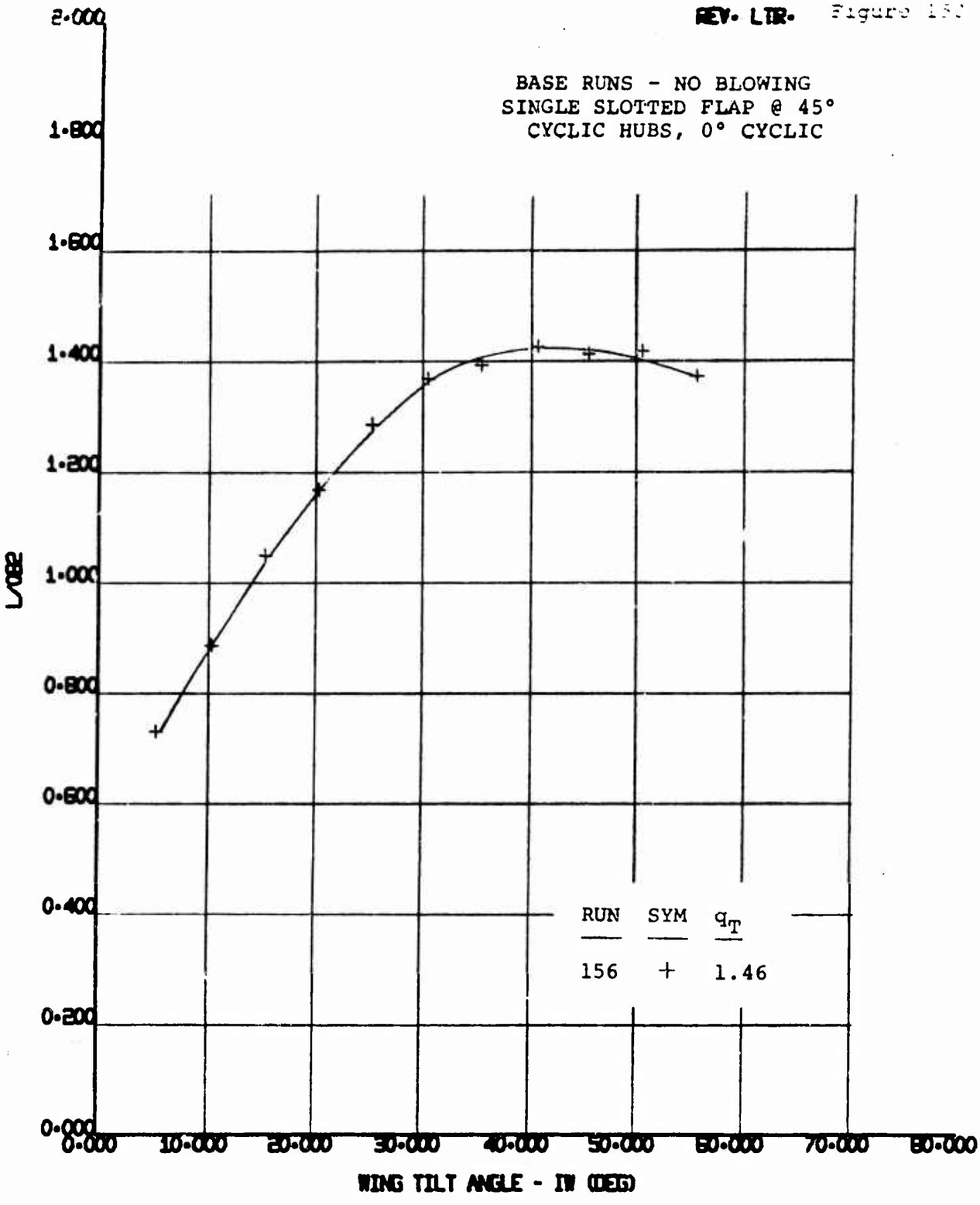

NOTES: (3) OUTBOARD FENCES OFF

170 HALF SPAN MODEL VR 040 0-3 L/QB2 VS WING TILT ANGLE	BWT 55 4/ 8/70

BASE RUNS - NO BLOWING
SINGLE SLOTTED FLAP @ 45°
CYCLIC HUBS, 0° CYCLIC

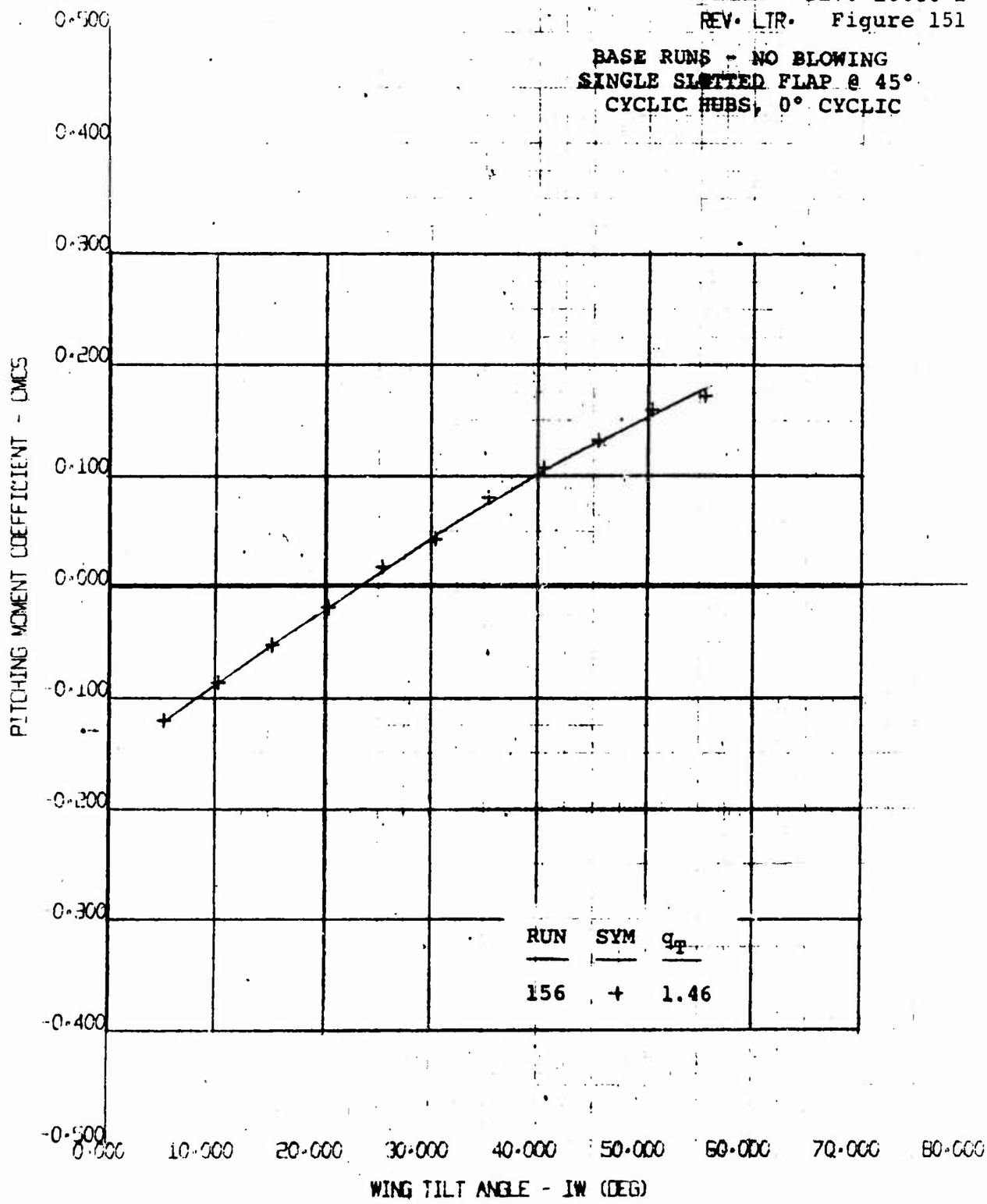

NOTES: (3) OUTBOARD FENCES OFF

170 HALF SPAN MODEL VR 040 0-3 CMCS VS TILT WING ANGLE	BVWT 55 4/ 6/70